Universitat de Girona

INHIBITION OF SIALYLTRANSFERASES IN PANCREATIC CANCER: EFFECTS ON THE EGFR PATHWAY AND ON THE TUMOUR PHENOTYPE

Laura Miró Domènech

Doctoral thesis

Inhibition of sialyltransferases in pancreatic cancer: effects on the EGFR pathway and on the tumour phenotype

Laura Miró Domènech

2022

Universitat de Girona

Universitat
de Girona

DOCTORAL THESIS

Inhibition of sialyltransferases in pancreatic cancer: effects on the EGFR pathway and on the tumour phenotype

Laura Miró Domènech
2022

Universitat de Girona

DOCTORAL THESIS

Inhibition of sialyltransferases in pancreatic cancer: effects on the EGFR pathway and on the tumour phenotype

Laura Miró Domènech
2022

Doctorate programme in Molecular Biology, Biomedicine and Health

Thesis supervisors	**Tutor**
Dr. Rosa Peracaula Miró	Dr. Anna Massaguer Vall-llovera

Dr. Anna Massaguer Vall-llovera

This thesis is submitted in fulfilment of the requirements to obtain the doctoral degree from the Universitat de Girona

AGRAÏMENTS

Ha arribat el moment d'escriure aquestes paraules, i us he de confessar que no ha sigut gens fàcil. Voldria donar les gràcies de tot cor a totes aquelles persones que en algun moment o altre m'heu acompanyat, ha sigut un regal poder compartir aquests últims anys amb vosaltres!

En primer lloc volia agrair a les meves directores, Rosa i Anna, l'oportunitat d'entrar al grup i començar la Tesi amb vosaltres. Tot i que les beques no m'ho van posar fàcil, al final ho vam aconseguir, gràcies per la paciència! Rosa, gràcies per ensenyar-me a ser constant, per animar-me a creure en el projecte i per donar-me suport en els moments bons i en els més difícils. Anna, gràcies per ensenyar-me que s'ha de lluitar i treballar dur per aconseguir els teus objectius. Gràcies també a tu Rafa, per obrir-me les portes del grup, per ensenyar-me a ser crítica i pel teu bon humor, els passadissos sempre eren més alegres quan hi erets tu!

Pedro, ¡sin ti todo esto no hubiera empezado! Gracias por ser mi apoyo durante los años de tesis, por compartir todo tu conocimiento científico, tu espíritu crítico e innovador, por hacerme ver que hay que espabilar y seguir luchando, pero por encima de todo eso, gracias por tu buen rollo, tus travesuras y las risas contigo.

Volia agrair també a les Bioquímiques: Montse, quina sort tenir algú com tu al costat durant aquests anys! Gràcies per la teva empatia, per l'alegria que transmets i per acompanyar-me sempre, tenim pendent un sopar! Esther, gràcies per escoltar-me i donar-me consell quan més ho necessitava. Jess, gràcies per tenir les portes del despatx sempre obertes i resoldre tots els meus dubtes de cultius. Marlon, gracias por ayudarme con los ensayos funcionales y por las conversaciones en cultivos, las horas pasaban más rápido contigo! Imma, gràcies pel teu bon rotllo i per fer que la feina al lab i a pràctiques fos molt més "fàcil"! I Júlia, gràcies per les teves aportacions a la tesi i a l'article, estic segura que el projecte es queda en bones mans.

Moltes gràcies al grup de Noves Dianes Moleculars del Càncer de l'IMIM: Pilar, Neus, Mireia i Noe. Gràcies per donar-me l'oportunitat de fer l'estudi *in vivo*, per la bona acollida al vostre lab i per tots els coneixements que he pogut aprendre al vostre costat.

Aquests anys no haguessin sigut el mateix sense els de la Granja!! Mil gràcies a tots per fer els dinars més divertits, pels sopars de Nadal, els scape rooms, les sortides a la platja fins tard i moltes aventures més! Iker, per continuar sentint les teves "carcajadas" particulars; Judit, per moltes converses interessants més; Pau, pels projectes futurs que un dia dinant vas imaginar; Irene, per la teva serenor i sinceritat; Mireia, per la teva experiència i consells; i

Sandra, gràcies per transmetre aquesta tranquil·litat, per fer que el teu despatx es convertís en un "confessionari" els últims temps i per moltes birres més per Vic! No m'oblido de les micros, Ellana, Paola, Laura i Eli, gràcies!! I finalment gràcies a tu, Carla, per ser un referent des del primer moment, per haver-me donat suport tots aquests anys, dins i fora de la uni, i sobretot per fer que em valorés quan ni tan sols jo creia en mi.

I mil gràcies als meus bioquímics preferits!! Adrià, merci per haver sigut el millor compi de despatx, i per les nostres conversacions justes i sinceres! Anna, no sé ben bé què dir que no t'hagi dit, gràcies de veritat per tot el que hem compartit aquests anys, per ser la millor confident que podria demanar, a nivell professional però sobretot a nivell personal, gràcies! Gràcies a tu Àlex, per deixar-me entrar una miqueta al teu cercle, i fer-me sentir com a casa!

A tu Adriana, gràcies per ser-hi sempre des de fa tants anys, per escoltar-me i donar-me suport en tot moment. I a totes les bionenes pels bons moments compartits des de la carrera, Maria i Eulàlia, per entendre'm a la perfecció, i a les de la plana, Ari i Jolis, gràcies per tot!

I per acabar, gràcies a la meva família. Papes, gràcies per creure en mi, per haver-me ensenyat que amb constància i esforç tot és possible, i aguantar-me en els moments difícils. Marta, gràcies per escoltar-me i acompanyar-me sempre amb amor, i per fer-me tieta, el millor regal que es pot demanar! Als del Toll, gràcies per cuidar-me com una filla més. Nutri, gràcies per ajudar-me amb la portada! I a tu Jacob, gràcies per ser al meu costat cada dia durant tot aquest temps, per la teva paciència infinita i el teu amor incondicional.

ACKNOWLEDGEMENTS

LIST OF ABBREVIATIONS

ABBREVIATION	DESCRIPTION
AREG	Amphiregulin
Asn	Asparagine
ATP	Adenosine triphosphate
BRCA	Breast-ovarian cancer syndrome
BSA	Bovine serum albumin
BTC	Betacellulin
CA19-9	Carbohydrate antigen 19-9
CAF	Cancer-associated fibroblast
CAR	Chimeric antigen receptor
CMAS	CMP N-acetylneuraminic acid synthase
CME	Clathrin-mediated endocytosis
CMP	Cytidine monophosphate
ctDNA	Circulating tumour DNA
CTL	Cytotoxic T-lymphocyte
CTLA-4	Cytotoxic T-lymphocyte-associated protein 4
CTP	Cytidine triphosphate
DMEM	Dulbecco's modified Eagle's Medium
DMSO	Dimethyl sulfoxide
DNA	Deoxyribonucleic acid
DPBS	Dulbecco's phosphate buffered saline
ECM	Extracellular matrix
EGF	Epidermal growth factor
EGFR	Epidermal growth factor receptor
EGN	Epigen
EMT	Epithelial-mesenchymal transition
EPR	Epiregulin
ER	Endoplasmic reticulum
FAK	Focal adhesion kinase
FBS	Fetal bovine serum
FC	Flow cytometry
FDA	Food and drug administration
Fuc	Fucose
FucT	Fucosyltransferase
GA	Golgi apparatus
Gal	Galactose
GalNac	N-acetylgalactosamine
GBP	Glycan binding proteins
Glc	Glucose
GlcA	Glucoronic acid
GlcNAc	N-acetylglucosamine
GnT	N-acetylglucosaminyltransferase

ABBREVIATION	DESCRIPTION
GPI	Glycosylphosphatidylinositol
GT	Glycosyltransferase
HB-EGF	Heparin-binding EGF-like growth factor
IL	Interleukin
KD	Knockdown
Kdn	2-keto-deoxynonoic acid
KRAS	Kristen Rat Sarcoma virus
Lith	Lithocolic acid
mAb	Monoclonal antibody
MAA-II	Maackia amurensis Lectin II
Man	Mannose
MDSC	Myeloid-derived supressor cells
MHC	Major histocompatibility complex
miR	MicroRNA
MRI	Magnetic resonance imaging
MSLN	Mesothelin
mTOR	Mammalian target of rapamycin
MTT	3-(4,5-dimethylthiazol-2-yl)-2,5-diphenyltetrazolium bromide
MUC	Mucin
NCE	Nonclathrin endocytic endocytosis
nEGFR	Nuclear epidermal growth factor receptor
Neu5Ac	5-N-Acetlylneuraminic acid
Neu5Gc	N-glycolylneuraminic acid
NK	Natural killer
NRG	Neuregulins
NSCLC	Non-small cell lung carcinomao
OST	Oligosaccharyltransferase
PanIN	Pancreatic intraepithelial neoplasia
PD-1	Programmed cell death protein-1
PDA	Pancreatic ductal adenocarcinoma
PET	Positron emission tomography
ppGalNAcT	Polypeptide-N-acetylgalactosaminyltransferases
PTB	Phosphotyrosine binding domains
PTM	Post-translational modifications
Rb	Retinoblastoma
rhE-selectin	Recombinant Human E-selectin
RT	Room temperature
RTK	Receptor tyrosine kinase
SA	Sialic acid
sEV	Small extracellular vesicle
Siglecs	Sialic-acid-binding immunoglobulin-like lectins
sLe^a	Sialyl-Lewis a
sLe^x	Sialyl-Lewis x
SNA	Sambucus nigra Agglutinin

ABBREVIATION	DESCRIPTION
SsaI	Soyasaponin-I
ST	Sialyltransferase
TGF	Transforming growth factor
TKD	Tyrosine kinase domain
TKI	Tyrosine kinase inhibitors
TM	Transmembrane
TME	Tumour microenvironment
TS	Transition-state
WB	Western blot
WT	Wild type
Xyl	Xylose

LIST OF FIGURES

LIST OF TABLES

TABLE OF CONTENTS

SUMMARY

Pancreatic ductal adenocarcinoma (PDA) presents a dismal prognosis mainly due to its delayed diagnosis, its aggressiveness, and resistance to existing therapies. Aberrant glycosylation and, in particular, the overexpression of several sialylated determinants such as sialyl-Lewis$^{x/a}$ (sLe$^{x/a}$), have been associated to cancer progression and metastatic spread, in addition to the modulation of the immune cell component of the tumour microenvironment.

Previous studies from our group demonstrated that the α2,3-sialyltransferases (ST) ST3GAL3 and ST3GAL4, two enzymes that transfer sialic acid (SA) to generate α2,3-sialylated determinants, promote the invasive and metastatic phenotype of PDA cell lines. In addition, these enzymes were shown to sialylate cell adhesion molecules involved in tumour progression, such as α2β1 integrin and E-cadherin, regulating their function and signalling pathways. These findings, together with the fact that expression levels of STs and SA levels are generally increased in the serum of cancer patients, being indicative of poor prognosis, highlight the importance of reducing hypersialylation in PDA. Blocking sialylation by modifying ST mRNA expression or by sialidase treatment has been used to study the role of tumour SA, but the application of these approaches to the clinical setting is complex. Nonetheless, the recent discovery and development of ST inhibitors have represented a new strategy to pharmacologically inhibit SA expression in tumours and have opened a path to therapeutically target STs.

The Epidermal Growth Factor Receptor (EGFR), an important membrane receptor involved in cell proliferation, contributes to several processes favouring cancer onset, progression, and metastatic spread in nearly all neoplasms, including PDA. EGFR is a glycoprotein membrane receptor that can be sialylated by STs that, in turn, can modulate its function. In this regard, the study of EGFR glycosylation in different cancer types has recently increased, although the role of EGFR sialylation in PDA progression is still unclear, and would be of high interest for scientists developing EGFR-targeted therapies.

Under these premises, in this study we principally aimed to gain insight into the role of the STs and their generated tumour sialoglycans on the phenotype of PDA cells; as well as to study their effect on the function and signalling of EGFR.

In the first part of this study we have focused on the implication of ST3GAL3 and ST3GAL4 on the glycosylation of EGFR in two PDA cell lines, BxPC-3 and Capan-1. We have first characterized the EGFR expression in control and ST knockdown (KD) cells (ST3GAL3

KD and ST3GAL4 KD) by flow cytometry (FC) and have shown that ST3GAL3 KD and ST3GAL4 KD cells do not alter basal EGFR expression levels. We have addressed how ST3GAL3 KD and ST3GAL4 KD alter the glycan pattern of EGFR by immunopurification of EGFR from cell lysates and subsequent immunoblotting to detect sLe^x, α2,3- and α2,6-SA expression on EGFR. We have shown that the expression levels of sLe^x on EGFR from ST silenced cells tended to decrease, in accordance with the general decrease of sLe^x on the cell surface glycoconjugates, although the expression of α2,6-SA was not significantly altered. The reduction of sLe^x on EGFR led to a higher EGFR activation induced by EGF in BxPC-3 and Capan-1 cells, to an increase in its dimerization and its capacity to trigger downstream signalling pathways, with a significant increase in the phosphorylation of AKT protein for both ST3GAL3 KD and ST3GAL4 KD BxPC-3 cells. Regarding the functional properties, we detected that the higher phosphorylation levels of EGFR on ST KD BxPC-3 cells were translated into an increase in cell proliferation induced by EGF, while for Capan-1 no significant changes were observed. Furthermore, we have studied whether ST3GAL3 KD and ST3GAL4 KD could increase cell sensitivity to EGFR-targeted drugs that are currently used in clinics for different tumour treatment, with the aim of improving PDA therapy by using a combined treatment strategy. Unfortunately, our results indicated that BxPC-3 and Capan-1 responsiveness to Erlotinib was not altered by the reduction of EGFR sialylation.

In the second part of this work, the potential of three ST inhibitors on the reduction of cell surface sialylation on PDA human and murine cells have been evaluated. Among the three inhibitors, Ac$_5$3F$_{ax}$-Neu5Ac produced the highest decrease on tumour sialoglycans in PDA cell lines, so it was selected as the best candidate to evaluate its effect on the tumour phenotype of PDA cells *in vitro* and on PDA tumours *in vivo*. Ac$_5$3F$_{ax}$-Neu5Ac treatment of human PDA cells caused a significant reduction on the cell surface expression levels of α2,3-SA and sLe^x, which led to an impairment in the E-selectin-mediated adhesion capacity and to a reduction in the migration and invasion capacities of the PDA cells. Besides, the effect of Ac$_5$3F$_{ax}$-Neu5Ac treatment was evaluated on four murine PDA cells, of which MSB262 and OBB452 were the ones that reduced more markedly their SA content upon treatment with the inhibitor and were selected for the functional assays. Ac$_5$3F$_{ax}$-Neu5Ac treatment significantly reduced migration and invasion capacity of MSB262 PDA cells although no significant reduction was found for OBB452 cells. Thus, MSB262 cells were injected into syngeneic mice to generate subcutaneous tumours that were posteriorly treated with Ac$_5$3F$_{ax}$-Neu5Ac. Importantly, the intratumoural Ac$_5$3F$_{ax}$-Neu5Ac treatment caused a reduction in the tumour volume, a reduction in their SA expression and altered the tumour immune

compartment, causing an increase in CD8$^+$ T cells and natural killer cells. Altogether, these results demonstrate that Ac$_5$3F$_{ax}$-Neu5Ac treatment effectively weakens the malignant phenotype of PDA cells and show a positive impact of reducing SA expression in PDA by inhibiting cell STs.

Overall, the results obtained demonstrate that ST3GAL3 and ST3GAL4 play a role in the glycosylation of EGFR, which modulates its activation and regulate downstream signalling pathways, promoting EGF-induced proliferation. Nevertheless, further research in PDA models is still needed to clarify the underlying molecular mechanisms. Finally, and up to our knowledge, this is the first work reporting the effect of the ST inhibitor Ac$_5$3F$_{ax}$-Neu5Ac in PDA cells and animal models, findings that might ease the way for the use of metabolic inhibitors to further evaluate the role of sialylated glycans in tumour progression and for their putative therapeutic application.

RESUM

L'adenocarcinoma ductal pancreàtic (PDA) presenta un pronòstic nefast degut principalment al seu diagnòstic tardà, la seva agressivitat i la resistència a les teràpies existents. La glicosilació aberrant i, en particular, la sobreexpressió de diversos determinants sialilats com el sialil-Lewis$^{x/a}$ (sLe$^{x/a}$), s'han associat amb la progressió del càncer i la formació de metàstasi, a part de la modulació del component immunitari cel·lular del microambient tumoral.

En estudis previs del grup s'ha demostrat que les α2,3-sialiltransferases (ST) ST3GAL3 i ST3GAL4, dos enzims que transfereixen àcid siàlic (SA) per generar determinants α2,3-sialilats, promouen el fenotip invasiu i metastàtic de les línies cel·lulars de PDA. A més, s'ha demostrat que aquests enzims sialilen molècules d'adhesió cel·lular implicades en la progressió del tumor, com la integrina α2β1 i la E-cadherina, regulant la seva funció i les vies de senyalització. Aquests resultats, juntament amb el fet que els nivells d'expressió de les STs i els nivells totals de SA s'incrementen generalment en el sèrum dels pacients amb càncer sent indicadors de mal pronòstic, posen de manifest la importància de reduir la hipersialilació en PDA. La disminució de la sialilació modificant l'expressió de l'ARNm de les ST o mitjançant el tractament amb sialidasa s'ha utilitzat per estudiar el paper de l'SA al tumor, però l'aplicació d'aquestes estratègies a l'àmbit clínic és complexa. No obstant això, el recent descobriment i desenvolupament d'inhibidors de les ST han representat una nova estratègia per inhibir farmacològicament l'expressió d'SA en tumors i han portat a considerar les STs com a possibles dianes terapèutiques.

El receptor del factor de creixement epidèrmic (EGFR), un receptor de membrana implicat en la proliferació cel·lular, contribueix en diversos processos que afavoreixen l'aparició, la progressió i la propagació del càncer en gairebé totes les neoplàsies, inclòs el PDA. L'EGFR és un receptor de membrana glicoproteic que pot ser sialilat per les STs que, alhora, poden modular la seva funció. En aquest sentit, l'estudi de la glicosilació de l'EGFR en diferents tipus de tumors ha augmentat recentment però el rol de la sialilació de l'EGFR en la progressió del PDA encara no està clar, i el seu estudi seria de gran interès per als científics que desenvolupen teràpies dirigides contra EGFR.

Sota aquestes premisses, en aquest estudi es planteja com a objectiu principal conèixer el rol de les STs, i els corresponents sialoglicans tumorals generats, en el fenotip de les cèl·lules de PDA; així com estudiar el seu efecte sobre la funció i la senyalització de l'EGFR.

En la primera part d'aquest estudi ens vam centrar en la implicació de les ST3GAL3 i ST3GAL4 en la glicosilació de l'EGFR en dues línies cel·lulars de PDA, les cèl·lules BxPC-3 i les Capan-1. Primer es va caracteritzar l'expressió d'EGFR en cèl·lules control i en cèl·lules silenciades (knockdown, KD) per les STs ST3GAL3 i ST3GAL4 (ST3GAL3 KD i ST3GAL4 KD) mitjançant citometria de flux i es va demostrar que en les cèl·lules ST3GAL3 KD i ST3GAL4 KD els nivells d'expressió basal d'EGFR es mantenen estables. Es va estudiar com la disminució dels nivells de ST3GAL3 i ST3GAL4 alteren el patró glucídic de l'EGFR mitjançant la immunopurificació d'EGFR a partir de llisats cel·lulars i la posterior immunodetecció per determinar l'expressió sLe^x, $\alpha2,3$- i $\alpha2,6$-SA en l'EGFR. Els resultats obtinguts van mostrar que els nivells d'expressió de sLe^x en l'EGFR de cèl·lules amb les ST silenciades tendeix a disminuir, d'acord amb la disminució general de sLe^x en els glicoconjugats de la superfície cel·lular, tot i que l'expressió d'$\alpha2,6$-SA no presentava una alteració significativa. La reducció de sLe^x en l'EGFR va portar a una major activació de l'EGFR (induïda per EGF) a les cèl·lules BxPC-3 i Capan-1, a un augment de la seva dimerització i de la seva capacitat per activar les vies de senyalització consegüents, causant un augment significatiu de la fosforilació de la proteïna AKT tant per les cèl·lules BxPC-3 ST3GAL3 KD com per a les ST3GAL4 KD. Pel que fa a les propietats funcionals, es va detectar que l'increment dels nivells de fosforilació de l'EGFR a les cèl·lules BxPC-3 silenciades es traduïa en un augment de la proliferació cel·lular induïda per EGF, mentre que per a Capan-1 no es van observar canvis significatius. A més, es va estudiar si la disminució dels nivells de ST3GAL3 i ST3GAL4 podrien augmentar la sensibilitat de les cèl·lules tumorals als fàrmacs dirigits a EGFR que s'utilitzen actualment en l'àmbit clínic com a tractaments anti-tumorals, amb l'objectiu de millorar la teràpia del PDA mitjançant una estratègia de tractament combinat. Malauradament, els nostres resultats van indicar que la resposta de les cèl·lules BxPC-3 i Capan-1 a Erlotinib no es veu alterada per la reducció de la sialilació d'EGFR.

En la segona part d'aquest treball, es va avaluar el potencial de tres inhibidors de les ST en la reducció de la sialilació de la superfície cel·lular en cèl·lules humanes i murines de PDA. D'entre els tres inhibidors estudiats, l'Ac$_5$3F$_{ax}$-Neu5Ac va ser el que va produir la disminució significativa dels sialoglicans tumorals en les línies cel·lulars de PDA i per aquest motiu va ser seleccionat per avaluar el seu efecte sobre el fenotip tumoral de cèl·lules de PDA *in vitro* i sobre tumors de PDA *in vivo*. El tractament de cèl·lules humanes de PDA amb l'Ac$_5$3F$_{ax}$-Neu5Ac va provocar una reducció significativa dels nivells d'expressió d'$\alpha2,3$-SA i sLe^x de la superfície cel·lular, que va causar una disminució de la capacitat d'adhesió mediada per E-

selectina i una reducció de les capacitats de migració i invasió de les cèl·lules de PDA. A més, es va avaluar l'efecte del tractament amb $Ac_5 3F_{ax}$-Neu5Ac en quatre línies cel·lulars murines de PDA, de les quals MSB262 i OBB452 van ser les que van presentar una reducció més gran del seu contingut d'SA després del tractament amb l'inhibidor i van ser seleccionades pels assajos funcionals. El tractament amb $Ac_5 3F_{ax}$-Neu5Ac va reduir significativament la capacitat de migració i invasió de les cèl·lules MSB262, però en les cèl·lules OBB452 no es va observar una reducció significativa. Així doncs, es van injectar cèl·lules MSB262 a ratolins singènics per generar tumors subcutanis que es van tractar posteriorment amb $Ac_5 3F_{ax}$-Neu5Ac. De manera rellevant, el $Ac_5 3F_{ax}$-Neu5Ac va provocar una reducció del volum del tumor, una reducció de la seva expressió d'SA i una alteració del component cel·lular immune del tumor, provocant un augment de les cèl·lules T $CD8^+$ i les cèl·lules natural killer. En conjunt, aquests resultats demostren que el tractament amb $Ac_5 3F_{ax}$-Neu5Ac disminueix eficaçment el fenotip maligne de les cèl·lules de PDA i evidencia l'impacte positiu de reduir l'expressió de SA als tumors de PDA mitjançant la inhibició de les ST.

En conclusió, els resultats obtinguts demostren que ST3GAL3 i ST3GAL4 tenen un rol important en la glicosilació de l'EGFR, que alhora modula la seva activació i regula les vies de senyalització conseqüents, promovent la proliferació induïda per EGF. No obstant això, altres investigacions en models de PDA són necessàries per esbrinar els mecanismes moleculars subjacents. Finalment, i fins al nostre coneixement, aquest és el primer treball que evidencia l'efecte de l'inhibidor de ST $Ac_5 3F_{ax}$-Neu5Ac en cèl·lules de PDA i en models animals, uns resultats que conviden a utilitzar inhibidors metabòlics per aprofundir en l'estudi del rol dels glicans sialilats en la progressió del PDA i posen de manifest l'interès per la seva possible aplicació terapèutica.

RESUMEN

El adenocarcinoma ductal pancreático (PDA) presenta un pronóstico nefasto debido principalmente a su diagnóstico tardío, su agresividad y la resistencia a las terapias existentes. La glicosilación aberrante y, en particular, la sobreexpresión de múltiples determinantes sialilados como sialil-Lewis$^{x/a}$ (sLe$^{x/a}$), se han asociado con la progresión del cáncer y la diseminación metastásica, además de la modulación del componente inmune celular del microambiente tumoral.

En estudios previos de nuestro grupo se ha demostrado que las α2,3-sialiltransferasas (ST) ST3GAL3 y ST3GAL4, dos enzimas que transfieren ácido siálico (SA) para generar determinantes α2,3-sialilados, promueven el fenotipo invasivo y metastásico de las líneas celulares de PDA. Además, se ha demostrado que estas enzimas sialilan moléculas de adhesión celular involucradas en la progresión tumoral, como la integrina α2β1 y la E-cadherina, regulando su función y vías de señalización. Estos resultados, junto con el hecho que los niveles de expresión de STs y los niveles totales de SA generalmente están aumentados en el suero de pacientes con cáncer, siendo indicativos de mal pronóstico, remarcan la importancia de reducir la hipersialilación en PDA. La disminución de la sialilación modificando la expresión del ARNm de ST o mediante el tratamiento con sialidasas se ha utilizado para estudiar el papel de los SA tumorales, pero la aplicación de estas estrategias al entorno clínico es todavía compleja. No obstante, el reciente descubrimiento y desarrollo de inhibidores de ST ha representado una nueva estrategia para inhibir farmacológicamente la expresión de SA en tumores y nos lleva a considerar las STs cómo posibles dianas terapéuticas.

El receptor del factor de crecimiento epidérmico (EGFR), un importante receptor de membrana involucrado en la proliferación celular, contribuye a varios procesos que favorecen el inicio, la progresión y la diseminación metastásica del cáncer en casi todas las neoplasias, incluido el PDA. EGFR es un receptor de membrana glicoproteico que puede ser sialilado por STs que, a su vez, pueden modular su función. En este sentido, el estudio de la glicosilación del EGFR en diferentes tipos de cáncer ha aumentado recientemente, aunque el papel de la sialilación del EGFR en la progresión del PDA aún no está definido y sería de gran interés para los científicos que desarrollan terapias dirigidas contra EGFR.

Bajo estas premisas, el objetivo principal de este estudio fue conocer el papel de las STs y los correspondientes sialoglicanos tumorales generados en el fenotipo de las células de PDA; así como estudiar su efecto sobre la función y señalización del EGFR.

En la primera parte de este estudio nos centramos en la implicación de ST3GAL3 y ST3GAL4 en la glicosilación de EGFR en dos líneas celulares de PDA, BxPC-3 y Capan-1. En primer lugar, se caracterizó la expresión de EGFR en células control y silenciadas (knockdown (KD) para ST3GAL3 y ST3GAL4 (ST3GAL3 KD y ST3GAL4 KD) por citometría de flujo y se demostró que los niveles de expresión de EGFR basal se mantienen estables en las células ST3GAL3 KD y ST3GAL4 KD. Se analizó cómo las células ST3GAL3 KD y ST3GAL4 KD alteran el patrón glucídico de EGFR a través de la inmunopurificación del EGFR a partir de lisados celulares y subsiguiente inmunotransferencia para detectar la expresión de sLe^x, α2,3 y α2,6-SA en EGFR. Se observó que los niveles de expresión de sLe^x en EGFR de células con las ST silenciadas tiende a disminuir, de acuerdo con la disminución general de sLe^x en los glicoconjugados de la superficie celular, aunque la expresión de α2,6-SA no presentó una alteración significativa. La reducción de sLe^x en EGFR condujo a una mayor activación de EGFR inducida por EGF en células BxPC-3 y Capan-1, a un aumento en su dimerización y su capacidad para activar las vías de señalización consiguientes, con un aumento significativo en la fosforilación de la proteína AKT en las células BxPC-3 ST3GAL3 KD y ST3GAL4 KD. En cuanto a las propiedades funcionales, se detectó que los niveles más altos de fosforilación de EGFR en las células BxPC-3 KD se traducían en un aumento de la proliferación celular inducida por EGF, mientras que para Capan-1 no se observaron cambios significativos. Además, se estudió si la disminución de los niveles de ST3GAL3 y ST3GAL4 podría aumentar la sensibilidad celular a los fármacos dirigidos a EGFR que se utilizan actualmente en clínica para el tratamiento de diferentes tumores, con el objetivo de mejorar la terapia del PDA mediante el uso de un tratamiento combinado. Desafortunadamente, nuestros resultados indicaron que la respuesta de las células BxPC-3 y Capan-1 a Erlotinib no se ve alterada por la reducción de la sialilación de EGFR.

En la segunda parte de este trabajo, se evaluó el potencial de tres inhibidores de las ST en la reducción de la sialilación de la superficie celular de células de PDA humanas y murinas. De los tres inhibidores, Ac$_5$3F$_{ax}$-Neu5Ac fue el que produjo la mayor disminución de sialoglicanos tumorales en las líneas celulares de PDA, por lo que fue seleccionado como el mejor candidato para evaluar su efecto sobre el fenotipo tumoral de las células de PDA *in vitro* y sobre tumores de PDA *in vivo*. El tratamiento con Ac$_5$3F$_{ax}$-Neu5Ac de células de PDA humanas provocó una reducción significativa en los niveles de expresión de α2,3-SA y sLe^x en la superficie celular, lo que condujo a una disminución de la capacidad de adhesión mediada por E-selectina y a una reducción de la migración e invasión de las células de PDA. Además, se evaluó el efecto del tratamiento con Ac$_5$3F$_{ax}$-Neu5Ac en cuatro líneas celulares

murinas de PDA, de las cuales MSB262 y OBB452 fueron las que presentaron una reducción más marcada de su contenido de SA tras el tratamiento con el inhibidor y fueron seleccionadas para los ensayos funcionales. El tratamiento con $Ac_5 3F_{ax}$-Neu5Ac redujo significativamente la migración y la capacidad de invasión de las células MSB262, aunque no se obtuvo una reducción significativa para las células OBB452. Así pues, se inyectaron células MSB262 en ratones singénicos para generar tumores subcutáneos que posteriormente se trataron con $Ac_5 3F_{ax}$-Neu5Ac. De manera relevante, el tratamiento intratumoural con $Ac_5 3F_{ax}$-Neu5Ac provocó una reducción del volumen tumoral, una reducción de su expresión de SA y alteró el componente celular inmunitario del tumor, provocando un aumento de las células T $CD8^+$ y las células natural killer. En conjunto, estos resultados demuestran que el tratamiento con $Ac_5 3F_{ax}$-Neu5Ac disminuye eficazmente el fenotipo maligno de las células de PDA y demuestra el impacto positivo de reducir la expresión de SA en PDA mediante la inhibición de las ST.

En conclusión, los resultados obtenidos demuestran que ST3GAL3 y ST3GAL4 juegan un papel importante en la glicosilación de EGFR, que a su vez modula su activación y regula las vías de señalización consiguientes, promoviendo la proliferación inducida por EGF. Sin embargo, se requieren otras investigaciones en modelos de PDA para determinar los mecanismos moleculares subyacentes. Finalmente, y hasta donde tenemos conocimiento, este es el primer trabajo que evidencia el efecto del inhibidor de ST $Ac_5 3F_{ax}$-Neu5Ac en células de PDA y en modelos animales, unos resultados que promueven el uso de inhibidores metabólicos para evaluar con más profundidad el papel de los glicanos sialilados en la progresión tumoral y ponen de manifiesto el interés para su futura aplicación terapéutica.

INTRODUCTION

1. Cancer

Cancer is a leading cause of death and represents an important limitation to the increase in life expectancy worldwide. In 2020, 19.3 million new cancer cases were estimated and almost 10.0 million cancer deaths occurred [1]. In most of the developed countries, cancer ranks to first or second cause of premature death (i.e. at ages 30-69 years)[2] and the global cancer burden in 2040 is expected to rise nearly a 50% from 2020, being a reflex of population aging and changes associated to socioeconomic development. These data evidence the need to improve the understanding of the mechanisms driving cancer genesis, progression, and metastasis formation to develop more efficient diagnostic methods and therapies.

The term cancer encompasses a large group of diseases characterized by an excessive and uncontrolled cell growth, and the potential of the cells to invade or spread to distant parts of the body. Carcinogenesis, the multistep process by which a cell ultimately becomes malignant due to the dysregulation of the multiple mechanisms that regulate normal cell proliferation and tissue homeostasis, begins when a phenotypically altered cell starts to grow out of control and forms an accumulation of cells called primary tumour. If this mass remains localized at the original site and is resectable, it is referred as a benign tumour. However, when it has the potential to detach from the primary tumour and colonize other parts of the body to establish and form a secondary tumour (metastasis), it is considered a malignant tumour [3,4].

Although more than 100 distinct types and subtypes of human cancers can be differentiated depending on the tissue or organ affected, Hanahan and Weingberg described a set of ten essential functional capabilities and enabling characteristics acquired by human cells during malignant transformation that are shared by all types of cancer cells (Figure 1). Very recently, Hanahan has proposed four new parameters as new hallmarks of cancer, encouraging the research community to continue with the experimental investigation and conceptual discussion to better define the basis of cancer disease [5,6].
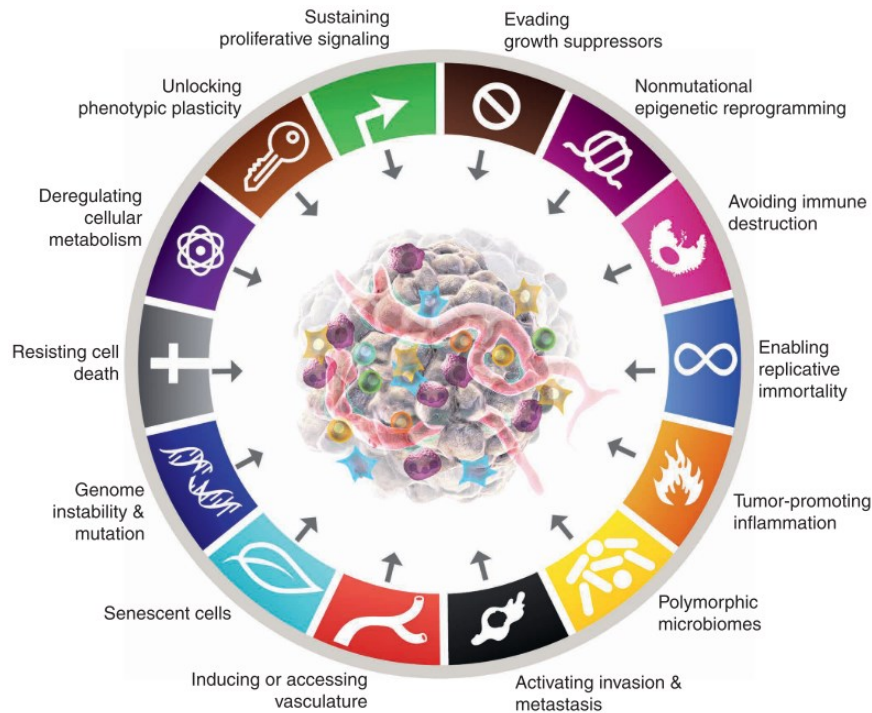
Figure 1. Hallmarks of Cancer. The fundamental characteristics that a cell acquires to become malignant are depicted in this figure, together with the two emerging hallmarks (unlocking phenotypic plasticity and senescent cells) and two enabling characteristics (nonmutational epigenetic reprogramming and polymorphic microbiomes) (extracted from Hanahan, 2022 [6]).

1.1 Stages of tumour progression

The process of tumour progression results from a complex molecular cascade of events, a large series of sequential and interrelated steps that disseminating tumour cells must complete to ultimately produce a metastasis [3,4,7,8]. In addition to the intrinsic properties of tumour cells, their interaction with extra-tumour factors, the action of stochastic factors, and epigenetic changes dictate the outcome of this process that can be summarized as follows:

a) The initiation of tumorigenesis normally results from the summation of oncogenes and inactivated tumour-supressor genes, genes that normally control the cell cycle or deoxyribonucleic acid (DNA) repair genes [9], which are responsible for the various

pathologic features characteristic of cancer, leading to a progressive growth of neoplastic cells and the formation of a benign tumour mass, with nutrients initially supplied by simple diffusion.

b) To exceed a diameter of 2mm, solid tumours must acquire new vasculature through the process of tumour **angiogenesis** [10–12], a process in which the synthesis and secretion of proangiogenic factors are of key importance. At this point, hypoxia represents a strong selective pressure and activates proangiogenic genes, anaerobic metabolism, cell survival, and invasion [13–15].

c) Specific cells escape from the primary tumour mass and migrate through the surrounding tissue starting a local **invasion**, a step that requires the ability of cells to detach from one another, and from the extracellular matrix (ECM), the remodelling of cell-surface adhesion receptors and ligands, and the degradation of ECM components by the secretion of proteolytic enzymes and glycosidases [16].

d) Tumour dissemination occurs via the **intravasation** of tumour cells into fine capillaries or lymphatic channels within the tumour, which represent a low resistance entrance pathway to vasculature and lymphatic system. Inside the blood vessels, the vast majority of circulating cells are rapidly destroyed but few of them are able to aggregate with host lymphocytes and platelets [17], which facilitate their survival by protecting them from hemodynamic shear forces and immune-mediated killing [18].

e) Surviving cells might arrest in the capillary beds of distant organs and enter in the small vessels by mimicking the homing of leucocytes [19,20], with the final aim to proliferate within the vessels or **extravasate** into the target organ site.

f) Proliferation and establishment of a **secondary tumour** in a new organ completes the metastatic process. The development of a new vascular network (angiogenesis) and the evasion of host immune system by the micrometastasis are required to maintain tumour growth. Finally, the metastatic cells can invade, penetrate to blood vessels, and enter again into circulation to extravasate and form additional **metastases**.

The outcome of the metastatic process is limited by the compliance of each of the sequential steps by metastatic cells, being the post-extravasation cell growth a major limiting step [21]. However, it also depends on multiple and complex interactions of the tumour cells with host homeostatic mechanisms, and specifically with the properties of the receptive tissue or organ, as postulated at the Paget's "seed and soil" theory [22]. In addition, the enriched tumour

microenvironment (TME) and the interaction of tumour cells with the host cells plays a critical role in the promotion of tumour growth, invasion, and metastasis [8,23].

1.2 Pancreatic ductal adenocarcinoma (PDA)

The **pancreas** is a glandular organ in the digestive and endocrine system, located in the abdominal cavity, behind the stomach. It is a retroperitoneal organ that can be divided histologically and functionally in two distinct components:, the **endocrine pancreas**, which is in charge of glucose metabolism, including the production of insulin, glucagon, somatostatin, and other important hormones; and, the **exocrine pancreas**, which facilitates food digestion and nutrient absorption in the small intestine via the secretion of pancreatic juice that contains digestive enzymes. The exocrine pancreas (95% of the pancreatic mass) is composed of acinar cells, structurally organized in functional units termed acini, which are responsible for the production and secretion of digestive enzymes and for their draining to the tubular network of ducts, formed by ductal cells, which secrete bicarbonate and mucins (MUC), and channel the pancreatic secretions to the duodenum to facilitate the digestive process [24].

Pancreatic ductal adenocarcinoma (PDA) is the most common neoplasia of the exocrine pancreas, accounting for more than 90% of all pancreatic malignancies [25]. Although the incidence of PDA is very low (around 3% of all new cancer cases per year), it represents the seventh leading cause of cancer-related mortality worldwide, with an overall 5-year survival rate of 11% in the United States (U.S.) [2]. Contrarily to most cancer types, and despite the efforts and achievements in PDA research, death rates are constantly rising. Projections indicate a more than two-fold increase in the number of cases by 2030, pushing PDA to the second cause of cancer-related deaths in the European countries as well as in the U.S [1,26,27]. PDA is associated with a dismal prognosis for several reasons: it is usually diagnosed at advanced stages due to the absence of symptoms or lack of specific ones, and due to its aggressive nature, with metastasis occurring in early stages [28]. In addition, it is characterised by resistance to existing therapies, including chemotherapy, radiotherapy, and molecular targeted therapy, being surgical resection the only treatment that increases the 5-year survival rate (15-20% approximately), although only 10-20% of all the patients have potentially resectable tumours [25]. Finally, the early onset of multiple genetic and epigenetic alterations, and the dense and complex TME also contribute to the discouraging prognosis. Considering all these data, global PDA research community, supported by several health-care organisations, have recognised that there is an urgent need to find reliable tumour markers

for an early detection and effective therapies in order to, at least, revert the negative tendency of the disease [29].

This malignancy is associated with several risk factors, including smoking, type 2 diabetes mellitus, and chronic pancreatitis that account for nearly 30% of all cases. Advanced age is another relevant risk factor [30], as most of cases are diagnosed between 60 and 80 years of age [31,32]. There is also a positive correlation between PDA and other risk factors such as male sex (with an incidence nearly 50% higher in men than in women) [31], obesity, cystic lesions of the pancreas, non-0 blood group, and diverse viral infections (e.g. *Helicobacter pylori*, hepatitis B, and C viruses) [33,34]. Moreover, about 10% of pancreatic cancer patients have a family history of the disease, which significantly increases their risk of developing the disease due to an inherited genetic predisposition. Other well-defined hereditary syndromes caused by germline mutations, such as familial atypical mole-multiple melanoma (FAMMM) syndrome (*CDKN2A*), Lynch syndrome (the mismatch repair genes), Li-Fraumeni syndrome (*TP53*), hereditary breast-ovarian cancer syndrome (*BRCA2*) among others, have been associated with PDA [32,35].

1.2.1 PDA progression model and precursor lesions

PDA arises from a series of non-invasive precursor lesions that as a consequence of genetic alterations, define the multi-step progression model of pancreatic carcinogenesis, initiated by acinar-to-ductal metaplasia (acinar cells trans-differentiation to a more ductal-like phenotype) [36,37], followed by pancreatic intraepithelial neoplasia (PanIN), dysplasia, *in situ* carcinoma, and eventually invasive carcinoma (Figure 2) [30,38,39].

PanINs are the most common precursor lesions to invasive PDA[40] and refer to microscopic lesions (<5mm diameter) that affect the smaller pancreatic ducts and are not directly visible by pancreatic imaging [41,42]. PanINs present a spectrum of morphological alterations and are characterised by varying amounts of mucins [43]. Considering the graded stages of dysplastic growth and cytonuclear atypia, PanINs are classified in two categories [44]. The low-grade (PanIN-1) lesions present hyperplasia but not dysplasia, with a flat (PanIN-1A) or papillary (PanIN-1B) mucinous epithelium, and low cytonuclear atypia. High-grade lesions include PanIN-2, which show increasing cellular atypia and a slight loss of nuclear polarity; and PanIN-3 lesions, advanced lesions also referred as high-grade dysplasia, *in situ* carcinoma or intraductal carcinoma, which exhibit severe nuclear atypia, luminal necrosis but are still restricted within the basement membrane. Importantly, in the last two decades several studies have challenged this linear and progressive model of PDA tumorigenesis proposing

alternative models [45,46], such as a direct progression from normal ductal epithelium to PanIN-2 state [44] or the presence of ductal complexes as intermediate states [47], although further investigations are required. In addition to the microscopic PanIN lesions, pancreatic cancers can also evolve from macroscopic precursor lesions, such as intraductal papillary mucinous neoplasms (IPMNs), and mucinous cystic neoplasms (MCN) [48–50].
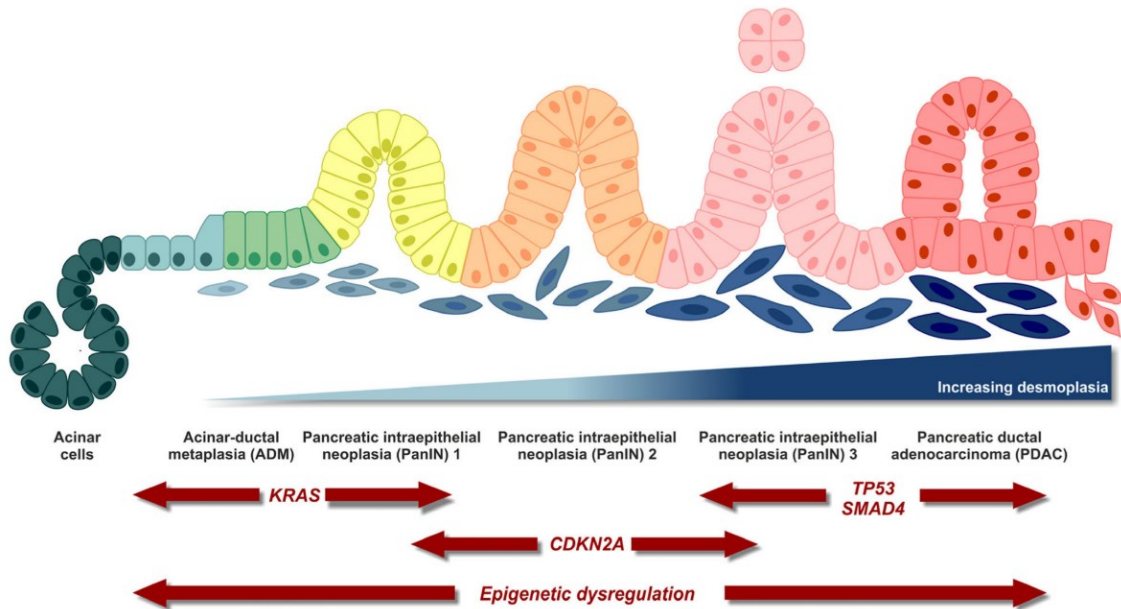
Figure 2. Precursor lesions of PDA: PanINs. Normal acinar cells progress to infiltrating PDA (left to right) through a histologically defined precursor lesions (PanINs), accompanied by genetic and epigenetic alterations (in red arrows) and increasing desmoplasia (Extracted from Orth, 2019 [28]).

The accumulation of multiple genetic alterations leads to PDA transformation preceding invasive adenocarcinoma, and the most frequent is mutational activation of the Kristen Rat Sarcoma virus (*KRAS*) oncogene, inactivation of tumour-suppressor genes including *CDKN2A*, *TP53*, and *SMAD4*, widespread chromosomal losses, gene amplifications [51], and telomere shortening [52]. **KRAS** mutations are detected in nearly all PDA cases (95%)[46], and is usually the first identified alteration in PDA [53], even found, although at low frequency, in low-grade PanIN lesions [54]. Thus, it is accepted as a driver mutation of the disease. Mutations in *KRAS* (not only its presence, but also its frequency [53]) play a critical role in early tumorigenesis as well as in metastasis as they dysregulate the GTPase activity, leading to uncontrolled cellular proliferation, angiogenesis, suppression of apoptosis, and evasion of immune system [55,56]. Inactivation of the tumour suppressor gene **CDKN2A**, present in 70-90% of PDAs [57,58], disrupts retinoblastoma (Rb) and p53 pathways (loss of function of *INK4A/p16* and *ARF/p14*, respectively), leading to uncontrolled cell-cycle progression and resulting in enhanced proliferation [59]. Inactivation of **TP53** gene, which encodes p53 DNA-binding protein, is detected in 50-70% of tumours but usually at high-grade PanIN lesions

and leads to deregulation of programmed cell death, leading to the survival and proliferation of tumour cells, and favouring angiogenesis [60]. Finally, the inactivation of **SMAD4** gene occurs in nearly 50% of PDAs at late stages and enhances cancer promotion by inhibiting the transforming growth factor (TGF) pathway [61], being considered a marker of complex PDA as it is associated with distant metastasis, and with worse overall survival (25,26).

In addition to these well-known altered genes, there are numerous genetic alterations at lower frequencies (with a prevalence of approximately 10%) [62], which include oncogenes and DNA repair genes such as *BRCA1, BRCA2, RPA1, ATM* [55,63], *BRAF, MYB, AKT2, EGFR, FHIT,* and *STK11*; and mutations in tumour-suppressor genes such as *MAP2K4, STK11, TGFBR1, TGFBR2, ACVR1B, ACVR2A, FBXW7,* and *EP300* [42,51]. Recently, whole genome analysis and genomic characterization studies of PDA [52,64] have revealed new insights into the complex molecular landscape of PDA and identified important modifications of known and novel candidate genes in PDA, as well as the main cluster of signalling pathways and processes that are genetically altered in a high percentage of PDA cases, such as TGF-β, Wnt/Notch, and Hedgehog [51]. Epigenetic dysregulation has also been described to contribute to PDA initiation and progression, including alterations in DNA methylation and histone modification and non-coding RNAs [42,62]. Moreover, overexpression of microRNAs (miR) in pancreatic cancer, such as miR-21, miR-34, miR-155, and miR-200, is thought to contribute to PDA progression, and considering that they are detectable in plasma, they could be useful diagnostic markers [65–67].

In conclusion, all the major genetic changes in invasive PDA are already present in pre-neoplastic lesions but its progression also corresponds to the increasing accumulation of genetic and epigenetic alterations, and the activation of a coordinated transcriptomal program [44]. Importantly, interactions between the neoplastic cells and the TME are of special relevance in PDA due to its high desmoplastic component and play a key role in tumour initiation, progression, and metastasis.

1.2.2 Role of tumour microenvironment in PDA

PDA's TME is characterised by a particularly high desmoplastic stroma, which can constitute up to 90% of the tumour volume [68,69]. Accumulating evidence has suggested that non-tumour cells composing the TME influence tumour proliferation, metabolism, cell death, therapeutic resistance, and immune profile (Figure 3) [28,70,71]. In addition, it is considered a source of therapeutic targets and novel biomarkers [72].

PDA stroma is formed by the accumulation of an altered ECM composed by non-cellular components and diverse cell types including fibroblasts, stellate cells, immune, and inflammatory cells (both lymphoid and myeloid cells)[73], neuronal cells and cells of the vasculature (endothelial cells and pericytes)[70,71,74]. The main cellular component of the TME are the cancer-associated fibroblasts (CAFs), either with myofibroblastic or inflammatory phenotypes [75], which are mainly derived from pancreatic stellate cells [74,76,77] that upon activation (by e.g. chronic inflammation, environmental factors such as reactive oxygen species or secretory molecules) start generating high amounts of ECM. During tumorigenesis and PDA progression there is a sustained crosstalk between tumour cells and stromal cells [76,78]. Cancer cells can secrete growth factors (e.g.VEGF, PDGF, EGF, and TGF-β) [79] and proteolytic enzymes to form a pro-tumour surrounding stroma, and activated CAFs secrete growth factors and cytokines (TGF- β, Interleukin (IL)-6, and IL-8 among others)[28,80] , and upregulate the expression of serine proteases and matrix metalloproteinases (MMPs) that promote tumour cell proliferation, survival, migration, invasion, and angiogenesis [81]. Accumulating evidence suggest that PDA stroma is altered to form an immunosuppressive niche and to support tumour progression. Hypoxia and desmoplasia, two interlinked key factors in PDA [82,83], represent barriers to T cell infiltration although they are associated to an accumulation of myeloid cells [73,84], as M2-like macrophages and myeloid-derived supressor cells (MDSCs), which are potent suppressors of T cell function [85]. Besides, the presence of immunosuppressive T and B subpopulations (regulatory T cells, γδ T cells, and regulatory B cells) in the TME help blocking the activation and the infiltration of effector T cells, supporting tumour immune-system evasion [86,87].
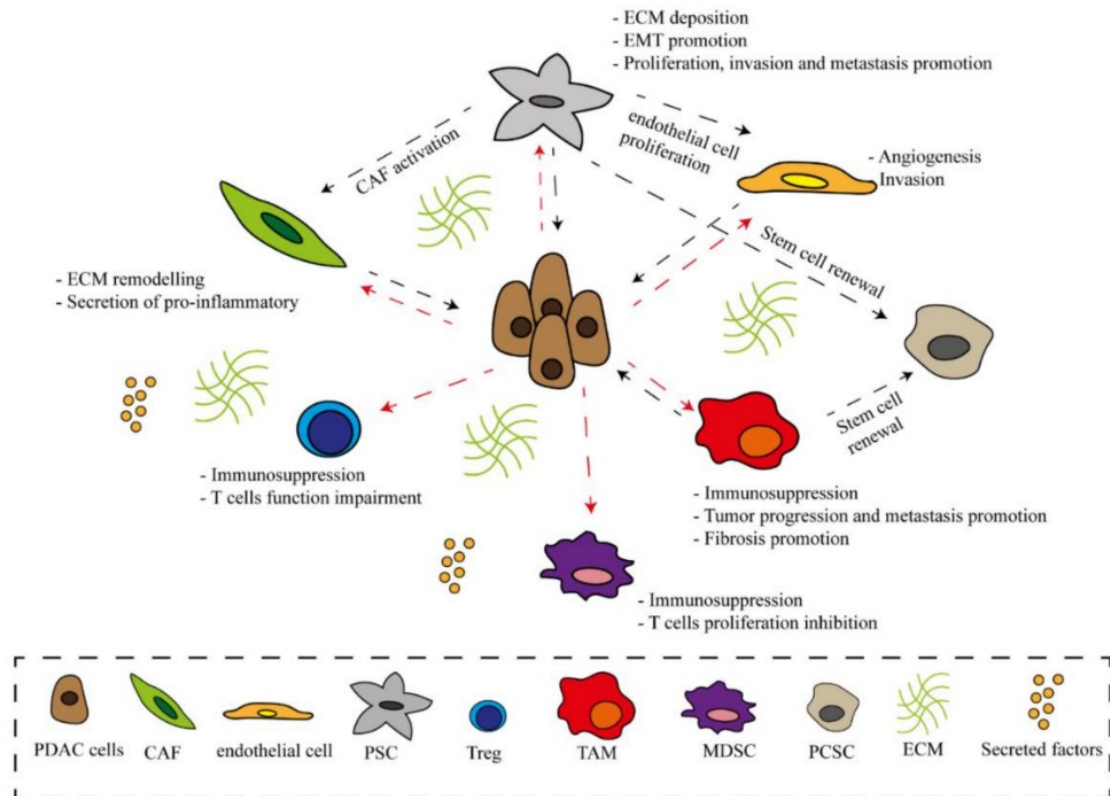
Figure 3. PDA interaction with TME. Cross talk between tumour cells and non-tumour cells in PDA microenvironment. Red arrows indicate inhibition and black arrows promotion or positive effect (extracted from Cortesi, 2021 [71]).

The acellular component of the stroma is mainly represented by ECM, a three-dimensional network composed by fibrillar collagens, fibronectin, elastin, laminin, proteoglycans, and matricellular proteins [70], as well as cytokines, enzymes, and growth factors [28,71]. It is of key importance in PDA as it provides physical scaffolds, favours tumour progression processes such as growth and migration through a coherent signalling function [88], as well as a physical barrier to immune cell infiltration and to anti-tumour drug penetration [72]. Interestingly, the formation of desmoplasia, regulated by the expression of *focal adhesion kinase 1* (FAK1) by PDA cells, has been recently pharmacologically targeted and considered as a potential therapeutic target [89].

1.2.3 PDA diagnosis, biomarkers and treatment

Unfortunately, despite the increasing research focused on improving PDA diagnosis, the vast majority of PDA patients are still diagnosed at late stages, when only 10-20% of patients have potentially resectable tumours [25]. Surgery in combination with chemotherapy and radiotherapy is usually the only treatment option [90,91]. The first reason for the late diagnosis is that clinical manifestations of PDA are usually inexistent until late-stages and if present, they are not specific (jaundice, unexplained weight loss, digestive problems deriving to back-

pain, nausea, new-onset diabetes mellitus, etc) [92,93]. Secondly, the existing tumour biomarkers used for PDA detection are still not completely reliable, and therefore, the discovery of novel ones with increased sensitivity and specificity would be of great importance. After the physical examination of the patient, imaging techniques are the currently used diagnostic tools, including multiple detector computed tomography (MDCT) [93,94] for initial stages of PDA and evaluation of the involvement of adjacent organs; dual or multi-phase dynamic contrast to analyse the vascular system involved and pancreatic lesions [95], and magnetic resonance imaging (MRI) for high resolution imaging of pancreatic ducts and cysts, as well as liver metastasis [96]. Positron emission tomography (PET) is normally used for monitoring the response to treatment and to detect recurrence after resection, as it is more sensitive than computer tomography [97]. Moreover, endoscopic ultrasonography (EUS) is used in most cases to obtain a definitive diagnosis, as it provides excellent resolution of the pancreas, and the vascular and lymphatic system involved, as well as the possibility to obtain a tissue sample required for tumour classification [98–100].

Referring to tumour markers, serum carbohydrate antigen 19-9 (CA19-9) is the only biomarker approved by the Food and Drug Administration (FDA) for monitoring PDA disease [25,101,102]. It is a carbohydrate antigen named sLe^a that is present on cell surface molecules such as gangliosides and MUC, and its expression is frequently elevated in PDA patients. Although it is routinely used as a biomarker of PDA, it is not sensitive enough to be used for general screening of asymptomatic population [102] since it is also elevated in other pathologies such as pancreatitis, jaundice, hepatic, and pancreatic cysts, and other cancers as colorectal and breast. Nonetheless, recent findings indicate that CA19-9 is upregulated 2 years prior to PDA diagnosis suggesting that it could be used to detect the disease in an early state [103]. The combination of this biomarker with albumin or IGF has shown to increase the sensitivity and specificity of the diagnosis, allowing to discriminate between PDA and chronic pancreatitis [104]. Other protein-based biomarkers have been described, although its sensitivity and specificity remained lower than desired [105]. Similarly, the presence of cell-free circulating tumour DNA (ctDNA) or circulating tumour cells (CTC) have been explored as novel non-protein biomarkers [106–110], since higher levels ctDNA encoding mutant *KRAS* and other frequently mutated genes in PDA such as *TP53* have been detected in early and late stages of PDA, rather than in benign pathologies or healthy patients [106,107,111]. Other approaches include the detection of systemic metabolic alterations [112], the analysis of circulating exosomes, including the presence of heparin sulphate on its outer layer [113], or the detection of miRNA [114], and the evaluation of plasma miRNA signatures [115].

On the basis that glycosylation is commonly altered during tumour progression, and glycan aberration increases progressively with malignant transformation, glycan alterations have been considered as putative reliable predictive biomarkers [116]. In the last decades, numerous glycoproteomic studies have focused on the analysis of aberrant glycosylation profiles of diverse glycoproteins involved in PDA progression with the aim to find an effective PDA biomarker [117–121] or future therapeutic targets (altered glycosylation as novel biomarker in cancer will be addressed at section 3.1).

Therapy for patients with PDA is still a challenge for the cancer research community since the majority of the patients are diagnosed in an advanced and unresectable stage of the disease, when chemotherapy alone or in combination with other treatments is the only option, although its effectivity is low [122]. Historically, very few effective drugs have been discovered for PDA treatment, mainly due to the high desmoplasia that impedes drug delivery, and to the high treatment resistance, which is associated with the activating mutation of *KRAS*, present in nearly all PDA cases, and other factors [91]. Currently, the most common treatments of PDA patients are surgery, chemotherapy (including neoadjuvant and adjuvant ones), radiation, and palliative care [31,123], and they are applied depending on the tumour stage and the patient's health status (Table 1)[123]. Until date, the most used chemotherapeutic agent is gemcitabine (approved for the U.S. FDA in 1997), a nucleoside analogue that moderately improves patient's survival rate and quality of life [124]. At present, gemcitabine is used in combination with other drugs to increase its efficacy. For instance, it can be used in combination with Erlotinib [125], a tyrosine kinase inhibitor (TKI) of Epidermal Growth Factor Receptor (EGFR)[126] for locally advanced, inoperable, or metastatic pancreatic cancer; it can also be administered with FOLFIRINOX (a combination of folinic acid (leucovorin), 5-fluorouracil, irinotecan, and oxaliplatin), although it generates severe toxicity and it is only recommended for patients with good performance status. The combination of gemcitabine with albumin-bound paclitaxel was introduced 10 years ago [127], with slightly softer side effects but improved efficacy, and finally, the combination of liposomal irinotecan with 5-fluoracil and leucovorin following first-line therapy with gemcitabine has also been approved by the FDA [128].

Table 1. Stage dependent treatment recommendations for pancreatic cancer. (Information extracted from Kleef, 2016 [25]).

Disease stage	Treatment recommendations
Resectable disease	• Upfront surgery followed by adjuvant therapy (gemcitabine or 5-fluorouracil)*
Borderline resectable disease	• Neoadjuvant chemotherapy with FOLFIRINOX or gemcitabine plus albumin-bound paclitaxel with or without chemoradiation followed by surgery • Upfront surgery followed by adjuvant therapy as above
Locally advanced disease	• Chemotherapy as for metastatic disease (see below) • Chemoradiation is not indicated after gemcitabine monotherapy, but is often used after combination chemotherapy as above (followed by surgery in highly selected cases)
Metastatic disease (first line)	• FOLFIRINOX (for patients with an ECOG performance status of 0-1)* • Gemcitabine plus albumin-bound paclitaxel (for patients with an ECOG performance status of 0-2)* • Gemcitabine monotherapy or best supportive care (for patients with an ECOG performance status of >2) • Radiotherapy can be used in selected circumstances for palliation of pain and the prevention of pathological fractures
Metastatic disease (second line)	• Following gemcitabine-based first-line therapy, 5-fluorouracil-based chemotherapy (5-fluorouracil and oxaliplatin or 5-fluorouracil and liposomal irinotecan)* • Following 5-fluorouracil-based first-line therapy, gemcitabine monotherapy or gemcitabine plus alumbin-bound paclitaxel • Radiotherapy can be used in selected circumstances for palliation of pain and the prevention of pathological fractures

ECOG, Eastern Cooperative Oncology Group; FOLFIRINOX, folinic acid (leucovorin), 5-fluorouracil, irinotecan and oxaliplatin. *Supported by data from randomized controlled trials.

In addition to the mentioned systemic therapies, the discovery of biologically targeted therapies and immunotherapies with higher specificity for PDA are of prominent importance. In this regard, diverse preclinical studies have focused on downstream effectors of the four major driver genes in PDA (*KRAS*, *CDKN2*, *TP53*, and *SMAD4*). For instance, targeting EGFR with cetuximab in addition to gemcitabine-based chemotherapy was evaluated in a phase III trial, although there was no significant improvement in clinical outcome probably due to the compensation mechanism exerted by integrin β1 [129,130]. The ErbB family inhibitor afatinib in combination with gemcitabine was evaluated in a phase II trial as first-line treatment for metastatic PDA, but the results were not favourable [131]. In addition, blocking other important pathways in PDA such as *mammalian target of rapamycin (mTOR)* [132–134] or targeting angiogenesis process [135] have been evaluated in several studies with discouraging results. Besides, the strategy of targeting epigenetic alterations in PDA, in conjunction with chemotherapy or with alternative therapeutic agents is being evaluated [136]. Altogether, despite all the preclinical efforts, no successful therapeutic strategy has been established so far.

Referring to immunotherapy, the number of preclinical trials for PDA is rapidly growing and, considering that it has already been implemented in some solid tumours, it has been accepted as an emerging option for the treatment of patients with PDA. Principally, trials have used passive products of the immune system (peptide vaccines and antibodies) in combination with chemotherapy (mainly gemcitabine). Therapeutic antibodies targeting immune checkpoints as *cytotoxic T-lymphocyte-associated protein 4* (CTLA-4) and *programmed cell death protein 1* (PD-1) axis were previously tested in melanoma and lung cancer showing promising results [137,138], however, in trials carried out with PDA patients, only 2% showed clinical benefits [139,140]. Several types of vaccines have been developed and tested including antigen, peptide, whole tumour, vector and dendritic cell vaccines (accurately reviewed by Rangelova and Kaipe [141]), as well as few adoptive transfer therapy trails [142,143]. Interestingly, preclinical studies demonstrated that the tumour-specific antigens CEA, mesothelin (MSLN), and MUC1, which are overexpressed in PDA, are promising determinants for chimeric antigen receptor (CAR) T cell therapy [144,145]. Overall, the clinical effectiveness of the clinical trials performed up to date is still limited, although the immunological effects observed in almost all trials show that immunotherapy is a feasible therapeutic option for PDA.

2. EGFR

The Epidermal Growth Factor Receptor (**EGFR**) is a transmembrane (TM) glycoprotein that belongs to the ErbB family of receptor tyrosine kinases (RTKs) and, in physiological conditions, exerts critical functions in the regulation of epithelial tissue development and homeostasis [146]. The ErbB family involves four distinct members with common structural elements, including EGFR (HER1/ErbB1), ErbB2 (HER2/Neu), ErbB3 (HER3), and ErbB4 (HER4) [147,148].

The human EGFR is encoded on the chromosome 7 short arm q22 and it is synthetized as a precursor of 1210 amino acid residues, which is then cleaved at the N-terminal to form the mature 1186 residue EGFR. Structurally, it consists of **i)** an extracellular, highly variable, cysteine rich N-terminal region, **ii)** a hydrophobic TM domain, and **iii)** an intracellular, highly conserved, C-terminal tail domain with tyrosine kinase activity (Figure 4). The extracellular region is subdivided into four domains, organised as tandem repeats of two types of domains. Domain I (L1) and III (L2) are leucine rich fragments involved in ligand binding, while domain II (CR1) and IV (CR2) are cysteine rich fragments involved in receptor dimerization. In particular, domain II contains the dimerization arm to form homo- or heterodimers with

other members of the ErbB family, and domain IV forms disulphide bonds to domain II, and links to the TM domain. The EGFR is anchored to the membrane by a single pass structure of the TM domain [149], which has also been suggested to be involved in receptor dimerization [150,151]. Finally, the intracellular domain can be subdivided in three regions: a flexible juxtamembrane segment; a tyrosine kinase domain (TKD) constituted by an N-lobe (principally a β-sheet structure), a C-lobe (a mainly α-helical structure), with an adenosine 5' triphosphate (ATP)-binding site located between them [152]; and a tyrosine rich C-terminal tail [153].
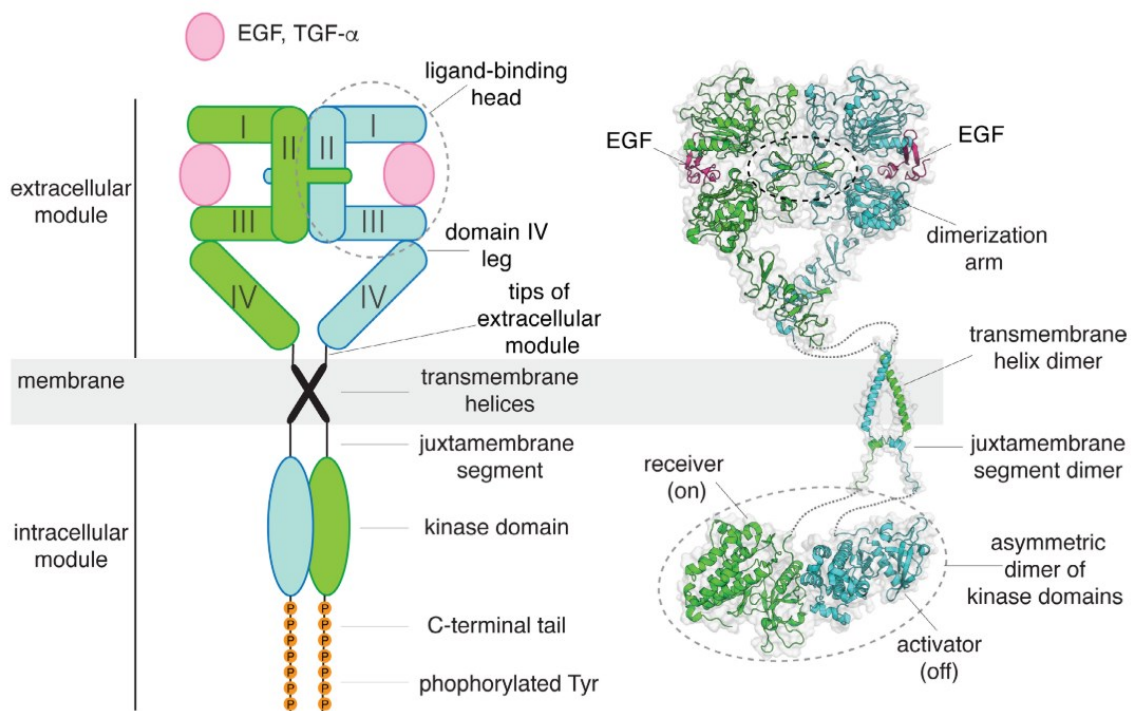
Figure 4. Structural representation of a ligand-bound EGFR dimer. Left, a schematic diagram of ligand-bound EGFR dimer. Right, crystal structures of EGFR fragments (extracellular dimeric domain bound to EGF, TM helix dimer, and intracellular asymmetric dimer of kinase domains (figure extracted from Huang, 2021[154]).

2.1 ErbB ligands

ErbB family of receptors can be activated by at least eleven different ligands in humans, all of which contain an EGF-like domain responsible for receptor binding and activation. Ligands are synthesised as TM precursors that undergo extracellular domain cleavage to release soluble ligands [155]. Ligands can be classified in three groups [156,157]. First, the group of ligands that exclusively bind to EGFR include EGF, TGF-α, amphiregulin (AREG), and epigen (EGN); a second group of ligands that bind both EGFR and ErbB4, which includes betacellulin (BTC), heparin-binding EGF-like growth factor (HB-EGF), and epiregulin (EPR); and the third group of ligands that consists of all the neuregulins (NRG1-NRG4), of

which NRG1 and NRG2 bind to ErbB3 and ErbB4, whereas NRG3 and NRG4 only bind to ErbB4 [157]. To date, no soluble ligand has been described for ErbB2 [157].

EGFR ligands have been shown to induce different cellular responses and intracellular trafficking of the receptor [158], resulting in a ligand functional selectivity, although they can auto- or cross-induce one another [159]. In that sense, each of the seven EGFR ligands has been described to be involved in diverse physiological processes, both in normal and disease states [160–166]. For instance, TGF-α increases proliferation through activation of EGFR downstream signalling and also induces mucous production and inhibition of gastric acid secretions [165]; and BTC is involved in the differentiation of pancreatic-β cells, as well as in reproductive processes and the control of neural stem cells [166]. Interestingly, a comparative study described an increased preference of EGF and TGF-α ligands for the formation of EGFR:ErbB2 heterodimers compared to EGFR:EGFR, whereas BTC and AREG showed a similar preference to induce both types of dimers [167]. Nonetheless, in this work we will focus on the EGF ligand, one of the main human EGFR activators, together with TGF-α.

2.2 EGF ligand

Human EGF is a 6kDa protein made up of 53 amino acids. It consists of a T-knot three-dimensional structure [168], stabilized by three intramolecular disulphide bonds formed between cysteines (with a conserved sequence pattern) that are basic to maintain its biological activities [169]. The three paired cysteines interact with the three contact sites between EGF and EGFR, the first located at domain I of EGFR, the second and the third at domain III, mainly by hydrophobic interactions of the residues involved, as well as by hydrogen bonds and Van der Waals contacts [168]. Physiologically, human EGF has been detected in a variety of body fluids and the innate concentration is regulated by diverse organs (not systemically) [170], ranging from high concentrations (50-500 ng/mL), as in bile, urine, or milk, to medium concentrations (5-50 ng/mL), as in tears or sperm, and to low concentrations (1-2 ng/mL) as in plasma or saliva [170]. Functionally, EGF binds to EGFR, activates its dimerization and intrinsic tyrosine kinase activity, initiating downstream signalling pathways that control cell proliferation, differentiation, survival, and motility (detailed at section 2.2.2) [171,172]

2.3 Ligand-induced dimerization and activation of EGFR

EGFR is expressed in almost all human cell types at levels ranging from 40000 to 100000 receptors per cell, while in cancer cells an overexpression of more than 10^6 receptors per cell is observed [171]. Ligand binding induces important conformational rearrangements in the

extracellular region of the receptor allowing its homo- or heterodimerization with other ErbB family members, the activation of its intracellular TKD and the trans-autophosphorylation of critical residues of the C-terminal tail, finally triggering the downstream signalling cascade. In a physiological state, EGFR is involved in the activation of genes responsible for cell proliferation, survival, and differentiation [146,173], although emerging roles of EGFR have been identified, such as in the regulation of autophagy and metabolism [174]. EGFR also plays a key role in wound healing and epithelial regeneration of diverse organs such as gastrointestinal, respiratory, skin, and corneal epithelia [175,176]. In addition, during embryogenesis, EGFR regulates morphogenesis of organs like teeth, brain, reproductive and gastrointestinal tracts, and cardiovascular system [177].

2.3.1 Dimerization

In the absence of bound ligand, the extracellular regions of EGFR form the closed, "tethered" structure, associated with its inactive state, in which the intramolecular interactions of domain II and domain IV maintain the domain II dimerization arm in an inaccessible position [178]. Upon ligand binding, domain I and III change their conformation to form the extended, "untethered" conformation of the receptor, breaking the domain II/IV tether and exposing the dimerization site (Figure 5) [179]. The formation of the dimerization interface with a homologous domain II is followed by reorganizations in the TM domain and juxtamembrane segment, which form interactions with the kinase domain and contribute to stabilize the EGFR dimer [180]. In contrast to the vast majority of RTKs, ligand binding to EGFR does not make a direct contribution to the dimerization interface, each EGFR monomer binds a ligand, and the receptors interact through domain II to form the dimers interface [171]. After the dimerization of the extracellular regions, the intracellular part of the receptors forms an asymmetric dimer that leads to kinase activation [181], in which the carboxy lobe of the "activator" TKD allosterically activates the amino lobe of the "receiver" TKD by inducing several conformational changes, and once activated it trans-phosphorylates tyrosines in the tail of the activator [181].
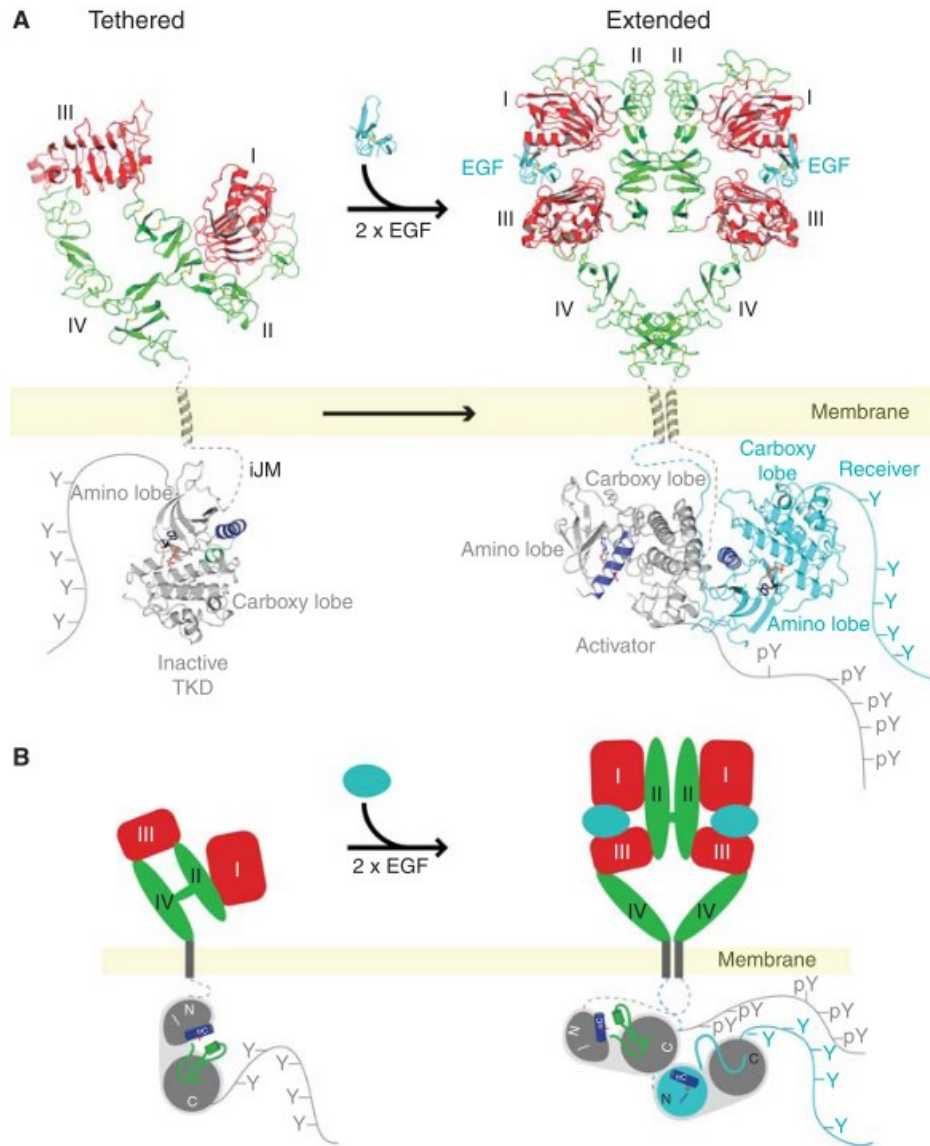
Figure 5. Model for EGF-induced dimerization and activation of EGFR. In the absence of bound ligand, the EGFR is largely monomeric, the extracellular region is maintained in a tethered position, and the TKD is inactive. Upon ligand binding, the receptor experiments a dramatic conformational change that "extends" the extracellular region, which dimerizes and induces intracellular TKD activation. In the asymmetric intracellular dimer, the "activator" TKD is represented in grey and the "receiver" kinase in cyan (figure extracted from Lemmon, 2014 [179]).

2.3.2 Activation of EGFR signalling pathways

The activation of EGFR by ligand binding induces the trans-autophosphorylation of tyrosine residues on the intracellular C-terminal tail, triggering the downstream signalling pathways. Each ligand induces the phosphorylation of a particular set of tyrosines, which act as docking sites for adaptor proteins and activate specific signalling pathways, accounting for the differences in ligand intrinsic activity. The main signalling pathways activated by EGFR are ERK MAPK, PI3K-AKT, SRC, PLC-γ1-PKC, JNK, and JAK-STAT, all of which are inter-

linked and stimulate a vast number of processes such as cell proliferation, growth, differentiation, migration, and inhibition of apoptosis. The phosphorylated tyrosine residues on EGFR include Y703, Y920, Y992, Y1045, Y1068, Y1086, Y1148, and Y1173, and also other tyrosine or serine, and threonine residues such as Y845, Y1101, T654, S971, or S1046/S1047 (Figure 6), that are phosphorylated later by other kinases (e.g. c-SRC, PKC, CaM kinase II). These phosphorylated residues serve as docking sites for the signal-transducing molecules containing phospho-tyrosine-binding residues, such as those with Src homology 2 (SH2) and phosphotyrosine binding (PTB) domains [182], which then stimulate the coupling of a large number of signalling effectors. For example, pY1173 binds to SHC (Src homology collagen), Grb2 (growth factor receptor binding protein 2), PLC-γ1, and SHP1; pY1068, pY1086, pY1148, and p1173 all bind to Grb2, activating ERK MAPK and PI3K-AKT signalling pathways [183], while pY1045 [184] and pS1046/47 [185,186] are involved in several negative regulatory loops in the EGF-stimulated EGFR, such as receptor internalization/downregulation and desensitization of the kinase domain.
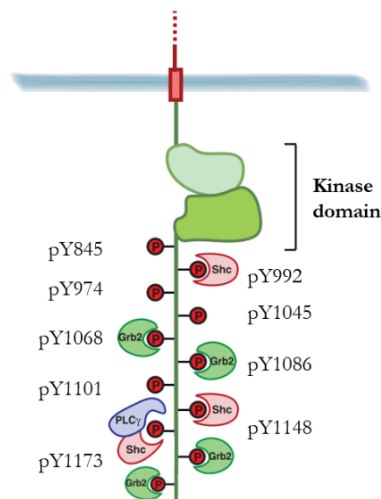
Figure 6. Important phosphorylation sites in the C-terminal region of EGFR and their interactions with signalling effectors. EGFR tyrosine residues that can potentially be phosphorylated and interact with SH2 or PTB domain containing-proteins to activate downstream signalling pathways. Some of the binding proteins and effectors are represented, although many others are involved: Shc (Src homology collagen), Grb2 (growth factor receptor binding protein 2), PLCγ (phospholipase C γ) (adapted from Conte and Sigismund, 2016 [170]).

The RAS-RAF-MEK-ERK MAPK pathway is the most important pathway downstream of EGF-induced EGFR activation, in which ERK MAPK initiate diverse physiological and pathological responses, including growth, proliferation, differentiation, migration, and inhibition of apoptosis [187]. In brief, Grb2 directly binds to the phosphorylated Y1068 and Y1086 residues, and SHC can be recruited by pY1148 and pY1173, leading to the recruitment

of Sos (a nucleotide exchange factor) to the plasma membrane to activate RAS. Activated RAS mediates RAF activation, by phosphorylating two important residues (S338 and Y341) that are relevant binding sites for MEK1/2. MEK1/2 binding allows its activation and the following activation of ERK1/2, which then catalyse the phosphorylation of multiple cytoplasmic and nuclear substrates including regulatory molecules and transcription factors to induce several biological responses.

PI3K-AKT is also one of the most important pathways activated upon EGFR activation, either by direct interaction with the p85α subunit of PI3K, by the interaction with the adaptor protein Grb2 or via activated RAS [188,189]. The PI3K-AKT-mTOR signalling pathway controls metabolism, proliferation, cell size, survival, and motility [183]. In short, PI3K binds to the receptor through its regulatory subunit (p85α), which binds to phospho-YXXM motifs (X indicates any amino acid) of the RTK, or can be activated by the binding of the adaptor protein GRB2, which binds preferentially to phospho-YXN motifs of the RTK. Grb2 binds to the scaffolding protein GAB, which in turn can bind to p85α [189]. Then, the PI3K catalytic domain (p110) phosphorylates the lipid phosphatidylinositol-4,5-biphosphate (PIP$_2$) to generate phosphatidylinositol-3,4,5-triphosphate (PIP$_3$), a potent secondary messenger that mediates PI3K activity. PIP$_3$ links PI3K to downstream effectors, including AKT, RHO, RAC, RAS, ARF, and GAB1/2 proteins. Once localized at the plasma membrane (PM), AKT is phosphorylated and mediate cell survival, by phosphorylating components of the cell death machinery (Bcl-2-associated death promoter (BAD), caspase-9 or FOXO1); mediating mTOR signalling cascade involved in the regulation of cell growth and autophagy; as well as cell metabolism and glycolysis in cancer [171].

The quality, amplitude and duration of the complex signalling network activated upon ligand binding to the EGFR are strictly regulated by several mechanisms including the compartmentalization and trafficking of the EGFR along the endocytic pathway (Figure 7). After the activation of EGFR at the PM, the first mechanism of regulation is EGFR internalization through multiple endocytic pathways, such as clathrin-mediated endocytosis (CME) and several nonclathrin endocytic pathways (NCE), which are active at different ligand concentrations and are cell type specific [158]. CME is active at low EGF concentrations and directs EGFR towards recycling instead of degradation, to maintain and prolong its signalling, and achieve a sustained proliferative response. Contrarily, NCE are only active at high EGF concentrations and are critical for long-term attenuation of EGFR signalling, since they direct EGFRs to lysosomal degradation (via EGFR ubiquitination) [190]. Furthermore, EGFR can be translocated to the nucleus, where it can regulate cell proliferation, tumour

progression, and DNA repair, by acting as a transcriptional co-activator [191–194]. In addition, other mechanisms have been described in nuclear translocation such as secondary phosphorylation [195], early loops involving miRNAs [196] and late mechanisms regulated by newly synthesized proteins and miRNAs [197].

2.4 EGFR and cancer

EGFR was one of the first identified oncogenes and has been described to contribute to several processes that are crucial for cancer onset and progression, including angiogenesis, metastasis, and apoptosis, in addition to its physiological role of promoting proliferation, growth, and cell survival [198]. It is activated in nearly all the solid neoplasms (e.g. lung, glioblastoma, head and neck, ovarian, breast, colorectal, prostate, and pancreatic) [199] either by gene mutation, amplification, or overexpression, although the EGFR aberration type, mutation frequency and distribution in functional domains differs among cancer types [200,201]. In many of the tumours, the number of EGFR receptors expressed by malignant cells can be up to 10-fold higher than in normal cells [171]. For instance, EGFR is overexpressed in between 30-50% of pancreatic tumours, 40-80% of non-small cell lung carcinomas (NSCLC) and 15-90% of breast tumours [199].

Diverse EGFR genetic alterations that are found in cancer induce a weakening of the negative-feedback mechanisms or an enhancement of positive regulation, prolonging the activation of EGFR signalling [197]. For example, the in-frame deletion of exons 2-7 of the extracellular domain of the receptor results in the most frequent EGFR mutant, the EGFR-variant III, which has been described to occur in diverse carcinomas such as glioblastoma, breast, ovarian, and lung cancers [202]. EGFRvIII is constitutively active due to the deletion of autoinhibitory residues, and because its abnormal conformation evades endocytic down-regulation, achieving a low intensity but prolonged signalling sufficient to enhance tumorigenicity [203]. Likewise, gene amplification or high polysomy, and small in frame deletions or mutations in the TKD have been found in human carcinomas [204], as well as many other genetic alterations summarised in Table 2.

Table 2. Genetic alterations of ErbB receptors in human carcinoma. Data extracted from Normanno, 2005 [204].

Receptor	Genetic alteration	Ligand dependence
EGFR	Gene amplification	+
	N-terminal truncation (EGFR vI)	-
	Deletion exons 14-15 (EGFRvII)	+
	Deletion exons 2-7 (EGFR vIII)	
	Deletion exons 25-27 (EGFR vIV)	+
	C-terminal truncation (EGFR vV)	+
	Tandem duplication exons 2-7	+
	Tandem duplication exons 18-25	-
	Tandem duplication exons 18-26	-
	Small in frame deletion or point mutations in the kinase domain (exons 18-21)	+

Furthermore, several alterations in the dimerization, intracellular trafficking of EGFR, protein turnover or in the regulatory loops are also responsible of dysfunctional EGFR regulation (Figure 7) [205,206]. Nuclear EGFR (nEGFR) localization in cancer cells promotes survival by acting as nuclear kinase or co-transcriptional activator and has been associated with poor overall survival in breast and NSCLC patients [207–211]. Another deregulation in EGFR trafficking is the secretion of EGFR inside small extracellular vesicles (sEVs) outside the tumour cells, which contribute to immune evasion, pre-metastatic niche preparation, angiogenesis, cancer cell stemness, and horizontal oncogene transfer [212]. Finally, EGFR signalling regulation can also be affected by the deficiency of one of its negative regulators, such as the E3 ubiquitin ligase CBL, ImmunoGlobulin-like domains 1 (LRIG1), Mitogen-Inducible Gene 6 (Mig6), Mucin 15 (Muc15) among others [213–216].
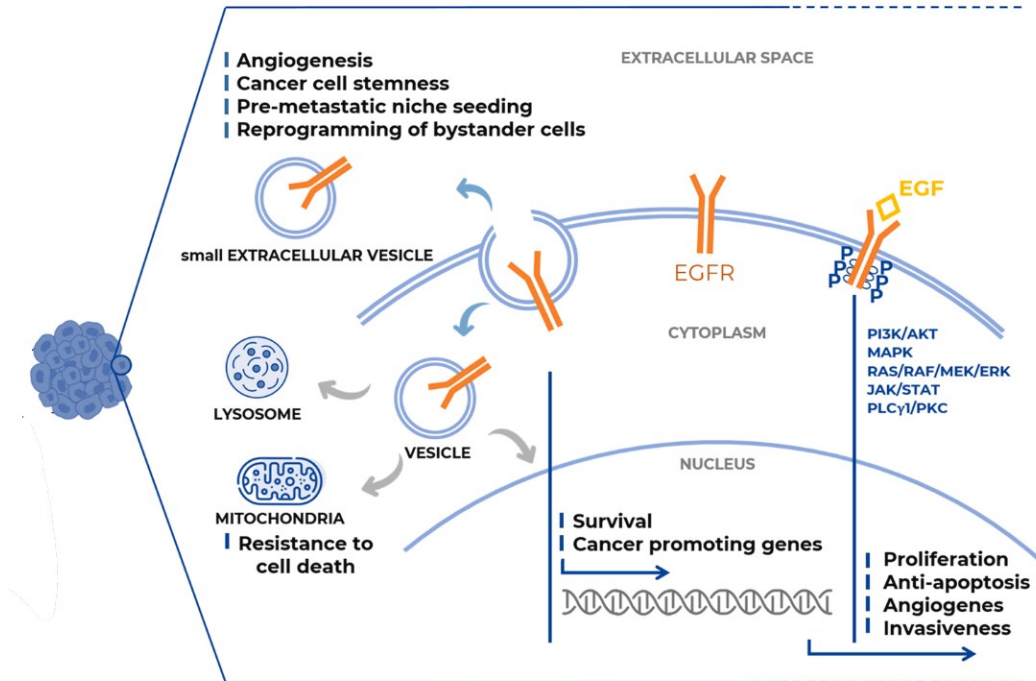
Figure 7.Schematic representation of EGFR trafficking (extracted and modified from Levantini, 2022 [202]).

2.5 EGFR targeted therapies

The critical role of EGFR in the cell signalling pathways makes it a primary target in cancer therapy. Inhibitors of this receptor have been among the most successful examples of targeted cancer therapies to date [217]. The anti-EGFR therapies can be subdivided into two important pharmacological approaches: monoclonal antibodies (**mAbs**) and small-molecule **TKIs**. The artificially-synthesized EGFR mAbs act as competitors of the natural EGFR-ligands for binding to the extracellular domain of EGFR, inhibiting the activation of the receptor. Small-molecule EGFR TKIs compete with ATP for binding to the intracellular TKD of EGFR, decreasing dimer auto-phosphorylation and downstream signalling [218].

During the last 30 years, several mAbs and TKIs EGFR have been developed and translated into clinics for cancer treatment [219]. Although the initial responses have been frequently encouraging, the development of chemoresistance after a treatment period has represented a major drawback, since it drastically decreases the response rates of anti-EGFR therapies. Thus, the development of anti-EGFR targeted drugs has evolved to overcome treatment resistance and improve the progression-free survival of patients [219,220].

On the one hand, all the small molecules TKIs that have been synthesised and evaluated can be categorised into first- to fourth generation of EGFR TKIs [219]. First generation TKIs are reversible competitors of the intracellular ATP binding site of EGFR and include Gefitinib

and Erlotinib, two therapeutic agents approved for cancer treatment by the FDA [221,222]. At least one single mutation on the exons encoding the TKD of EGFR (L858R and del19) is required for the treatment with TKIs to obtain positive clinical responses. Second-generation TKIs are irreversible inhibitors that target EGFR and other ErbB-family members such as ErbB2, and include afatinib (BIBW2992, approved by the FDA), dacomitinib (PF-00299804), and neratinib (HKI-272) among others. Nonetheless, the secondary drug resistance appears frequently, being the EGFR gatekeeper T790M mutation the most important mechanism (threonine substitution alters the ATP binding pocket and increases the receptor affinity for ATP, preventing the binding of TKIs). Third-generation TKIs, including Osimertinib (AZD9291) and Olmutinib (HM617l3) among others, were designed to overcome T790M mutation, as they selectively and covalently bind mutant EGFR^{T790M} active site over wild-type EGFR [223], and are proposed for patients with resistance to the first- and second-generation TKIs. Finally, fourth-generation TKIs are being developed with novel design strategies mainly to target triple mutant EGFR with C797S mutation. Currently, there are at least five inhibitors at phase I clinical trial (BLU-945, BLU-701, TBQ3804, BBT-176, and BPI-361175), although any of them has not yet been approved for the clinical use[224].

On the other hand, Cetuximab (Erbitux) and Panitumumab (Vectibix) are the two mAbs currently used in cancer treatment, although resistance to these inhibitors has limited their use [217]. Cetuximab binds to the EGFR with higher affinity than the natural ligands TGF-α and EGF, and promotes receptor internalization and degradation without its activation, resulting in a decrease of the receptor availability at the PM and less activation of downstream signalling. Indeed, it has been described to bind to the mutant receptor EGFRvIII, to inhibit cell cycle progression as well as the production of pro-angiogenic factors [217].

Recently, many other strategies have been designed as novel therapies, including combination therapies and multitarget agents, such as the use of anti-EGFR agents with drugs targeting other signalling pathways (e.g. PI3K inhibitor pictilisib) [225], or the dual inhibition of the extra- and intracellular domains of the EGFR (with mAbs and TKIs against EGFR) [226]. Interestingly, a strategy for selective delivery of the anti-EGFR agent to EGFR-overexpressing cancer cells has been developed, which consists of the use of nanoparticles containing a cytotoxic agent and coated with an anti-EGFR mAb (EDV EnGeneIC Dream Vector)-D682), and is currently in a phase II trial [227]. Likewise, diverse types of nanoparticles conjugated to EGF or other types of ligands have been studied in pancreatic cancer showing promising results [228,229].

3. Glycobiology

Glycobiology is the study of the structure, biosynthesis, biology, and evolution of saccharides (also called carbohydrates, sugar chains, or glycans) that are widely distributed in nature, and of the proteins that recognize them [230]. Glycans were first considered as a source of energy or as structural materials, without other biological activities. However, the development of new technologies to study their complex structures and functions during the 1980s opened a new field in molecular biology. At present, glycobiology is one of the fields in the natural sciences that is growing faster due to the relevant biological roles of glycans in most of the living organisms [231].

Glycosylation, defined as the enzymatic process that produces glycosidic linkages of saccharides to other saccharides, proteins, or lipids [232], is one of the most important post-translational modifications (PTM). Together with other relevant PTM such as phosphorylation, methylation, and ubiquitination, it helps explaining how the complexity and diversity characteristic of different cell types can be generated from the limited number of protein coding genes of the human genome. Glycosylation is considered the most complex PTM and probably one of the most frequent, with 50-80% of all proteins described to have potential glycosylation sites [233,234]. Glycans are ubiquitously present in all cells in nature, usually expressed on its outer surface and ECM, although they can also be in organelles such as the Golgi apparatus (GA), the endoplasmic reticulum (ER), lysosome, cytosol, and the nucleus. Glycans play crucial roles in several physiological functions and, therefore, they are involved in multiple human diseases, including cancer [232].

The basic structural units of glycans are the monosaccharides, carbohydrates that cannot be hydrolysed into a simpler form, which are typically attached to other monosaccharides or to other molecules by a covalent glycosidic linkage, generating α- or β-linkages via the hydroxyl group of the anomeric center of one unit and the hydroxyl of the second molecule. In mammals, carbohydrates are composed of ten common monosaccharide units, all derived from glucose [235,236]: glucose (Glc), galactose (Gal), *N*-acetylglucosamine (GlcNAc), *N*-acetylgalactosamine (GalNAc), fucose (Fuc), mannose (Man), xylose (Xyl), glucoronic acid (GlcA), iduronic acid (IdoA), and 5-N-Acetlylneuraminic acid (Neu5Ac or sialic acid (SA)) (Figure 8).
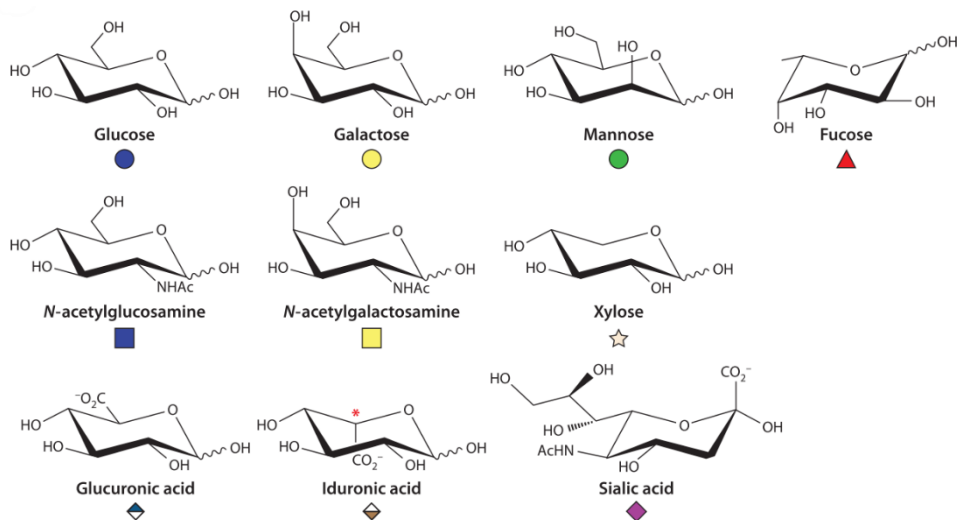
Figure 8.Chemical structures of human monosaccharides and depiction of each glycan according to the Consortium for Functional Glycomics (CFG) notation. All monosaccharides are shown as their free reducing sugars (extracted and modified from Rakus and Mahal, 2011 [235]).

3.1 Glycoconjugates

The term glycoconjugate is used to refer to compounds formed by one or more monosaccharide or oligosaccharide units (glycon) covalently linked to a non-glycosyl part (aglycon) that can be a protein or a lipid; and are classified according to the nature of this linkage. The most common classes of glycoconjugates in mammalian cells are represented at Figure 9, and include glycosylphosphatidylinositol (GPI)-anchored glycoproteins, proteoglycans, glycosphingolipids, and glycoproteins [232].
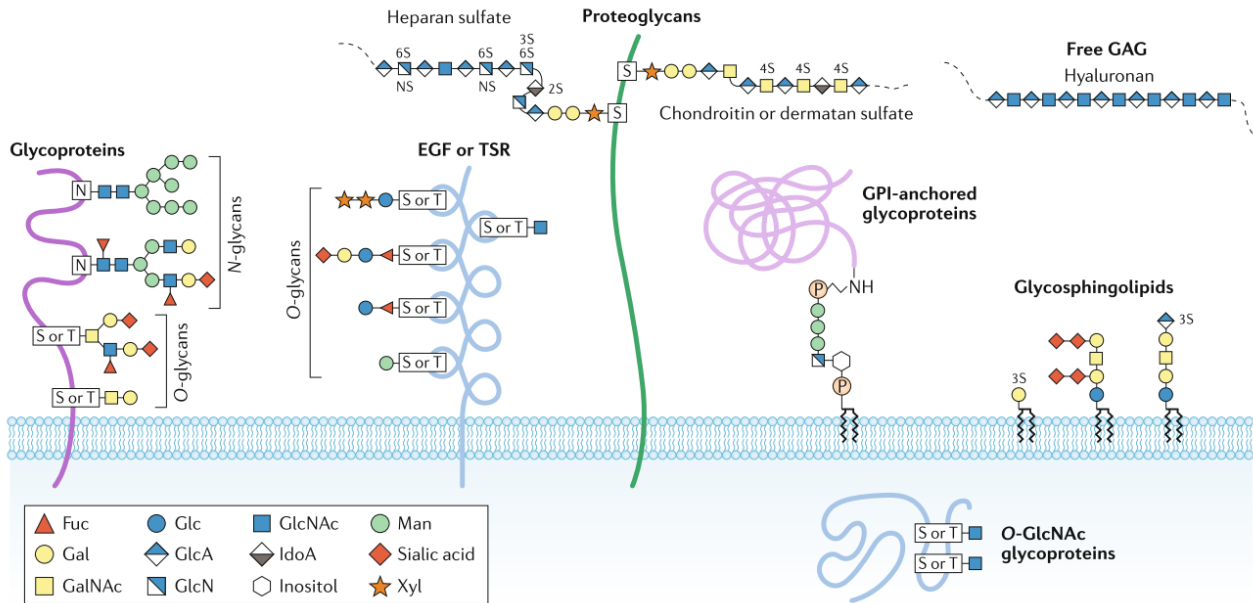
Figure 9. Major types of glycosylation in humans. Schematic representation of the most common glycan structures on animal cells and monosaccharides in CFG notation. Glycoproteins can contain *N*-glycans, attached to Asn (N) of the consensus glycosylation motif Asn-X-Ser/Thr (in which X denotes any amino acid except for Pro), or *O*-glycans, attached to Ser (S) or Thr (T) residues. Different types of *O*-glycosylation are represented, mucin-type glycans, *O*-linked fucose (Fuc) and *O*-linked mannose (Man), which often occurs in specific proteins or protein domains, such as epidermal growth factor (EGF) repeats, thrombospondin type I (TSR) repeats or dystroglycan. Proteoglycans represent a major class of glycoproteins, defined by the presence of long glycosaminoglycan (GAG) chains attached to proteins. Glycosylphosphatidylinositol (GPI)- anchored glycoproteins and glycosphingolipids represent another wo major class of glycoconjugates (extracted from Reily, 2019 [237]).

Contrary to proteins, glycan structures are not encoded directly in the genome; their biosynthesis, assembly, and addition to aglycons are produced as PTM driven by the regulated action of several enzymes (glycosyltransferases (GT) and glycosidases), generating a high number of glycan combinatorial possibilities.

Protein glycosylation is produced in a site-specific manner and not all the potential glycosylation sites are occupied on a given protein, generating a variation termed as macroheterogeneity. Likewise, the presence (or absence) and the specific composition of glycans in a particular glycosylation site of a given protein can derive into the formation of numerous "glycoforms" of the protein, a diversity that is cell-type specific, and can be rapidly modified by glycosylation and deglycosylation reactions taking place primarily in the GA, creating the phenomenon known as microheterogeneity [230].

Glycans can have an effect on many of the physicochemical properties of the glycoprotein they are attached to, such as its conformation, folding, flexibility, charge and hydrophobicity, subcellular trafficking, turnover, and half-life. Thus, glycosylation can modulate many cellular and molecular processes, including receptor activation, signal transduction, endocytosis, and

cell adhesion and drives the concomitant regulation of physiological and pathological events, such as cell growth, migration, differentiation, tumour metastasis, and host-pathogen interactions [238].

Referring to glycoproteins, glycans can be classified into two major groups, according to the covalent bond established between them and the polypeptide backbone: via an asparagine (Asn) (*N*-linked glycans) or via serines or threonines (O-linked glycans). In very few cases, the linkage can be via a tryptophan residue (*C*-linked glycan), but this will not be further addressed in this thesis.

3.1.1 *N*-glycosylation

In *N*-glycosylation, the glycan chains are covalently attached to Asn residues of the protein by an *N*-glycosydic bond. All eukaryotic *N*-glycans begin with a GlcNAc attached through a β-glycosylamine linkage between the hydroxyl group of its anomeric carbon and the amide nitrogen of the Asn side chain (GlcNAc β1-Asn), in an Asn belonging to a consensus amino acid sequence, Asn-X-Ser/Thr in which "X" is any amino acid except proline [239]. Nonetheless, recent work has demonstrated other possible consensus sequences [240].

All human *N*-glycans are generated from a core oligosaccharide of three Man residues and two GlcNAc (Man$_3$GlcNAc$_2$), linked to the Asn (Manα1,3(Manα1,6) Manβ1,4GlcNAcβ1,4GlcNAcβ1-Asn-X-Ser/Thr). According to the residues attached to the core sequence, *N*-glycans are classified into **a) high mannose** or oligomannose type, when all the terminal monosaccharides (at the non-reducing end) of the glycan are Man **b) complex** *N*-glycans, when no Man are found at the terminal positions of the glycan, and **c) hybrid** *N*-glycans, when there are both Man and other monosaccharides at the terminal positions of the glycan. The complex ones are subdivided according to the number of GlcNAc attached to the core (branches or *antennae*), into bi-, tri-, and tetrantennary structures, being the biantennary structures the most abundant extracellular glycans in vertebrates (Figure 10)[241].
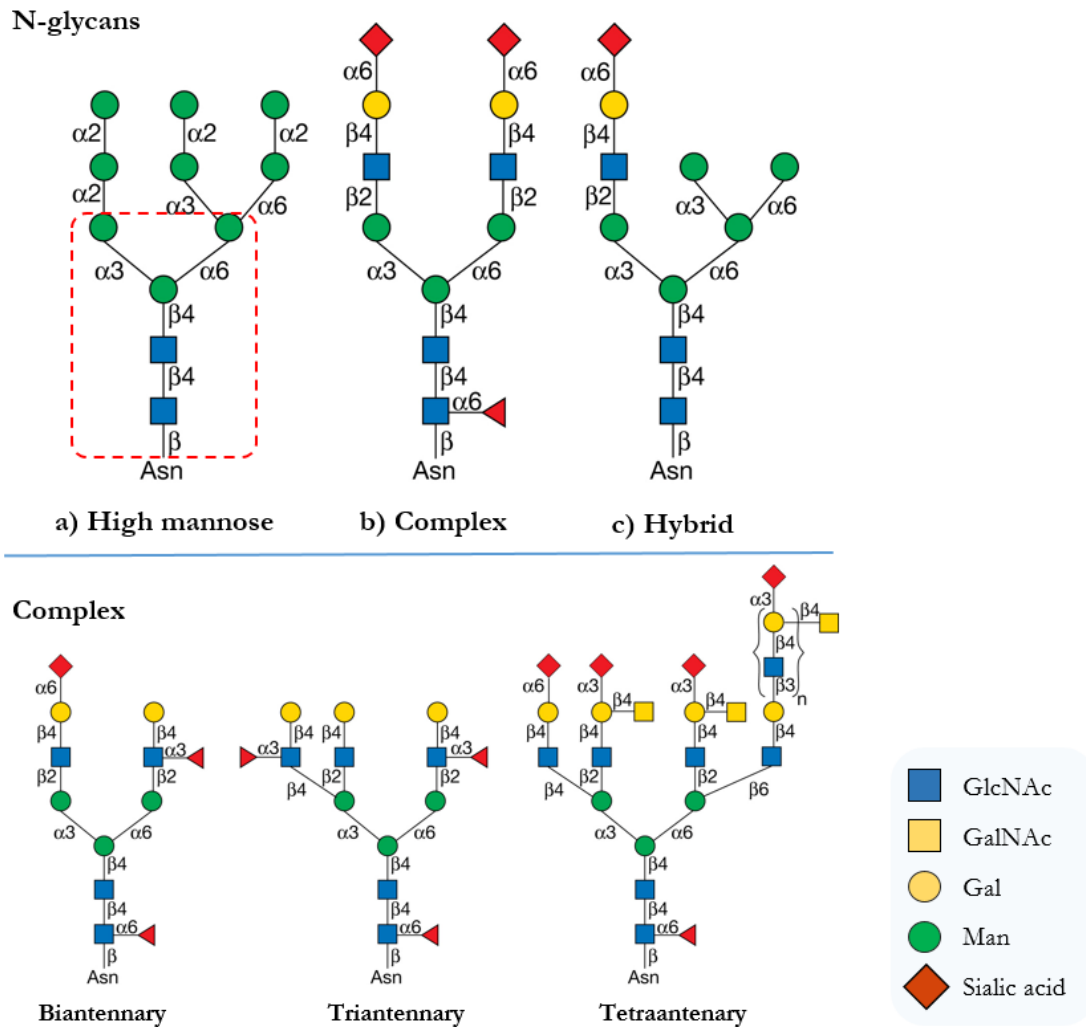
Figure 10. Types of *N*-glycan and complex *N*-glycans found on mature glycoproteins. Top panel: a) High mannose type, b) Complex type, c) Hybrid type structures. The dashed red box highlight the core or common penta-saccharide region that the three types of *N*-glycans share. Bottom panel: Biantennary, Triantennary and Tetraantenary complex *N*-glycan typical structures. A LacNac unit (bracketed) on any branch may be repeated many times (extracted and modified from Essentials of Glicobiology[230]).

N-glycan biosynthesis occurs in two different organelles, the ER and GA, where the enzymes that catalyse this process are located. This process occurs in three major phases:

i) **The synthesis of the lipid-linked precursor oligosaccharide:** this is a highly conserved phase in eukaryotes that takes place at the ER cytoplasmic membrane, starting with the transfer of a GlcNAc-1-P to a dolichol-phosphate (Dol-P), to generate Dol-P-P-GlcNAc. Next, a second GlcNAc and five Man residues are transferred to Dol-P-P-GlcNAc to form GlcNAc2Man5-P-P-Dol, which is "flipped" into the luminal side of the ER. Subsequently, GlcNAc$_2$Man$_5$-P-P-Dol is extended by the addition of four Man and three Glc residues, transferred from Dol-P-Man and Dol-P-Glc, respectively, to form the 14-sugar mature *N*-glycan precursor Glc$_3$Man$_9$GlcNAc$_2$-P-P-Dol.

ii) Transfer of the *N*-glycan precursor to nascent proteins: the oligosaccharide part of $Glc_3Man_9GlcNAc_2$-P-P-Dol precursor is transferred by oligosaccharyltransferase (OST) to the Asn (Asn-X-Ser/Thr) of the proteins as they emerge from the translocon in the ER membrane.

iii) Processing of the oligosaccharide: after the transfer of the precursor oligosaccharide by OST to the nascent protein, the processing of the glycan occurs in the ER and GA by the action of glycosidases and GTs. The **early processing** in the ER lumen begins with the sequential removal of three Glc residues by two glucosidases, and the removal of a Man residue by an ER mannosidase, reactions that are tightly related to glycoprotein folding and protein fate (to GA processing or to degradation). Misfolded glycoproteins are recognised at this point by degradation-enhancing α-mannosidase I-like (EDEM) proteins and targeted to ER degradation. Next, the high-mannose glycoprotein is transferred to the *cis*-Golgi cisternae, where three Man residues are sequentially removed ($Man_5GlcNAc_2Asn$) by α1-2 mannosidases IA and IB (MAN1A1, MAN1A2). In the **late processing** steps, the biosynthesis of hybrid and complex *N*-glycans is initiated in the *medial*-Golgi by the addition of a Glc residue to the core α1-3 Man residue of the $Man_5GlcNAc_2Asn$ by the action of an N-acetylglucosaminyltransferase (GnT) (MGAT1). Subsequently, most glycans are trimmed by the action of two α-mannosidase II enzymes (MAN2A1 and MAN2A2), which remove terminal Man residues (α1-3Man and α1-6Man), and then a second Glc residue is added to the α1-6Man in the *N*-glycan core by the action of MGAT2, to form the precursor for all biantennary, complex *N*-glycans. If the second mannosidase is inactive, the first hybrid *N*-glycans are formed ($GlcNAcMan_4GlcNAc_2$). Besides, hybrid and complex *N*-glycans can suffer additional branching by the addition of GlcNAc to α1-3Man and α1-6Man to yield tri- and tetra-antennary *N*-glycans, or the transfer of a bisecting GlcNAc, attached to the core βMan. Finally, the **maturation** of *N*-glycans (Figure 11) takes place in the *medial*- and *trans*-Golgi, where further monosaccharide additions convert the limited glycan repertoire into a complex and extensive array of mature *N*-glycans. Monosaccahride can be added to the *N*-glycan core (α1-6Fuc is the main core modification in vertebrates), or can also be added to elongate the branches, by the transfer of β-linked Gal and GlcNAc residues. Furthermore, additional monosaccharide residues can be added for the "decoration" or "capping" of the glycan *antennas*, including SA, Fuc, Gal, and GlcNAc among the most important ones. To facilitate its presentation to lectins and antibodies, these capping sugars are normally α-linked. Overall, the final glycan product will depend on the

monosaccharide donor availability and the presence and accessibility of different GTs within the *medial-* and *trans-*GA.
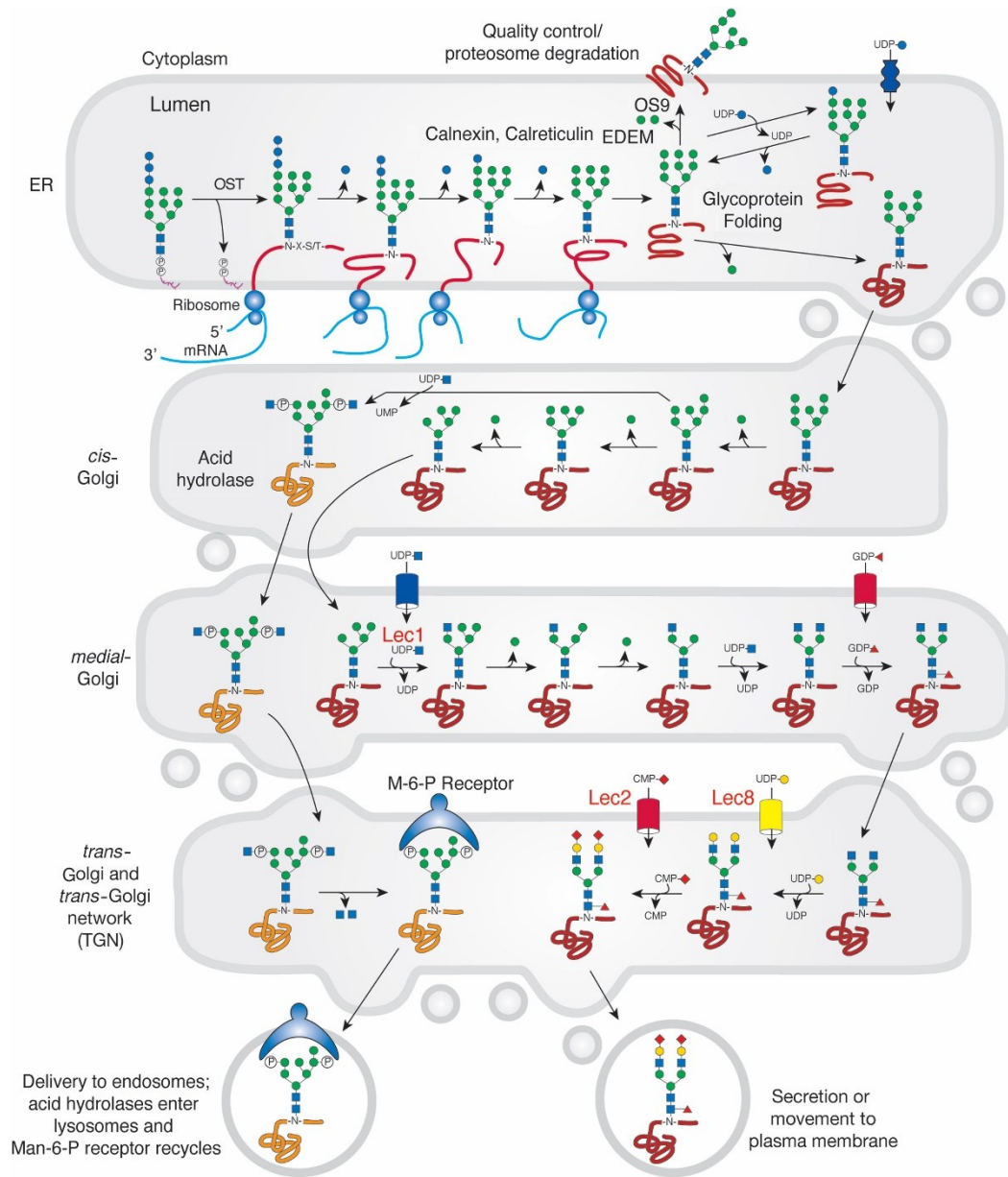
Figure 11. N-glycans biosynthesis and maturation in the secretory pathway. Extracted from Essentials, 4th edition [230].

3.1.2 *O*-glycosylation

In *O*-glycosylation, the glycans are linked to a protein via the hydroxyl group of a Ser/Thr residue of the polypeptide chain. There are several types of *O*-glycans, including α-linked *O*-Fuc, β-linked *O*-xylose, α-linked *O*-mannose, β-linked *O*-GlcNAc, α- or β-linked *O*-galactose and α- or β-linked *O*-glucose glycans [230,236]. However, the most common *O*-glycosylation type in animals is the linkage via a GalNAc molecule, creating the **O-GalNAc glycans** or also called mucin-type-*O*-glycans [242].

O-glycosylation is an evolutionary conserved PTM that, unlike *N*-linked glycosylation, begins when protein synthesis starts and folding is already completed [242,243]. A large family of enzymes named polypeptide-N-acetylgalactosaminyltransferases (ppGalNAcT) initiates the *O*-glycosylation process in the *cis*-Golgi by adding a single GalNAc residue, and the elongation process of the glycoprotein is followed by the stepwise addition of other monosaccharides within the GA by GTs [242,243].

The first common structure GalNAcα-Ser/Thr, also named Thomsen-nouvelle antigen or Tn-antigen, is used as a substrate to form extended chains by the addition of Gal or GlcNAc residues catalysed by GTs (Figure 12), giving place to core 1 and core 3 structures, from which most of the additional *O*-glycan core types are formed (core 1-4 in addition to Tn-antigen and Sialyl-Tn antigen)[244]. Besides Gal and GlcNAc, other sugars are found in *O*-glycans including GalNAc, Fuc, and SA, generating mainly linear or bi-antennary chains with variable length, from a single GalNAc to more than 20 monosaccharide residues. *O*-GalNAc glycans are heavily expressed on MUCs, contributing to its conformation and to its adhesive properties and thus, *O*-GalNAc glycans have an important role in protecting the epithelia in mucus sites, as they provide a barrier (by forming a mucus) to many external threats such as intestinal microbes. Furthermore, the overexpression of MUCs in several types of cancers and the aberrant glycosylation carried on these protein have been related to tumour progression, invasiveness, metastasis formation, and drug resistance [245].
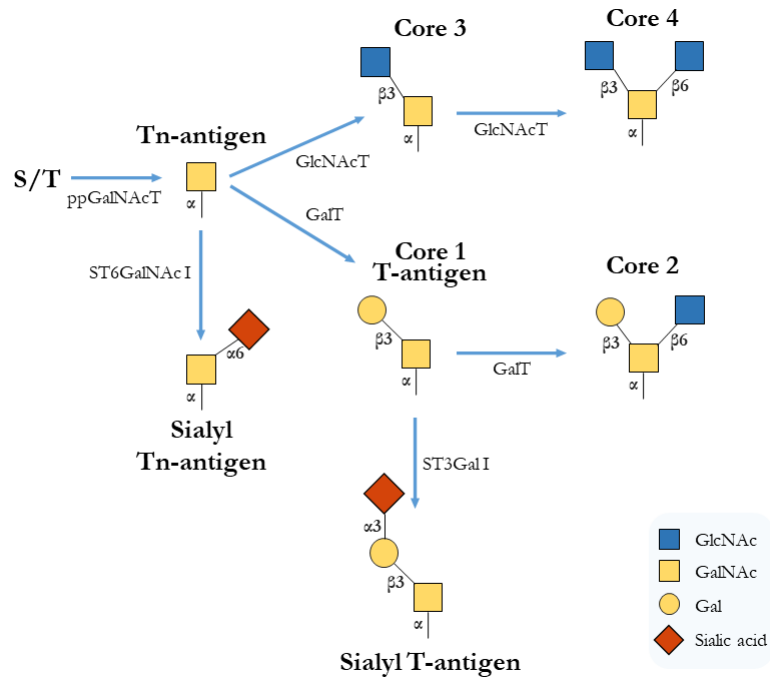
Figure 12. Biosynthesis of *O*-glycans. Representation of the most common mucin-type *O*-glycosylation core 1-4 biosynthetic pathways in mammals. Data for the figure was extracted from Essentials 4th edition, 2022; Bennet et al., 2012; and Tran et al., 2013 [230,242,243].

3.2 Sialic acids and sialyltransferases

SA are a family of nine-carbon backbone sugars that are typically attached to the outermost ends of glycoconjugate chains [246], commonly added to *N*- or *O*-linked glycans of glycolipids or glycoproteins. There are two major SA core structures (Figure 13), the 2-keto-deoxynonoic acid (Kdn) and neuraminic acid (Neu) [230,247], sharing the nine-carbon backbone and differing at the C5-position. In mammals, the following two derivatives of Neu are the most common SA structures: *N*-acetylneuraminic acid (Neu5Ac) and its hydroxylated form, *N*-glycolylneuraminic acid (Neu5Gc). However, humans lack Neu5Gc due to an inactivating mutation of a hydroxylase that catalyses the reaction of CMP-Neu5Ac to CMP-Neu5G [246,247] and thus, the most common SA in humans is the Neu5Ac. Importantly, the carboxylate group at C1-position of Neu5Ac is normally deprotonated at physiological pH, conferring a negative charge to the glycan [230]. The glycerol-like side chain (C-7, C-8, and C-9, each carrying a hydroxyl group) can establish hydrogen bonds and the N-acetyl group facilitates hydrophobic interactions, all of them participating in binding specificities and functions of sialylated glycans [230]. In addition, the four SA core molecules (Kdn, Neu, Neu5Ac, and Neu5Gc) can be naturally modified via esterification (with acetyl, lactyl, sulfate or phosphate), O-methylation, lactonization, or lactamization, giving rise to over 50 variations [246,247]. These modifications, together with the net negative charge, can strongly influence in

the physicochemical properties of the glycans and in its recognition by glycan binding proteins (GBPs) such as sialic-acid-binding immunoglobulin-like lectins (Siglecs), thus conditioning their physiological roles.
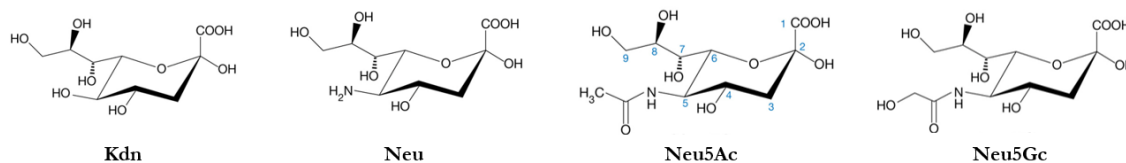
Figure 13. SA core molecules. From left to right, Ketodeoxynonulosonic acid (Kdn), Neuraminic acid (Neu), N-acetylneuraminic acid (Neu5Ac), and N-glycolylneuraminic acid (Neu5Gc) (extracted and modified from Essentials 4th edition[230]).

Sialylation, the process of adding SA residues to terminal non-reducing positions of oligosaccharide chains of glycoproteins and glycolipids, is one of the most relevant "capping" reactions in the biosynthesis of glycans, which provides diversity, both in structure and function to the glycans. Sialylation is catalysed by a family of GTs enzymes known as **sialyltransferases** (STs). In all vertebrates, STs are type II TM glycoproteins predominantly located at the *trans*-Golgi, which use the nucleotide sugar CMP-Neu5Ac as a donor to transfer SA to the glycan chains. STs can generate different linkage types when binding SA to the glycan chain and, based on the linkage and glycan type, they have been classified into four major subfamilies: ST3Gal, ST6Gal, ST6GalNAc, and ST8Sia. SAs can be transferred via their C-2 anomeric carbon in α-configuration, commonly to the C-3 or C-6 positions of Gal by α2,3-STs (ST3Gal I-VI) and α2,6-STs (ST6Gal I-II) respectively. SAs can also be attached to the C-6 position of GalNAc in α2,6-linkage by ST6GalNAc I-VI and additionally, SA can be attached to the C-8 or C-9 position of another SA molecule, generating a linear homopolymer of SA also referred as polysialic acid structure by ST8Sia I-VI [230,248].

In human and murine genomes, there are twenty known genes encoding STs enzymes. Six of these genes (*ST3GAL1, ST3GAL2, ST3GAL3, ST3GAL4, ST3GAL5,* and *ST3GAL6*) encode for α2,3-STs enzymes, which transfer SA in an α2,3 linkage to the Gal of type-1, or -2 structures in glycoproteins or glycolipids (Galβ1,3GalNAc or Galβ1,4GlcNAc structures respectively). In mammals, α2,3-sialylation of *N*-glycans is catalysed by the enzymes ST3Gal III, ST3Gal IV and ST3Gal VI, being ST3Gal III and ST3Gal IV the principal enzymes since *ST3GAL3* and *ST3GAL4* genes are broadly expressed [249]. α2,3-STs compete with other GTs such as α1,2-FucTs (fucosyltransferase), α1,3-GalT, GlcNAcTs, and GalNAcTs for the transfer of additional monosaccharide residues to the terminal Gal residue, enzymes that cannot act when α2,3-SA has previously been linked to Gal terminal residues by α2,3-STs [230].

ST6GAL1 and *ST6GAL2* genes codify for the α2,6-STs that transfer SA to Gal in α2,6-linkage, while *ST6GALNAC1-6* genes codify for the α2,6-STs that transfer SA to GalNAc. In addition, *ST8SIA1-6* genes codify for the α2,8-STs that transfer SA to other SA residues [230].

In vertebrates, Neu5Ac is synthetized in the cytosol (detailed process represented at figure 14), converted to activated cytidine monophosphate (CMP)-Neu5Ac (donor) in the nucleus by condensation with cytidine tryphosphate (CTP), returned to the cytosol and transferred into Golgi compartments by a CMP antiporter. At *trans*-Golgi, where the STs reside, SAs are transferred to lipid and protein glycans, which are transported to the cell surface to be part of the PM or secreted [230].
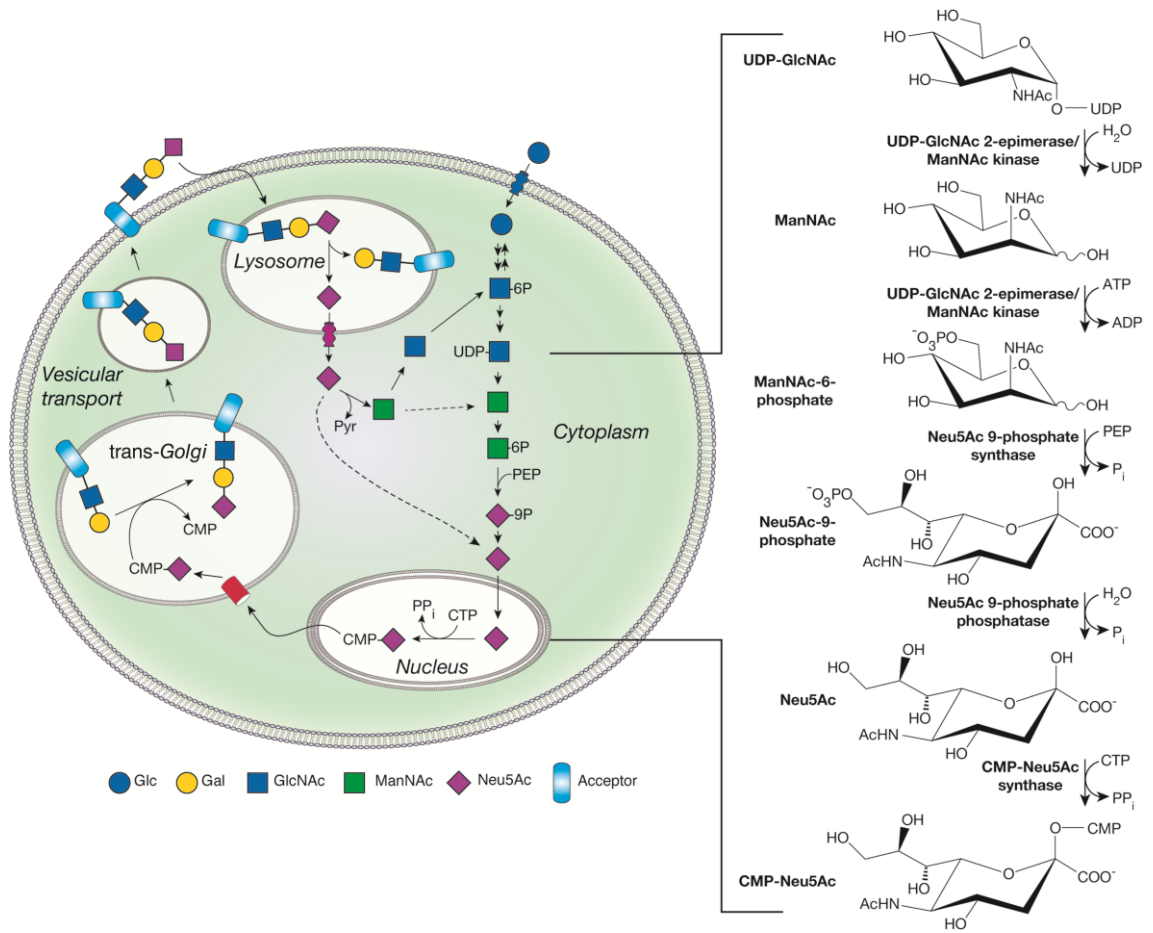
Figure 14. Metabolism of N-acetylneuraminic acid in vertebrate cells. On the left, schematic pathways and compartments of biosynthesis of Neu5Ac: biosynthesis in the cytosolic compartment, converted to activated CMP-Neu5Ac in the nucleus, transferred to lipid and protein glycans in the Golgi, transported to the cell surface, secreted or recycled into lysosomes and degraded. On the right, details of enzymatic steps leading to CMP-Neu5Ac biosynthesis (extracted from Essentials 4th edition [230]).

The presence of SA on glycoconjugates is regulated by the activity of STs (which is mainly regulated at gene transcription level and also by PT controls, epigenetic events, and Golgi pH [250], as well as by the availability of the SA nucleotide sugar donor (conditioned by the activity of the enzymes that regulate its synthesis) and the co-localization of substrate and enzymes in the Golgi compartments. Moreover, SA can be removed from the glycoconjugates by the enzymatic activity of sialidases (also called neuraminidases) either intracellularly to recycle sialoglycans, or on the cell-surface to regulate sialylation and modulate receptor-mediated signalling [230].

SAs have been described to play diverse important roles, which are not mutually exclusive. The presence of SA modulates the biophysical environment of sialoglycoproteins such as mucins, conferring a negative charge and inducing its hydrophilic properties to promote its efficacy as hydrating molecules. SAs have also been described to mask underlying glycans and prevent its recognition by glycan-binding proteins. They are specifically recognised by SA-binding proteins, which mediate important biological processes. Among the most important roles, SAs are involved in the modulation of cellular recognition, cell signalling, cell adhesion, neural signalling and plasticity, and glomerular filtration, and are used as binding sites for many human pathogens and toxins, facilitating its colonization and spreading [247,251–255]. Considering the roles of SA in modulating several important biological processes, its deregulation or modification has been reported in numerous diseases, including cancer, an issue that will be addressed in section 3.4.2.

3.3 Lewis blood group determinants

The Lewis blood group antigens are a set of glycans that carry Fuc residues in α1,3/α1,4 linkage (Figure 16). Type-1 and type-2 structures in *N*-glycans, *O*-glycans and glycosphingolypids [256] can be further modified by the sequential action of diverse FucT and STs, which catalyse the addition of Fuc and SA residues to generate type-1 and type-2 Lewis antigens. Some of the members of Lewis blood group antigens play important roles as selectin ligands on glycoproteins, being involved in several physiological processes such as the extravasation of the leucocytes to the tissues, as well as many pathological processes such as tumour cell extravasation and metastasis formation [256–263]. Thus, given their potential role in tumorigenesis and metastasis in various cancers, we will give special emphasis to **sialyl Lewis A** (sLe^a) Neu5Acα2,3Galβ1,3(Fucα1,4)GlcNAc and **sialyl Lewis X** (sLe^x) Neu5Acα2,3Galβ1,4(Fucα1,3)GlcNAc antigens.

For the biosynthesis of sLe^a antigen, type-1 glycan chains (Galβ1,3GlcNAc) are used as precursor structures by the α2,3-STs ST3Gal III and, with lower catalytic efficiency by ST3Gal IV, which catalyse the transfer of a SA residue to the terminal Gal in α2,3-linkage, generating the Dupan-2 antigen. Then, the addition of a Fuc residue in α1,4-linkage to the GlcNAc by the FucTs FucT III and FucT V generates sLe^a antigen [264] (Figure 15).

For the biosynthesis of sLe^x antigen, type-2 glycan chains (Galβ1,4GlcNAc) are used as precursors, and initially modified by the addition of α2,3-linked SA to the terminal Gal catalysed by the ST3Gal III, ST3Gal IV, and ST3Gal VI STs. In the subsequent step, the addition of a Fuc to the GlcNAc in α1,3-linkage by the action of a α1,3-FucTs FucT III, FucT V, FucT VI, or FucT VII finally produces the sLe^x antigen [265–268] (Figure 15).
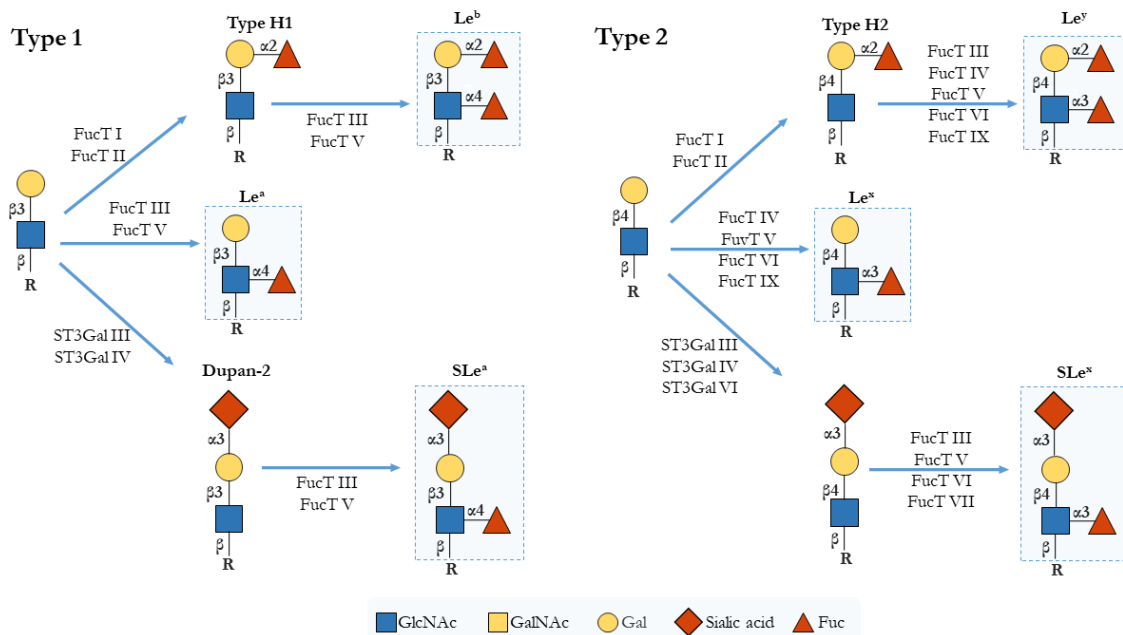
Figure 15. Schematic representation of type I and II Lewis antigens. Lewis and sLe structures are depicted (highlighted by the dashed blue boxes). The key enzymes involved in their synthesis are indicated (adapted from Pinho, 2015 [232]).

Interestingly, recent studies have focused on the particular importance of some of these enzymes in the biosynthesis of sLe antigens, although results differ between the tissues studied. In humans, ST3Gal IV was reported to be the major STs in the biosynthesis of E-, P- and L-selectin ligands in leukocytes [269]. Nonetheless, diverse studies from our group reported that in pancreatic cancer cell lines both ST3Gal III and ST3Gal IV participate in the biosynthesis of sLe^x antigen [270,271]. Referring to FucTs, it has recently been described that FucT III, FucT VI, and FucT VII are the enzymes that more importantly contribute to sLe^x biosynthesis pathway [272,273].

3.4 Altered glycosylation in cancer

Aberrant expression of glycans and glycoconjugates has been associated with numerous pathologies, including congenital disorders [274], immunodeficiencies and cancer [232,257,275]. During the last decades, aberrant glycosylation has emerged as a hallmark of cancer due to its contributions in malignant transformation of cancer cells, tumour progression, and ultimately, metastasis formation. Additionally, increasing evidence propose glycans as a novel source of clinical biomarkers, and consider glycans and the biosynthetic pathways involved in glycan structures as promising targets for cancer therapy, due to their ability to modulate diverse stages of tumour progression and metastasis [276].

In cancer, glycan alterations have been related to cell-cell adhesion, cell-matrix interactions, activation of oncogenic signalling pathways, tumour angiogenesis, immune modulation, and induction of pro-metastatic phenotypes [232,277,278]. Glycan alterations can occur in core structures of *O*-glycans and *N*-glycans, present either on the tumour cell surface or in secreted glycoproteins and host elements [3]. The principal alterations found in cancer are truncated *O*-glycans, highly branched *N*-glycans, diverse fucosylated and sialylated terminal structures, and alterations in glycosphingolipid expression (Figure 16)[279]. Among these changes, the formation of highly fucosylated glycans, such as Lewis antigens (Le[a/b] and Le[x/y]), and sialylated antigens (such as sLe[x] and sLe[a]), are of special relevance during the neoplastic transformation.
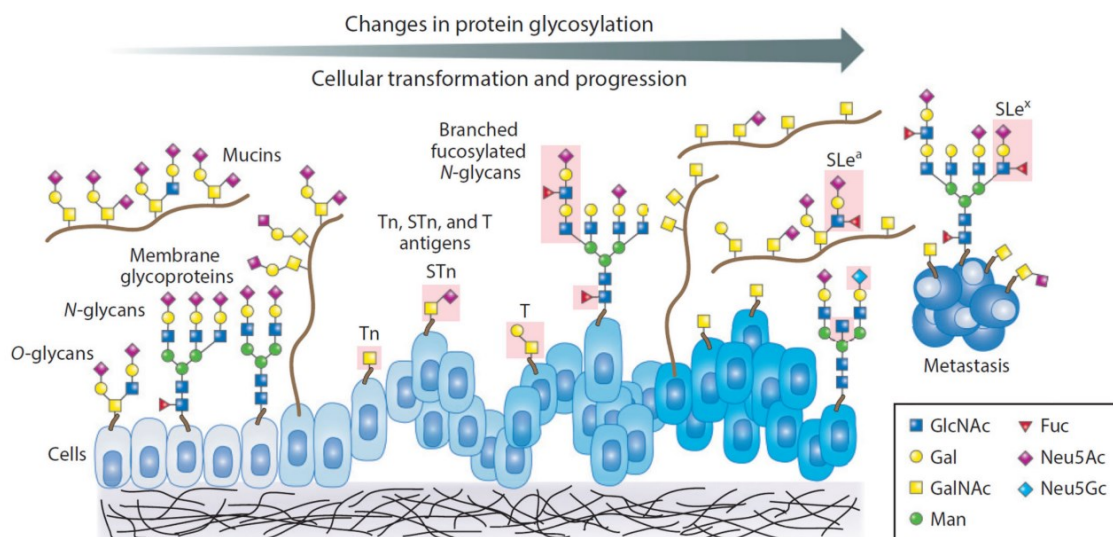
Figure 16. Alterations in protein glycosylation during cellular transformation and progression. The main changes in the glycosylation of membrane or soluble proteins are highlighted in pink, changes in O-glycans (T, Tn, and STn antigens) and altered branching and fucosylation of N- and O-glycans, including changes in sialylated Lewis antigens (sLe[x] and sLe[a]) (extracted from Stowell, 2015 [236]).

These modified glycans, also called tumour-associated carbohydrate antigens (TACAs) as they are generated during tumorigenesis and cancer development, offer the possibility to discriminate the glycosylation pattern of proteins expressed either on normal or tumour cells [276]. Although it remains insufficiently understood, diverse mechanisms have been proposed as the origin of the main glycan alterations: changes in expression levels of GTs and glycosidases [242,280], whose expression is frequently deregulated in cancer, changes of GTs location in the ER and GA [281], modified molecular chaperone activity [282], and substrate and donor availability [283,284]. Recently, alterations in glycosylation have been linked to the acquisition of the cancer hallmarks capabilities proposed by Douglas Hanahan [285], reinforcing the concept that glycosylation plays crucial roles during all steps of tumour progression, regulating tumour proliferation, invasion, angiogenesis, and metastasis [3,232].

3.4.1 Altered glycosylation affects key cell receptors and influences their activity, as well as tumour cell adhesion and invasion capabilities

RTKs are glycosylated TM receptors that regulate key processes in malignant transformation and cancer progression such as cell division, differentiation, migration, and angiogenesis. Recently, it has been reported that alterations in the glycosylation of RTKs can cause its aberrant activation and signalling. Glyosaminoglycans (GAGs), glycosphingolypids, and gangliosides have been described as modulators of RTKs activation and signal transduction for receptors such as EGFR, FGFR, MET, and IGFR [286–288]. Besides, *N*-glycans on RTKs are important regulators of cell proliferation and arrest. For instance, as commented above, *N*-glycan branching of EGFR has been described to modulate tumour cell phenotype in several cancer types. Its aberrant glycosylation promotes the retention of the receptor at the cell surface mediated by the galectin lattice, facilitating its activation [289–291]. In addition, the increase of α2,3-sialylation, linked to the increase of sLe epitopes, caused a more invasive phenotype on gastric carcinoma cells through the hyperactivation of the RTKs MET and RON [292,293].

Referring to tumour cell-cell interactions, increasing evidence suggest that the glycosylation of cadherins, principally E-cadherin, affects its stability and thus, mediate cell-cell adhesion, cell motility, and cell growth differentiation. Dysregulated *N*-glycosylation of E-cadherin might be present on diverse cancer types, modulating protein junctions between cancer cells and its adhesive capabilities [294–297]. Fucosylation of E-cadherin by FUT8 (α1,6-FucT) was reported to promote breast cancer cell migration [276] as well as to increase cell-cell adhesion in human colon carcinoma cells [298]. Furthermore, previous research from our group reported

that alterations in E-cadherin and α2β1-integrin sialylation, caused by *ST3GAL3* and *ST3GAL4* overexpression, resulted in enhanced migratory and invasive properties of PDA cells [271,299].

The integrin family of receptors comprise the major regulators of the adhesion of cells to the ECM elements (collagens, fibronectin and laminin among others), regulating cell growth and proliferation. Importantly, diverse glycan modifications have been reported to affect the expression of integrins: β-1,6 branching of complex *N*-glycans on integrins catalysed by the Gn-T III promoted invasion and metastasis in melanoma cells, similarly to the highly *N*-glycosylated α5β3 integrin [276]. Sialylation and fucosylation are also involved in the modulation of integrin functions. The overexpression of ST3GAL3 in PDA cells caused an increase in sialylated antigens (sLe^x) on α2β1 integrin, leading to FAK phosphorylation and increased invasive phenotype [299]. Moreover, the inhibition of fucosylation in liver cancer cells supressed migration and the intracellular FAK signalling linked to β1 integrin [300].

3.4.2 Hypersialylation in cancer

In cancer cells, glycan chains of glycoconjugates are often terminated by numerous sialylated determinants. This hypersialylation correlates with higher malignancy, invasion, and cancer cell survival [301–303]. First, regarding to the physicochemical properties, hypersialylation of glycans confers a negative charge to the glycan chain that contributes to cell-cell and cell-matrix detachment, thus promoting invasion to other tissues and metastasis [3,258,304]. Second, the increased expression of selectin ligands at the cell surface, such as sLe^x and sLe^a, enhances the metastatic properties of cancer cells by their interaction with the E-selectin expressed on the activated endothelium, which allows their extravasation. [305–307].

The aberrant expression of these sialylated determinants in tumours is linked to the enzymes regulating their addition and removal (STs and sialidases, respectively), being ST3Gal III, ST3Gal IV, and ST3Gal VI of critical importance [308]. In addition to sialylated determinants, a more generic increase in α2,3 and α2,6-sialylation resulting from the overexpression of ST3Gal and ST6Gal STs, and the dysregulated activity of sialidases, have been reported as a hallmark of cancer [285,309–313].

Several STs are implicated in cancer, but *ST6GAL1* has been the most studied ST in recent years. *ST6GAL1* is upregulated in numerous types of cancer (including pancreatic, prostate, colon, breast, and ovarian cancer) [314–316], contributing to increase tumour aggressiveness, metastasis and resistance to chemotherapy. The mechanisms by which ST6Gal I mediated-

α2,6-sialylation facilitates tumour progression and metastasis are still poorly understood, although recent research has provided valuable results: upregulation of *ST6GAL1* blocked apoptotic signalling via the increased α2,6-sialylation of FasR [317]; *ST6GAL1* mediated sialylation was reported to enhance HIF-1α signalling, protecting tumour cells against hypoxia [318]; and *ST6GAL1* overexpression was reported to promote survival signalling and resistance to cytotoxic stress under serum growth factor withdrawal situations, sustaining proliferative capacity of tumour cells [319]. In addition, increased α2,6-sialylation of EGFR has been described as a key factor in modulating its activation and the sensitivity of tumour cells to EGFR-targeted drugs [320–322]. Finally, ST6Gal I activity has been described to inhibit galectin binding and function, modulating tumour immunity [323].

Regarding *ST3GAL3* and *ST3GAL4*, the increased expression of sLe[x], caused by *ST3GAL4* overexpression, was reported to induce invasive phenotype in gastric cancer cells through the activation of c-Met pathway [293] and RON RTK [292]. In ovarian cancer, *ST3GAL3* down-regulation sensitized cisplatin-resistant cells to cisplatin, meaning that targeting α2,3-linked SA might contribute to prevent resistance and relapse of this cancer type. Similarly, it has been recently revealed that increased α2,3-sialylation in PDA cells can be recognised by Siglec-7 and Siglec-9 expressed on myeloid cells, modulating its function in multiple stages of tumour-associated macrophage (TAM) differentiation towards a reduced pro-inflammatory profile, by upregulating PD-L1, IL-10, IL-6, and CD206, to promote immune system evasion [322]. Moreover, previous studies from our research group demonstrated that *ST3GAL3* and *ST3GAL4* were overexpressed in PDA tissues compared to control ones [271,324], and proved that the increase in α2,3-SA in PDA cell lines derived of *ST3GAL3* and *4* overexpression positively correlated with E-selectin adhesion and cell migration capabilities. In further studies, it was demonstrated that the injection of PDA cells overexpressing α2,3-STs into athymic nude mice increased metastasis formation and reduced mice survival [270,271,299,325]. Additionally, *ST3GAL3* and *ST3GAL4* knockdown (KD) in PDA cell lines impaired cell migration and invasive capabilities, as well as its binding and rolling to E-selectin, reinforcing the importance of α2,3-sialylation in the PDA metastatic process [326].

Considering all these findings in diverse cancer models, and the fact that expression levels of STs and total serum sialylation levels are generally increased in cancer patients, normally being indicative of a poor prognosis, aberrant sialylation has been considered as a therapeutic target and inhibitors of STs activity have emerged as a pharmacological therapy for cancer.

3.5 EGFR glycosylation

The extracellular region of ErbB family members is heavily glycosylated, accounting to nearly 50 kDa of the total molecular weight of the receptor (~175 kDa) [327]. This PTM has been shown to modulate receptor structure, functionality, and therapeutic response and thus, it has represented a source of novel clinical biomarkers and therapeutic targets for human cancers. Twelve potential sites for *N*-glycosylation have been identified along the extracellular region of EGFR (Figure 17) [327,328], eleven of which consist of the typical *N*-glycosylation consensus sequences (N-X-S/T, where X is any amino acid except proline) (N104, N151, N172, N328, N337, N389, N420, N504, N544, N579, N599), and another one (N32) that is known to be an atypical glycosylation site (N-X-C) [329,330]. Nonetheless, other studies have proposed additional residues as potential glycosylated and fucosylated sites [328,331].
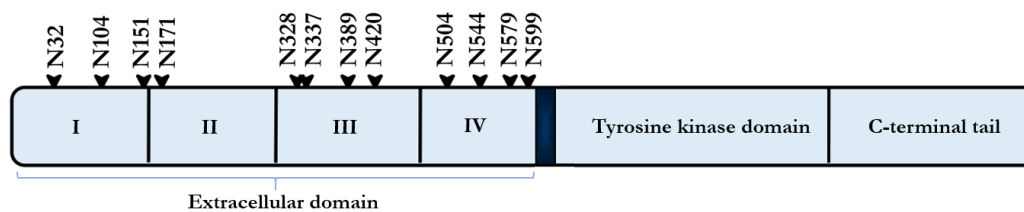
Figure 17. *N*-glycosylation sites of EGFR. Schematic diagram of the structural protein domain and *N*-glycosylation sites of EGFR. The amino acid numbering is for the mature form of the receptor and does not include signal peptides of the *N*-terminal 24 amino acids of EGFR (extracted and modified from Takahashi, 2022 [332]).

The site specific *N*-glycosylation status of EGFR has been described for endogenous and recombinant EGFR expressed in different cancer cell types, indicating that most of the *N*-glycosylation sites are 100% glycosylated (only some of them are partially or not glycosylated) and that the most common glycan types are high-Man or complex ones [332].

Several studies have reported that *N*-linked glycosylation of the EGFR affects its conformation, which is crucial for the regulation of its dimerization and function [333]. In a normal state, a basal *N*-glycosylation of EGFR has been described to be required for the proper sorting to the cell surface and for ligand binding [330,334–336]. Besides, considering that aberrant glycosylation is a common feature in cancer development and progression, several works have demonstrated that in diverse cancer types, EGFR-bound glycans modulate the malignancy of tumour cells [331,337–339]. The glycome of EGFR and its neighbouring receptors has been described to highly influence on the ability of EGFR to trigger oncogenic signalling, by allowing the correct folding of the receptor, its trafficking to the cell membrane and stabilizing its expression there [340,341]. *O*-linked glycosylation has also been described to affect ErbB-dependent oncogeneicity, as demonstrated in glycoengineered gastrointestinal cell

models in which the activation threshold of EGFR and ErbB2 was significantly altered [342,343]. Importantly, since the glycosylation profile of the ErbB receptors determines their stability and residence time at the PM, it might alter the therapeutic effect of EGFR-targeted drugs and thus, the combination of anti-EGFR agents with drugs targeting its glycosylation has been considered as a promising strategy to treat cancer and to overcome acquired TKI resistance [344,345].

The specific *N*-glycosylation plays a key role in the regulation of receptor properties, including receptor trafficking to the cell surface, ligand-binding, dimerization capacity, phosphohrylation and endocytosis [332]. For instance, it has been reported that the *N*-glycans on N420 of EGFR are involved in dimerization, as their deletion promote ligand-independent dimerization and autophosphorylation [346], while N-glycan on N579 contributes to stabilize the tethered conformation of EGFR, by preventing ligand-independent dimerization [347]. Another mechanism by which *N*-glycans functionally regulate EGFR is the interaction of specific *N*-glycans with carbohydrate recognition molecules such as lectins, as suggested in the study performed with diverse lung adenocarcinoma cell lines, in which the binding of the pulmonary surfactant protein D (SP-D) to *N*-glycans of EGFR down-regulated EGF signalling in these cells [348]. Similarly, the specific terminal structures of the EGFR *N*-glycans interact with carbohydrate recognition molecules, such as galectin-3, an interaction that regulates receptor endocytosis [290,349].

Referring to EGFR *N*-linked terminal sialylation and fucosylation, several studies have addressed their impact on EGFR activation and resistance to EGFR therapies in different tumour cell models, by either up-regulating or down-regulating a specific sialyl- or FucT that can modify the pattern of EGFR glycosylation. Depending on the tumour cell model and the GTs up- or down-regulated, some studies reported that specific EGFR glycosylation patterns favour EGF binding to the receptor and the consequent EGF-induced dimerization, as well as to increase its autophosphorylation threshold [350], thus increasing tumour cell malignancy [320,321,331,343,351–353]. In addition, it has been recently postulated that aberrant glycosylation patterns on EGFR in cancer cells, may contribute to the evasion of antitumour immunity via interaction with inhibitory immune receptors [320–322,354]. Nonetheless, other studies reported the contrary, describing that some EGFR glycosylation patterns reduce its activation [351,352,355].

3.6 Sialyltransferase inhibitors

In the last two decades, several ST inhibitors have been identified in natural products or microbial metabolites, specifically designed or discovered via high-throughput screening methods. Based on their properties or origin, most of these inhibitors can be classified into five groups: i) acceptor analogues, ii) donor analogues, iii) bisubstrate analogues, iv) transition-state (TS) analogues and v) inhibitors from nature. Importantly, although many of these inhibitors have low-cell permeability and are not suitable for therapeutic intervention, some of them have shown promising effects *in vivo* and can potentially be used for clinical treatment of cancer metastasis.

i) Acceptor analogues

STs catalyse the transfer of a SA residue from a sugar nucleotide donor to a glycoconjugated acceptor, and their specificity is determined by the terminal structure of the acceptor glycan (Figure 18). To date, few acceptor analogues inhibitors have been synthesized but most of them exhibit only modest activity. The ones with remarkable inhibitory activity towards α2,6- or α2,3-STs respectively are the 6'-deoxy analogue, an analogue of methyl N-acetyl-β-lactosaminide from lactose [356], and the imino-linked methyl 5a'-carba-β-lactoside, a carba-oligosaccharide with a similar structure to the natural activated oligosaccharides [357].
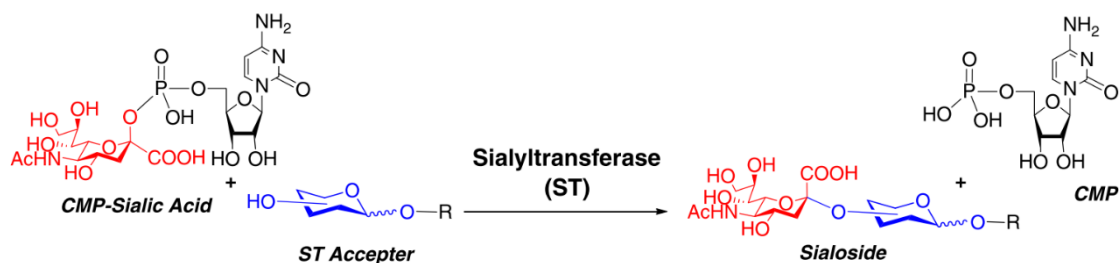
Figure 18.ST mechanism of action. Transfer of SA to a suitable glycan (ST accepter) using CMP-SA catalysed by STs (extracted from L.Wang et al. 2016 [358]).

ii) Donor analogues

Most of the inhibitors designed and synthetized recently are CMP-SA analogues (donor analogues), small molecules that bind to the active site of STs and prevent SA transfer by competing for its binding with the natural donor CMP-Neu5Ac. Based on the structural part of the CMP-Neu5Ac to which they resemble, these inhibitors can be classified into two subgroups: the cytidine analogues and the SA analogues.

First, the **cytidine analogues**, which generally contain a cytidine component that is essential for binding to the enzyme [359], helped to determine that the environment in the active site significantly differs between STs subtypes, since the methylcytosine derivatives of CMP

selectively inhibited ST3Gal III and ST3Gal IV, but not ST6Gal I [360]. In addition, CMP-Neu5Ac cytidine analogues such as cyclopentane α-hydroxyphosphonate coupled with cytidine phosphoramidite or with 5'-amino-5'-deoxyuridine fragment, were shown to block ST8SIA2-mediated polysialylation [361], as well as to strongly inhibit ST6Gal I by mimicking the planar structure of the donor in the TS (Figure 19) [362,363].
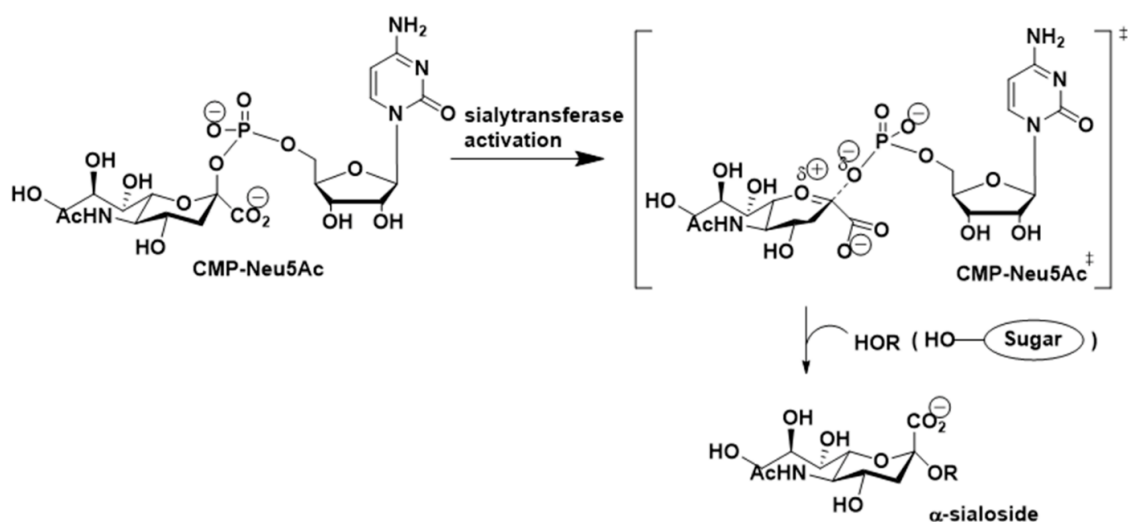
Figure 19. Proposed mechanism of ST-catalysed reactions and transition state (extracted from Pérez et al., 2021[364]).

Second, the **SA analogues**, include the 2-deoxy-2-fluorosugar nucleotide that had reduced ability to inhibit fucosyl- and STs [365] and the peracetylated analogue of Neu5Ac, called 2,4,7,8,9-pentaacetyl-3Fax-Neu5Ac-CO2Me (**Ac₅Fₐₓ-Neu5Ac**), recently reported by Paulson and co-authors [366]. Ac5Fax-Neu5Ac is characterized by a fluorine atom at the 3-position of the SA backbone (proximal to the endocyclic oxygen) that prevents SA transfer by destabilizing the oxocarbenium ion-like TS of the catalytic process [367,368]. Ac5Fax-Neu5Ac is able to cross the cell membrane by passive diffusion (due to the acetylation) and inside the cell, it is deacetylated by esterases and converted into activated CMP-3F-NeuAc (by the CMP N-acetylneuraminic acid synthetase (CMAS)), an extremely poor substrate for STs due to the electron-withdrawing effect of the fluorine atom, with the consequent inhibition of the synthesis of sialoglycoproteins (Figure 20). Moreover, the structural similarity of the inhibitor with the natural donors induces feedback inhibition of the *de novo* synthesis of CMP-Neu5Ac, by inhibiting UDP-GlcNAc 2-epimerase/ManNAc kinase (GNE), which is involved in N-acetylmannosamine (ManNAc) biosynthesis, the metabolic precursor of SA [369,370].
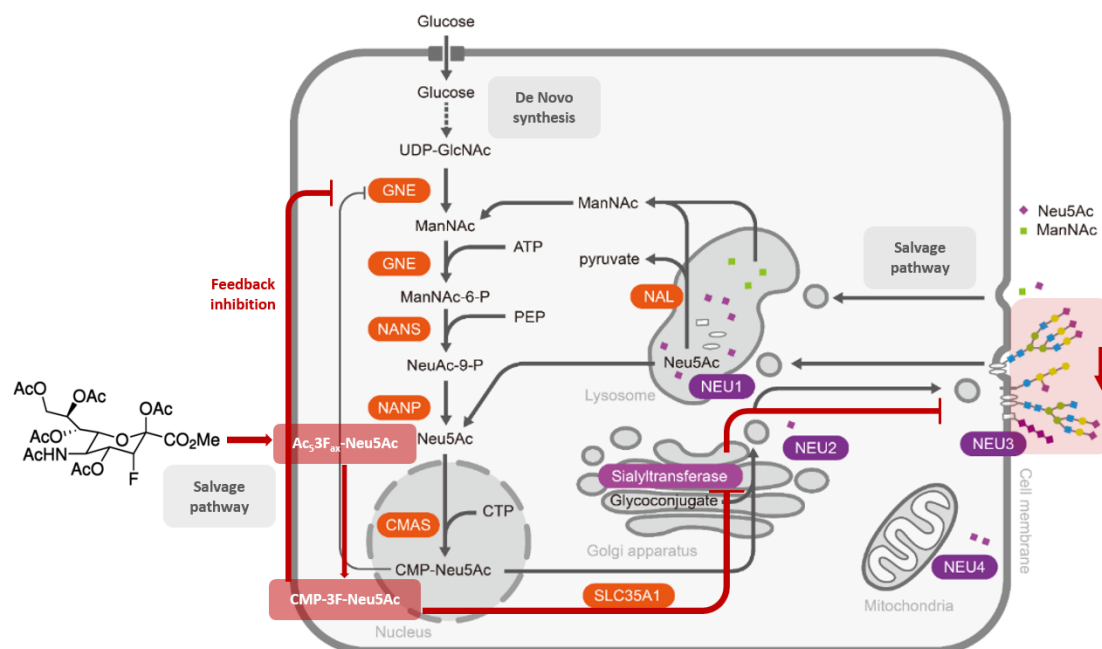
Figure 20. Biosynthesis of SA and mechanism of action of Ac$_5$3F$_{ax}$-Neu5Ac ST inhibitor. Ac$_5$3F$_{ax}$-Neu5Ac enters the cell by simple diffusion and it is activated into a poor substrate for STs (CMP-3F$_{ax}$-Neu5Ac), inhibiting STs action and preventing *de novo* formation of Neu5Ac.

Ac$_5$3F$_{ax}$-Neu5Ac was reported to effectively reduce the synthesis of sialylated glycan epitopes and to alter the cellular glycome in different cell models, and even in *in vivo* assays. In that sense, Büll and coauthors reported that Ac$_5$3F$_{ax}$-Neu5Ac had the potency to cause depletion of α2,3- and α2,6-linked SAs in B16F10 murine melanoma cells, and consequently diminish adhesion and migratory cell capacities, and *in vivo* tumour growth [371]. In a posterior study, Ac$_5$3F$_{ax}$-Neu5Ac was reported as a global ST inhibitor *in vivo*, reducing sialylation in all the analysed tissues, although it produced kidney and liver dysfunction [372]. In order to selectively direct the inhibitor to cancer cells and reduce cytotoxicity, the inhibitor was encapsulated into poly (lactic-co-glycolic acid) nanoparticles coated with antityrosinase-related protein-1 antibodies, and its administration resulted in long-term SA blockade and prevented metastasis formation in a murine lung metastastis model [373]. This compound was also shown to suppress the interaction of α4 integrins with E-selectin, MADCAM1, and VCAM1 receptors by altering α4 integrin sialylation, thus preventing the entrance of myeloma cells into the protective bone marrow, where they are less sensitive to chemotherapeutics such as bortezomib [374]. Recently, Boltje group developed potent sialylation inhibitors via modification of the SA backbone of Ac$_5$3F$_{ax}$-Neu5Ac to generate C-5-modified 3-fluoro SA analogues, showing that the substitution of the natural N-acetamide group with a carbamate functionality increased the potency of the novel inhibitors due to a more efficient metabolism to its CMP analogue [375].

iii) Bisubstrate analogues

These inhibitors are designed to mimic donor and acceptor substrates and contain covalently bound motifs of donor and acceptor substrates. Usually formed by a lactose unit connected to an intact CMP-Neu5Ac, or a CMP-KDN, linked by a thioether or alkanedithiols, they have been described to modestly inhibit both α2,3- and α2,6-ST activity [376,377]. Although recent advances have been shown referring to the specific residues of the donor or acceptor fragment of the inhibitors involved in protein-ligand molecular interactions [378], further investigations are needed to clarify the potential of bisubstrate analogues.

iv) Transition state analogues

These compounds mimic the oxocarbenium-like TS of the STs mechanism (Figure 19), and several of them are generated by the addition of a planar structure bound to the CMP (resembling the geometry and charge distribution of CMP-Neu5Ac in the transition state) and the replacement of the carboxylate group with phosphonate [379–381]. Recently, the characterization of crystal structures of several STs, molecular docking and molecular dynamics simulations, as well as computational analysis have provided valuable knowledge of the binding of these compounds to the catalytic site of each STs, and the relevance of designing selective TS-based inhibitors for each STs subfamily [367,368,382–385].

v) Natural products
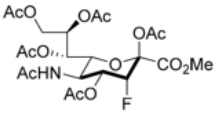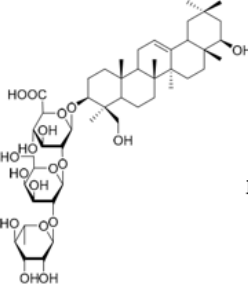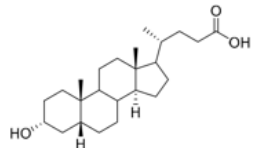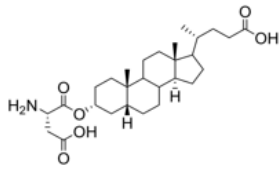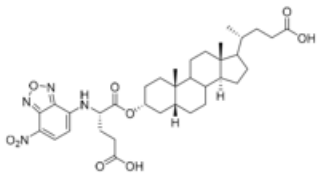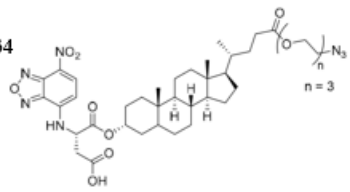
Natural products have been used as a source to obtain ST inhibitors, although their identification and purification processes are still a limiting factor. One of the more important compounds included in this group is the **Soyasaponin-I** (SsaI), a rigid pentacyclic system with a trisaccharide component derived from crude soybean saponin [386]. This inhibitor was initially described to compete with CMP-Neu5Ac for the binding to ST3Gal I, selectively reducing α2,3-linked SA expression without affecting other surface glycans [386], and posterior studies also related SsaI sialic inhibition with impaired adhesion, migratory, and metastatic abilities of breast and melanoma tumour cells [387,388].

Another subgroup of the nature-derived inhibitors are the steroidal compounds, which includes **lithocolic acid** (Lith), a compound that mimic the pentacyclic ring of SsaI, and its synthetic derivatives [389]. Among these derivatives, Lith-O-Asp was shown to reduce α2,3- and α2,6-sialylation by inhibiting ST3Gal I, ST3Gal III, and ST6Gal I, and to reduce migration ability *in vitro* and metastasis formation *in vivo* [390]. Another Lith derivative that showed encouraging results was **AL10**, a selective inhibitor of α2,3-STs activity, that was reported to impair cell adhesion, migration, and invasion of lung cancer cells by decreasing

sialylation of α5, αv, and β1 integrins, as well as to supress lung metastasis *in vivo* [391]. Recently, two Lith-O-Asp analogues (FCW34 and FCW36) were generated following the Lith extension strategy, in which one or more ethylene glycol units were added to the cyclopentane ring side chain of Lith-O-Asp to form the isozyme-specific, cell-permeable STs inhibitors. FCW34 inhibitor was shown to inhibit tumour growth, metastasis, and angiogenic activity in diverse breast cancer animal models [392]. In addition, there are many other STs inhibitors derived from natural products such as flavonoids, alginate oligosaccharides and ginsenosides that have been recently reviewed by Pietrobono et al [393].

Among all the above mentioned ST inhibitors, few of them have shown promising results in *in vivo* biological and preclinical studies (Table 3) and some of them are commercially available (Ac$_5$3F$_{ax}$-Neu5Ac, SsaI, Lith, and Lith-O-Asp). However, the discovery of subtype-selective and effective ST inhibitors is still necessary [364].

Table 3. Selected promising ST inhibitors as antimetastasic candidates. EC_{50} refers to the half maximal effective concentration, and IC_{50} refers to the half maximal inhibitory concentration of the inhibitors (extracted and adapted from Perez et al., 2021 [364]).

Inhibitor Name	Chemical Structure	ST Inhibition	ST Subtype Selectivity	Preclinical Data	Clinical Data
Peracetylated-3F$_{ax}$-Neu5Ac		EC_{50} = 26.8 μM (α2,3-sialylation, B16F10 cells)	N.D.	Impaired cancer cell adhesion to ECM components, inhibited cell migration, and reduced tumour growth in vivo	N.D.
Soyasaponin-I		K_i = 2.3 μM (ST3Gal-I); inhibited the expression of α2,3-linked sialic acids on B16F10 cell surface	N.D.	Enhanced cell adhesion to ECM proteins and decreased the migration ability of B16F10 cells but showed no effect on cell invasiveness; reduced pulmonary metastasis in vivo	N.D.
Lithocolic acid		IC_{50} = 21 μM (rST3Gal-I)	N.D.	N.D.	N.D.
Lith-O-Asp		IC_{50} = 37 μM (rST3Gal-I), 15.8 μM (hST6Gal-I), 12.2 μM (hST3Gal-III)	Non-selective	Inhibited migration and invasion abilities of lung and breast cancer cells in vitro; reduced lung metastasis in vivo; supressed tube formation in HUVEC and upregulated angiogenic inhibidors; inhibited the integrin/FAK/paxillin signaling pathway and its corresponding downstream effectors	N.D.
AL10		IC_{50} = 0.88 μM (rST3Gal-I), 1.50 μM (hST6Gal-I)	Non-selective	Inhibited adhesion, migration, actin polymerization and invasion of α2,3-ST-overexpressing A549 and CL1-5 cells; supressed lung metastasis in vivo	N.D.
FCW34		IC_{50} = 1.74 μM (hST3Gal-III), 3.60 μM (hST6Gal-I), >500 μM (rST3Gal-I)	ST3Gal-III and ST6Gal-I selective	Diminished migration ability of MDA-MB-231 cells; attenuated sialylation of integrin β1, β3, β4, and β5; exhibited in vivo metàstasis inhibition and decreased tumour growth; inhibited talin/integrin/FAK/paxillin and integrin/ NFκB signalling pathways; lessened neovascularization in a transgenic zebrafish model	N.D.

AIMS & SCOPE

Tumour aberrant glycosylation, in particular several sialylated determinants such as sLe$^{x/a}$, has been associated with cancer progression and metastasis spread as well as in modulating the immune component of the TME. In this regard, STs, which are the enzymes that transfer the SA to generate those tumour sialylated determinants, have been postulated as potential therapeutic targets. Previous studies performed in our group determined the importance of the α2,3-STs ST3GAL3 and ST3GAL4 in the tumour phenotype of PDA cell lines as well as the effect of ST3GAL3 and ST3GAL4-mediated sialylation on cell adhesion molecules involved in tumour progression, such as α2β1 integrin and E-cadherin. Considering the key role of EGFR on intracellular signalling pathways involving cell proliferation, apoptosis and metastatic spread, the study of EGFR glycosylation in several cancer types has increased in the recent years. Nonetheless, the role of EGFR sialylation on PDA progression is still unclear. This knowledge would be of interest to develop anti-EGFR combined cancer therapies. Besides, the recent discovery and development of ST inhibitors have represented a potent strategy to therapeutically target tumour cell STs and reduce tumour cell sialylation.

Based on this evidence, the **main goal** of this thesis is to gain insight into the role of the STs and their corresponding tumour sialoglycans on the phenotype of PDA cells as well as to study their effect on the function and signalling of EGFR. In order to accomplish this purpose, two studies were defined addressing the following aims and specific sub-objectives:

1. To determine the impact of α2,3-STs ST3GAL3 and ST3GAL4 knockdown on EGFR signalling in BxPC-3 and Capan-1 PDA cells:

   1.1. To determine the effect of ST3GAL3 KD and ST3GAL4 KD on EGFR sialylation pattern by immunopurification of EGFR from PDA cells.

   1.2. To study the effect of ST3GAL3 KD and ST3GAL4 KD on EGFR activation, dimerization, downstream signalling and cell proliferation rate upon EGF-induction.

   1.3. To assess the sensibility of ST3GAL3 KD and ST3GAL4 KD PDA cells to the anti-EGFR drugs Erlotinib and Cetuximab.

2. To assess the effect of three potential ST inhibitors on the reduction of sialylation of PDA human and murine cells and to evaluate their effect on the tumoural phenotype of these cell lines *in vitro* as well as their effect in an *in vivo* mice model:

   2.1. To determine the potential of three ST inhibitors to reduce cell sialylation in BxPC-3 and Capan-1 human PDA cell lines and identify the best candidate to proceed with the following sub-objectives.

   2.2. To study the effect of the SA reduction caused by the ST inhibitor treatment on the E-selectin adhesion, migration and invasion capabilities of human and murine PDA cells *in vitro*.

   2.3. To generate pancreatic subcutaneous tumours from murine PDA cells in immunocompetent syngeneic mice in order to evaluate the effect of intratumoural STs inhibitor injections on tumour growth, tumour SA expression and tumour immune component.

MATERIALS & METHODS

1. Cell lines

The origin, genetic background and routine culture conditions for the human and mice pancreatic adenocarcinoma cell lines are described in this section.

1.1 Human PDA cell lines

The human PDA cell lines used in this study are BxPC-3 and Capan-1:

BxPC-3 was obtained from the cell repository at Hospital del Mar Medical Research Institute (IMIM), Barcelona, Spain. This cell line was originally obtained from a 61-year-old woman's adenocarcinoma and it has been considered as a non-metastatic cell line. Particularly, these cells contain wild type (WT) *KRAS* [394]. It has medium expression of ST3GAL3 and ST3GAL4 STs genes, and express medium levels of sLe^x [326].

Capan-1 was purchased from the American Type Culture Collection (ATCC, HTB-79) and is a well-differentiated cell line. It was obtained from a liver metastasis of a 40-year-old male with a pancreatic adenocarcinoma, and it has been described to have a high tumorigenic and metastatic potential [394]. This cell line has medium expression of ST3GAL3 and ST3GAL4 STs genes, and express high levels of sLe^x [270,324,326]. Regarding genetic alterations, this cell line presents the four most common mutations in PDA, affecting *KRAS*, *TP53*, *CDKN2A/p16,* and *SMAD4* genes.

To investigate the role of ST3GAL4 and ST3GAL3 in human PDA, our group previously targeted both genes for silencing through shRNA technology in BxPC-3 and Capan-1 cell lines, generating the corresponding ST3GAL3 and ST3GAL4 Knocked Down (KD) cell lines. Parental cells were simultaneously transduced with a scramble control containing a non-targeting sequence (shScramble cells). For the expression of sLe^x, sLe^a and α2,3- and α2,6-SA were characterized by flow cytometry (FC) and Western Blot (WB) [326].

Cells were cultured at 37 °C in a 5% CO_2 humidified atmosphere. BxPC-3 and Capan-1 were routinely grown in Dulbecco's modified Eagle's Medium (DMEM) from Gibco, supplemented with 100 U/mL penicillin, 100 U/mL streptomycin and 2 mM L-glutamine, and 10% fetal bovine serum (FBS) for BxPC-3 and 20% for Capan-1 cells. BxPC-3 or Capan-1 KD cells or cells containing irrelevant vector (shScramble) were cultured with DMEM containing puromycin dihydrochloride (Sigma) at a final concentration of 1.5 μg/mL for BxPC-3 and 1 μg/mL for Capan-1 cells. Cells were grown in adherent conditions until 70-80% of confluence was reached and passaged following conventional protocols. All cell lines were routinely tested with the Venor® GeM OneStep Mycoplasma Detection Kit (Minerva Biolabs) to confirm the absence of mycoplasma.

1.2 Murine PDA cell lines

Murine PDA cell lines MLK2343, MLK2242, MLK2300, MJU241, MJU222, MJU215, ATQ79, ATQ1730, MSB188, MSB262, OBB452, and OBB473 were obtained from the Spanish National Cancer Research Center (CNIO) Experimental Oncology group (kindly given by Dra.Guerra, CNIO, Madrid).

MLK2343, MLK2242, MLK2300, MJU241, MJU222, MJU215 cell lines were extracted and generated from mice with TetoCre (+/T): Kras (+/LSLG12Vgeo) p53 (lox/lox) genotype (LSL). ATQ79 and ATQ1730 cell lines from ELA (+/E) TetoCre (+/T) Kras (+/LSLG12Vgeo) p53 (+/+). MSB188 from Tg-Pdx1-Cre (+/+) Kras LSLG12D (+/KI) Raf 1 (+/lox) Ptf1-Cre (+/T) P53 (+/+); MSB262 from Tg-Pdx1-Cre (+/+) Kras LSLG12D (+/KI) Raf 1 (+/+) Ptf1-Cre (+/T) P53 (+/+) (KC); OBB452 from Tg.Pdx1-Cre (+/T) Kras_LSLG12D (+/KI) p53_ lox (+/lox) (KPC); and OBB473 from Tg.Pdx1-Cre (+/T) Kras_LSLG12D (+/KI) p53_ lox (+/lox) (KPC).

Cells were cultured at 5% CO_2 and 37 °C stable temperature. DMEM (Gibco), supplemented with 10% FBS, 100 U/mL penicillin, 100 U/mL streptomycin, and 2 mM L-glutamine, was

used for all cell lines. Mycoplasma absence was confirmed by routinely testing all cell lines with Venor® GeM Mycoplasma Detection Kit (Minerva Biolabs).

2. Cell lysis

Cells were seeded in individual 60-mm cell culture dishes or in 6-well plates until they reached a confluence of 75-80% or until the treatment was finished (STs Inhibitor treatment). Cells were washed twice with cold Dulbecco's phosphate buffered saline (DPBS, Lonza) and incubated with Tris or phosphate RIPA lysis buffer on ice for 15 min. Tris based RIPA lysis buffer (25 mM Tris-HCl pH 7.4, 1% NP-40 (v/v), 100 mM NaCl, 2 mM EDTA, 10 mM sodium fluoride, 1 mM PMSF, 0.2 mM sodium orthovanadate, and complete™ ULTRA tablets protease inhibitors cocktail (Roche)) was used for EGFR immunopurification assays and phosphate based RIPA lysis buffer (20 mM Sodium Phosphate pH 7.4, 150 mM NaCl, 1% Triton X-100, 250 μg/mL sodium orthovanadate, and cOmplete™ ULTRA tablets protease inhibitors cocktail (Roche)) was used for the other experiments. Afterwards, cells were detached using a cell scrapper, collected and mechanically lysed with a 25-gauge needle. Then, lysates were cleared by centrifuging at 14000 g for 10 min at 4 °C and the protein concentration in the supernatants was quantified with the QuickStart™ Bradford Protein Assay (Bio-Rad) kit (see Materials & Methods section 3) and immediately used for subsequent analysis or stored at -80 °C.

For PDA murine cell lines, total protein extracts were provided by the group "Cancer Molecular Targets" of the associated Unit Hospital del Mar Medical Resarch center (IMIM)-Institute of Biomedical Research of Barcelona (IIBB). Lysates were prepared using Laemmli Buffer 1X (2% SDS, 40% glycerol, 5% 2-mercaptoethanol (β-ME), 0.005% bromophenol blue, 62.5 mM Tris HCl, pH 6.8), boiling at 100 °C for 10 min and centrifuged for 5 min at 13000 g.

3. Protein quantification

Protein concentration in the cell lysates was determined using the QuickStart™ Bradford Protein Assay (Bio-Rad) kit in 96 well plates (Corning) following manufacturer's instructions and using Bovine Serum Albumin (BSA) as standard (Bio-Rad). The standard curve was diluted with the equivalent lysis buffer concentration of the diluted samples. Each sample and standard curve was prepared in triplicate and absorbance was read at 595 nm with the Synergy 4 automated microplate reader (BioTek).

4. SDS-PAGE

Prior to SDS-PAGE, protein lysates were diluted with 4x Laemmli Buffer containing 5% v/v β-ME as a reducing agent, to a final concentration of 1x for Laemmli Buffer and 1.25% for β-ME. In order to denature the proteins, samples were heated for 5 min at 95 °C. Different quantities of cell lysates were loaded into 5% acrylamide gels for stacking and 8% acrylamide gels for resolving for all the experiments except for AKT and MAPK protein analysis (10% acrylamide resolving gel) and dimerization assay (3% acrylamide for stacking and 5% acrylamide for resolving gel). 3 µL of protein molecular weight standards from 10 to 180 kDa (Thermo Scientific PageRuler Prestained Protein Ladder) were also loaded into the gels. Mini-Protean Tetra Cell (Bio-Rad) was used to run electrophoresis at 100-120 V.

5. Western blot

Following electrophoresis, proteins were transferred onto PVDF membranes (Immobilon-P® membrane 0.45 µm, Millipore) either at 100V for 4 h or at 30 V overnight at 4 °C in Tris-glycine transfer buffer (191 mM glycine, 24 mM Tris, and 20% methanol). After transferring the proteins, membranes were washed with TBS-T (Tris Buffered Saline [10 mM Tris-HCl pH 7.5, 100 mM NaCl] containing 0.1% tween-20) for 5 min at room temperature (RT), and blocked at RT for 1 h to overnight (ON) with the corresponding blocking solution (BSA or non-fat dry milk).

After blocking, membranes were washed with TBS-T as described above and incubated with a specific primary antibody or lectin, using conditions specified in Table 4. The buffer composition for lectin incubation was: 100 mM Tris-HCl pH 7.6, 150 mM NaCl, 1 mM CaCl$_2$, and 1 mM MgCl$_2$.

Table 4. WB analyses conditions. Primary antibodies and lectins used for immunoblotting and incubation conditions.

Protein/glycan structure	Antibody-lectin	Host	Dilution	Incubation time	Blocking solution
EGFR	Ab52894 Abcam	Rabbit	1/5000 in TBS-T 3% milk	1 h RT	TBS-T, 3% milk
EGFR	Sc-373746 (A-10) Santacruz Biotechnology	Mouse	1/1000 in TBS-T 3% milk	1 h RT	TBS-T, 3% milk
Total pTyr	p-Tyr Ab (PY20) HRP sc-508 Santacruz Biotechnology	Mouse	1/3000 in TBS-T 3% BSA	1 h RT	TBS-T, 3% BSA
p-Y1068	p-EGFR Ab Tyr 1068 (1H12) #2236 Cell Signaling Technology (CST)	Mouse	1/1000 in TBS-T 5% milk	ON 4 ºC	TBS-T, 5% milk
p-Y1173	p-EGFR Ab Tyr 1173 (53A5) #4407 CST	Rabbit	1/1000 in TBS-T 5% BSA	ON 4 ºC	TBS-T, 5% BSA
p-Y1045	p-EGFR Ab Tyr 1045 #2237 CST	Rabbit	1/1000 in TBS-T 5% BSA	ON 4 ºC	TBS-T, 5% BSA
p-S1046/1047	p-EGFR Ab Ser 1046/1047 #2238 CST	Rabbit	1/1000 in TBS-T 5% BSA	ON 4 ºC	TBS-T, 5% BSA

Protein/glycan structure	Antibody-lectin	Host	Dilution	Incubation time	Blocking solution
Total AKT	#9272 Cell Signaling Technology	Rabbit	1/2000 in TBS-T 5% BSA	ON 4 ºC	TBS-T, 5% BSA
p-AKT	#4058 Cell Signaling Technology	Rabbit	1/2000 in TBS-T 5% BSA	ON 4 ºC	TBS-T, 5% BSA
Total MAPK	#9102 Cell Signaling Technology	Rabbit	1/2000 in TBS-T 5% BSA	ON 4 ºC	TBS-T, 5% BSA
p-MAPK	#9101 Cell Signaling Technology	Rabbit	1/2000 in TBS-T 5% BSA	ON 4 ºC	TBS-T, 5% BSA
ErbB2	Sc-33684 (3B5) Santacruz Biotechnology	Mouse	1/1000 in TBS-T 3% milk	ON 4 ºC	TBS-T, 5% milk
ErbB3	Sc-285 (C-17) Santacruz Biotechnology	Rabbit	1/1000 in TBS-T 5% BSA	ON 4 ºC	TBS-T, 3% BSA
sLe^x	551314 (CSLEX1 clone) BD biosciences	Mouse	1/70 in TBS-T 0,5% BSA	2 h, RT or ON, 4 ºC	TBS-T, 3% BSA
sLe^a	Ab3982 Anti-CA 19-9 (121SLE) Abcam	Mouse	1/1000 in TBS-T, 0,5% BSA	1 h RT or ON, 4 ºC	TBS-T, 3% BSA
a-tubulin	Sc-5286 (B-7) Santacruz Biotechnology	Mouse	1/500 in TBS-T, 3% BSA	1 h, RT or ON, 4 ºC	TBS-T, 5% BSA

Protein/glycan structure	Antibody-lectin	Host	Dilution	Incubation time	Blocking solution
a2,3-SA	Biotinylated *Maackia Amurensis Agglutinin II* (MAA-II)	-	1/500 in lectin buffer	2 h RT	TBS-T, 2% PVP
a2,6-SA	Biotinylated *Sambucus Nigra Agglutinin* (SNA)	-	1/1000 in lectin buffer	2 h RT	TBS-T, 2% PVP

After incubation, the membranes were washed 3 times with TBS-T and incubated for 1 h at RT with the corresponding secondary antibodies or streptavidin conjugated to peroxidase, as listed below in Table 5.

Table 5. WB analysis conditions. Peroxidase-conjugated detection reagents and usage conditions.

Secondary reagent	Host	Dilution
Peroxidase-Conjugated Anti-mouse IgG (H&L Chain Specific) Millipore (401215)	Goat	1/10000 in TBS-T, 0,5% milk
Peroxidase-Conjugated Anti-mouse IgG + IgM Jackson Immune Research (115-035-044)	Goat	1/40000 in TBS-T, 0,5% BSA
Peroxidase-Conjugated Anti-rabbit IgG (H&L) ThermoFisher (31460)	Goat	1/400000 in TBS-T 3% milk
Streptavidin-Peroxidase Conjugate GE Healthcare (RPN1231V)	-	1/100000 in TBS-T, 1 % BSA

After secondary antibody incubation, membranes were washed again and incubated with tempered Immobilon Western Horseradish Peroxidase (HRP) Substrate (EMD Millipore). Chemiluminescence was visualized using the imaging system Fluorchem SP (AlphaInnotech, San Leandro, CA, USA) under non-saturating conditions.

Densitometry analysis was performed with the Fluorchem SP software or with ImageJ software (NIH)). The density of the bands was normalized to the total EGFR or tubulin levels and relative quantity was expressed as fold change compared to control cells (shScramble).

6. Stripping

In order to remove the antibodies previously attached to the membrane and reblot them with another primary antibody, a stripping protocol was used. Briefly, membranes were washed thoroughly thrice with double-distilled water and twice with TBS solution (10 mM Tris-HCl pH 7.5, 100 mM NaCl) (5 min washes at RT). Then, membranes were incubated with Restore™ WB Stripping Buffer (Thermo Scientific) at the shaker during 10 min at RT and for 20 min more at 37 ºC (20 mL for entire membranes or 10 mL for half-membranes). Membranes were washed again with TBS solution (2 x 10 min washes) and with TBS-T (2 x 5 min washes), in order to get rid of the stripping buffer, and then blocked with corresponding blocking solution for at least 2 h at RT. Ordinary WB protocol was followed from that point on.

Stripping protocol was used in different experiments. First, it was used to corroborate the presence of sLe^x on EGFR following EGFR immunopurification. Second, membranes used for pAKT and pMAPK determination were stripped and used to determine total-AKT and total-MAPK presence, using the conditions specified in Table 4. Finally, stripping protocol was also used to reblot the membranes with an antibody against α-tubulin, a constitutively expressed protein that was used as a loading control of the WB.

7. Immunoprecipitation

BxPC-3 KD, Capan-1 KD and control cells were seeded on 100-mm dishes and allowed to grow to 70-75% confluence. Cells were lysed in ice-cold Tris-based RIPA lysis buffer as specified at Material & Methods section 2 and protein concentration was quantified.

500 µg of total protein lysate for BxPC-3 and 500 µg, 1000 µg, or 2000 µg for Capan-1 were used to purify EGFR and detect *Sambucus nigra Agglutinin* Lectin (SNA), *Maackia amurensis* Lectin II (MAA-II) and sLe^x on EGFR respectively. Cell lysates were first pre-cleaned incubating them with Cytiva™ Protein-A sepharose (Sigma Aldrich,17078001) for 2 h at 4 ºC on a 0.22 µm Spin-X Centrifuge Tube Filter (Costar, Corning, NY) according to manufacturer's protocol. Meanwhile, 1 mg of the SureBeads™ Protein A Magnetic Beads

(Bio-Rad) was incubated with 2 µg of an anti-EGFR antibody (Abcam, ab52894) for 45 min at RT in incubation buffer (50 mM Tris-HCl pH 7.4, 150 mM NaCl, 0.05% BSA, and 1% Tween-20). Then, magnetic beads were washed thrice with washing buffer (50 mM Tris-HCl pH 7.4, 150 mM NaCl, and 1% Triton 100X) to get rid of the unbound antibody and pre-cleared lysate was incubated for 4 h at 4 ºC and in vortex gentle shaking. Magnetic beads were washed again and incubated at 100 ºC for 8 min with 50 µL of 2x Laemmli buffer containing 2.5% β-ME to elute EGFR bound protein. Eluted samples were loaded into an acrylamide gel and blotted against anti-sLe^x antibody, SNA or MAA-II lectin following the protocols described above.

8. EGFR activation assay

To study EGFR activation in BxPC-3 KD, Capan-1 KD and control cell lines, cells were treated with EGF and then analysed by WB. Cells were seeded into 100-mm dishes, allowed to attach and grow to 70% confluence during 48 h for BxPC-3 cells or 72 h for Capan-1 cells, starved the following 24 h in incomplete DMEM (0%FBS), and treated for 10 min at 37 ºC with the optimal EGF dose, which was previously determined (20 ng/mL for BxPC-3 cells and 40 ng/mL for Capan-1 cells). Next, cells were lysed and the same quantity of protein for each sample was electrophoresed and analysed by WB with a mouse mAb against total phosphotyrosines conjugated to HRP (PY20, sc-508) and a primary antibody against EGFR (A-10, sc-373746), as specified in Table 4. Specific phosphorylated EGFR residues levels were also analysed: p-Y1068 (#2236) and p-Y1173 (#4407), involved in proliferation signalling, and p-S1046/47 (#2238) and p-Y1045 (#2237), and α-tubulin as a loading control. For the analysis of AKT and MAPK proteins activation, 20 µg of protein (exceptionally 10 µg for BxPC-3 MAPK analysis) were electrophoresed and analysed in parallel by Western blotting with primary antibodies against phospho-AKT (#4058) and phospho-MAPK (#9101). Afterwards, membranes were stripped and reblotted with primary antibodies against total-AKT and MAPK proteins.

9. Dimerization analysis

In order to analyse EGFR dimerization in KD and control BxPC-3 and Capan-1 cells we performed chemical cross-linking experiments as previously described by Panosa et al. [395] with minor modifications. Briefly, BxPC-3 and Capan-1 cells were seeded in 6-well plates, allowed to attach for 24 h with 10 or 20% FBS containing DMEM, and then starved during 24 h with incomplete DMEM (0% FBS). Cells were lysed with 150 µL of ice-cold Sodium

Phosphate RIPA buffer and harvested following the protocol described at section 3, and protein concentration in cell lysates was determined by QuickStart™ Bradford Protein Assay (Bio-Rad). Then, aliquots of 75 µg of protein were activated by adding 150 nM Human Recombinant EGF (Thermo Fisher Scientific) for 30 min at RT. For each assay, not activated control BxPC-3 and Capan-1 cells were used as negative control. Then, 30 mM glutaraldehyde (Sigma) was added to induce EGFR cross-linking and after 1 min, the reaction was stopped by adding 0.2 M glycine pH 9. After that, 4x Laemmli Buffer containing 5% β-ME was added and samples were boiled during 5 min. Lysates were loaded onto 5% polyacrylamide gels, electrophoresed for 1 h at 200 V, and transferred onto PVDF membranes at 100 V for 3 h at 4 °C in Tris-Glycine transfer buffer. EGFR dimer formation was analysed by Western blotting with specific primary antibodies against EGFR (Ab52894) and ErbB3 (sc-285), using conditions detailed in Table 4.

10. Cell proliferation analysis

To assess cell proliferation capacity of KD cells vs control ones, 3000 cells/well were seeded in 96-well plates, allowed to attach for 24 h, starved for 24 h in incomplete DMEM and treated with incomplete DMEM supplemented with 50 ng/mL EGF along the assay in a final volume of 100 µL per well (DMEM supplemented with 50 ng/mL EGF was changed every 48 h). We seeded an identical plate for each incubation time, considering the beginning of EGF treatment as the starting point of the assay. After 0 h, 48 h, 96 h, and 120 h of EGF treatment we determined cell proliferation by MTT (3-(4,5-dimethylthiazol-2-yl)-2,5-diphenyltetrazolium bromide, Sigma) assay: EGF containing DMEM was removed carefully and cells were washed twice with 200 µL/well of cold DPBS. A 10% MTT (Sigma) solution diluted in incomplete DMEM was added to each well and plates were incubated for 2 h at 37 °C. After that time, DMEM was removed and purple formazan crystals were dissolved by adding 200 µL/well of dimethyl sulfoxide (DMSO) (Sigma). Plates were gently agitated at RT for 2 min and absorbance was read at wavelength of 570 nm with the Synergy 4 automated microplate reader (BioTek). Cell viability of ST3GAL3 KD and ST3GAL4 KD cells was expressed as relative levels compared to untreated cells, which was calculated by dividing the mean absorbance of each treated sample by the mean absorbance of the corresponding untreated cells (each sample was tested by quintuplicated).

11. Cytotoxicity assay

To assess the responsiveness of BxPC-3 KD, Capan-1 KD and control cells to the EGFR inhibitors Erlotinib (sc-202154, Santa Cruz Biotechnology) and Cetuximab (Erbitux) cytotoxicity assays were performed.

First, a seeding test was carried out to determine the optimal initial cellular concentration as explained below. Different number of cells per well (1000, 2000, 3000, 4000, and 5000 cells/well) were seeded in quintuplicate in 96-well plates and after 24 h and 48 h of incubation at 37 ºC and humidified 5% CO_2 atmosphere, cells were observed with a CKX41 inverted microscope (Olympus) to assess the cell confluence in the wells. 5000 cells/well was chosen as the optimal cell concentration for BxPC-3 and Capan-1 cells.

Erlotinib was dissolved in DMSO to obtain a 2 mg/mL (4652.24 µM) stock solution. Cetuximab, provided by the Pharmacy service of the Catalan Institute of Oncology (ICO) of Girona (Hospital Josep Trueta, Girona, Spain), was at 5 mg/mL. For each assay, necessary aliquots of the drug solution were diluted in DMEM to obtain the fresh working solutions (DMSO final concentration in the culture media was always <1%).

5000 cells per well were seeded in 96-well plates in culture medium and allowed to attach for 24 h at 37 ºC. Increasing concentrations of Erlotinib solution (0 µM, 1.25 µM, 2.5 µM, 5 µM, 10 µM, 25 µM, and 50 µM) or Cetuximab (50 µg/mL, 100 µg/mL, 250 µg/mL, 400 µg/mL, and 500 µg/mL) were added to the wells (quintuplicates for each condition) in a final volume of 100 µL.

Cells were incubated during 48 h at 37 ºC and then, treatments were removed by carefully aspirating the DMEM and cell viability was determined by MTT assay as described above.

For each experiment, cell viability was calculated by dividing the mean absorbance of each treatment by the mean absorbance of control cells, treated with the vehicle alone. The concentration that reduces the cell viability by 50% (IC_{50} ± standard error SE) was stablished for each compound by non-linear regression and curve fitting using Synergy 4 automated microplate reader Gen5 software.

12. Flow cytometry analysis

FC was used to characterize carbohydrate determinants (sLe[x], sLe[a], α2,3-SA, α2,6-SA, and terminal β-galactose) expression on the membrane of human and murine PDA cell lines and to quantify their expression after STs Ac_5F_{ax}-Neu5Ac inhibitor treatment.

Cells were grown in flasks or petri dishes up to a confluence of 70-80%, trypsinized, resuspended in PBS, 2% BSA and counted. $1x10^5$ cells for each experimental sample were collected in eppendorfs and washed with cold PBS. Exceptionally, for $Ac_5 3F_{ax}$-Neu5Ac inhibitor treatment, cells were seeded into 24-well plates, allowed to attach for 24 h, and treated during 72 h with 100 μM STs inhibitor for BxPC-3 cells, 400 μM STs inhibitor for Capan-1 cells, and 200 μM STs inhibitor for OBB452 and MSB262 cells. $Ac_5 3F_{ax}$-Neu5Ac inhibitor was reconstituted in DMSO to a 90.66 mM stock solution, and diluted with DMEM to obtain the working concentration. For untreated control cells, DMEM with the corresponding concentration of the vehicle (DMSO) was added during treatment. After the incubation, cells were washed and all the cells contained in each well were collected in an Eppendorf tube to proceed with the cytometry protocol (cells were not counted at this point of the experiment).

Cells were pelleted by centrifugation at 2600 rpm for 8 min at 4 ºC, the supernatant was removed and the pellet was resuspended in 100 μl of primary antibodies or biotinylated lectins diluted in PBS 2% BSA as specified in Table 6 and 7, and then incubated during 30 min at 4 ºC. The anti sLe^x and anti-sLe^a mAbs were used both for human and murine cell lines since they are Ab directed to the specific glycan structures. Unstained cells (negative control) were incubated with PBS 2% BSA alone. Next, cells were washed again with PBS and then resuspended with 100 μl of PBS 2% BSA in the presence of the corresponding diluted secondary antibody for 30 min at 4 ºC in the dark. Then, cells were washed with PBS and resuspended in 300 μl of PBS 2% BSA for fluorescence analysis with the Acea NovoCyte® Flow Cytometer. At least $1x10^4$ cells were gated and analysed with the NovoExpress® software, and the median fluorescence of the cells was determined. Three or more independent assays were undertaken for each sample and the mean ± SD value was calculated. No cell aggregation or loss of viability was observed after antibody or lectin incubations.

Table 6. Primary and secondary antibodies conjugated to fluorescent dyes used for FC analysis of PDA human and murine cell lines.

Antibody	Host	Dilution	Supplier
Sialyl Lewis X 551314 Anti-CD15s (CSLEX1 clone)	Mouse	1/10	BD biosciences
Sialyl Lewis A Ab3982 Anti-CA19-9 [121SLE] antibody	Mouse	1/500	Abcam
EGFR Anti-human antibody (Ab-3) (Clone 225)	Mouse	1/100	Calbiochem, Sigma
Alexa Fluor™ 488 Anti-mouse IgG (H&L) (A11029)	Goat	1/400	Invitrogen

Table 7. Biotinylated lectins and streptavidin conjugated fluorescent dyes used for FC analysis of PDA human and murine cell lines.

Lectin/Conjugated Fluorophore	Dilution	Supplier
Biotinylated *Sambucus Nigra Agglutinin* (SNA) (B-1305)	1/100	Vector Laboratories
Biotinylated *Maackia Amurensis Agglutinin II* (MAA-II) (B-1265)	1/50	Vector Laboratories
Biotinylated *Peanut Agglutinin* (PNA) (B-1075-5)	1/100	Vector Laboratories
Alexa Fluor™ 488 conjugated streptavidin (S32354)	1/1000	Invitrogen

13. E-selectin binding assay

150000 control BxPC-3 and Capan-1 cells were seeded into 6-well plates, allowed to attach for 24 h and treated with the optimal dose of $Ac_5 3F_{ax}$-Neu5Ac ST inhibitor (Merck): 100 μM for BxPC-3 and 400 μM for Capan-1 during 72 h at 37 °C. $Ac_5 3F_{ax}$-Neu5Ac inhibitor treatment was performed as described at section 12.

In parallel, 2 µg/mL of the goat anti-human IgG (Fc) Affinity Purified Antibody (Merck, Sigma Aldrich) in a final volume of 100 µL was added to each well of a 96-well maxisorp microplate (Thermo Fisher Scientific) and incubated for 1 h at RT. Then, the antibody was removed, wells were carefully washed twice with sterile DPBS and blocked with 100 µl of DPBS solution containing 1% BSA (sterile filtered). After 1 h incubation at RT, wells were washed again with DPBS and 2 µg/mL of Recombinant Human E-selectin/CD62 Fc Chimera (rhE-selectin) (R&D Systems) diluted in 100 µl of DPBS (Ca+ and Mg+) was added to each well, with the exception of the negative control wells. rhE-selectin was incubated ON at 4 ºC to achieve the optimum binding to the antibody.

The following day, after 72 h of STs inhibitor treatment, cells were detached from the 6-well plates by trypsinization and 75000 cells/well for BxPC-3 and 50000 cells/well for Capan-1 were seeded into the 96-well maxisorp plates, which were previously washed to remove the unbound rhE-selectin. Cells were allowed to bind to rhE-selectin for 1 h at 37 ºC and then gently washed twice with DPBS. The remaining rhE-selectin bound-cells were estimated with the CellTiter 96R Aqueous One Solution Cell Proliferation Assay based colorimetric method (MTS, Promega) following the manufacturer's protocol. Briefly, fresh DMEM (100 µl) containing MTS (20 µl) was added to each well and cells were incubated between 1 and 2 h in the dark at 37 ºC. Finally, plates were agitated at RT for 2 min and the absorbance was read at a wavelength of 490 nm using the microplate automated reader Synergy 4 (BioTek). Quintuplicates were analysed for each sample, and each value of absorbance was normalized versus the corresponding negative control (without E-selectin). Adhesion of treated cells was expressed as a percentage of the untreated cells, which was calculated by dividing their mean absorbance by the mean absorbance of untreated cells. Three independent assays were carried out.

14. Transwell migration assay

Modified Boyden chambers in 24-well plates were used to evaluate cell migration. Prior to the migration experiments, 150000 BxPC-3 or Capan-1 control cells, 15000 OBB452 cells and 12000 MSB262 cells were seeded into 6-well plates and treated with 100 µM (BxPC-3), 400 µM (Capan-1), or 200 µM (OBB452 and MSB262) $Ac_5 3F_{ax}$-Neu5Ac STs inhibitor during 72 h at 37 ºC. For untreated cells, DMEM with the corresponding concentration of the vehicle (DMSO) was added during treatment period.

Prior to use, 8 µm pore size ThinCerts™ inserts (Greiner Bio-one) were coated during 1 h with 200 µL of 0% FBS DMEM with 0.001% Collagen type I from calf skin (Sigma) and 500

µL of 0% FBS DMEM were added in the lower chamber. Meanwhile, cells were trypsinized, washed twice with 0% FBS DMEM and resuspended in either DPBS, 1% BSA or 0% FBS DMEM. Just before seeding, untreated cells were incubated for 20 min at RT with anti-sLe^x (Clone CSLEX1) mouse mAb (BD biosciences, 1/10) or with anti CA-19.9 [121SLE] mouse mAb (Abcam, 1/500) in DPBS, 1% BSA. A mouse IgM [B11/7] antibody (Abcam) was used as an isotype control. DMEM with 0.001% Collagen type I was removed from the inserts and $2.5x10^4$ cells for BxPC-3, $5x10^4$ cells for Capan-1, $2x10^4$ for OBB452, and $3.5x10^4$ for MSB262, in a final volume of 100 µL were seeded into the top chamber and 500 µL of DMEM was added at the bottom as a chemoattractant. Cells were allowed to migrate for 18 h for BxPC-3, 22 h for Capan-1 or 24 h for OBB452 and MSB262 in the incubator and after that time, cell migration was evaluated by fixing, staining, and quantifying the covered area of the bottom part of the membrane. In short, the inserts were fixed with a 4% paraformaldehyde (PFA) solution in PBS (Santa Cruz Biotechnology) for 15 min and stained with 0.3% violet crystal solution (Scharlau) during 30 min. Then, inserts were thoroughly washed thrice with PBS and non-invading cells were removed from the upper part of the insert using humidified cotton swabs. Finally, at least 20 random fields for each transwell were photographed at 10x magnification under a CKX41 bright-field microscope (Olympus) and the cell covered area was quantified using ImageJ software (code for cell coverage is described below).

15. Transwell invasion assay

The invasive potential of treated and control BxPC-3, Capan-1, OBB452, and MSB262 cells was determined using a modified Boyden chambers assay in 24-well plates. Cells were seeded in 6-well plate and treated with Ac$_5$3F$_{ax}$-Neu5Ac for 72 h as described at section 12.

Before seeding the cells, the 8 µm pore size ThinCerts™ inserts (Greiner Bio-one) were rehydrated with a layer of 35 µg of basement membrane matrix (Matrigel, Corning) diluted in cold DPBS (final volume per well: 70 µL) and incubated between 50 and 60 min to let the Matrigel polymerize. Meanwhile, cells were trypsinized, washed twice with 0% FBS DMEM and resuspended in either DPBS, 1% BSA or 0% FBS DMEM. Just prior to cell seeding, untreated cells were incubated for 20 min at RT with anti-sLe (Clone CSLEX1) mouse mAb (BD biosciences, 1/10) or with anti CA-19.9 [121SLE] mouse mAb (Abcam, 1/500) in DPBS, 1% BSA. A mouse IgM [B11/7] antibody (Abcam) was used as an isotype control. $4x10^4$ cells for BxPC-3, $5x10^4$ cells for Capan-1, $5x10^4$ cells for OBB452, and $2.5x10^4$ cells for MSB262 in a final volume of 200 µL were seeded into the top chamber and 500 µL of

complete DMEM was added at the bottom as a chemoattractant. Cells were allowed to invade for 24 h for BxPC-3 and OBB452, 72 h for Capan-1, or 48 h for MSB262, in the incubator and then, cell invasion was evaluated by fixing, staining and quantifying the covered area of the bottom part of the membrane, as described above at section 14.

16. Code for cell coverage analysis

A Macro for Fiji software (ImageJ) was generated in order to automate image processing and quantification with the following code, written by X. Sanjuan. Important note: in order to reduce the code length, each jump of paragraph has been represented as (JUMP):

```
run("Options...", "iterations=1 count=1 black edm=Overwrite do=Nothing"); (JUMP)
MyDir = getDirectory("Choose a Directory"); (JUMP) MyList = getFileList(MyDir); (JUMP)
for(i=0;i<lengthOf(MyList);i=i+1) (JUMP) { (JUMP) if(endsWith(MyList[i], ".tif")) (JUMP)
{ (JUMP) open(MyDir+MyList[i]); (JUMP) MyImatge= getTitle(); (JUMP) MyImatge_ID=
getImageID(); (JUMP) run("Set Scale...", "distance=0 known=0 pixel=1 unit=pixel");
(JUMP) selectImage(MyImatge_ID); (JUMP) run("Split Channels"); (JUMP)
selectImage(MyImatge + " (green)"); (JUMP) MyTrueImatge_ID= getImageID(); (JUMP)
selectImage(MyImatge + " (blue)"); (JUMP) run("Close"); (JUMP) selectImage(MyImatge +
" (red)"); (JUMP) run("Close"); (JUMP) selectImage(MyTrueImatge_ID); (JUMP)
run("Median...", "radius=1"); (JUMP) run("Threshold..."); (JUMP) waitForUser("if neede
adjust threshold"); (JUMP) run("Convert to Mask"); (JUMP) run("Options...", "iterations=1
count=1 black edm=Overwrite do=Open"); (JUMP) run("Set Measurements...", "area
area_fraction redirect=None decimal=2"); (JUMP) run("Measure"); (JUMP)
selectImage(MyTrueImatge_ID); (JUMP) close(); (JUMP) selectWindow("Threshold");
(JUMP) run("Close"); (JUMP) } (JUMP) }
```

17. *In vivo* study of STs inhibitor effect

17.1 Syngeneic mice tumour generation

A total of 20 adult C57BL female mice were commercially acquired from Charles River and were housed in the animal facility of the Barcelona Biomedical Research Park (PRBB). This study had the perceptive authorizations from the Animal Research Ethics Committee (CEEA) from PRBB. 10-week aged mice were housed in groups of 4 or 5 animals per cage in a controlled environment (22±2 °C of temperature, 40-70% humidity, 12 h light/dark cycle). Mice free access to water and rodent chow was guaranteed during the experiment.

For tumour generation, 0.5×10^6 MSB262 cells were resuspended in incomplete DMEM and matrigel was added in 1:1 ratio. The cells were injected subcutaneously with a 29-gauge needle at the posteriors flanks of the mice. The following days, mice were observed and the presence of tumours was determined by palping them. After 2 weeks approximately, when palpable tumours of around 100 mm^3 appeared, we started Ac$_5$3F$_{ax}$-Neu5Ac STs inhibitor treatment: mice were distributed in four experimental groups: 10 mg/kg STs inhibitor group (n=7), 20 mg/kg STs inhibitor group (n=5), DMSO group (n=3), which received excipient injections, and control group (n=3), which were injected with physiological saline solution alone. Three intra-tumoural injections per week in a total volume of 20 µl were administered under isoflurane anaesthesia during 15 days or until the tumour volume exceeded 1000 mm^3. Mice were then sacrificed in CO_2 euthanasia chamber and tumour samples were collected to perform posterior analyses. Mice presenting compromised general welfare during the experiment were sacrificed following ethical guidelines.

Tumours were weighted and the three perpendicular diameters were measured with a calliper to estimate the tumour volume. General aspects were annotated such as tumour shape, consistence, subcutaneous or intramuscular localization, and vascularization.

For FC analysis, tumour samples were kept in cold DPBS and tumour digestion protocol was performed immediately in order to obtain a cellular suspension (described at section 17.2). Digested samples were preserved at -80 °C in FBS, 10% DMSO for posterior analysis.

17.2 Tumour digestion

Tumours were mechanically disaggregated with a carbon steel surgical blade and incubated with the digestion buffer (1 mg/mL collagenase, 5% FBS, 2 u/mL DNAsa in DPBS) for 40 min at 37 °C. Samples were agitated every 5-10 min to enhance the digestion process. After that time, cells were filtered with a 100 µm Cell Strainer and centrifuged at 30 g for 5 min at RT to discard remaining cell debris. Supernatant was centrifuged at 300 g for 5 min at RT and the pellet was resuspended with FBS containing 10% DMSO and frozen with a Nalgene® Mr.Frosty freezing container. Samples were preserved at -80 °C until they were used for FC analysis.

17.3 Immune component and tumour infiltrates analysis by flow cytometry

To study the immune component and the presence of tumour infiltrates, cellular suspension samples obtained from the tumours were processed by using the Cytek® Aurora spectral flow cytometer and analysed using the SpectroFlo software.

Cryotubes containing tumour cells were defrosted in complete DMEM (10% FBS) and centrifuged to discard DMSO from the media. Pellets were resuspended in complete DMEM, then cells were centrifuged again and resuspended in DPBS, 5% FBS to proceed with the antibody staining (except for the unstained controls, which were incubated with DPBS, 5% FBS alone). First, cells were incubated for 30 min at 4 °C and darkness with Live/Dead staining, washed twice with DPBS, 5% FBS and blocked with CD16 antibody for 15 min at 4 °C and in the dark (to block Fc receptors). Then, cells were washed again and incubated with a mix containing a panel of antibodies conjugated to specific fluorophores in DPBS, 5% FBS for 1 h at 4 °C and darkness as described in Table 8. After immunostaining, cells were washed once, resuspended in DPBS, 5% FBS and kept on ice until they were analysed by FC. Prior to the analysis of the samples, we performed a Set Up experiment to create the reference controls for each fluorescent tag with UltraComp eBeads™ Compensation Beads (ThermoFisher Scientific). SpectroFlo software was used to acquire and analyse the samples, to perform the spectral unmixing and identify and exclude the auto-fluorescence signals. At least 1.5×10^5 live cells were gated and analysed with the SpectroFlo software.

Table 8. FC antibody panel. Primary antibodies conjugated to fluorescent dyes used for FC analysis of murine digested tumour samples.

Antibody/Conjugated Fluorophore	Host/Isotype	Dilution	Supplier
Brilliant Violet 510™ anti-mouse CD8a Antibody (100752)	Rat IgG2a, κ	1/1000	BioLegend
APC anti-mouse CD3 Antibody (100235)	Rat IgG2b, κ	1/500	BioLegend
PerCP-Cy™5.5 Rat Anti-Mouse CD45 (550994)	Rat LOU	1/200	BD biosciences
APC-Cyanine7 anti-mouse CD4 (565650)	Rat DA, also known as DA/HA IgG2a, κ	1/400	BD biosciences

Antibody/Conjugated Fluorophore	Host/Isotype	Dilution	Supplier
PE/Cyanine7 anti-mouse Ly-6G Antibody (127618)	Rat IgG2a, ϰ	1/1000	BioLegend
FITC anti-mouse/human CD11b Antibody (101206)	Rat IgG2b, ϰ	1/4000	BioLegend
PE-Cy™5 Anti-Mouse CD45R/B220 (561879)	Rat IgG2b, ϰ	1/200	BD biosciences
Brilliant Violet 785™ anti-mouse F4/80 Antibody (123141)	Rat IgG2a, ϰ	1/100	BioLegend
Alexa Fluor® 700 anti-mouse Ly-6C Antibody (128023)	Rat IgG2c, ϰ	1/200	BioLegend
PE/Dazzle™ 594 anti-mouse CD49b (pan-NK1.1 cells) Antibody (108923)	Rat IgM, ϰ	1/1000	BioLegend
Brilliant Violet 650™ anti-mouse/human CD45R/B220 Antibody (103241)	Rat IgG2a, ϰ	1/100	BioLegend
Anti-mouse CD16 antibody	Rat IgG2a, λ	1/100	BioLegend
LIVE/DEAD™ Fixable Violet Dead Cell Stain Kit, for 405 nm excitation (L34963)	-	1/100	Life Technologies

17.4 Sialic expression analysis of tumour samples by flow cytometry

Glycan structures expression of tumour cells after STs inhibitor tumour treatment was analysed by FC. Tumour cells were defrosted in complete DMEM (10% FBS) and centrifuged to discard DMSO from the media. Pellets were resuspended in complete DMEM and then centrifuged again and resuspended in DPBS, 3% BSA to proceed with the antibody staining (except for the unstained control, incubated with DPBS, 3% BSA alone). First, cells were incubated for 30 min at 4 °C with the corresponding biotinylated SNA or MAA-II lectin (see specifications in Table 9). After the lectin incubation, cells were washed once with DPBS, 3% BSA and incubated with 200 µl of a DPBS, 3% BSA solution containing CD45.2 PerCP/Cyanine 5.5 conjugated mAb and the Alexa Fluor™ 488 conjugated streptavidin for 30 min at 4 °C and darkness. Finally, cells were washed and resuspended in 500 µl of a DPBS, 3% BSA and cell fluorescence was acquired with the Acea NovoCyte® Flow Cytometer.

Samples were acquired and analysed by using the NovoExpress® software, a minimum of 1.5×10^4 cells within the gated region were analysed as described above.

Table 9. FC antibodies and lectins. Conjugated primary antibody, biotinylated lectins and streptavidin conjugated fluorescent dyes used for FC analysis of PDA murine cell lines.

Lectin/Conjugated Fluorophore	Dilution	Supplier
Biotinylated *Sambucus Nigra Agglutinin* (SNA) (B-1305)	1/100	Vector Laboratories
Biotinylated *Maackia Amurensis Agglutinin II* (MAA-II) (B-1265)	1/50	Vector Laboratories
PerCP/Cyanine5.5 anti-mouse CD45.2 Antibody monoclonal (109827)	1/100	BioLegends
Alexa Fluor™ 488 conjugated streptavidin (S32354)	1/1000	Invitrogen

18. Statistical analysis

All statistical analyses were performed using GraphPad-Prism8. Normality analyses were performed using the Shapiro-Wilk normality test. Statistical differences between paired groups were assessed using Student's t-test, for parametric comparisons or Mann-Whitney U test, for nonparametric comparisons. Statistical significant results were considered when $p < 0.05$ using a 95% confidence interval (*$p < 0.05$; **$p < 0.01$; ***$p < 0.001$). Otherwise stated, all data is presented as mean $\pm$ SD of at least 3 independent experiments. Kaplan Meier survival test and long-rank test were used to plot mice survival. All figures were designed with GraphPad-Prism8.

RESULTS & DISCUSSION

1. Chapter I. Impact of α2,3-sialyltransferases knockdown on EGFR signalling in BxPC-3 and Capan-1 PDA cells

1.1 Results

To determine the role of α2,3-ST in PDA, in a previous study of our group, we knocked-down ST3GAL3 and ST3GAL4 with specific shRNAs (shST3GAL3_6-10 and shST3GAL4_1-5, respectively) in BxPC-3 and Capan-1 human PDA cell lines [326]. The expression of sialylated determinants on ST3GAL3 and ST3GAL4 KD cells was characterized by FC and WB with lectins and specific antibodies. Results showed a significant decrease in α2,3-sialylated determinants, highlighting a reduction of the α2,3-SA epitope sLe^x (Neu5Acα2,3Galβ1,4[Fucα1,3]GlcNAcβ1-R) of about 37-73%, depending on the cell line and the silenced ST. The BxPC-3 and Capan-1 KD cells with highest reduction in sLe^x expression were the ones silenced with shST3GAL3_9 and shST3GAL4_1 and they were selected for subsequent experiments. The decrease in sLe^x levels was of 37% for BxPC-3 ST3GAL3 KD cells and of 68% in the ST3GAL4 KD cells, while in Capan-1 cells, both KD

cells showed similar decreases: 73% for ST3GAL3 KD and 64% for ST3GAL4 KD cells. The reduction in α2,3-SA was associated with an increase in α2,6-SA levels (BxPC-3: 41% in ST3GAL3 KD cells and 35% in ST3GAL4 KD cells. Capan-1: 12% in ST3GAL3 KD cells and 35% in ST3GAL3 KD cells) compared to control cells, which contained an irrelevant vector, shScramble [326]. Interestingly, ST3GAL3 and ST3GAL4 downregulation resulted in a significant impairment of important tumorigenic and metastatic capabilities of KD cells compared to control cells, showing a decrease in cell migration and invasion, and an impaired binding and rolling to E-selectin [326].

Considering the key role of EGFR in intracellular signalling pathways involving cell proliferation, apoptosis, and metastatic spread [396], we aimed to evaluate the role of ST3GAL3 and ST3GAL4 in EGFR glycosylation pattern, and its effect on EGFR activity and downstream signalling during PDA progression. To this end, we first characterized EGFR expression on BxPC-3 and Capan-1 PDA models and the corresponding ST3GAL3 KD and ST3GAL4 KD cells.

1.1.1 EGFR expression levels on control and ST3GAL3 KD and ST3GAL4 KD BxPC-3 and Capan-1 cells

First, the basal expression of EGFR on control, ST3GAL3 KD and ST3GAL4 KD BxPC-3 and Capan-1 cells was analysed by FC after indirect immunofluorescence staining using a specific mAb against EGFR. Both BxPC-3 and Capan-1 ST3GAL3 KD and ST3GAL4 KD cells showed similar EGFR expression levels relative to their corresponding control cells (Figure 21A). These results were confirmed by EGFR immunoblotting of whole cell lysates, indicating that silencing of ST3GAL3 and ST3GAL4 genes does not alter basal EGFR expression levels (Figure 21B). It should be noted that BxPC-3 cells expressed about 4.5-fold higher levels of EGFR in comparison to Capan-1 cells (Median fluorescence values: 868171 vs 188024.5 (BxPC-3 vs Capan-1)), a difference that is in accordance with the high heterogeneity in phenotypes and genotypes of PDA cell lines, which are, indeed, representative of PDA subtypes [394].

A

B
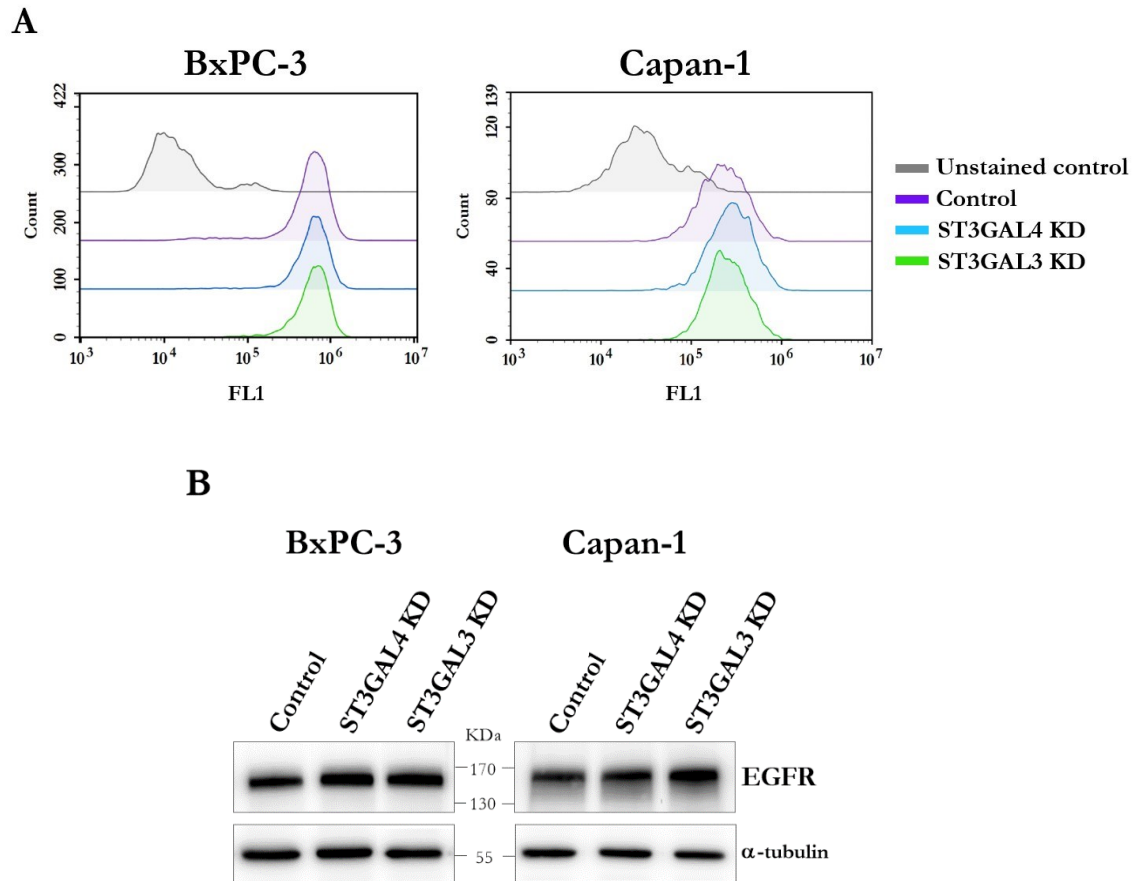
Figure 21. Analysis of EGFR expression level in BxPC-3 and Capan-1 ST3GAL3 and ST3GAL4 KD cells and control ones. A. FC representative histograms corresponding to EGFR cell surface expression levels on BxPC-3 (left) and Capan-1 (right) KD and control cells. An irrelevant antibody was used as a negative control for the unstained cells. **B.** Representative EGFR immunoblots for BxPC-3 (left) and Capan-1 (right) of ST KD and control cells. Membranes were stripped and immunoblotted again to detect total α-tubulin as loading control.

1.1.2 Effect of ST3GAL3 and ST3GAL4 downregulation on EGFR sialylation pattern

Previous results of the group described that α2,3-ST KD generated a reduction of α2,3-SA determinants such as sLe^x and sLe^a, and an increase in α2,6-SA levels on the overall cell surface glycoconjugates of the KD cells [326]. Based on these results, we evaluated whether the KD of ST3GAL3 and ST3GAL4 could specifically affect the glycosylation pattern of EGFR in BxPC-3 and Capan-1 KD cells.

To analyse EGFR sialylated determinants, we first immunopurified EGFR from cell lysates using an anti-EGFR mAb and protein-A bound to magnetic beads. Immunoprecipitated samples were immunoblotted for sLe^x antigen, α2,6-SA and α2,3-SA glycan structures using CSLEX mAb, SNA, which selectively binds SA preferentially α2,6-linked to a terminal Gal, and MAA-II, which binds SA in α2,3-linkage, respectively. Finally, membranes were stripped and immunoblotted using an anti-EGFR antibody to detect the EGFR levels.

In both BxPC-3 and Capan-1 cell models, α2,6-sialylated glycans and sLe[x] epitopes were detected in EGFR. When comparing the level of these sialylated determinants between the KD cells and their corresponding control cells, lower level of sLe[x] could be observed in all KD cells (Figure 22), although the differences were not statistically significant. For Capan-1 cells, the decrease in sLe[x] levels was similar for both ST3GAL3 KD and ST3GAL4 KD cells, while for BxPC-3 model results showed a higher decrease for ST3GAL4 KD cells than for ST3GAL3 KD cells. Interestingly, these sLe[x] reductions are in agreement with the glycosylation changes detected on the total cell surface glycoconjugates of the KD cells [326].
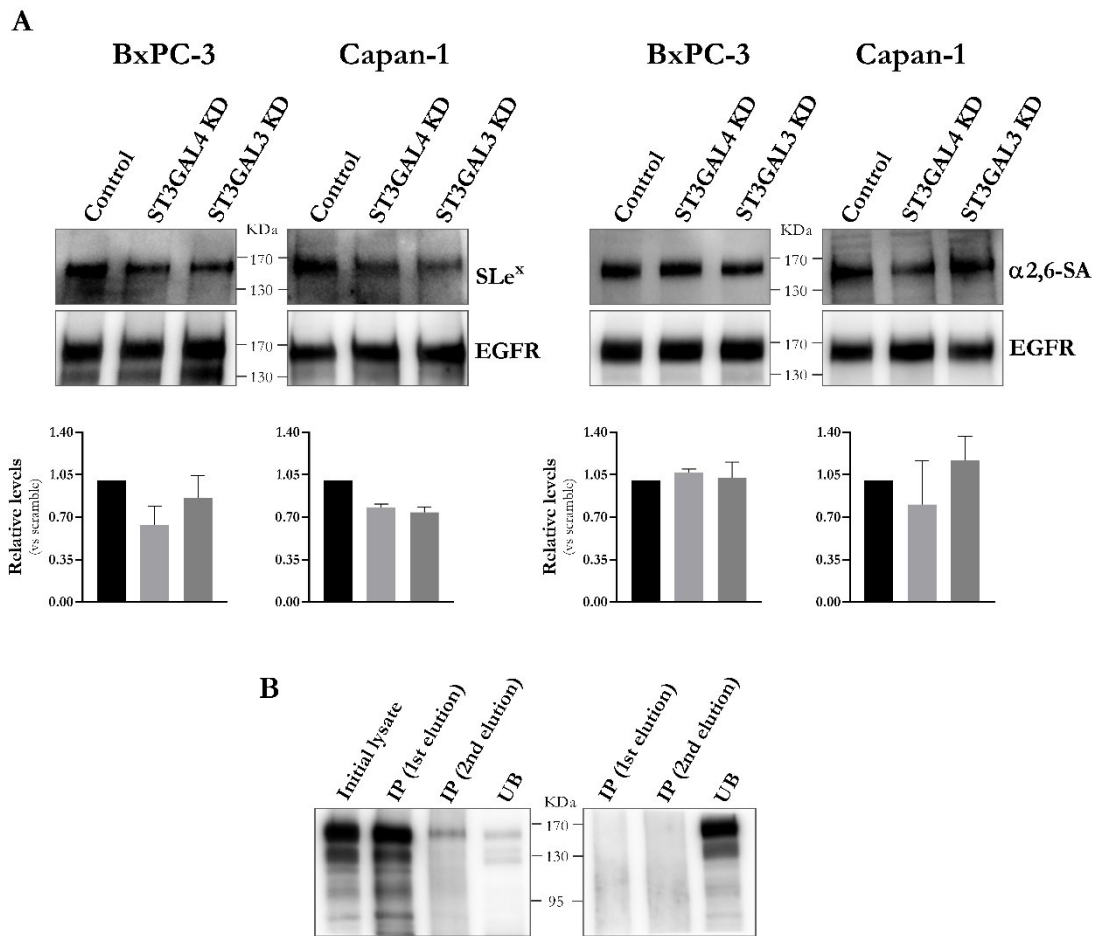
Figure 22. Analysis of the EGFR glycosylation pattern in BxPC-3 and Capan-1 ST3GAL3 KD and ST3GAL4 KD and control cells. A. EGFR was immunopurified from total cell lysates and then immunoblotted with anti-sLe[x] mAb or SNA lectin. Representative immunoblots are shown. Membranes were stripped and immunoblotted for EGFR. Densitometric analyses of the bands were carried out, values were normalized to total EGFR and relative levels vs control cells were determined. Plots show the mean ± SD of three (for BxPC-3) and two (for Capan-1) independent experiments. **B.** Representative EGFR immunoblots of EGFR IP (left) and negative control IP (right) are shown. Left panel: 20 μg of BxPC-3 cell lysate (IP input), 1st elution (equivalent to 40 μg of initial input), 2nd elution (equivalent to 100 μg of initial input) and UB (equivalent to 20 μg of initial input). Right panel: 1st elution (equivalent to 40 μg of initial input), 2nd elution (equivalent to 100 μg of initial input) and UB (equivalent to 20 μg of initial input).

Concerning α2,6-SA detected on EGFR, results showed very similar levels for both BxPC-3 KD cells and the corresponding controls. Similarly, in the Capan-1 cell model, there were no significant differences between KD and control cells, although the relative levels between experiments showed more dispersion (Figure 22 A). Regarding α2,3-SA, we did not detect its expression using MAA-II on immunopurified EGFR from BxPC-3 or Capan-1 cells (data not shown). The total amount of immunoprecipitated EGFR was similar between KD and control cells (Figure 22 A bottom panel). Considering that the KD of STs did not significantly alter the levels of EGFR expression by either FC or WB (Figure 21), we assumed that the immunopurification efficiency was comparable for all the KD and control cells. In addition, we carried out an assay to confirm the efficiency and specificity of the mAb used for the IP and found that nearly all the EGFR was eluted on the first elution and that a minor quantity of EGFR remained on the unbound (UB) or flow-through (Figure 22 B, left panel). In parallel, we performed the IP using an irrelevant antibody as a negative control, and found that all the protein remained on the unbound portion, confirirming the specificity of the IP (Figure 22 B, right panel).

Overall, these results point out that the KD of ST3GAL3 and ST3GAL4 tends to decrease the expression of sLe^x on EGFR, in accordance to the general decrease of sLe^x on the glycoconjugates expressed on the cell surface of BxPC-3 and Capan-1 PDA cells.

1.1.3 Effect of ST3GAL3 and ST3GAL4 KD on EGFR activation and downstream signalling

To investigate whether ST3GAL3 KD and ST3GAL4 KD in BxPC-3 and Capan-1 cells can alter EGFR activity, the downstream signalling of the receptor was evaluated in control and KD cells.

After a period of starvation, cells were treated for 10 min with EGF to activate the receptor and then we evaluated by WB the phosphorylation of the cytosolic domain of EGFR in the whole cell lysates using a polyclonal antibody against phosphorylated tyrosines. Previously, the optimal EGF dose to analyse EGFR activation in each cell line was determined by activating the cells with doses ranging from 10 ng/mL to 40 ng/mL EGF and then analysing EGFR phosphorylation by WB. We determined that the optimal dose was 20 ng/mL for BxPC-3 and 40 ng/mL for Capan-1 (data not shown). Results showed higher levels of total phosphotyrosine residues in ST3GAL3 KD and ST3GAL4 KD cells compared to control ones in both Capan-1 and BxPC-3 cell lines upon EGF activation, although differences were not statistically significant (Figure 23). The increase in the phosphorylation levels was

remarkable in the region of high molecular weight proteins (170 kDa), corresponding to EGFR, particularly for BxPC-3 cells. An increase in the phosphorylation level was also detected at the region above 55 kDa in both cell models, which could correspond to activated AKT protein, one of the key downstream signalling pathways that can be activated by EGFR upon EGF induction [158].
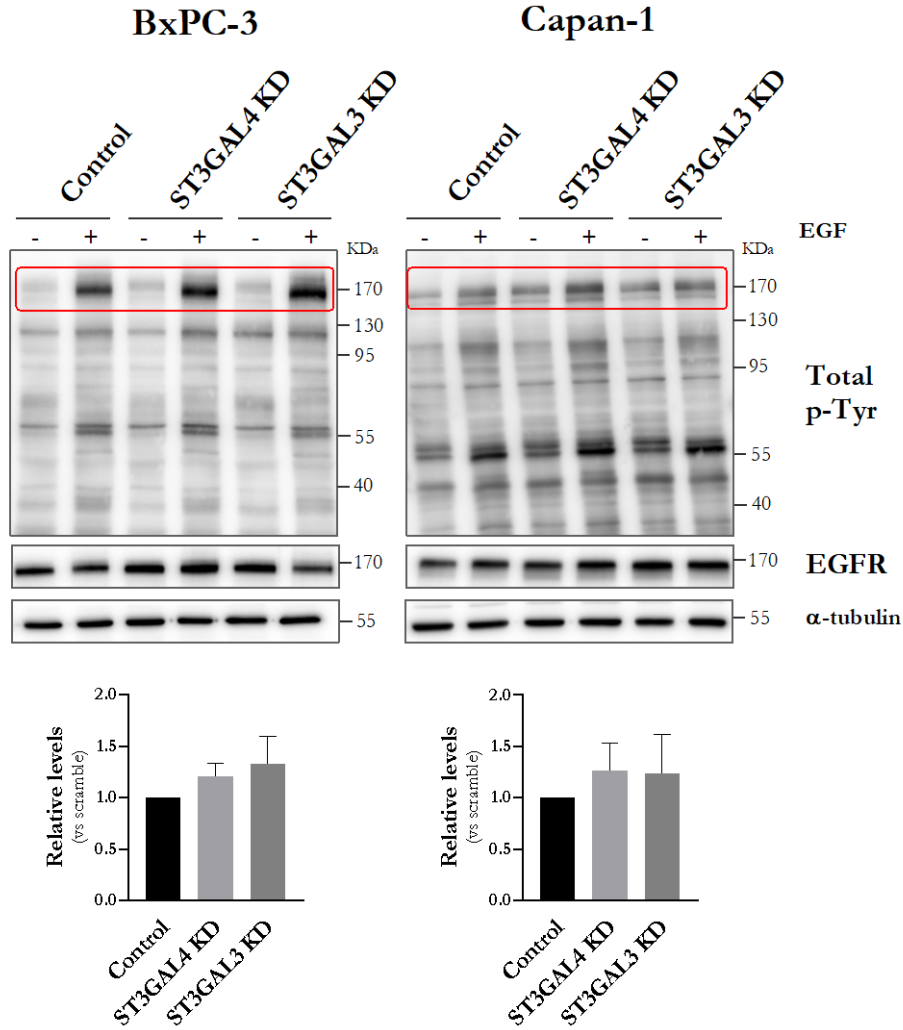
Figure 23. Analysis of the total phosphorylation levels of EGFR after EGF treatment. Cells were exposed to 20 ng/mL (BxPC-3) or 40 ng/mL (Capan-1) of EGF for 10 min, whole cell lysates were obtained and immunoblot analyses for total-phosphotyrosine residues were carried out. Representative blots are shown. Membranes were stripped and immunoblotted for EGFR, to assess EGFR levels of the cell lines in the different conditions. Tubulin levels in the stripped membranes were determined as loading control. Densitometric analyses of at least three independent blots of total phosphotyrosine residues are shown, values were normalized to total EGFR. Plots show the mean ± SD.

Based on these results, we explored the phosphorylation levels of specific tyrosine (Y) and serine (S) residues of the C-terminal intracellular domain of EGFR, which have been described to play an important role in specific functions of the receptor: Y1068 and Y1173, involved in proliferation, and S1046/47 and Y1045, involved in receptor internalization.

Cells were activated with EGF and the corresponding lysates were immunoblotted with antibodies against these specific phospho-residues. Regarding BxPC-3 cell line, an increase of Y1173, Y1068, and Y1045 residues phosphorylation was detected in ST3GAL3 KD cells compared to control cells (Figure 24A and B), although it was not statistically significant, while for ST3GAL4 KD cells no differences could be appreciated. Regarding Capan-1 models, ST3GAL4 KD cells showed a statistically significant higher phosphorylation in S1046 and Y1068 residues (Figure 24C and D), although no significant differences were detected for Y1045 residue. For ST3GAL3 KD Capan-1 cells no differences could be appreciated. Besides, we were not able to detect Y1173 phosphorylated residue after EGF treatment in this cell model.
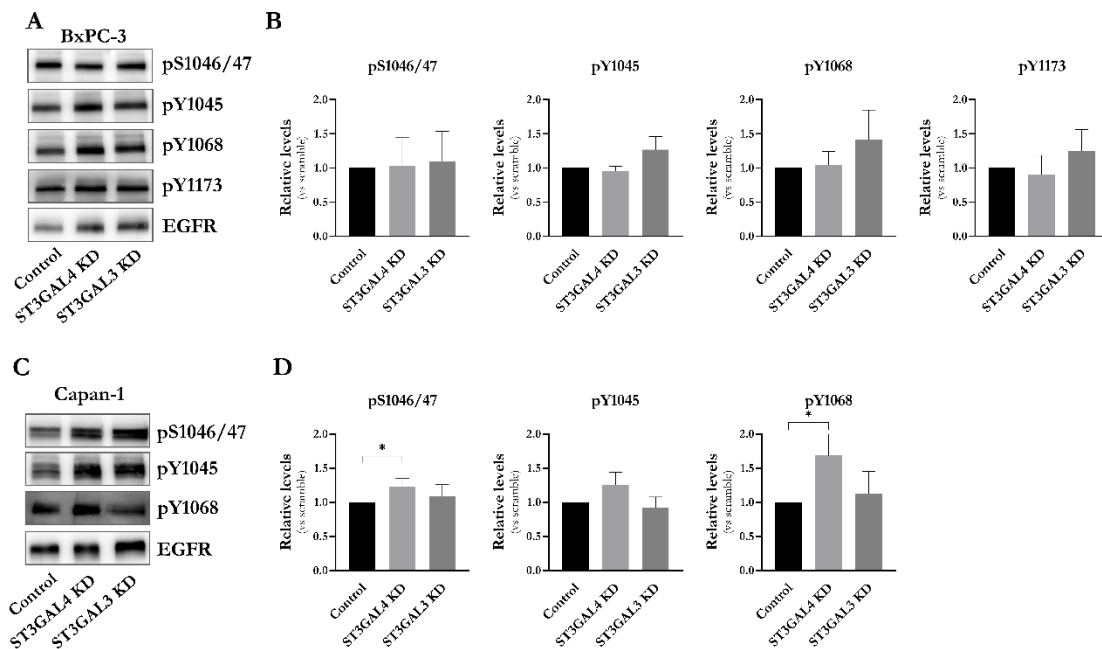
Figure 24. Analysis of EGFR phosphorylation in ST3GAL3 KD and ST3GAL4 KD cells. A (BxPC-3) and **C** (Capan-1) representative immunoblot images of the phosphorylation levels of specific tyrosine or serine residues of EGFR after EGF-treatment. **B** (BxPC-3) and **D** (Capan-1) plots of the densitometric analyses of at least three independent experiments of these tyrosine residues of EGFR. Values were normalized to total EGFR. Plots show Mean ± SD. *: $p < 0.05$.

Altogether, these findings reveal that after EGF treatment, there is a higher increase in EGFR phosphorylation levels in the KD cells compared to control cells, particularly in ST3GAL3 KD BxPC-3 and ST3GAL4 KD Capan-1 cells, which affects specific residues of the receptor involved in the EGFR proliferative and internalization signalling pathways.

Given the increased phosphorylation levels of Y1068 and Y1173 residues of EGFR, involved in proliferative signalling, we compared the activation of two downstream signalling pathways between control and the corresponding ST3GAL3 KD and ST3GAL4 KD cells.

In particular, we determined the activation of AKT and MAPK proteins [183] after EGF-induced EGFR activation. WB results showed a statistically significant increase in the phosphorylation levels of AKT in all BxPC-3 and Capan-1 KD cells compared to control cells after EGF-treatment (Figure 25A and B). However, it must be pointed out that in the case of ST3GAL3 KD and ST3GAL4 KD Capan-1 treated cells a similar AKT phosphorylation was detected compared to ST3GAL3 KD and ST3GAL4 KD untreated cells (Figure 25C and D), and therefore this activation cannot be exclusively attributed to the receptor activation by EGF. Regarding MAPK phosphorylation levels, no differences were found except for ST3GAL3 KD Capan-1 cells, which displayed a decrease in MAPK phosphorylation in comparison to control cells (Figure 25A and B). Nonetheless, we observed an increase in MAPK phosphorylation for untreated ST3GAL4 KD Capan-1 cells compared to untreated control cells (Figure 25D), meaning that for Capan-1 cells and similar to the activation of AKT, the activation of MAPK cannot be exclusively attributed to the receptor activation by EGF.

A BxPC-3
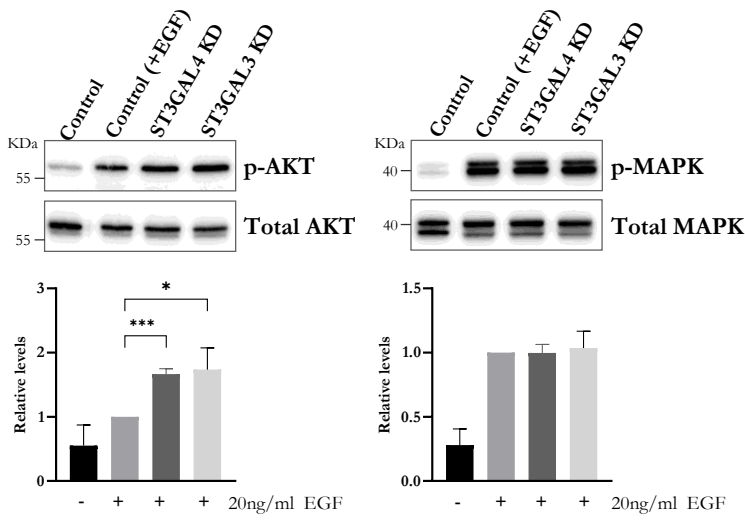
B Capan-1
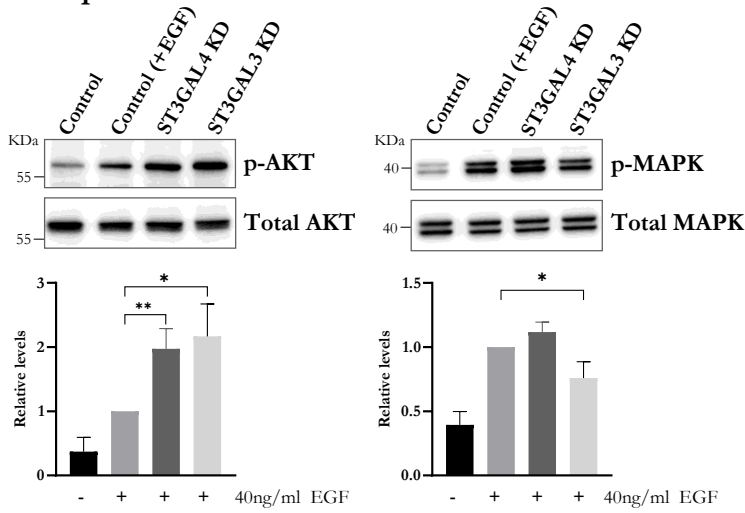
C BxPC-3
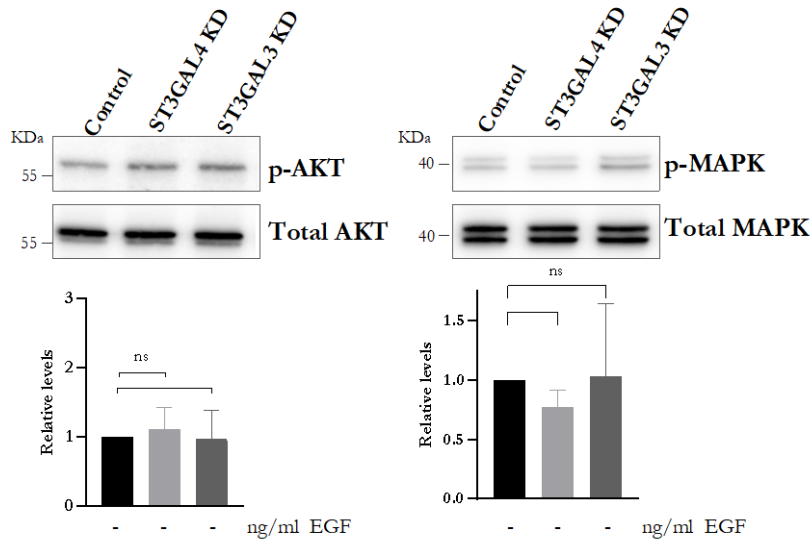
D Capan-1
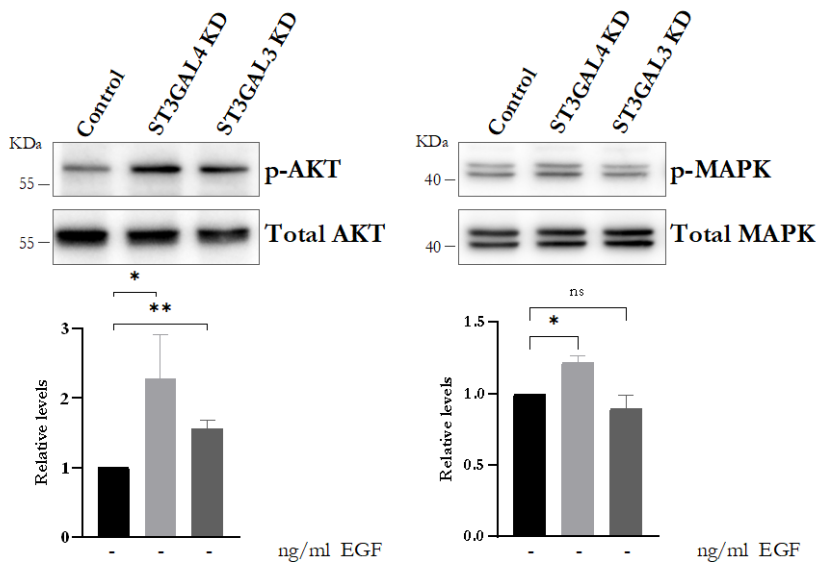
Figure 25. Study of ST3GAL3 KD and ST3GAL4 KD effect on AKT and MAPK signalling pathway. To determine the activation of AKT and MAPK proteins their phosphorylation levels were analysed by WB after EGF treatment: **A** for BxPC-3 cells and **B** for Capan-1 cells. AKT and MAPK phosphorylation levels of untreated BxPC-3 (**C**) and Capan-1 (**D**) cells were also analysed. Three blots from independently generated cell lysates were analysed by densitometry, values were normalized to AKT or MAPK total levels and represented as phosho/total (p/t) AKT or p/t MAPK, the relative levels vs treated control cells are shown for A and B, and the relative levels vs the control untreated cells are shown for C and D. Plots represents Mean ± SD. *, p < 0.05, **, p < 0.01, and ***, p < 0.001.

1.1.4 Analysis of EGFR dimerization

EGFR exists predominantly in an inactive monomeric form, and upon ligand binding, it undergoes a conformational rearrangement that allows it to form active homodimers or heterodimers with other members of the ErbB receptors family, such as ErbB2 or ErbB3, and activate the intracellular signalling pathway [396].

It has been described that alterations in the glycosylation of EGFR, such as sialylation or fucosylation of EGFR *N*-glycans, can affect its conformation, which plays an essential role in regulating the receptor dimerization [333]. Therefore, we next analysed whether the ability of EGFR to dimerize upon EGF induction could be altered in the ST3GAL4 KD cells in comparison to control cells, using glutaraldehyde as crosslinking agent. We carried out the experiment with ST3GAL4 KD cells because they showed higher phosphorylation of EGFR residues, mainly in the Capan-1 model, and higher decrease in sLe^x compared to ST3GAL3 KD cells in the BxPC-3 model.

WB experiments revealed that BxPC-3 ST3GAL4 KD cells showed increased EGFR homodimerization level compared to control cells in response to EGF treatment, while similar levels of monomeric EGFR were detected in the different samples. For Capan-1 cells, we also detected increased EGFR homodimerization in ST3GAL4 KD cells compared to control cells, although the bands corresponding to EGFR homodimers were less intense than in BxPC-3 cells (Figure 26). No dimer formation was detected in BxPC-3 and Capan-1 untreated cells.
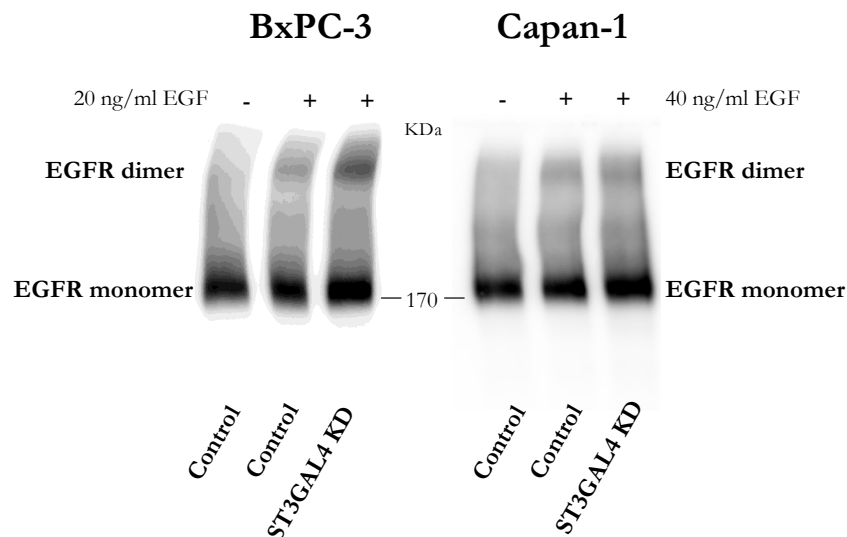
Figure 26. Analysis of EGFR dimerization of control and ST3GAL4 KD BxPC-3 and Capan-1 cells. EGFR dimerization was induced by EGF and analysed using glutaraldehyde crosslinking agent. Dimer formation was determined by WB analysis. Representative immunoblot images are shown for BxPC-3 (left) and Capan-1 (right).

We assessed the capacity of EGFR to form heterodimers with other members of the ErbB family, ErbB2 and ErbB3, after EGF treatment using the same approach. EGFR-ErbB3 dimer formation was of special interest since it has been described that glycosylation alterations in EGFR can alter its ability to dimerize with ErbB3 receptor and modify downstream AKT pathway activation, as ErbB3 contains seven binding sites for PI3K [171]. However, we could not detect the formation of EGFR-ErbB3 or EGFR-ErbB2 heterodimers in the immunoblots (results not shown).

Altogether, these results indicate that the KD of α2,3-STs leads to a higher activation of EGFR signalling upon EGF treatment as shown by an increase in EGFR homodimerization and by an increase in the level of specific EGFR phosphorylated residues, and global AKT phosphorylation.

1.1.5 Analysis of cell proliferation upon EGF induction in ST3GAL3 KD and ST3GAL4 KD PDA cell lines

To gain insight into the role of ST3GAL3 and ST3GAL4 in EGFR functional characteristics, we investigated whether the increase in EGFR activation described above can lead to a different cell proliferation rate of ST3GAL3 KD and ST3GAL4 KD BxPC-3 cells, and ST3GAL4 KD Capan-1 cells, after EGF stimulation. The experiment was carried out with ST3GAL4 KD Capan-1 cells because they showed higher phosphorylation of EGFR residues, and because we detected that the decrease of sLe^x expression on ST3GAL3 KD Capan-1 cells was not stable at that moment. First, we performed a cell number titration to determine the optimal cell number per well to maintain cells in exponential growth phase until the end of the experiment (5 days), and 3000 cells/well was selected as the optimal initial cell concentration for both BxPC-3 and Capan-1 cells.

After 24-hours of starvation, cells were treated with 50 ng/mL EGF in DMEM without FBS during the entire assay. Cell number was quantified by MTT assay at different time points along the experiment (0 h, 48 h, 96 h, and 120 h) and proliferation of KD cells was compared to control cells. As shown at figure 27, ST3GAL3 KD BxPC-3 cells displayed a significantly higher proliferation rate at every time point compared to control cells, whereas ST3GAL4 KD BxPC-3 cells only showed increased proliferation at 96 h and 120 h, although it was not statistically significant. Regarding Capan-1 cells, we could not detect differences in the proliferation rate between the treated ST3GAL4 KD and control cells.

These results might partially be explained by the lower expression of EGFR in Capan-1 cells compared to BxPC-3 cells, suggesting that Capan-1 cells are probably less EGFR-dependent for their proliferation.
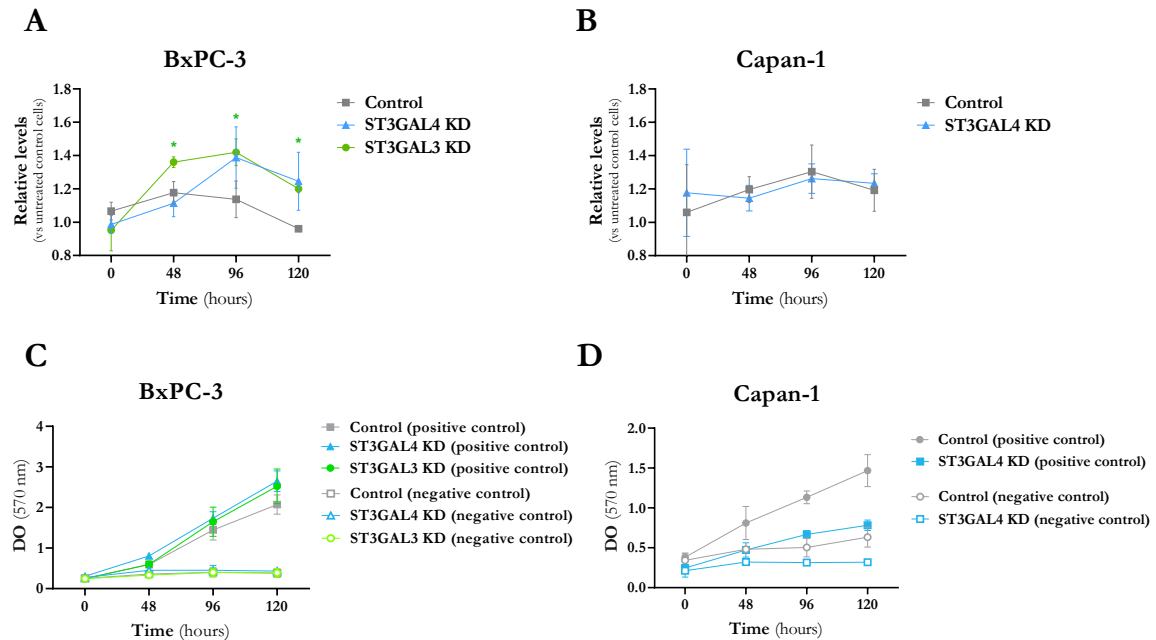
Figure 27. Cell proliferation induced by EGF in control and STs KD BxPC-3 (A) and Capan-1 (B) cells. The proliferation of the cells was measured by an MTT assay. The relative levels of absorbance of treated cells (50 ng/mL EGF) vs the corresponding untreated cells (negative control) are shown at different time points in the graphs. Cell proliferation of positive and negative controls ($DO_{570\,nm}$) is shown at different time points in the graphs for BxPC-3 (**C**) and Capan-1 (**D**) cells. Positive control cells were cultured with complete DMEM, and negative control with incomplete DMEM (0% FBS), both without EGF. Each point represents the mean ± SD of at least three independent experiments, *, $p < 0.05$.

Overall, these findings suggest that reduction of ST3GAL3 and ST3GAL4 expression in the higher EGFR expressing BxPC-3 cells can lead to increased activation of the proliferation signalling pathways upon EGF treatment, and, accordingly, to increased proliferation and growth of the cells. Nevertheless, these results are not in the same line as others published by Li et al. and Qi et al. using other cancer cell models highlighting that there is no consensus on the role of α2,3-STs in regulating EGFR glycosylation and determining its activity after EGF stimulation [397,398]. Therefore, further studies are needed to clarify ST implication on EGFR glycosylation and, ultimately, on cancer progression.

1.1.6 Sensitivity of ST3GAL3 and ST3GAL4 KD cell lines to EGFR-targeted drugs

EGFR-targeted drugs are widely used as a specific treatment for different types of cancers, including breast, lung, prostate, and pancreas among others [399], and have been described to be effective in delaying or stopping tumour progression [217,219]. However, the overexpression

of EGFR as well as EGFR mutations often lead to chemoresistance and decreases the effectivity of EGFR-directed therapies [400–402].

Different strategies have been designed to overcome drug resistance, such as the combination of drugs targeting different signalling pathways in cancer growth [225,403] or the combination of TKIs with other agents. For instance, dual inhibition of extra and intracellular domains of EGFR has been considered a useful strategy [226].

Following the latter strategy, we explored whether the alteration of EGFR glycosylation pattern could modify the anti-proliferative effect of the EGFR-targeted drug Erlotinib (a TKI that binds to the EGFR intracellular domain), which is being used in PDA treatment.

BxPC-3 and Capan-1 STs KD and their corresponding control cells were treated with different concentrations of Erlotinib ranging from 1.25 μM to 50 μM, and the dose that inhibits the cell proliferation by 50% (IC_{50}) was determined after 48 h of treatment. IC_{50} values were very similar between KD and control cells, indicating that responsiveness to Erlotinib was not altered in the ST KD cells (Figure 28). On the basis of these results, no effect of α2,3-ST KD on PDA cells sensitivity to Erlotinib could be established.

C   **IC_{50} Erlotinib** (μM)

	Control	ST3GAL4 KD	ST3GAL3 KD
BxPC-3	17.14 ± 3.51	21.71 ± 3.38	17.55 ± 6.93
Capan-1	>50	>50	n.d
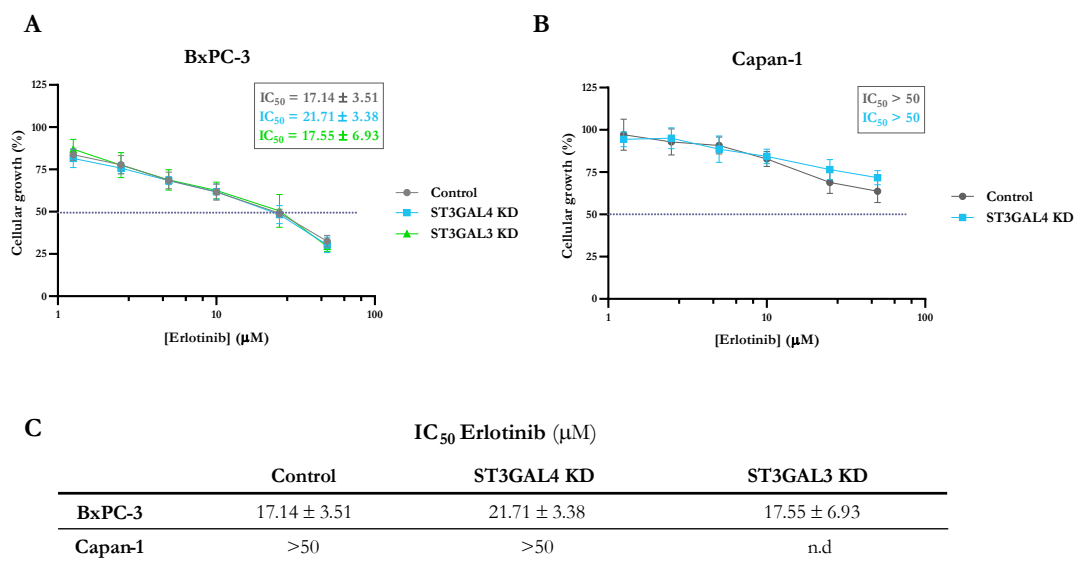
Figure 28. Sensitivity of BxPC-3 and Capan-1 control and STs KD cells to Erlotinib. Erlotinib cytotoxicity curves for BxPC-3 **(A)** and Capan-1 cells **(B)**, plots represent cellular growth (mean $\pm$ SD) normalized to untreated cells of at least three independent experiments. The doses of Erlotinib that inhibit the cell proliferation by 50% (IC_{50} values, μM) are represented as mean $\pm$ SD of at least three independent experiments **(C)**.

Similar experiments were carried out with Cetuximab, a mAb that acts as a competitor to EGFR ligands and blocks ligand-induced EGFR activation. Although previous studies reported that PDA cells and pancreatic tumour xenografts were responsive to Cetuximab treatment, our results showed that BxPC-3 and Capan-1 cell viability was not decreased upon

Cetuximab treatment, indicating that these cell lines were not sensitive to this drug (IC_{30}>500 µg/mL, data not shown).

1.2 Discussion

Aberrant glycosylation has been proposed as a hallmark of cancer due to its contribution in carcinogenesis, cancer progression, and metastasis [285,404,405]. Many of the recent studies in this field have focused on the identification of specific tumour-associated alterations on glycosylation -new tumour biomarkers- and the underlying mechanisms that give rise to them [236,406,407]. Aberrant glycan expression in pancreatic cancer is associated to an increase in the sLe^a and sLe^x antigens [117,270,326,408–415], and in branched and fucosylated *N*-glycans [337,416–420], which are linked to disease progression and poor prognosis [404].

Previous studies performed in our group, together with other reports [269,316,421,422], highlight the importance of the α2,3-STs ST3GAL3 and ST3GAL4 in regulating processes involved in the progression and metastasis of PDA and other cancers, such as cell migration, cell invasion and E-selectin adhesion, suggesting that ST3GAL3 and ST3GAL4-mediated sialylation can be related to malignancy [270,271,299,326]. Moreover, we described how changes in the sialylation pattern of α2β1 integrin and E-cadherin, which are key cell adhesion molecules that mediate pancreatic cancer cell adhesion and invasion, can alter their functional role. In addition, Mereiter et al. [279] underlined the importance of ST-mediated glycosylation of RTKs such as EGFR and ErbB2, which are also involved in cancer progression and resistance to existing therapies [320,331,352].

In the recent years, multiple studies have been conducted to examine how altered glycosylation can interfere with RTK functions in cancer development. EGFR glycan changes and their functional consequences have been extensively studied in lung, breast, ovarian, and colon cancer cells among others [322,331,352,353,355,423]. For instance, Cheng et al. showed that bisecting GlcNAc on EGFR from breast cancer cells inhibits its malignant phenotype via downregulation of EGFR/Erk signalling [355]. In the same line, Park and colleagues revealed that the reduction of ST6Gal I-mediated sialylation on EGFR augments its phosphorylation and downstream activation of ERK kinase in colon cancer cells [352]. Nonetheless, up to our knowledge there are few studies exploring how alterations in the glycosylation of EGFR on PDA cells can affect its activation and signalling, and consequently affect PDA progression [320,343,351].

For this reason, in the present study we have focused on the implication of ST3GAL3 and ST3GAL4 in the glycosylation of EGFR in two PDA cell lines, BxPC-3 and Capan-1. We have addressed how ST3GAL3 KD and ST3GAL4 KD alters the glycan pattern of EGFR and modulates its activation by EGF, its dimerization and the capacity to trigger downstream

signalling pathways. Regarding the functional properties, we have studied if the cell proliferation induced by EGF is altered. To go further, we have studied whether ST3GAL3 KD and ST3GAL4 KD can increase cell sensitivity to EGFR-targeted drugs that are currently used in clinics for different tumour treatments, with the aim of improving PDA therapy by using a combined treatment strategy.

1.2.1 EGFR sialylation is partially mediated by ST3GAL3 and ST3GAL4

First, we analysed EGFR expression of the BxPC-3 and Capan-1 ST3GAL3 KD and ST3GAL4 KD cells and their respective controls by FC. Our results, in the same line as previously published studies [320,322,343], corroborated that ST3GAL3 KD and ST3GAL4 KD did not alter EGFR basal expression. BxPC-3 cells displayed a higher EGFR expression level compared to Capan-1 cells, according to what has been previously described [424], a feature that we have to bear in mind for the following results. The difference in the EGFR expression levels that we could observe between the two cell lines could be explained by the different genetic complexity of PDA cell lines, which reflects the tumour heterogeneity that can be found in PDA [394].

Concerning EGFR glycosylation, it has been described that EGFR contains 12 potential *N*-glycosylation sites in the extracellular domain that can be potentially glycosylated. In particular, EGFR glycosylation was fully characterized in A431 cells, which express large amounts of EGFR, showing that eight of the twelve canonical sites were glycosylated and that EGFR *N*-glycans contained 17% of oligomannose-type (Man5GlcNAc2 to Man8GlcNAc2), 73% of bi-, tri- and tetra-antennary complex-type structures, with 24% neutral and 59% α2,3-sialylated (up to tetrasialo). EGFR glycosylation from CL1-0 and CL1-5 human lung cancer cell lines has also been characterized [331] showing oligomannose structures and complex sialylated *N*-glycan structures, containing both α2,3 and α2,6-SAs [331], although glycan composition was different among the different cell lines since glycosylation is cell-type specific.

We focused our study on the sialylation pattern of EGFR in BxPC-3 and Capan-1 PDA cells, two cell lines that express high and moderate EGFR levels respectively. Results showed that the immunopurified EGFR from both cell models contained α2,6-SA and sLe^x antigen, although we could not detect α2,3-SA using MAA-II, a lectin that does not bind to α2,3-SA of sLe antigens [230].

We determined whether EGFR sialylation could be altered by the KD of ST3GAL3 and ST3GAL4, which codify for the enzymes that are involved in the last steps of sLe[x] biosynthesis. The KD of ST3GAL3 and ST3GAL4 led to a modest decrease in sLe[x] expression on EGFR in both BxPC-3 and Capan-1 models, results that are in line with the global decrease in sLe[x] levels that we had previously described for ST3GAL3 KD and ST3GAL4 KD cells [326]. However, we did not detect any clear difference in α2,6-SA levels on EGFR, in contrast to the moderate increase observed in the general cell sialome. For Capan-1 cells, the sLe[x] reduction on EGFR was similar between ST3GAL3 KD and ST3GAL4 KD cells while for BxPC-3 we found a higher sLe[x] decrease for ST3GAL4 KD cells than for ST3GAL3 KD ones. Interestingly, these results are in agreement with the changes described for the total cell sialylation in our previous study [326] - a significantly higher decrease in sLe[x] for BxPC-3 ST3GAL4 KD cells than for ST3GAL3 ones-, reinforcing the idea that ST3GAL4 has a critical role in sLe[x] biosynthesis and for EGFR sialylation [269].

It would be plausible to hypothesize that the modest decrease in EGFR sLe[x] is due to the compensation mechanisms used by other α2,3-STs or by the α2,6-ST, ST6Gal I. In that sense, a recent study reported that there is a low level of compensation among α2,3-ST for EGFR sialylation in HeLa cells and that ST3Gal VI is the α2,3-STs with the most important effect on EGFR α2,3-sialylation. In addition, the authors stated that α2,3-STs could compete with ST6Gal I for the sialylation of the same target protein [398].

1.2.2 ST3GAL3 KD and ST3GAL4 KD modulate EGFR activation and downstream signalling

The KD of ST3GAL3 and ST3GAL4 genes in both BxPC-3 and Capan-1 models led to an increase in the total phosphorylation status of the cells when cells were treated with EGF. This increase correlated with an increase in the phosphorylation of EGFR-specific tyrosine and serine residues, although the increase in the phosphorylation of specific residues was only statistically significant for Capan-1 ST3GAL4 KD cells.

A possible mechanism that could link the KD of α2,3-STs with a higher EGFR activation status would be the modification of the EGFR sialylation pattern, as described in the literature. In this regard, and consistent with our results that show a modest decrease in sLe[x] in α2,3-ST KD BxPC-3 cells, Liu et al. [331] also showed that reducing the terminal sialylation and α1,3-fucosylation on EGFR enhanced its dimerization and activation in lung cancer cells. In the same line, Park et al [352] described that α2,6-sialylation of EGFR inhibited EGF-induced EGFR tyrosine phosphorylation in colon cancer cells. Conversely, Rodrigues et al. [322] found

that ST6GAL1 silencing did not alter EGFR activation status in colorectal cancer cells. Moreover, it was reported that ST6Gal I-mediated sialylation of EGFR correlates with its activation in pancreatic cancer cells [320]. Overall, there is no consensus on the role of EGFR sialylation and its implication on EGFR activation, and the reason for this discrepancy is still currently unclear. The reported studies have used diverse cancer cell models and methodological approaches, which could account for the different results obtained. In addition, it should be taken into consideration that global cellular sialylation indirectly regulates EGFR phosphorylation by modulating the activity of other kinases responsible for EGFR phosphorylation apart from directly regulating EGFR auto-phosphorylation [353]. After all, the studies carried out so far analysing the effect of EGFR sialylation on its activity and exploring the underlying mechanisms that regulate EGFR activation are not conclusive.

In reference to the phosphorylation of specific EGFR residues after EGF-treatment, we found an increase in the phosphorylation levels of Y1068 (for BxPC-3 and Capan-1 KD cells) and Y1173 (for BxPC-3 KD cells), two residues that are responsible for the activation of two major downstream pathways of EGFR, PI3K/AKT and MAPK, involved in cell proliferation [353,396]. Thus, we analysed the AKT and MAPK phosphorylation status upon EGF-treatment in ST3GAL3 KD and ST3GAL4 KD cells and control cells. Our results showed a significant increase in AKT phosphorylation in ST3GAL3 KD and ST3GAL4 KD cells compared to the control ones both in Capan-1 and BxPC-3 models, while no differences were observed in MAPK phosphorylation levels. In the absence of EGF, there were no differences in the AKT phosphorylation levels between KD and control cells, except for ST3GAL3 KD and ST3GAL4 KD Capan-1 cells, whose basal level of pAKT was slightly higher with respect to control cells. These observations indicate that reduction of EGFR sialylation may increase the ability of the receptor to activate cell proliferation, mainly through the AKT pathway. However, it cannot be excluded that other EGFR-residues such as Y1101 [425], a Src-dependent phosphorylated residue, as well as other cell receptors with TK activity might be also involved in the activation of the AKT pathway [426], since in ST3GAL4 KD BxPC-3 cells the higher phosphorylation of AKT did not correlate with an increased activation of the specific EGFR residues described above. In line with our findings, FUT7 has been shown to catalyse the α2,3-fucosylation of EGFR, which leads to its phosphorylation and activation and, ultimately, to the phosphorylation of signalling molecules Erk1/2 (MAPK) and AKT in follicular thyroid carcinoma cells [427].

It should be noted that, we found a similar increase in the levels of AKT phosphorylation between control and KD Capan-1 cells in the presence or absence of EGF treatment, indicating that the increased activation of the AKT signalling pathway may be driven by changes in the glycosylation of other members of the ErbB family, together with other membrane receptors that activated this signalling pathway. For instance, the phosphorylation status of ErbB3, which has been described to promote the direct activation of the PI3K/AKT pathway by facilitating ErbB2-ErbB3 dimer formation in the presence of its ligand NRG [171,428,429]; or the α2,6-sialylation of the ErbB2 receptor that has been described to enhance AKT downstream signalling in gastric cancer cells [354]. Besides, the presence of paracrine or autocrine mitogenic loops has been described in pancreatic cancer cells [430], which might promote the activation of proliferation pathways even if the cells are cultured in growth factors-deprived conditions. Additionally, the expression of certain oncogenes or loss of particular tumour suppressor genes, such as mutations of EGFR/PI3K or amplification of AKT itself, can result in overactivation of AKT in many tumours [431]. In particular, the overactivation of AKT2 has been observed in about 30-40% of pancreatic cancers [431]. Thus, although Capan-1 cell line has been described to have low levels of AKT activation [432], we might hypothesize that the increased AKT phosphorylation levels in Capan-1 cells could be due to a permanent overactivation of this signalling pathway.

1.2.3 EGFR dimerization is regulated by ST3GAL3 and ST3GAL4-mediated sialylation

Several studies have reported the importance of *N*-glycosylation on the functional properties of EGFR, including ligand binding and dimerization among others [341,346,347], which are closely related to EGFR conformation. In EGFR dimerization, *N*-glycans are mainly involved in stabilizing the inactive state and regulating the EGFR transition from the tethered form to an active extended form [433]. Moreover, it has been described that sialylation could supress EGFR dimerization by attenuating EGF binding [331,352,353].

In the present study, we addressed the influence of the ST3GAL4 KD on the capacity of EGFR to form dimers upon EGF-binding. To this end, we analysed the dimer formation capacity of EGFR in BxPC-3 and Capan-1 cells with reduced ST3GAL4 expression. As we hypothesized, results showed an increase in EGFR homodimers formation in BxPC-3 ST3GAL4 KD cells compared to control ones, confirming that the decrease in EGFR sialylation results in an increased EGFR dimerization capacity. A similar trend was observed in Capan-1 cell models, although the levels of EGFR dimerization were lower. This higher

homodimerization of EGFR would allow a higher autophosphorylation of the intracellular domains of the receptors compared to control cells, as observed in ST3GAL4 KD cells.

Similarly, distinct reports have described that ST silencing enhances EGFR signalling by promoting EGFR dimerization. Park and coauthors reported that ST6GAL1 KD, and the concomitant loss of α2,6-sialylation, promotes EGFR phosphorylation, internalization of receptor and increases cellular growth in response to EGF in human colon cancer cells [352]. In the same line, Liu at al. established that overexpression of STs and FucTs in A549 lung cancer cells supress EGFR dimerization and phosphorylation upon EGF treatment, and confirmed their findings by sialidase and fucosidase treatments [331]. Similarly, Mathew et al., in an attempt to reproduce these experiments, observed a slight reduction of EGFR dimerization after α2,6-sialylation overexpression in SW1990 pancreatic cancer cells, although they were not able to achieve statistically significant results [351].

In a further attempt to address the role of EGFR sialylation in the capacity of EGFR to form dimers, we also studied the ability of EGFR to form heterodimers with ErbB2 and ErbB3 receptors upon EGF activation. However, we could not detect ErbB2 nor ErbB3 heterodimers. These findings could be partially explained by the fact that EGF is the main ligand activating EGFR and ErbB2 heterodimer formation, but ErbB2-ErbB3 heterodimers are preferentially stimulated by NRG binding [434]. Thus, in future experiments it would be interesting to evaluate ErbB3 sialylation pattern in ST3GAL3 KD and ST3GAL4 KD cells and its involvement in EGFR-ErbB3 dimer formation and subsequent activation of downstream signalling pathways preferentially activated by ErbB3, such as the PI3K/AKT pathway.

In addition, multiple studies have been performed so far to analyse the role of specific EGFR and ErbB3 *N*-glycan sites in regulating EGFR function. Asn 420 and Asn 579 in EGFR are considered as crucial *N*-glycan linking sites for maintaining the tethered form in the absence of ligands. In this regard, the loss of *N*-glycans linked to those residues leads to EGFR spontaneous dimerization in the absence of ligand [333,346,347,435]. For future investigations, it would be of great interest to specifically analyse the glycan pattern of EGFR in ST3GAL3 KD and ST3GAL4 KD cells in comparison to the control cells by mass spectrometry, and to stablish possible links between the specific *N*-glycan site modifications and EGFR functional alterations. Nonetheless, the high amount of purified protein that is needed to perform mass spectrometry experiments might represent a handicap to overcome.

1.2.4 Alteration of EGFR glycan pattern induced by ST3GAL3 and ST3GAL4 KD can lead to enhanced proliferation upon EGF induction in PDA cell lines

One of the main objectives in this work was to analyse if the ST3GAL3 KD and ST3GAL4 KD and subsequent decrease in sLe^x epitopes on EGFR could lead to functional changes at the cellular level. To accomplish this goal, we performed a proliferation assay inducing the cells with EGF along the experiment and we quantified the cell number at different time points by an MTT assay. In accordance with the increase in EGFR phosphorylation, BxPC-3 ST3GAL3 KD cells displayed a statistically significant increase in the proliferation rate after 48 h, 96 h, and 120 h compared to control cells, while BxPC-3 ST3GAL4 KD cells also showed a higher proliferation rate than control cells although it was not statistically significant. We did not find any significant difference on the proliferation rate between STs KD cells and the control BxPC-3 cells when cultured with complete media or with incomplete media without EGF-treatment (Figure 27 C), which point out that the differences in the proliferation rate between ST3GAL3 KD cells and control cells might be specifically related to changes in the EGFR glycosylation pattern. Unfortunately, we could not detect any differences in proliferation for Capan-1 cells after the EGF stimulation. In addition, cell proliferation of ST3GAL4 KD cells was slightly lower compared to control cells, both for the positive and the negative controls. Considering that Capan-1 cells express lower EGFR levels than BxPC-3 cells, we hypothesise that this cell line might be less EGFR-dependent for their proliferation. Very recently, Qin and collaborators [427] performed a study with thyroid carcinoma cells and, contrarily to what we described, they found that increased α1,3-fucosylation and sLe^x on EGFR by enhanced FUT7 expression (a key FucT involved in the last stages of sLe^x biosynthesis), led to an increase in EGFR activation and proliferation rate.

Other studies have focused on the role of EGFR glycosylation on cancer cell proliferation in different types of tumours but there is no general consensus [319,343,352,397,398,436–439]. On the one hand, Li et al. demonstrated that the EGFR glycosylation status mediates cell proliferation through EGFR/ERK signalling pathway in colorectal cancer cells, showing that reduced EGFR *N*-glycosylation and EGFR total expression by tunicamycin treatment resulted in impaired cell proliferation [397]. On the other hand, Chugh et al. showed that KD of GALNT3 in CD18/HPAF and BxPC-3 PDA cells lead to Tn and T carbohydrate antigens increase on EGFR and ErbB2, resulting in a significant increase in proliferation [343].

The discrepancies found in these studies indicate that the alteration of the EGFR-glycosylation status might differently affect EGFR activity on different cancer cell types. In

addition, the reduction of general glycosylation by different inhibitors (3Fax-Peracetyl Neu5Ac or SsaI) or by silencing of GTs might also affect other glycoproteins involved in the biological processes that are regulated by EGFR. Thus, although understanding the mechanism by which altered EGFR glycosylation can result in increased or impaired EGFR activation is complex, this knowledge could enable the development of novel therapeutic strategies to treat each cancer type.

1.2.5 ST3GAL3 and ST3GAL4-mediated EGFR sialylation might affect the sensitivity to anti-EGFR drugs

There are two important pharmacological approaches in anti-EGFR therapies, mAbs and TKIs, which target different domains of EGFR structure [217]. At present, both are widely used for the treatment of different types of cancers [219]. However, EGFR overexpression as well as EGFR mutations lead to important chemoresistance, decreasing the response rates of anti-EGFR therapy [400–402]. To date, and with the aim of overcoming resistance to existing therapies, multiple studies have focused on the hypothesis that alteration of the EGFR-sialylation status might affect the anticancer activity of the EGFR-targeted drugs, either by increasing or decreasing cell sensitivity to mAbs or TKIs [320–322,331,422,440].

In that sense, multiple studies have demonstrated that the expression levels of α2,3- or α2,6-SA on EGFR inversely correlate with cancer cell sensitivity to TKIs or mAbs, although the results indicate that some difference exist among cancer cell types [320,322,352,423,440]. Examples of these studies include the following: **i)** Wang's group reduced α2,3-linked sialylation by treating ovarian cancer cells with the sialylation inhibitor SsaI and showed a significant impairment of tumour invasion capacity when combining SsaI with AG1478 (an EGFR TKI)[423], **ii)** Rodrigues et al., demonstrated that overexpression of ST6GAL1 in SW48 colorectal cancer cells decreases Cetuximab-induced cytotoxicity. However, their results were not confirmed when they KD ST6GAL1 in Caco-2 cells [322], and **iii)** C.M. Britain and coauthors found that reduction of α2,6-SA expression by silencing ST6GAL1 in ovarian cancer cells increased Gefitinib sensitivity, by increasing Gefitinib mediated-apoptosis, while ST6GAL1 KD in BxPC-3 pancreatic cancer cells enhanced Gefitinib-induced cell death [320]. On the contrary, Yen et al. demonstrated that reduced SA expression in some of the TKI-resistant lung cancer cell lines reduced the antineoplastic effect of Gefitinib while in other TKI-resistant cells they were not able to observe a clear correlation between EGFR sialylation and Gefitinib sensitivity. Mathew and coauthors demonstrated that the sialylation

increase caused by 1,3,4-*O*-Bu₃ManNAc treatment sensitizes SW1900 pancreatic cancer cells to the TKIs Erlotinib and Gefitinib.

In this study, we analysed the anti-proliferative effect of the TKI Erlotinib and the mAb Cetuximab in ST3GAL3 KD and ST3GAL4 KD BxPC-3 and Capan-1 cells. Unfortunately, we could not establish a clear correlation between EGFR sialylation levels and the sensitivity of the cells to the drugs. In addition, although it has been described that PDA cells and tumour xenografts are sensitive to Cetuximab [424,441–444], we could not detect alterations in BxPC-3 and Capan-1 cell viability when treated with Cetuximab. It would be plausible to speculate that the differences in the EGFR sialylation pattern described in this study for ST3GAL3 KD and ST3GAL4 KD PDA cells are not sufficient to alter cell sensitivity to Erlotinib or Cetuximab.

For future research and bearing in mind that we observed an increase on EGFR activation in ST3GAL3 KD and ST3GAL4 KD cells in comparison to control cells, it would be interesting to perform an assay in concordance with Britain et al. recent publication. In this study, they showed that cells expressing higher ST6Gal I levels had higher EGFR activation and increased invasive ability than cells expressing lower ST6Gal I levels. Interestingly, these differences were suppressed by Erlotinib treatment. These results suggested that Erlotinib can counteract the pro-tumorigenic effect of the ST6Gal I-mediated EGFR sialylation and concomitant increase of its activation [321]. In addition, and in line with Mathew et al. latest report, it would be interesting to address if changes in EGFR-sialylation can alter EGFR intracellular trafficking, as it is a key process regulating TKI and mAbs interaction with EGFR [205]. Altogether, the discrepancies between the published studies and our results highlight the importance of investing further efforts in understanding the mechanism by which altered EGFR sialylation, brought by the modification of STs expression or by sialidase treatment, can determine the effect of EGFR-targeted drugs on cancer cells.

1.2.6 Concluding remarks and future directions

In summary, in this part of the study we have shown that ST3GAL3 and ST3GAL4 play a role in the glycosylation and activation of EGFR. Based in the generalized idea that sialylation can be related to malignancy in cancer, it was counterintuitive to think that less EGFR sialylation could be associated with increased EGFR activation. However, our results showed that a modest reduction of EGFR sialylation caused by ST3GAL3 KD and ST3GAL4 KD leads to enhanced EGFR activation and downstream activation of the AKT signalling pathway, which in BxPC-3 KD cells was translated to an increase in cell proliferation rate

upon EGF activation. Nonetheless, we could not establish any correlation between EGFR sialylation levels and the sensitivity of the PDA cells to the EGFR-targeted drugs Erlotinib and Cetuximab. Thus, further research could help clarifying the molecular mechanism by which the reduction of sLe^x on EGFR can modulate EGFR conformation, dimerization, downstream signalling, and intracellular trafficking among others [338,351,445]. Finally, investing further efforts in the study of anti-EGFR targeted drugs in combination with the alteration of EGFR sialylation has the potential to pave the path for the development of novel therapies for PDA.

Miró Domènech, L.

2. Chapter II. Reduction of sialic acid on PDA cells by a sialyltransferase inhibitor and study of its effect on E-selectin adhesion, migration and invasion capabilities of PDA cells *in vitro* and its potential to reduce tumour growth and alter tumour immune component in syngeneic mice

2.1 Results

2.1.1 Sialic acid characterization of human PDA cells

In order to investigate the effect of several reported ST inhibitors to decrease cell SA determinants, the expression levels of sLe^x, sLe^a, α2,3-SA- and α2,6-SA were characterized in two human PDA cell lines: BxPC-3 and Capan-1.

Cell surface glycan expression was analysed by FC for BxPC-3 and Capan-1 cells using specific mAbs against sLe^x and sLe^a antigens, and the specific carbohydrate-binding lectins MAA-II and SNA, which preferentially bind to SA attached to terminal Gal in α2,3- and α2,6-linkage respectively. Capan-1 cells expressed nearly a 5-fold higher level of sLe^x and 3-fold higher level for sLe^a than BxPC-3 cells (Figure 29). The analysis of the expression of α2,3- and α2,6-SA determinants showed that both cell lines expressed higher α2,3-SA than

α2,6-SA levels. Both cell lines expressed similar levels of α2,6-SA while for α2,3-SA, BxPC-3 was the cell line with the highest levels (a 1.5-fold increase vs Capan-1 cells) (Figure 29).
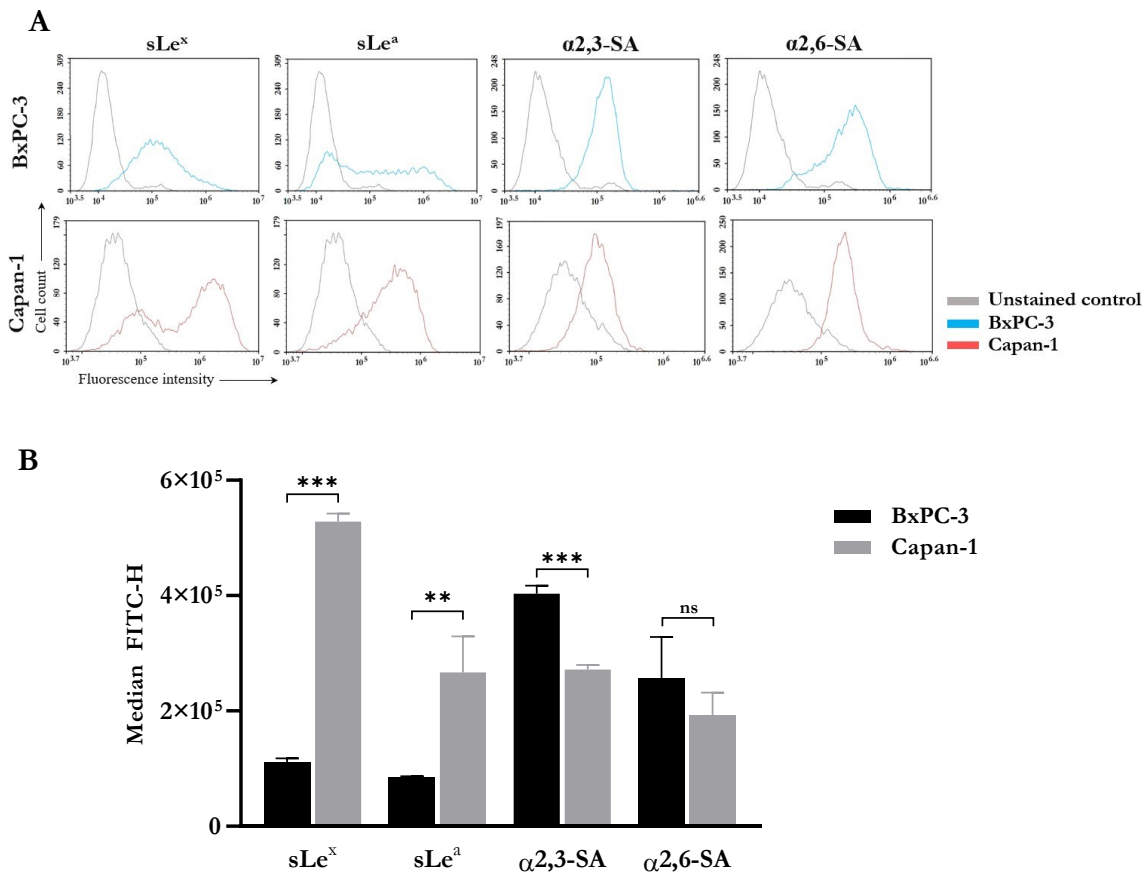
Figure 29. Analysis of cell surface sialoglycan expression in BxPC-3 and Capan-1 PDA cells. A. Representative histograms of the different glycan structures expression on the cell surface of BxPC-3 and Capan-1 cell lines: sLe^x, sLe^a, α2,3-SA detected with MAA-II lectin and α2,6-SA detected with SNA lectin. **B.** Median fluorescence for each glycan structure for BxPC-3 and Capan-1 cells are represented. Plot shows mean ± SD of at least three independent experiments. *, $p < 0.05$, **, $p < 0.01$, and ***, $p < 0.001$.

2.1.2 Treatment of STs inhibitors on PDA cell lines

Up to date, there is extensive biological evidence demonstrating that STs and the sialylation processes they catalyse are of critical importance for tumour progression, adhesion, and migration of human cancer cells. Thus, STs are considered as potentially important targets for the development of new treatment strategies against tumour progression and metastasis formation. Several types of STs inhibitors have been developed in recent years, and importantly they are moving forward to cell-permeable STs inhibitors, which easily exert their action on tumour cells and potentiate the forthcoming application to cancer treatment.

In this study, we assessed the potential of three different inhibitors that have previously been described in other tumour cell types to reduce the sialylation.

First, we tested **AL10 STs inhibitor**, which is a cell permeable Lith analogue that has been described to repress α2,3-STs activity in lung cancer cells and to impair cell adhesion, migration, and metastasis formation of A549 and CLI.5 tumour cells [391]. BxPC-3 and Capan-1 cells were seeded into 24-well plates and treated with 1.25 μM, 2.5 μM, 5 μM or 10 μM of AL10 for 48 h. Cells were detached and the effect of AL10 on glycan expression pattern was analysed by FC, by indirect immunofluorescence staining with mAbs against sLe[x] and sLe[a] antigens, and with the MAA-II lectin. For BxPC-3 cells, 2.5 μM AL10 treatment slightly reduced sLe[x] and α2,3-SA around 18%, but this trend was unexpectedly not observed at higher AL10 doses for sLe[x] (data not shown). Contrarily, AL10 treatment caused an increase in sLe[a] expression of 21% compared to untreated cells (Figure 30, top panel). For Capan-1 cells, we could not detect any differences on glycan expression between treated and control cells (Figure 30, bottom panel). The effect of the ST inhibitor was not predictable as it was not dose dependent and the results were different between cell lines.
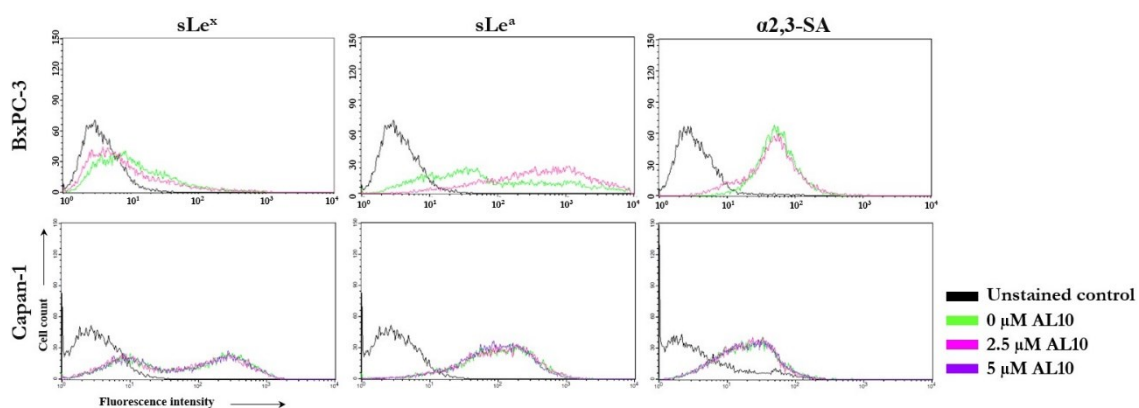
Figure 30. Analysis of AL10 effect on cell surface glycan expression in BxPC-3 and Capan-1 pancreatic cancer cells by FC. Representative histograms of the different glycan structures expression on the cell surface of treated and control BxPC-3 (top panel) and Capan-1 (bottom panel) cells: sLe[x], sLe[a], and α2,3-SA detected with MAA-II lectin (from left to right).

To address if AL10 could have any effect on cell cytotoxicity, an MTT assay was conducted in BxPC3 and Capan-1 cells. The results showed that cell viability was not affected by AL10 treatments at 1.25 μM, 2.5 μM or 5 μM doses (data not shown). Finally, we tested if the inconsistent effect of AL10 on PDA cell surface sialylation could be due to the poor permeability of the compound that compromises its capacity to cross cell membranes and inhibit STs activity' at the intracellular compartments. After 48 h of treatment with 2.5 μM and 5 μM AL10 on BxPC-3 and Capan-1 cells, the remaining AL10 on the cell media was quantified by measuring its fluorescence emission at 470/540 nm and compared to the initial AL10 fluorescence. Results showed a decrease of around 30% for BxPC-3 and around 18% for Capan-1 of AL10 at both 2.5 μM and 5 μM in the cell media, suggesting that the

compound was partly cell permeable or that the compound had been degraded during the treatment time. In a further attempt to determine if the inhibitor was able to permeate through cell membrane and reach the cytoplasm and subcellular organelles, we performed an internalization assay: BxPC-3 cells were seeded and after a 24 h treatment with 5 μM or 50 μM AL10, they were fixed and stained with Hoecht dye (nucleus) and observed under a confocal microscope. Unfortunately, the fluorescence signal emitted by AL10 and detected on the cytoplasm was negligible, suggesting that the AL10 compound was not cell permeable or that it was degraded during the incubation time (data not shown). Thus, we concluded that AL10 compound did not effectively block cell sialylation on BxPC-3 and Capan-1 cells and decided to explore other STs inhibitors.

Secondly, we tested **Soyasaponin-I** (**SsaI)**, a ST inhibitor described to decrease the expression of α2,3-STs in melanoma and breast cancer cells, and to reduce the metastatic potential of tumour cells [386–388]. In order to study the effect of SsaI on BxPC-3 and Capan-1 cells sialic expression, we seeded the cells in a 24 well-plate and treated them for 72 h with increasing SsaI concentrations, from 0 μM to 100 μM for BxPC-3 cells and from 0 μM to 200 μM for Capan-1 cells. Unfortunately, as represented in the FC profiles (Figure 31), none of the tested doses of SsaI altered sLe^x, sLe^a, α2,3-, or α2,6-SA determinants expression on cell surface glycoconjugates.
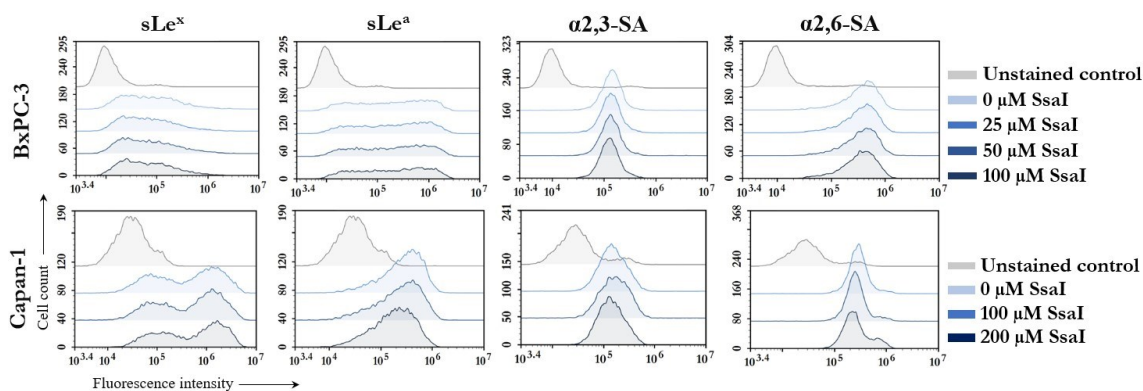
Figure 31. Analysis of SsaI effect on cell surface glycan expression in BxPC-3 and Capan-1 pancreatic cancer cells by FC. Representative histograms of the different glycan structures expression on the cell surface of treated and control BxPC-3 (top panel) and Capan-1 (bottom panel) cells: sLe^x, sLe^a, α2,6-SA detected with SNA lectin, and α2,3-SA detected with MAA-II lectin (from left to right).

Finally, we tested the commercially available inhibitor **Ac$_5$F$_{ax}$-Neu5Ac**, a membrane permeable fluorinated analogue of SA, described to drastically reduce the expression of α2,3 and α2,6-linked SA in B16F10 melanoma cells, to impair cell migration capacity and to reduce *in vivo* tumour cell growth [371].

2.1.3 Ac$_5$3F$_{ax}$-Neu5Ac significantly reduced cell surface sialylation in BxPC-3 and Capan-1 cells

First, the effective dose of Ac$_5$3F$_{ax}$-Neu5Ac and the best treatment time for each cell model was determined. In an initial experiment, BxPC-3 cells were incubated for 48 h and 72 h with increasing concentrations of Ac$_5$3F$_{ax}$-Neu5Ac (0 μM, 100 μM, 200 μM, 500 μM) and results indicated that 100 μM was the optimal dose after 48 h and 72 h of treatment, since it caused the highest decrease in the expression of sLe^x, α2,3- and α2,6-SA determinants (Figure 32). Although the decrease in cell surface expression of sLe^x, α2,3- and α2,6-SA determinants was considerable at 48 h, it was a 20% higher after 72 h of treatment leading to a reduction of the expression levels up to 80% for sLe^x, to 66% for α2,3-SA and to a 57% for α2,6-SA (Figure 32A). In a further attempt to find the effective dosage of the inhibitor for BxPC-3 cells, we decreased the dose up to 50 μM or 25 μM. However, the maximal effect of the inhibitor was observed at the 100 μM dose, indicating that from 0 μM to 100 μM the Ac$_5$3F$_{ax}$-Neu5Ac acts in a dose-dependent manner for BxPC-3 cells (Figure 32A). For Capan-1 cells, we carried out an initial experiment with increasing doses (0 μM, 50 μM, 100 μM, 200 μM, 400 μM) at 72 h of treatment and found that the optimal dose was 400 μM (Figure 32B). In this case, the inhibitor maintained its dose-dependent effect until 400 μM concentration. At 400 μM it caused a 10-20% higher decrease compared to 200 μM dose, leading to a reduction of 69% for sLe^x, to 37% for sLe^a, to 36% for α2,3-SA, and to a 18% for α2,6-SA.
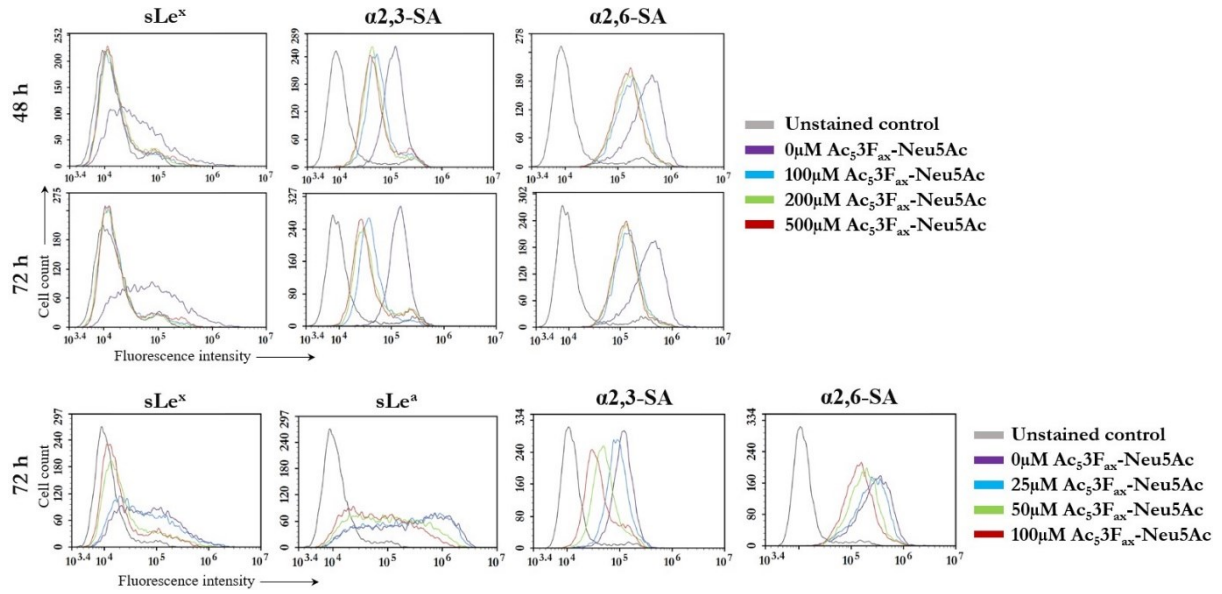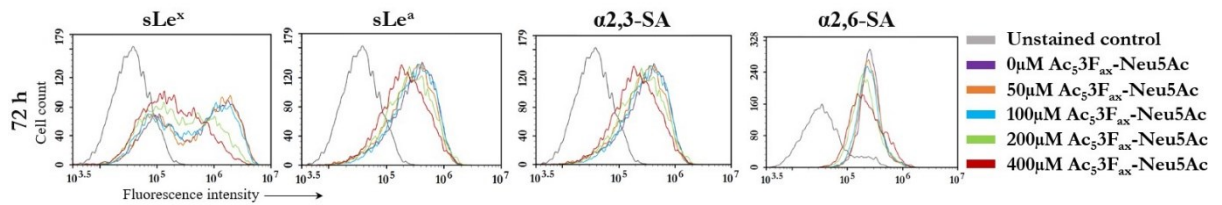
Figure 32. Analysis of Ac₅3Fₐₓ-Neu5Ac effective dose and treatment time for cell surface glycan inhibition in BxPC-3 and Capan-1 PDA cells by FC. Representative histograms of the different glycan structures expression on the cell surface of treated and control BxPC-3 **(A)** and Capan-1 **(B)** cells: sLeˣ, sLeᵃ, α2,3-SA detected with MAA-II lectin and α2,6-SA detected with SNA lectin (from left to right). For BxPC-3, 48 h (top panel) or 72 h (intermediate panel) of treatment, and increasing doses (0 μM, 100 μM, 200 μM, 500 μM) of Ac₅3Fₐₓ-Neu5Ac inhibitor, and 72 h treatment at increasing doses (0 μM, 25 μM, 50 μM, 100μ M) of Ac₅3Fₐₓ-Neu5Ac inhibitor (bottom panel). For Capan-1, 72 h of treatment and increasing doses (0 μM, 50 μM, 100 μM, 200 μM, 400 μM).

Ac₅3Fₐₓ-Neu5Ac treatment could significantly reduce the expression of both α2,3-linked and α2,6-linked SAs, as well as the expression of sLeˣ and sLeᵃ sialylated antigens in BxPC-3 and Capan-1 cells at 100 μM and 400 μM of Ac₅3Fₐₓ-Neu5Ac, respectively, similarly to the published studies performed in diverse cancer cell models [374]. Next, using the reported conditions of the inhibitor we determined that the most prominent reduction observed was in the sLeˣ expression levels of treated cells in both cell models –around 80% (86% ± 7.4 for BxPC-3 cells and 82.5% ± 7.3 for Capan-1 cells) – comparing the median fluorescence values of the treated cells vs its relative control (Figure 33). Referring to sLeᵃ, the reduction in the expression levels was higher in BxPC-3 cell model –up to 76.4% ± 6.4 – than in Capan-1 cells –up to 34.4% ± 6.1 – (Figure 33). Lectins' analyses showed, on the one hand, a decrease of 82.9% ± 1.4 for Capan-1 cells and of 74.0% ± 6.5 for BxPC-3 in α2,3-SA expression using MAA-II lectin, and a minor reduction of α2,6-SA expression for both BxPC-3 (56.8% ± 2.0)

and for Capan-1 (28.4% $\pm$ 6.2), indicating that in these two PDA cell models the effect of the inhibitor is more pronounced on α2,3-SA than on α2,6-SA expression, as previously described by Büll et al. for murine melanoma cells [371]. Importantly, the used concentrations of Ac$_5$3F$_{ax}$-Neu5Ac did not alter tumour cell viability (data not shown).

The reduction of the expression of sLe^x, α2,3- and α2,6-SA determinants in protein extracts from treated and control BxPC-3 and Capan-1 cell lysates was analysed by WB (Figure 33C), and results were in agreement with the ones obtained for cell membrane glycoconjugates determined by FC [446].
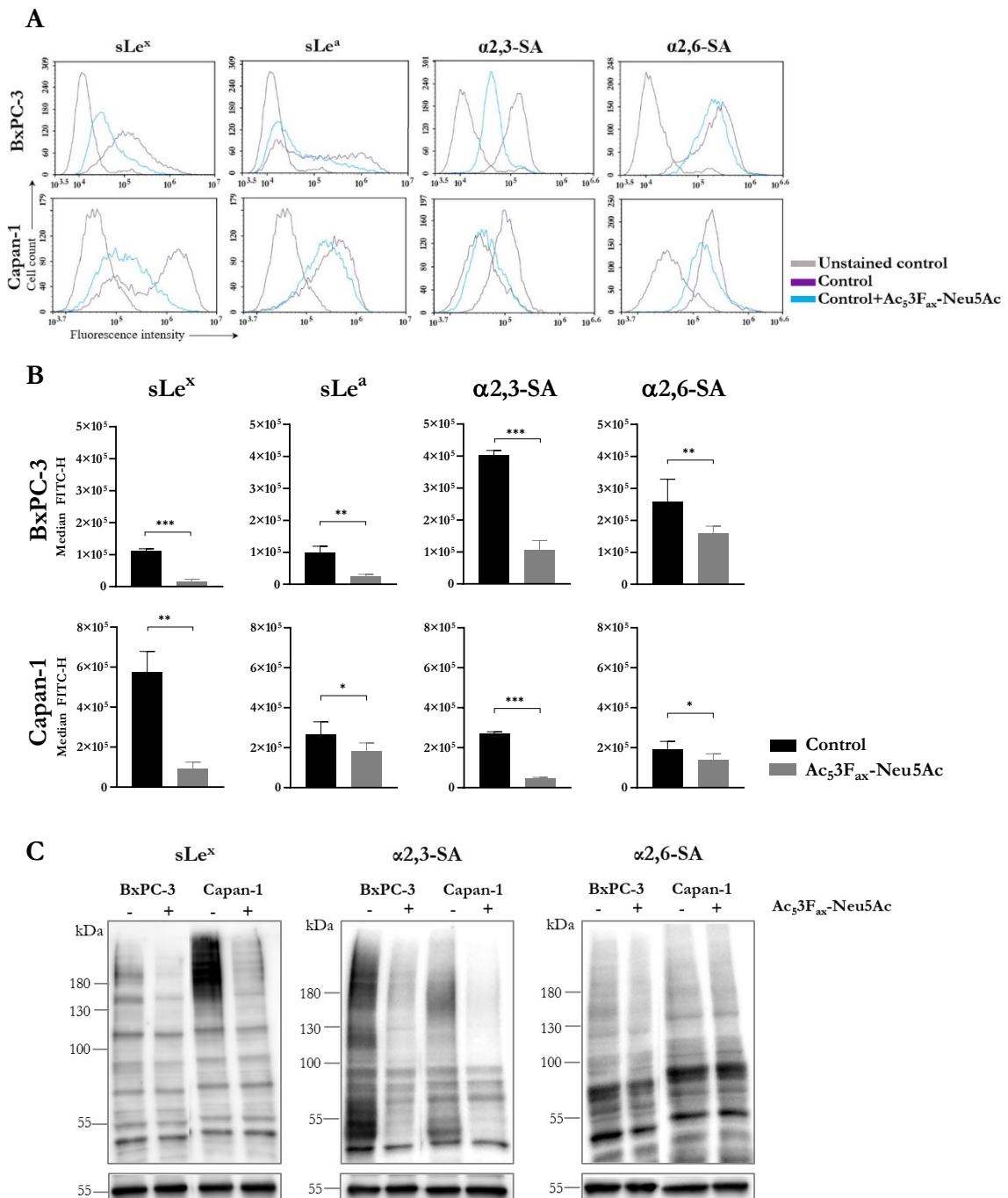
Figure 33. Analysis of Ac$_5$3F$_{ax}$-Neu5Ac effect on cell surface glycan expression in BxPC-3 and Capan-1 PDA cells by FC. A. Representative histograms of the different glycan structures expression on the cell surface of treated and control BxPC-3 (top panel) and Capan-1 (bottom panel) cells: sLe^x, sLe^a, α2,6-SA detected with SNA lectin and α2,3-SA detected with MAA-II lectin (from left to right). **B.** Median fluorescence for each glycan structure of treated and control BxPC-3 and Capan-1 cells are represented. Plots show mean ± SD of at least three independent experiments. *, $p < 0.05$, **, $p < 0.01$, and ***, $p < 0.001$. **C.** Representative blots of the expression of the sialylated glycan structures sLe^x, α2,3-SA and α2,6-SA from the cell lysates of treated and control BxPC-3 and Capan-1 cells (top). Immunodetection of tubulin after stripping membranes, as loading control (bottom). Images extracted and modified from Júlia Lopez' Master's Thesis, 2022 [446].

Overall, we showed that Ac$_5$3F$_{ax}$-Neu5Ac efficiently decreased sLe^x and sLe^a levels in BxPC-3 and Capan-1 cells as well as α2,3-SA and α2,6-SA levels, leading to a generalised decrease of the sialylation pattern of these cells. Nonetheless, the blockage of sialylation by the Ac$_5$3F$_{ax}$-Neu5Ac treatment did not lead to the complete loss of α2,3- and α2,6- linked SAs.

When comparing the results obtained in this study with a previous study performed in our group, where we analysed the changes in the cell sialylation pattern caused by ST3GAL3 and ST3GAL4 KD in PDA cells, we can conclude that the Ac$_5$3F$_{ax}$-Neu5Ac STs inhibitor reduced SA expression more effectively than the KD of the STs [326]. In addition, and contrary to what we previously observed when KD α2,3-STs, Ac$_5$3F$_{ax}$-Neu5Ac STs inhibitor also reduced the expression of α2,6-SA. Again, these results corroborate that it has the ability to act on α2,3- and α2,6-STs, leading to a global decrease of the cell sialylation and preventing compensation mechanisms displayed by the diverse STs subtypes.

Next, to investigate if the Ac$_5$3F$_{ax}$-Neu5Ac treatment could have an effect on the ST KD BxPC-3 and Capan-1 cells, in which we had previously silenced ST3GAL4 expression by shRNA technique, we treated ST3GAL4 KD cells with Ac$_5$3F$_{ax}$-Neu5Ac for 72 h, following the protocol described above, and analysed their cell surface glycan expression by FC. Data represented at Figure 34 showed that combining the KD of ST3GAL4 with STs inhibitor treatment resulted in higher reduction of cell surface sLe^x expression in both BxPC-3 and Capan-1 cells, although the difference between the expression levels of control and ST3GAL4 KD cells, both treated with the inhibitor, was not statistically significant. When analysing the expression of the other sialylated determinants (sLe^a, α2,6-SA and α2,3-SA), we could not detect an additive effect of ST KD and the ST inhibitor treatment. Thus, we concluded that the Ac$_5$3F$_{ax}$-Neu5Ac treatment had enough potency to reduce cell surface SA expression on BxPC-3 and Capan-1 cells since we obtained a maximal reduction of sialoglycans expression by treating control cells with the inhibitor, and did not observe an additive effect when treating ST3GAL4 KD cells with Ac$_5$3F$_{ax}$-Neu5Ac. For this reason, BxPC-3 and Capan-1 control cells were used to carry out the following experiments.
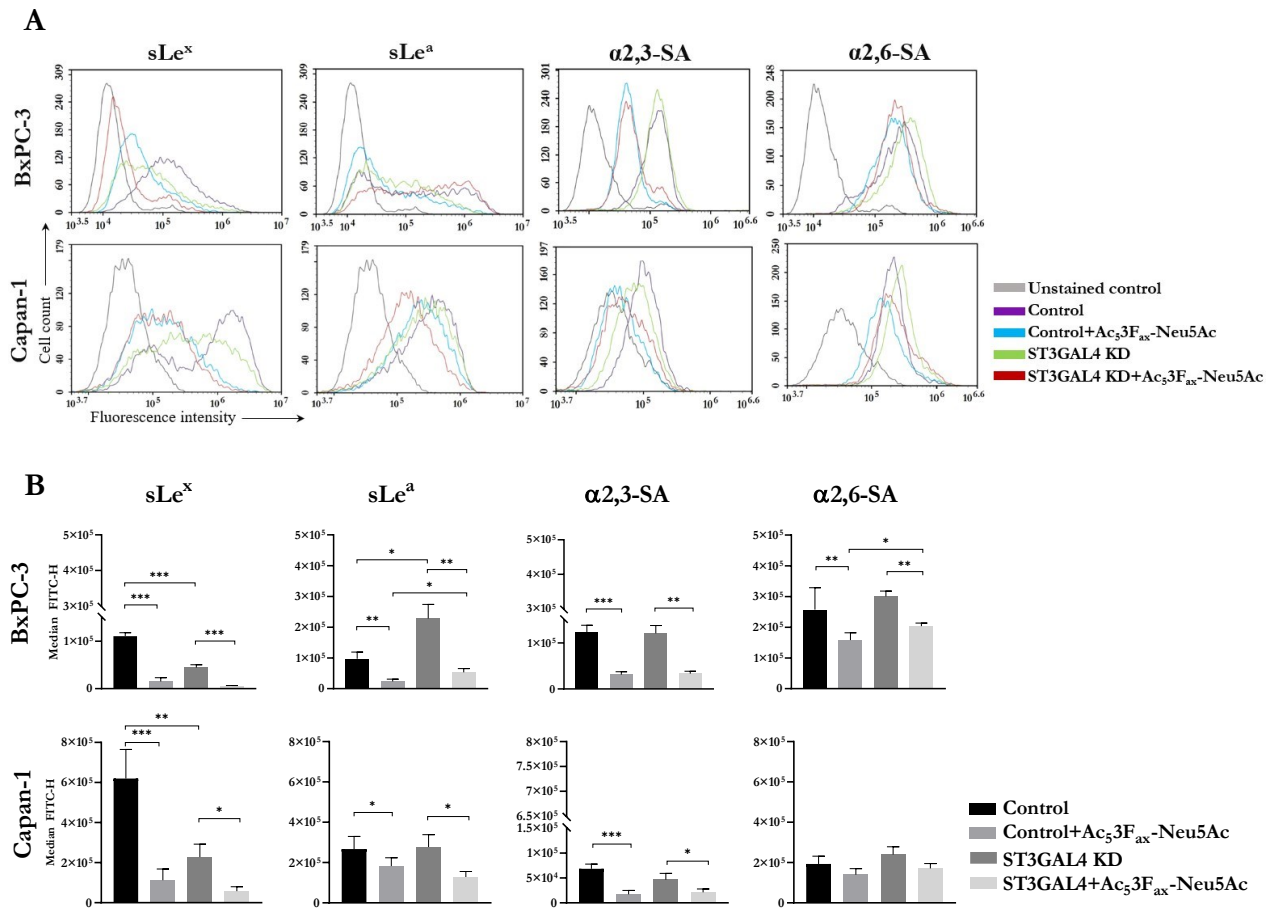
Figure 34. Analysis of Ac$_5$F$_{ax}$-Neu5Ac effect on cell surface glycan expression in BxPC-3 and Capan-1 control cells and ST3GAL4 KD pancreatic cancer cells by FC. A. Representative histograms of the different glycan structures expression on the cell surface of treated and control BxPC-3 (top panel) and Capan-1 (bottom panel) cells: sLe^x, sLe^a, α2,3-SA detected with MAA-II lectin and α2,6-SA detected with SNA lectin (from left to right). **B.** Median fluorescence for each glycan structure of treated and control and ST3GAL4 KD BxPC-3 and Capan-1 cells are represented. Plots show mean ± SD of at least three independent experiments. *, $p < 0.05$, **, $p < 0.01$, and ***, $p < 0.001$.

Next, the effect of Ac$_5$F$_{ax}$-Neu5Ac on cell adhesion, and migration and invasion was analysed on control BxPC-1 and Capan-1 cells.

2.1.4 Ac$_5$F$_{ax}$-Neu5Ac treatment impaired E-selectin binding in BxPC-3 and Capan-1 cells

Interactions of selectins and their ligands play a crucial role in several steps of cancer metastasis, including intravasation to the circulatory system and transport to the lymphoid organs and/or distant sites, and adhesion to the endothelium at these sites to establish a secondary tumour. It has been described that the carbohydrate antigens sLe^x and sLe^a expressed by metastatic cancer cells facilitate the arrest of these cells by the E-selectin present on the activated endothelium [447]. With the aim of exploring if the decrease of surface SA caused by Ac$_5$F$_{ax}$-Neu5Ac in BxPC-3 and Capan-1 cells can lead to alterations in its

107

adhesion capacity, we performed an *in vitro* assay to analyse the binding of treated vs non treated PDA cells to rhE-selectin/Fc Chimera. rhE-selectin/Fc Chimera was previously linked to a Fc-secondary antibody to optimize E-selectin orientation and facilitate cell binding. Cell adhesion was quantified by an MTS assay.

First, we confirmed that both BxPC-3 and Capan-1 control cells had the ability to adhere to rhE-selectin/Fc Chimera, and revealed that Capan-1 cells had slightly higher adhesion levels to E-selectin than BxPC-3 cells (data not shown), a difference that might be explained by the higher sLe^x and sLe^a levels of Capan-1 cells. When comparing the adhesion capacity to E-selectin of ST inhibitor treated vs control cells, our results showed that Ac$_5$3F$_{ax}$-Neu5Ac treatment significantly reduced the adhesion capacity of Capan-1 and BxPC-3 cells to rhE-selectin, as represented at Figure 35. BxPC-3 treated cells displayed a reduction of 58.4% ± 14.5 in the adhesion capacity in comparison to non-treated control cells, while in Capan-1 treated cells the reduction was of 74.8% ± 11.1 compared to control cells. The important reduction in sialylated determinants, especially sLe^x-sLe^a in the ST inhibitor treated cells can explain their important decrease in E-selectin adhesion. In conclusion, these results revealed that the blockade of tumour sialylation with Ac$_5$3F$_{ax}$-Neu5Ac impairs the ability of BxPC-3 and Capan-1 cells to bind to rhE-selectin *in vitro*, and in consequence, the treatment of tumour cells with Ac$_5$3F$_{ax}$-Neu5Ac is likely to reduce their metastatic potential.
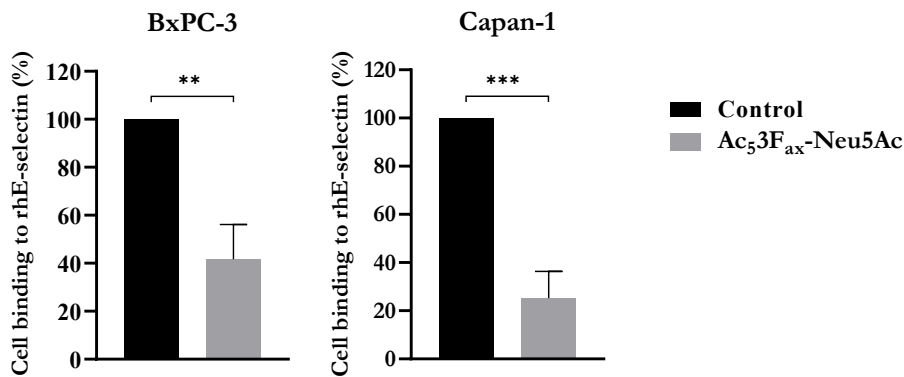
Figure 35. Ac$_5$3F$_{ax}$-Neu5Ac treatment impairs cell adhesion to rhE-selectin in human PDA cells. BxPC-3 (left) and Capan-1 (right) cell adhesion was quantified after 90 min incubation over rh-E-selectin-Fc Chimera coated 96-well plates (previously incubated with Fc secondary antibody) with MTS-based colorimetric assay. Plots represent mean ± SD of adherent cells normalized to non-treated (control) cells of at least three independent experiments. Unpaired Student t-test was performed *, $p < 0.05$; **, $p < 0.01$, and ***, $p < 0.001$.

2.1.5 Ac$_5$3F$_{ax}$-Neu5Ac treatment reduced cancer cell migration

Aberrant sialylation has been described to modulate tumour progression, adhesion, migration, and invasion in several cancer cells [232,276,277,279]. Recently, diverse studies have

demonstrated that overexpression of STs correlates with increased migration capacity in PDA cells [270,271,326], and that overexpression of sLe antigens on cell membrane glycoconjugates plays a crucial role in enhancing mobility and metastatic capacities.

To investigate the potential of $Ac_5 3F_{ax}$-Neu5Ac to modulate the migratory capacity of BxPC-3 and Capan-1, cells were pre-treated with the ST inhibitor as previously described and allowed to migrate in modified Boyden chambers coated with Type-I collagen. Results showed that sialylation blockade produced by $Ac_5 3F_{ax}$-Neu5Ac treatment significantly impaired cancer cell migration in both cell lines. The reduction in cell migration comparing treated versus untreated cells was of 31% ± 15.5 in BxPC-3 and 25.0% ± 4.9 in Capan-1 cells (Figure 36). To determine if the reduction in cell migration observed in treated cells could be explained by sLe^x and sLe^a reduced expression, control cells were incubated with anti-sLe^x mAb CSLEX and anti-sLe^a mAb 121SLE for 20 min prior to their seeding in the transwells. BxPC-3 and Capan-1 cells treated with the anti-sLe^x mAb presented reduced migration ability in comparison to their respective controls, a reduction of 61.3% ± 3.3 in BxPC-3 and of 49.2% ± 5.0 in Capan-1. These levels of reduction were higher than the ones obtained after the $Ac_5 3F_{ax}$-Neu5Ac treatment, which could be explained by the non-complete blocking of sLe^x in the $Ac_5 3F_{ax}$-Neu5Ac treated cells. Regarding the anti-sLe^a mAb incubation, BxPC-3 cells presented a similar migration capacity compared to its untreated control, while Capan-1 incubated cells showed a slight increase in migration – up to 14.1% ± 8.0– vs untreated control cells, suggesting that sLe^a is not playing a role in modulating cell migration process in these PDA cells.
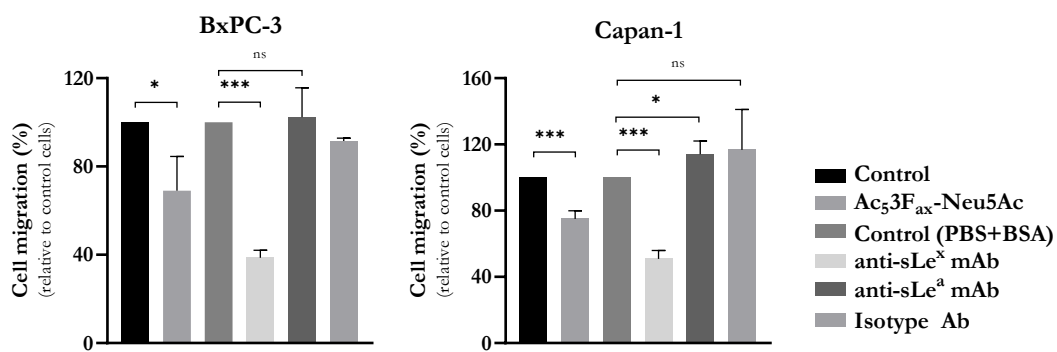
Figure 36. $Ac_5 3F_{ax}$-Neu5Ac treatment impairs cell migration of BxPC-3 and Capan-1 cells by reducing sLe^x expression. BxPC-3 (left) and Capan-1 (right) cells were pre-treated for 72 h with ST inhibitor. For the mAb treatments, cells were detached after the inhibitor treatment and incubated for 20 min at RT with the corresponding Ab. Then, cells were allowed to migrate through Collagen type-I coated transwells, for 18 h or 22 h for BxPC-3 and Capan-1 respectively. Migrated cells were fixed, stained and the area occupied by the cells was quantified with ImageJ software. Data of at least three independent experiments are represented as mean ± SD. *, $p < 0.05$; ** $p < 0.01$, and ***, $p < 0.001$.

2.1.6 Ac$_5$3F$_{ax}$-Neu5Ac treatment reduced cancer cell invasion

To assess if Ac$_5$3F$_{ax}$-Neu5Ac treatment had the potential to impair the invasion capacity of PDA cells, Matrigel-coated transwell invasion assays were performed. Prior to their seeding, BxPC-3 and Capan-1 cells were treated with Ac$_5$3F$_{ax}$-Neu5Ac during 72 h and allowed to invade for 24 h or 72 h, for BxPC-3 and Capan-1 cells respectively. The results showed that Ac$_5$3F$_{ax}$-Neu5Ac treatment significantly reduced cell invasion of pancreatic cancer cells, with a decrease of 25.3% $\pm$ 3.6 in BxPC-3 treated cells and a slight decrease of 12.6% $\pm$ 3.4 in Capan-1 treated cells in comparison to their respective untreated controls (Figure 37). To investigate the role of cell sialylation in cell invasion *in vitro*, cells were pre-incubated with blocking antibodies against sLe^x and sLe^a antigens and then allowed to invade in matrigel-coated transwells. The invasion capacity of BxPC-3 cells treated with anti-sLe^x and anti-sLe^a antibody was significantly reduced to a 38.7% $\pm$ 7.4 and to a 46.2% $\pm$ 26.6 vs untreated control cells, respectively, which pointed out a relationship between the reduction of sLe^x and sLe^a expression caused by Ac$_5$3F$_{ax}$-Neu5Ac treatment and the decrease in the invasiveness of BxPC-3 cells. Contrarily, the effect of the treatment with anti-sLe^x antibody in Capan-1 cells, which showed a decrease in the invasive capacity to a 26.0% $\pm$ 6.8, was not conclusive, since the isotype control also showed a significant decrease with respect to control cells (Figure 37). Overall, these results pointed out a relationship between the reduction of sLe^x expression caused by Ac$_5$3F$_{ax}$-Neu5Ac treatment and the decrease in the invasiveness of pancreatic cancer cells, which was not as clear with sLe^a expression and needs to be further investigated.
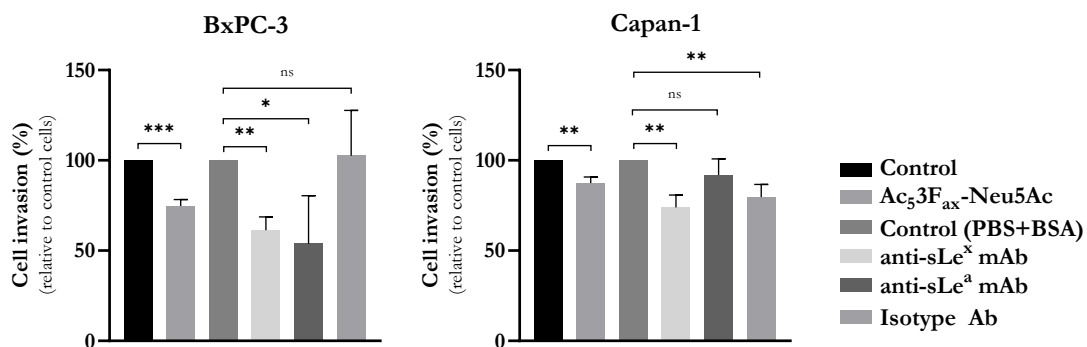
Figure 37. SA blockade caused by Ac$_5$3F$_{ax}$-Neu5Ac impairs cell invasion of BxPC-3 and Capan-1 cells *in vitro.* BxPC-3 (left) and Capan-1 (right) cells were pre-treated for 72 h with the SA inhibitor. For the mAb treatments, cells were detached after the inhibitor treatment and incubated for 20 min at RT with the corresponding Ab. Then, cells were allowed to invade in Matrigel coated inserts for 24 h or 72 h, for BxPC-3 and Capan-1 respectively. Invading cells were fixed, stained and the area occupied by the cells was quantified with ImageJ software. Data of at least three independent experiments are represented as mean $\pm$ SD *, p < 0.05; ** p < 0.01 and ***, p < 0.001.

Overall, Ac$_5$3F$_{ax}$-Neu5Ac effectively impaired the migration and invasion capacities of BxPC-3 and Capan-1 cells, as well as their ability to bind to E-selectin *in vitro*, a crucial mechanism regulating metastasis. Collectively, these results prompted us to evaluate the potential of Ac$_5$3F$_{ax}$-Neu5Ac to block sialylation *in vivo* on subcutaneous tumours generated in syngeneic immunocompetent C57BL mice and to assess if Ac$_5$3F$_{ax}$-Neu5Ac tumour treatment might affect tumour growth, modulate immune response or determine mice survival.

2.1.7 *In vivo* model in immunocompetent syngeneic mice: PDA tumours generated subcutaneously from murine pancreatic cancer cells

Blocking sialylation by genetically modifying ST expression or by sialidase treatment has been used to study the effects of sialoglycan expression on various cancer cells *in vitro* and appeared to be a useful approach to decipher the role of tumour SAs. To date, several studies have been performed *in vivo* to study the effect of sialylation blockade in established tumours and in their metastasis formation capacity although the application of these approaches to the clinical setting is complex. Nonetheless, the recent discovery of STs inhibitors have represented a new strategy to pharmacologically inhibit SA expression in tumours *in vivo* and could ease the path for a putative translation to the clinic. In this regard, Bull et al. demonstrated that Ac$_5$3F$_{ax}$-Neu5Ac effectively impaired melanoma cell growth and prevented metastasis formation *in vivo* [373,448]. Moreover, they reported that intratumoural injections of Ac$_5$3F$_{ax}$-Neu5Ac blocked sialylation in tumours, reduced tumour growth and modulated the immune response to create a TME permissive for immunotherapy.

To study the potential effect of Ac$_5$3F$_{ax}$-Neu5Ac on pancreatic tumours *in vivo,* sialoglycan expression pattern of murine pancreatic cancer cell lines and the effect of Ac$_5$3F$_{ax}$-Neu5Ac on those cell lines was first characterized. Afterwards, *in vitro* studies were performed to determine the effect of Ac$_5$3F$_{ax}$-Neu5Ac on murine PDA cell lines invasive capacities, and finally, subcutaneous tumours were generated into syngeneic C57BL mice to assess Ac$_5$3F$_{ax}$-Neu5Ac effect *in vivo*.

2.1.7.1. Syngeneic mice PDA cells characterization

To select the appropriate murine cell line to carry out the *in vivo* assay, the expression of α2,3-SA and α2,6-SA, as well as the expression of sLe^x and sLe^a sialylated antigens were characterized on twelve murine pancreatic cancer cell lines by WB and FC in 4 of them. First, whole cell lysates were immunoblotted with specific lectins (SNA and MAA-II) and with mAbs against sLe^x and sLe^a antigens. WB results (Figure 38) showed a similar pattern of bands below 95 kDa in all the lanes, suggesting unspecific binding, and some bands at high MW, both in sLe^x and sLe^a WBs proteins.
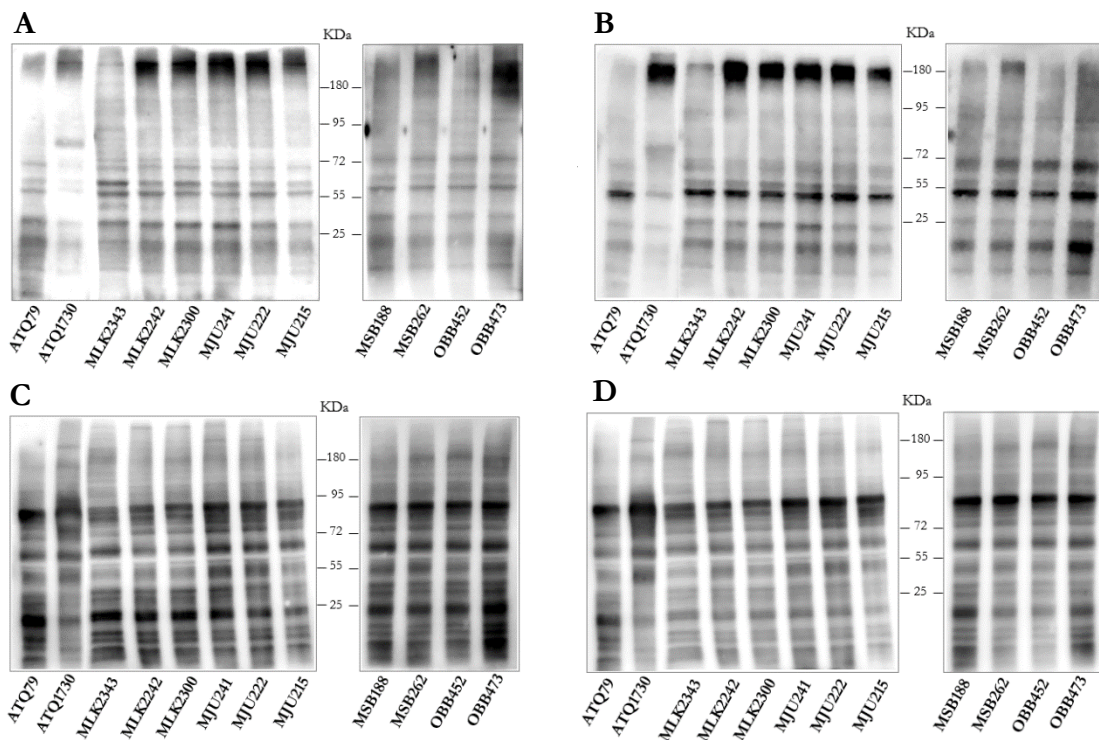
Figure 38. Sialoglycan pattern characterization of murine PDA cell lines by WB. Representative blots showing immunodetection of SLe^x (**A**) and sLe^a (**B**) antigens as well as α2,3- (**C**), and α2,6-SA (**D**) by WB of total cell lysates of the different murine PDA cell lines.

To investigate if this signal was specific for sLe^x and sLe^a, OBB473, OBB452, MSB262, and MJU241 cells, which showed different signal intensity in this region, were also analysed by FC. SNA and MAA-II detection also showed similar pattern among the cell lines and were also analysed by FC. SLe^x and sLe^a antigens were not detected on cell surface glycoconjugates of any of the four murine cell lines OBB473, OBB452, MJU241, and MSB262 by FC (Figure 39). Regarding α2,3/6-SA expression, FC analyses showed that OBB473, OBB452, and MSB262 cell lines expressed high levels of α2,6-SA (detected by SNA lectin) and moderate levels of α2,3-SA (detected by MAA-II lectin), while MJU241 cell line presented low levels of α2,6-SA expression and undetectable α2,3-SA expression (Figure 39).
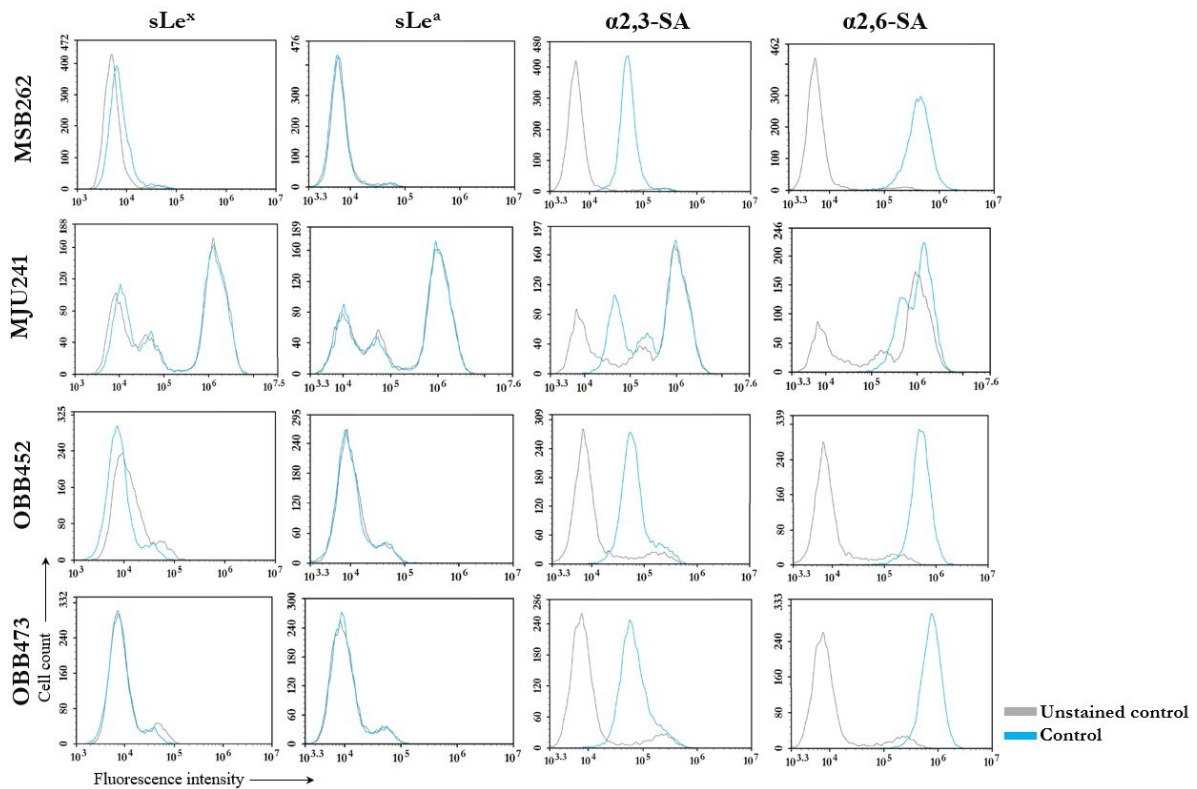
Figure 39. Cell surface glycan analysis of murine PDA cell lines by FC. Representative histograms of the cell surface glycans structures detected by sLe^x and sLe^a antibodies, and the lectins SNA (α2,3-SA) and MAA-II (α2,6-SA).

Next, to confirm these results, we immunoblotted MJU241, OBB473, and OBB452 cell lysates, together with Capan-1 cell lysate as a positive control (presents high sLe^x expression levels) and did not detect any signal for sLe^x at high molecular weight for the murine cells lysates, while Capan-1 did show signal for sLe^x (Figure 40). A control WB without the primary antibody against sLe^x to discard that the signal was derived from unspecific secondary antibody binding was performed with cell lysates from MJU222, MSB262, and MLK242 murine cells and Capan-1 cells and no signal was detected. The difference in sLe^x expression of the murine cell lines when comparing this last WB (figure 40), that contained a positive control, with the previous WB (Figure 38) without a positive control, could be explained by an over-exposition of the membrane that generated an unspecific signal in all lanes. Altogether, these results indicate that we were not able to detect the expression of sLe^x on these cell lines, probably due to the poor reactivity of the conventional anti-sLe^x antibodies (mAb) against mice tissues and cells. The poor reactivity of the mAb could be attributed to the fact that an important proportion of terminal SA in WT mice is in the form of Neu5Gc, whereas most existing mAbs react with glycans containing terminal Neu5Ac [449].
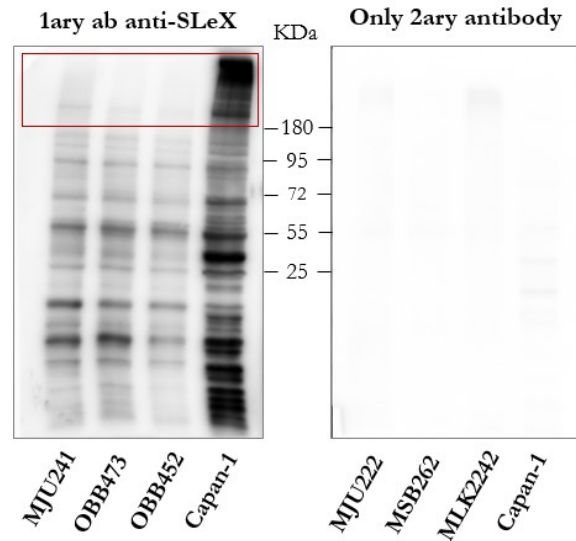
Figure 40. Pancreatic cancer cell lines immunoblots of sLe^x from total cell lysates. Blots showing immunodetection of sLe^x with Capan-1 cell line as a positive control (left) and (right) immunoblot without primary antibody (only secondary antibody) as a negative control. Red square indicates sLe^x immunoreactive bands.

2.1.7.2. STs inhibitor treatment decreased sialic acid expression on murine MSB262 and OBB452 cell lines

Next, we assessed the optimal dose of Ac_5F_{ax}-Neu5Ac and the best treatment time for OBB473, OBB452, MSB262, and MJU241 cell lines to decrease cell surface SA expression. Cells were incubated for 48 h and 72 h with increasing concentrations of Ac_5F_{ax}-Neu5Ac (0 µM, 50 µM, 100 µM, 200 µM). Results indicated that 200 µM was the optimal dose and 72 h the optimal treatment time, as it caused the highest decrease in α2,3-SA and α2,6-SA expression for all the cell models, except for MJU241 cells that were not sensitive to Ac_5F_{ax}-Neu5Ac. MSB262 and OBB452 cell lines were selected as the best candidates to carry out the following experiments, as they displayed the highest reduction in SA expression upon Ac_5F_{ax}-Neu5Ac treatment.

Once the optimal dose of the inhibitor and the treatment time were established, the reduction of α2,3- and α2,6-SA expression and the subsequent increase of the exposed terminal Gal residues (specifically detected by PNA lectin) were analysed by FC (Figure 41). Results showed that Ac_5F_{ax}-Neu5Ac treatment led to a significant decrease in α2,6-SA expression in OBB452 cells –up to 63.4% ± 12.0– and in MSB262 cells –up to 68.2% ± 5.7–. Regarding α2,3-SA expression, a decrease of 29.6% ± 8.36 was detected in MSB262 treated cells while for OBB452, Ac_5F_{ax}-Neu5Ac treatment caused an increased expression of α2,3-SA. Accordingly, a large increase in the exposure of Gal residues was detected in both treated cell lines (989.2% in OBB452 and 108.8% in MSB262) (Figure 41).

Contrarily to what we described for BxPC-3 and Capan-1 human pancreatic cancer cells, Ac_5F_{ax}-Neu5Ac had a more relevant effect on α2,6-SA than on α2,3-SA expression in the OBB452 and MSB262 murine cells.
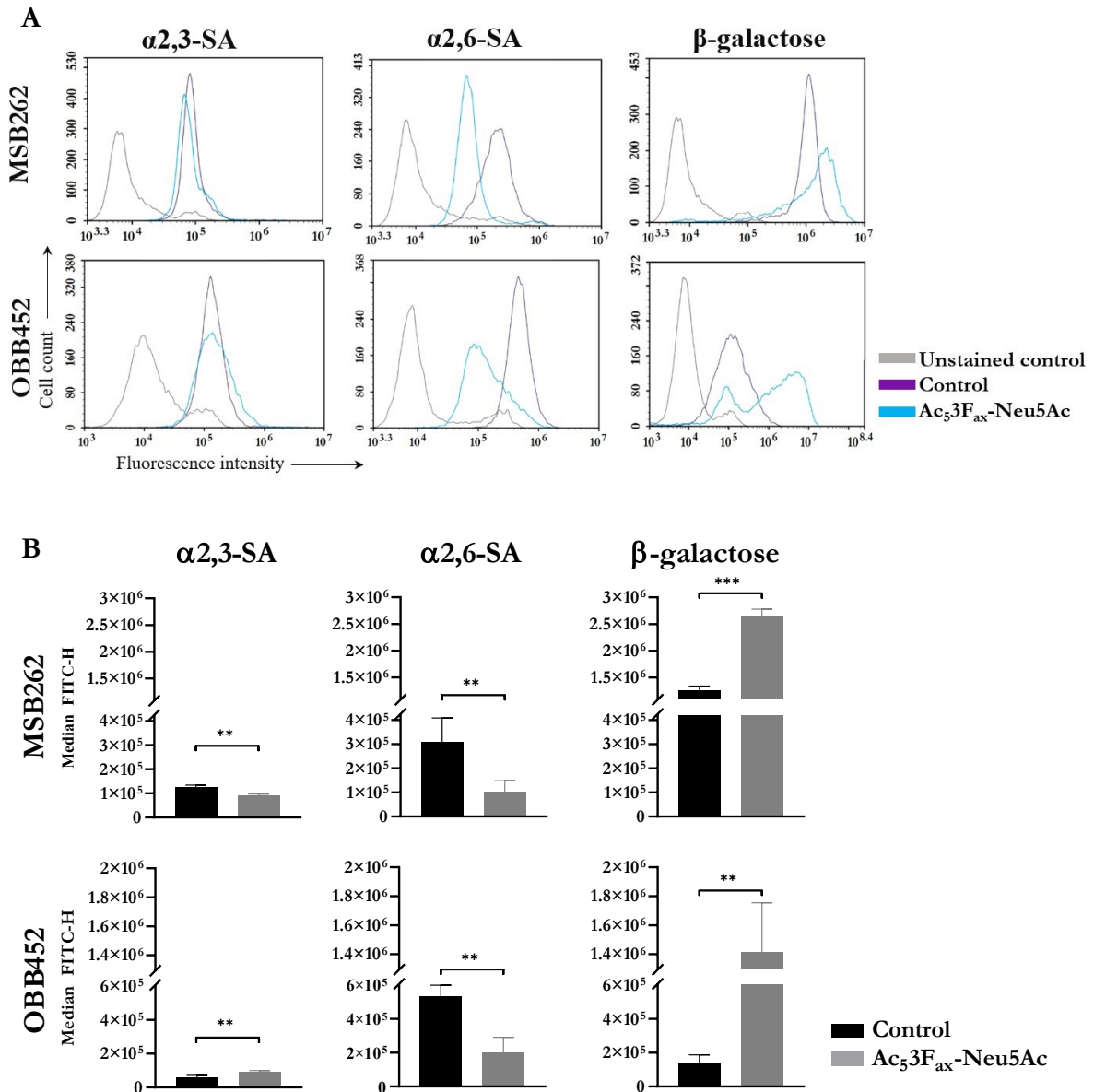
Figure 41. Ac_5F_{ax}-Neu5Ac reduced sialylation in OBB452 and MSB262 murine pancreatic cancer cell lines. A. Representative histograms showing the expression levels of α2,3-SA, detected by MAA-II lectin; α2,6-SA, detected by SNA lectin; or the exposure of terminal β-galactose by PNA lectin. **B.** Median fluorescence for each glycan structure of treated (200 μM Ac_5F_{ax}-Neu5Ac) and control OBB452 and MSB262 cells are represented. Plots show mean ± SD of at least three independent experiments. * $p < 0.05$; ** $p < 0.01$, and ***, $p < 0.001$.

2.1.7.3. STs inhibitor effect on migration and invasion *in vitro* assays

The effect of Ac_5F_{ax}-Neu5Ac was analysed *in vitro* in migration and invasion assays. OBB452 and MSB262 cells were pre-treated with 200 μM Ac_5F_{ax}-Neu5Ac during 72 h and allowed to migrate in modified Boyden chambers coated either with Type-I collagen for migration

assays or with Matrigel for invasion assays. Results showed that $Ac_5 3F_{ax}$-Neu5Ac treatment significantly impaired cancer cell migration in MSB262 treated cells in comparison to untreated control cells (reduction of 23.2% ± 8.0), but had no effect on OBB452 cell migration (Figure 42A). Results of the Matrigel-coated transwell assay indicated that the invasion capacity of MSB262 cells was significantly impaired by $Ac_5 3F_{ax}$-Neu5Ac treatment, causing a reduction of 19.6% ± 2.1 of the invasion capacity vs control cells. Again, OBB452 treated cells had similar invasion capacity to their untreated control cells, indicating that $Ac_5 3F_{ax}$-Neu5Ac treatment did not impair cell invasion in this cell line (Figure 42B).

Altogether, these results confirmed that $Ac_5 3F_{ax}$-Neu5Ac blocks SA expression in mice cell lines *in vitro* without affecting cell viability (data not shown), and showed that cell sialylation plays a key role in regulating migration and invasion processes in MSB262 murine PDA cells, but not in OBB452 ones, suggesting that the reduction in α2,3-SA is important to alter cell functional capabilities tightly linked to PDA progression and metastasis formation.
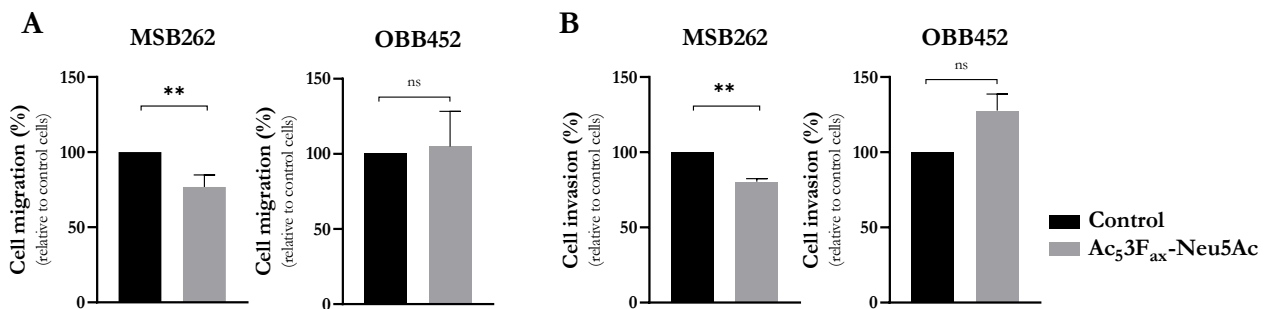
Figure 42. $Ac_5 3F_{ax}$-Neu5Ac treatment impaired cell migration and invasion of MSB262 but not OBB452 cells. OBB452 (left) and MSB262 (right) cells were pre-treated for 72 h with the ST inhibitor and allowed to (**A**) migrate through Collagen type-I coated transwells, for 24 h or (**B**) invade into Matrigel coated inserts for 24 h (OBB452 cells) or 48 h (MSB262 cells). Migrated/invading cells were fixed, stained and the area occupied by the cells was quantified with ImageJ software. Data of at least 3 independent experiments are represented as mean ± SD *, p < 0.05 and ** p < 0.01.

2.1.7.4. Effect of Ac53Fax-Neu5Ac on the growth of tumours generated by subcutaneous injection of MSB262 cells in syngeneic mice

With the aim of analysing the effect of $Ac_5 3F_{ax}$-Neu5Ac on tumour growth and its putative correlation to increased mice survival time, 0.5×10^6 MSB262 cells were injected into each posterior flank of C57BL immunocompetent mice to generate subcutaneous tumours. Based on the data published by Büll et al. and our own results, indicating that cells recover basal SA levels 2 days (for α2,6-linked SA) or 4 days (for α2,3-linked SA) after $Ac_5 3F_{ax}$-Neu5Ac treatment removal, and considering the treatment schedule and dosage used in their *in vivo* study, we decided to apply the following treatment regimen. When palpable tumours appeared, mice were intratumourally administered with 10 mg/kg or 20 mg/kg of $Ac_5 3F_{ax}$-

Neu5Ac three times per week during two weeks (Figure 43A). Injections with physiological saline solution or excipient (DMSO) were used as controls.

Intratumoural injections with 10 mg/kg $Ac_5 3F_{ax}$-Neu5Ac resulted in a significant reduction of the tumour volume compared to control group (that comprised the mice injected with physiological saline solution and with DMSO) 8 days after the start of the treatment and that was sustained until the end of the treatment (Figure 43B). Likewise, 20 mg/kg $Ac_5 3F_{ax}$-Neu5Ac injections resulted in a decrease of tumour volume, although it was only statistically significant at day 10 of drug administration (Figure 43B).

On the other hand, results showed a trend of 10 or 20 mg/kg $Ac_5 3F_{ax}$-Neu5Ac administration to increase median mice survival time although it was not statistically significant (Figure 43C). We hypothesize that the lack of significance might be explained by the extremely fast growth of tumours, which forced us to sacrifice the mice earlier than expected, following ethical guidelines, and hinder the study of mice survival. Moreover, increasing the number of animals per group would probably help to improve statistical power of the experiment.

Overall, these findings suggest that the treatment with this SA mimetic effectively slows down pancreatic tumour growth, being 10 mg/kg $Ac_5 3F_{ax}$-Neu5Ac dose the more effective one, and that further studies are needed to overcome the assay limitations described and determine the effect of $Ac_5 3F_{ax}$-Neu5Ac on mice survival.
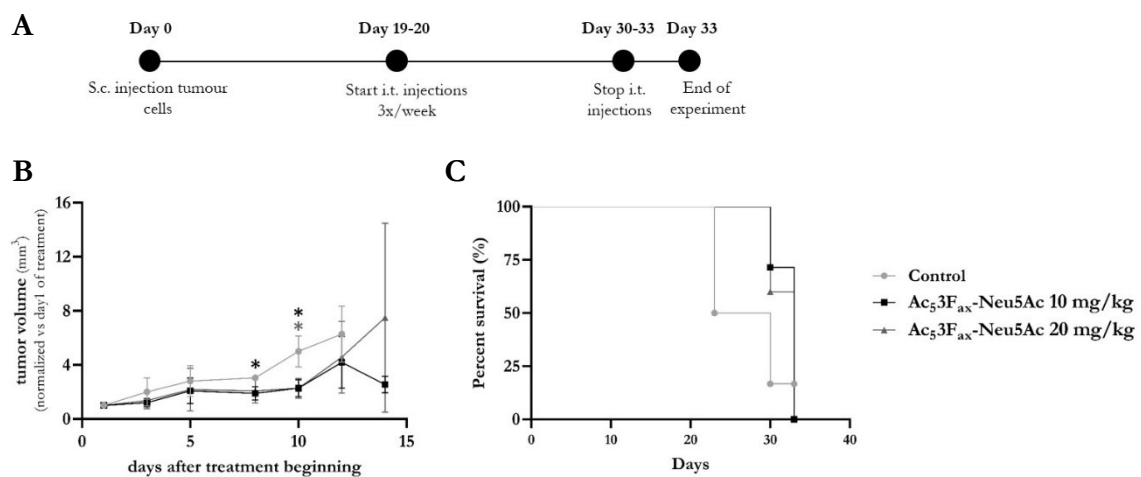
Figure 43. Effect of intratumoural $Ac_5 3F_{ax}$-Neu5Ac injections in tumour growth. A. Time-based diagram of the experiment. **B.** MSB262 cells were inoculated subcutaneously and tumours were treated with PBS, DMSO, 10 mg/kg or 20 mg/kg $Ac_5 3F_{ax}$-Neu5Ac. Tumour volume was measured thrice per week since the beginning of the tumour treatment. Tumour volumes are represented as mean values of each group $\pm$ SD, and normalized vs their tumour volume of the first day of administration. * p < 0.01. **C.** Kaplan-Meier curve corresponding to mice survival of each mice group are represented.

2.1.7.5. Ac$_5$3F$_{ax}$-Neu5Ac reduced sialic acid expression on tumour cells and altered the tumour immune component

To determine if Ac$_5$3F$_{ax}$-Neu5Ac administration could block SA expression on tumour cells *in vivo*, tumours were collected after two weeks of 10 or 20 mg/kg Ac$_5$3F$_{ax}$-Neu5Ac intratumoural injections and were analysed by FC. Leukocyte marker CD45.2 was used to differentiate tumour cells (CD45.2 negative) and the immune cells (CD45.2 positive).

Regarding the changes in SA expression, FC results with SNA and MAA-II lectins revealed that 10 mg/kg Ac$_5$3F$_{ax}$-Neu5Ac injections caused a reduction of 15.7% ± 2.5 on α2,6-SA expression and a significant reduction of 23.6% ± 5.3 on α2,3-SA expression on treated-mice tumour cells in comparison to control-mice tumour cells (Figure 44). For tumours administered with 20 mg/kg Ac$_5$3F$_{ax}$-Neu5Ac, we could only detect a slight decrease of SA expression.

When comparing the percentage of CD45.2$^+$ cells vs CD45.2$^-$ cells of the tumours, we detected an increase of the immune cell to tumour cell ratio in the 10 mg/kg Ac$_5$3F$_{ax}$-Neu5Ac treated tumours compared with control-injected tumours, indicating that Ac$_5$3F$_{ax}$-Neu5Ac injections potentiate the infiltration of immune cells into the tumour mass (Figure 44).

Next, we assessed the effect of Ac$_5$3F$_{ax}$-Neu5Ac on the immune cell composition: T-lymphocytes (CD4$^+$ and CD8$^+$), B-cells, natural killer (NK) cells, granulocytes, monocytes and macrophages in the MSB262 generated tumours after two weeks of treatment. Results revealed an increase in the percentage of infiltrating T cell population (CD3+) in treated-mice tumours compared with control-mice tumours (treated with either PBS or DMSO), being significant for the 10 mg/kg Ac$_5$3F$_{ax}$-Neu5Ac treated tumours. In particular, we detected a significant increase in the CD4$^+$ and CD8$^+$ T cell population within the viable, tumour-infiltrating leucocyte population (CD45$^+$ cells) in the 10 mg/kg Ac$_5$3F$_{ax}$-Neu5Ac treated tumours with respect to control tumours. Moreover, Ac$_5$3F$_{ax}$-Neu5Ac injections increased the percentage of NK cells, especially in the 10 mg/kg Ac$_5$3F$_{ax}$-Neu5Ac treated tumours. The percentage of myeloid regulatory cells (granulocytes and monocytes) in the 10 mg/kg Ac$_5$3F$_{ax}$-Neu5Ac treated tumours showed an increasing trend, while the percentage of B cells and macrophages remained unaltered in that group with respect to the control one (Figure 44).

These results collectively suggest that Ac$_5$F$_{ax}$-Neu5Ac treatment at the dose of 10 mg/kg Ac$_5$F$_{ax}$-Neu5Ac significantly alters the immune cell component of the TME by increasing infiltrating T cell population, including CD8$^+$ T cells; and an increasing trend of infiltrating NK cells, altogether, increasing the immune response against the tumour. Nonetheless, further assays would help to determine the consequences of the increasing trend in infiltrating granulocytes and monocytes in the 10 mg/kg Ac$_5$F$_{ax}$-Neu5Ac treated tumours.
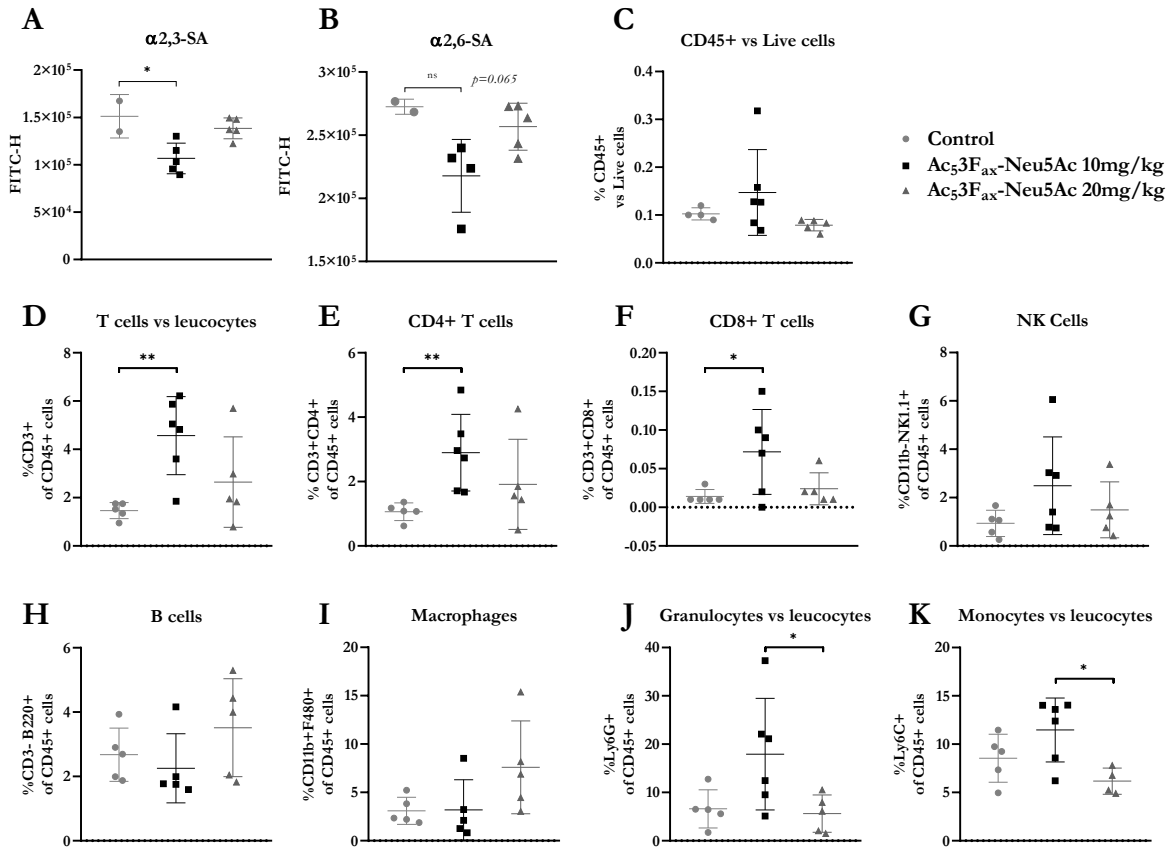
Figure 44. Intratumoural Ac$_5$F$_{ax}$-Neu5Ac injections reduced SA expression of tumour cells and altered the immune cell composition of the tumour. Analysis of cell surface sialoglycans expressed by MSB262 tumour cells isolated from control or 10 mg/kg and 20 mg/kg Ac$_5$F$_{ax}$-Neu5Ac treated tumours by FC. Dot plots showing mean ± SD of (**A**) α2,6-SA and (**B**) α2,3-SA expression levels of the different treatment groups. **C.** Analysis of immune infiltrating cells, dot plots showing mean ± SD of (**D**) CD3$^+$CD45.2$^+$ T cells, (**E**) CD4$^+$ T cells, (**F**) CD8$^+$ T cells, (**G**) CD11b$^+$ NK1.1$^+$ cells, (**H**) CD3$^-$B220$^+$ B cells, (**I**) CD11b$^+$ F480$^+$ Macrophages and (**J**) Ly6G$^+$, or (**J**) Ly6C$^+$ myeloid cells in the tumours of the different treatment groups (n=6). * p < 0.05 and ** p < 0.01.

2.2 Discussion

Aberrant sialylation has been closely associated with cancer progression and metastatic spread, promoting cell migration and invasion, angiogenesis, cancer cell survival, resistance to apoptosis, and evasion of the immune system among others. Considering that STs catalyse a late stage reaction in sialoglycan formation and have a major role in promoting tumour progression, they have been postulated as potential cancer biomarkers. In addition, diverse strategies have been developed to inhibit ST activity, and in consequence, to reduce cellular hypersialylation. Extensive literature, including some of the works of our group [270,271,299,326], reported that the silencing of STs by genetic modification causes a reduction in the sialome of diverse cancer cell models, and effectively diminishes their pro-tumorigenic capacities and metastatic potential. In addition, in the past two decades research in this field has focused on the development of ST inhibitors as potential therapeutic agents for clinical treatment of cancer progression and metastasis formation. Currently, many of the developed inhibitors are not appropriate for clinical use as they present low cell-permeability, cell toxicity or other limitations to overcome, although some of them have shown promising results *in vivo*.

In this chapter of the thesis, we have investigated the potential of three ST inhibitors to block SA expression in PDA BxPC-3 and Capan-1 cell models: AL10, SsaI, and Ac_53F_{ax}-Neu5Ac. Considering that Ac_53F_{ax}-Neu5Ac exerted the major reduction on the SA expression of PDA human cells, we have set the focus on this inhibitor and carried out *in vitro* functional experiments with human and murine PDA cell lines, and performed an *in vivo* assay. Importantly, up to our knowledge, this is the first study that reports the effect of the ST inhibitor Ac_53F_{ax}-Neu5Ac in PDA cell models and analyses its effect on tumour growth and tumour immunity *in vivo*. Despite the fact that further studies are warranted to understand the underlying mechanisms, the data presented in this work might pave the way for the broader use of these metabolic inhibitors to evaluate the role of sialylated glycans in tumour progression and for its possible therapeutic application.

2.2.1 Sialic acid characterization of PDA human cells

SA expression of BxPC-3 and Capan-1 cells was previously characterized in our lab [326] and data presented in this thesis confirmed that Capan-1 cell model expresses higher sLe^x levels than BxPC-3, similar α2,6-SA levels for both cell lines, while BxPC-3 expresses higher α2,3-SA levels than Capan-1 cells. The only difference between the two studies was the expression levels of sLe^a for both cell lines, which was higher on Capan-1 cells than on BxPC-3 cells in this study, contrary to what was previously described in [326]. This variability could be attributed

to the use of two different anti-sLe[a] antibodies: for the first study, we used an antibody produced by De Bolós et al. (57/27 Anti-CA 19-9) [450] that is not available at the present, so for the study herein we used a commercial one (121SLE, Ab3982, Abcam).

2.2.2 AL10 and SsaI sialyltransferase inhibitors do not significantly decrease sialic acid expression on BxPC-3 and Capan-1 cells

AL10 was first developed by Chiang et al. in 2010 as a non-competitive inhibitor of α2,3-ST and appeared to have a potent anti-cancer effect. Chiang et al. demonstrated that AL10 effectively impaired cell migration and invasion *in vitro* in lung cancer cells by inhibiting integrin-mediated signalling, without causing cytotoxicity. Furthermore, it was the first STs inhibitor exhibiting important anti-metastatic activity *in vivo* since it supressed experimental lung metastasis in a murine model [391]. Similarly, Su et al. established that AL10 treatment supressed Chemokine ligand 19 (CCL19)-stimulated proliferation, invasion and anti-anoikis by blocking Chemokine receptor 7 (CCR7) sialylation in breast cancer cells, as well as inhibiting tumorigenicity of breast cancer in animal models [451]. Thus, it was considered a good candidate to perform further preclinical assays as a novel pharmacologic compound for cancer treatment. In this study, we aimed to determine the potential of this inhibitor to block sialylation in PDA cell models and showed that 2,5μM AL10 inhibitor slightly diminished the expression of cell surface α2,3-linked SA (determined by MAA-II lectin and sLe[x]) on BxPC-3 cells. However, the results were not dose-dependent and not consistent for other α2,3-sialylated epitopes such as sLe[a] and therefore we did not proceed with further functional studies. Unfortunately, AL10 inhibitor did not block SA expression on Capan-1 cells. We hypothesized that poor cell permeability of AL10 in the PDA cell lines could be one of the reasons to explain its lack of activity.

Other Lith analogues have been described as potent anti-cancer compounds in line with the findings described for AL10 inhibitor. First, Chen et al. found that Lith-O-Asp effectively decreased some ST enzymes activity *in vitro* and inhibited migration and invasion in diverse lung and breast cancer cell lines. In addition, Lith-O-Asp delayed cancer cell metastasis and spontaneous metastasis formation in animal models probably by inhibiting integrin sialylation and FAK/paxillin signalling pathway and expressing antiangiogenesis factors [452]. Very recently, Fu et al. reported that FCW34 and FCW66 ST inhibitors selectively impaired induced cell migration via inhibition of α2,3-ST3Gal III-catalyzed *N*-glycoprotein sialylation in MDA-MB-231 breast cancer cells. Likewise, they showed that the decrease of *N*-

glycosylation caused by FCW34 treatment impaired cancer cell metastasis via regulation of talin/integrin/FAK/paxillin and integrin/NFϰB signalling pathways [392].

Notwithstanding, the discrepancies between our data and the findings described in these studies, together with the fact that most of the studies showing potent activity for these inhibitors have been performed in lung and breast cancer models, let us to hypothesise that the inhibitor effect might be cancer-type specific. Therefore, further investigations in more PDA models are required to elucidate the impact of AL10 inhibitor on PDA.

Referring to SsaI inhibitor, it was discovered two decades ago by Tsai group [386] and it has been reported to be a potent α2,3-ST inhibitor in diverse cancer cell and animal models. Tsai group described in the early 2000's that SsaI caused a two-fold decrease in α2,3-STs activity on breast and melanoma cancer cells, impaired cell migration capacity of those cells, and although it enhanced cell adhesion, it reduced the ability of melanoma cells to generate pulmonary metastasis [387,388]. Few years later, it was reported by Wang group that SsaI inhibited cell migration and dissemination in an *in vivo* mouse model transplanted with ovarian cancer cells, and acted in synergy with an EGFR inhibitor to enhance its anti-tumour effects on epithelial ovarian cancer (EOC) cells, findings that were lately reconfirmed on clear-EOC cell lines [422,438]. Nevertheless, we found that SA expression of BxPC-3 and Capan-1 PDA cells remained intact after the inhibitor treatment at all of the tested doses, indicating that SsaI was not able to block SA expression on these cell lines. The cell permeability of this compound was not investigated in these PDA cells and could be one of the reasons that could explain its lack of activity. In conclusion, additional evidence are required to explain why SsaI inhibitor significantly generates a sialylation blockade in breast, melanoma and ovarian cancer models but does not alter SA expression on the studied pancreatic cell models.

2.2.3 Ac_5F_{ax}-Neu5Ac inhibits cell surface sialylation in human and murine PDA cells

In order to inhibit cell sialylation, Rillahan and colleagues synthetized the ST inhibitor Ac_5F_{ax}-Neu5Ac in 2002 and described that it was able to inhibit sialylation in human leukaemia cell lines at a concentration around 64 μM [366], a dose that was later described by Büll et al. to be sufficient to reduce α2,3- and α2,6-sialylation by more than 90% in murine melanoma cell lines [371]. In this Thesis, we first performed a Ac_5F_{ax}-Neu5Ac dose-finding *in vitro* study, similarly to what was described by Rillahan et al.[366], and found that the most effective dose for human PDA BxPC-3 cells (100 μM) was in line with the described data, while the optimal dose for the murine cell lines was slightly higher (200 μM). For Capan-1

cells, the dose required to achieve the highest reduction in all the SA determinants was 400 µM, resembling the findings described by Natoni and colleagues, who treated highly metastatic multiple melanoma murine cells with 300 µM $Ac_5 3F_{ax}$-Neu5Ac [374]. Referring to the treatment time, we showed that the optimal treatment time for all the cell lines was 3 days, which was in accordance with the previous studies [366,371–373], with the exception of Natoni et al. report [374], in which cells were treated with the inhibitor for 7 days.

In this study, we have shown for the first time that $Ac_5 3F_{ax}$-Neu5Ac treatment efficiently inhibit cell surface sialylation of human and murine PDA cells without affecting cell viability. In line with the findings described by Natoni et al. [374], $Ac_5 3F_{ax}$-Neu5Ac treatment led to an important reduction of sLe^x expression around 85% on human PDA cells and a reduction of 75-85% in the expression of α2,3-linked SA, in accordance with the data showed by Rillahan and Büll [366,371]. The decrease in α2,6-SA was lower (28-38%) than for α2,3-SA (75-85%) for the human PDA cell lines, in accordance with Büll et al. [371], which suggests $Ac_5 3F_{ax}$-Neu5Ac blocks α2,3-STs more effectively than α2,6-STs. Regarding murine cell lines, we have shown that $Ac_5 3F_{ax}$-Neu5Ac treatment inhibited α2,3- and α2,6-sialylation in MSB262 cell line by 30% and 65% respectively, which was a lower reduction than what was achieved for leukaemia and myeloma cell lines. Contrarily to the trend observed in human PDA cell lines, in the murine MSB262 cells $Ac_5 3F_{ax}$-Neu5Ac treatment resulted in higher decrease of α2,6-SA than α2,3-SA [371].

Moreover, although direct evidence is lacking, we hypothesised that the remaining SA expression that we were not able to eliminate might represent SA that is internalized from the cell culture media, STs that might have lower affinity to the inhibitor or the presence of stable sialoglycans with a slow turnover.

Considering the results obtained in a recent study of our lab [326], in which we analysed the sialylation changes on ST3GAL3 and ST3GAL4 STs KD PDA cells, we concluded that $Ac_5 3F_{ax}$-Neu5Ac treatment caused a more efficiently and generalised SA expression reduction than the specific ST silencing in PDA cell models, suggesting that this ST inhibitor might be considered as a promising candidate to reduce hypersialylation present on most cancer cells.

In this regard, we carried out an experiment to decipher if the combination of two strategies to inhibit ST activity, the genetic modification of cells to silence STs with shRNA and the cell treatment with the $Ac_5 3F_{ax}$-Neu5Ac inhibitor, could lead us to achieve a maximal reduction of cell sialylation. Interestingly, we confirmed that the inhibitor effect alone was

sufficient to reduce cell sialylation since the reduction obtained for the ST3GAL4 KD cells treated with the inhibitor was either similar or lower than the one obtained by treating control cells with the same dose of the inhibitor.

2.2.4 $Ac_5 3F_{ax}$-Neu5Ac effect on E-selectin binding

Tumour metastasis is a multistep process in which malignant cells separate from the primary site, intravasate into blood vessels to travel to a distant organ, where they adhere to the vascular endothelium and penetrate into the secondary tissue to form new tumour colonies. During the dissemination of tumour cells, tethering, rolling and firm adhesion steps are of crucial importance before the extravasation to secondary tumour sites, and glycoproteins are involved in all of them. It has been extensively described that sLe antigens found on the surface of circulating adenocarcinoma cells act as ligands to selectins expressed on activated endothelial cells, being E-selecting of particular importance in the adhesion of tumour cells to endothelial cells and by extension, to tumour invasion and metastasis [453]. During the last decades, the inhibition of selectin-ligands through diverse experimental interventions has been used to target metastasis and tumour growth, which are of particular importance to fight against PDA, since metastasis formation occurs in most of the detected PDA cases.

Paulson's group described in the early 90's that the cell adhesion by E-selectin was mediated by the carbohydrate antigen sLe^x [454], but few years later Takada and co-authors postulated that sLe^a could also act as a ligand for E-selectin expressed on cytokine-activated human endothelial cells [453]. Posterior studies demonstrated that both carbohydrate antigens are expressed on the cell surface of circulating tumour cells [309,455] and bind to E-selectin expressed on activated endothelium. Nonetheless, some of them revealed that sLe^x was the main ligand by completely inhibiting the adhesion to E-selectin when blocking PDA cells with anti-sLe^x antibodies [326,456,457], while others postulated that in tumours of the digestive tract such as colon and pancreas, with the exception of the liver, tumour cells bind to E-selectin preferentially via sLe^a rather than sLe^{x} [453].

In this study, we have shown that $Ac_5 3F_{ax}$-Neu5Ac treatment of BxPC-3 and Capan-1 PDA cells, and the subsequent reduction of sialylated determinants including sLe^x and sLe^a expression, led to a significant impairment of the adhesion of tumour cells to human recombinant E-selectin. The results observed – reduction of around 60% for treated BxPC-3 cells and 75% for treated Capan-1 cells in comparison to untreated control cells– were in consonance with our previous findings with these PDA cell lines [326], and with studies performed by other groups. In this regard, Rillahan et al. and Natoni et al. demonstrated that

reduction of sLe^x and sLe^a caused by Ac$_5$3F$_{ax}$-Neu5Ac treatment, led to a significant decrease in the interaction between tumour cells and E-selectin in human leukaemia and melanoma cells [366,374]. Besides, SsaI was also described to block sialylation and inhibit tumour cell adhesion to endothelial monolayers [387].

Moreover, genetic modification strategies have been used to block cell sialylation in PDA cell models, as well as in other carcinomas such as lung or colon cancer, remarking the relevance of sLe antigens in the adhesion of tumour cells to E-selectin, involved in the last steps of the metastatic cascade. For instance, the reduction of sLe antigens expression derived from the invalidated expression of FUT3 in BxPC-3 cells was associated to an inhibition of the E-selectin adhesion and a decrease of the metastatic power of the genetically modified cells (16). Similarly, Zhan et al. demonstrated that the KD of FUT3 in Capan-1 cells impaired cell adhesion to E-selectin and inhibited TGF-β-induced epithelial-mesenchymal transition (EMT), suggesting a significant relation between those sialylated determinants and EMT in PDA [459]. In line with these findings, the restoration of FUT1 expression, which is normally decreased in human metastatic PDA cells and outcompetes for the same substrate of α2,3-STs to catalyse the transfer of SA, led to a decrease in the adhesive and metastatic properties of BxPC-3 cells, and a decrease in metastasis formation after xenograft transplantation into nude mice [460]. In parallel, previous results from our group revealed that the overexpression of ST3GAL3 and ST3GAL4 in PDA cell lines, which catalyse the final steps of sLe antigens biosynthesis, was associated with an increased adhesion and metastatic capacity of PDA cells *in vitro,* and a higher metastasis formation when injected into athymic nude mice [270,271].

Collectively, Ac$_5$3F$_{ax}$-Neu5Ac was capable of reducing sLe antigens in PDA cells and, consequently, impaired their adhesion to E-selectin, which is a key step that facilitates tumour cell extravasation, and is closely associated with an invasive and metastatic phenotype of PDA.

2.2.5 Ac$_5$3F$_{ax}$-Neu5Ac effect on cell migration and invasion capacities

Throughout the course of disease, cancer cells experience several essential events, being adherence to proteins of the ECM, migration on and degradation of ECM proteins and invasion into nearby tissues of critical importance, as well as the spreading to distant organs to form a metastatic tumour. Although the molecular mechanisms underlying these processes are yet not fully understood, there is growing evidence indicating that the interactions between cell-cell and cell-ECM might be clearly altered during the tumour cell dissemination

[16,461,462]. Several studies have demonstrated that SA determinants modulate cell-ECM adhesion and migratory processes of various human cancer models, including pancreatic, gastric and breast cancer [270,271,293,299,326,421,463,464]. Indeed, previous studies from our lab established a correlation between the α2,6-SA cell surface levels and the adhesion capacity to ECM components, such as collagen and fibronectin, as well as a correlation between α2,3-SA expression level, and migration and metastatic ability [270,325].

In the present study, we have evaluated whether the sialylation decrease caused by Ac5F$_{ax}$-Neu5Ac treatment might alter the migratory and invasive capacities of BxPC-3, Capan-1, MSB262 and OBB452 pancreatic cancer cell lines. In agreement with previous studies, we have demonstrated that targeting α2,3- and α2,6-sialylation with the ST inhibitor Ac5F$_{ax}$-Neu5Ac could effectively impair the tumour progression related abilities of pancreatic cancer cell lines, supporting the idea that cell sialylation has a determinant role in the regulation of migration and invasion processes.

BxPC-3 and Capan-1 treated cells showed a significant reduction in the migratory (30-25%) and invasive abilities (25-12% respectively) compared to untreated cells, in line with the findings described by Büll et al. [371], which demonstrated that Ac5F$_{ax}$-Neu5Ac inhibitor remarkably impaired adhesion to ECM components and migration of melanoma cells. Likewise, results obtained with other STs inhibitors (SsaI and AL10) showed that inhibition of α2,3-sialylation impaired cell motility, adhesion and migration through ECM components and cell invasion in ovarian and lung cancer cells [387,391,438]. Furthermore, previous studies have stated that the overexpression or down-regulation of ST3GAL3 and ST3GAL4 genes, and the concomitant increase or decrease of sLe^x levels respectively, correlates with cell migration and invasive phenotype of PDA cells [270,271,325] and other cancer models such as gastric or breast [421,464]. In this work, we performed blocking experiments by treating the human PDA cells with anti-sLe^x and anti-sLe^a antibodies. In accordance with previous results, we found that blocking sLe^x led to a significant reduction in BxPC-3 and Capan-1 cell migration and invasion abilities, which reinforces the importance of sLe^x determinant in the modulation of invasion and migration processes.

Considering that one of the main characteristics of PDA is a particularly high desmoplasia [71,72], many studies have converged on the idea that the adhesion and migration through the ECM protein type I collagen has a determinant role in favouring a more motile phenotype on PDA cells and promoting its metastatic potential. Moreover, the interactions between tumour cell-ECM proteins, mainly collagen, have been described to be dependent on α1β2

integrin adhesion molecule in diverse pancreatic cancer cell lines [325], and it has been postulated that sialylation levels (in particular of sLe^x antigen) of integrins and E-cadherin modulate the tumour cell ECM adhesion and migration capacities [305,465–467]. Recently, Gomes et al. proposed a possible molecular mechanism that could explain the increase of invasion capability of ST3GAL4 overexpressing gastric cancer cells, suggesting that sLe^x expression on secreted or membrane glycoproteins mediates the induction of tumour cell invasion via the activation of the tyrosine kinase receptor c-Met and its downstream signalling effectors Scr, FAK, and RhoA GTPases activation [293], results that where lately demonstrated in PDA ST3GAL3 silenced cell models [299].

We also evidenced that the reduction of cell sialylation in the PDA murine cell line MSB262 induced by Ac$_5$3F$_{ax}$-Neu5Ac treatment also led to significant impairment of cell motility and invasion capacity of the cells, despite the fact that the expression levels of sLe^x on this cell line were undetectable, suggesting that the decrease in α2,3- and α2,6-SA determinants may be sufficient to alter the invasive and motile phenotype of this tumour cells.

Overall, we have demonstrated that the treatment of human and murine PDA cells with Ac$_5$3F$_{ax}$-Neu5Ac inhibitor and the concomitant decrease of cell membrane α2,3-sialylation impairs tumour cell migration and invasion processes, key steps on tumour progression and metastasis. Although systemic administration of Ac$_5$3F$_{ax}$-Neu5Ac is not feasible yet, it would be of great therapeutic interest to direct the administration to tumour cells to reduce its malignant phenotype and stop disease progression. Nonetheless, further studies are warranted to further investigate the underlying molecular mechanisms causing tumour cell phenotypical changes during cancer progression and in particular, to determine the sialylation carriers and their influence on the modulation of cell-cell or cell-ECM interactions, migration and invasion.

2.2.6 Ac$_5$3F$_{ax}$-Neu5Ac intratumoural injections supresses tumour growth by enhancing and immune permissive tumour microenvironment

Given the importance of aberrant SA expression in cancer, an increasing number of studies have focused on ST inhibitors on the last decades. Nonetheless, the pharmacological application of these inhibitors and their therapeutic potential are understudied yet. In the present work, we have explored the potential of the inhibitor Ac$_5$3F$_{ax}$-Neu5Ac to block SA expression on established pancreatic tumours, and its putative effect on tumour growth and tumour immunity. As far as we know, we have demonstrated for the first time that the administration of repeated intratumoural injections of Ac$_5$3F$_{ax}$-Neu5Ac in established

pancreatic tumours blocked SA expression in tumour cells and caused a decrease in the tumour growth rates. Moreover, it derived to an increase of the immune cell to tumour cell ratio in the treated tumours and a switch of the immune TME from an immunosuppressive to a more permissive one, via an increase in infiltrating T cell numbers.

Previous results described in this study, together with findings from others [366,371–374], demonstrated that Ac_5F_{ax}-Neu5Ac effectively causes a cell sialylation blockade *in vitro,* without affecting cell viability or proliferation. In addition, Büll et al. recently evidenced that repeated intratumoural administrations of 10 mg/kg inhibitor did not generate toxicity [448]. On the one hand, considering that the sensitivity for the inhibitor of each cell type can differ [371], and that tumour cells present higher preference to take up SA compared with other tissues [468,469], we decided to administer 10 mg/kg and 20 mg/kg. On the other hand, the administration of the ST inhibitor to the mice had to be intratumoural to retain the inhibitor in the tumour mass and limit systemic exposure, since Macauley and colleagues had previously described that the intravenous administration of 300 mg/kg inhibitor caused severe nephrotoxicity and ended in kidney failure [372]. For these reasons, the safe administration of the inhibitor to humans has not been feasible so far and further investments are needed to improve this prototype drug to make intratumoural injections possible or to develop a tumour-cell targeted delivery system. In this regard, Büll et al. encapsulated the SA-blocking glycomimetic into biodegradable nanoparticles coated with mAbs targeting tumour cells, which directed the delivery of the inhibitor into melanoma cells, preventing metastasis formation in a murine lung metastasis model [373].

In the present work, we established that after 2 weeks of intratumoural administration, tumour growth was slowed down in the 10 mg/kg group, but not in the 20 mg/kg group in comparison to control tumours, indicating that 10 mg/kg administration is sufficient to effectively stop tumour growth *in vivo,* probably due to the SA blockade locally in the tumour and TME. Referring to mice survival, we could not significantly determine whether the administration of the inhibitor and the concomitant reduction of tumour growth could prolong the mice survival time. In that sense, some methodological considerations need to be addressed and improved for future experiments. First, in terms of SA expression and tumour generation, we selected the optimal murine cell line, however, we found that in general the tumours grew faster than expected (one possibility would be to reduce the number of injected cells) and wounds appeared in some tumours. The reason why these wounds appeared is not currently clear although we think that the use of a distinct tumour-generating cell model might be a solution. Second, considering the total body weight of the

mice, we hypothesize that the start of inhibitor treatment might be established at a smaller tumour volume, so we could extend the tumour follow up. Third, it would be of special interest to generate orthotropic tumours in the pancreas as they offer tissue site-specific pathology, a more realistic influence of the TME and allow the study of Ac_5F_{ax}-Neu5Ac effect on metastasis formation.

Interestingly, we have found that Ac_5F_{ax}-Neu5Ac had the potency to reduce SA expression in established subcutaneous tumours generated by pancreatic cancer murine cells, in line with Büll et al. results [448]. Moreover, blocking of SA expression altered the TME, leading to an increase of the immune cell to tumour cell ratio in the treated tumours. In particular, we described a marked increase in tumour infiltrating $CD4^+$ and $CD8^+$ T cells, and NK cells, indicators of a reversion of the immunosuppressive TME [71,470]. Although it was not statistically significant, we observed increasing percentages of granulocytes and monocytes, cells that are usually classified as immunosuppressive ones. Nonetheless, it has been described that myeloid cells can adopt a pro- or anti-tumorigenic profile depending on the TME composition and SAs expressed by tumour cells [471], indicating that further studies are warranted to clarify the role of MDSCs in PDA models [472]. An important drawback to overcome was the fact that, although pancreatic tumours are highly heterogenic, the vast majority are classified as "cold" tumours, meaning that the infiltration of immune cells is very low [473]. Thus, the absolute numbers of each immune cell subtype present on the tumour samples analysed by FC was limited.

The molecular mechanisms by which SA blockade leads to these changes in the TME remains undetermined. However, there is growing evidence that blocking SA interactions of tumour cells with immune modulatory Siglecs of immune cells hampers the formation of an immunosuppressive TME [474–477]. Recently, Rodriguez et al. revealed that enhanced sialylation of PDA tumour cells is sensed by the myeloid cell receptors Siglec-7 and Siglec-9, and promotes the differentiation of monocytes into macrophages with an immune-suppressive phenotype, via upregulation of CD206, PD-L1 and immunosuppressive cytokines [478]. In parallel, several studies have shown that the binding of α2,8-SA to Siglec-7 dampens NK cell activation and function, enhancing tumour immune evasion [479–483]. Other studies have shown that Siglec-7 and Siglec-9 bind to SAs on both *O-* and *N*-glycans, preferably to sialylated antigens such as sialyl-T or sLe^x generated by the activity of two enzymes, ST3Gal I and ST3Gal IV, which are upregulated in PDA patients [478,484]. In addition to Siglecs, the interactions of galectins with β-galactoside residues present on glycosylated proteins might be altered by the inhibitor-induced SA blockade, influencing key processes of PDA

progression such as cell-cell adhesion, migration and signalling as well as driving immune evasion as reviewed by Martínez-Bosch and colleagues [485].

Although SA blockade had an extensive effect on tumour cells and TME, it has been postulated that the increased cell death and growth inhibition after $Ac_5 3F_{ax}$-Neu5Ac treatment results from the higher number and activation status of cytotoxic T cells [448], a concept that could partially explain the observed reduction in tumour growth of the 10mg/kg treated group. It has been postulated that hypersialylation on tumour cells can affect two of the most powerful mechanisms that cytotoxic T lymphocytes (CTLs) use to eliminate tumour cells. First, the presence of SA inhibits the granule-mediated cytotoxicity, as described by Lee et al., who demonstrated that tumour-derived SA-containing gangliosides (GM1-3, GD1a) inhibited trafficking and exocytosis of lytic granules from CTLs [486]. Second, there is evidence that Fas-mediated cytotoxicity is inhibited by the hypersialylation of the FasR on tumour cells, thus desensitizing and protecting them from Fas-induced apoptosis. Interestingly, it was reported that the α2,6-sialylation of Fas receptor expressed on colon carcinoma cells inhibit Fas capacity to induce apoptosis by blocking its internalization and the assembly of the DISC complex upon Fas ligand binding [317]. Büll et al. observed increased clustering between desialylated melanoma cells and $CD8^+$ T cells with a transgenic T-cell receptor compared to control cells [448], suggesting that SA blockade facilitates tumour cell-T cell interactions. Besides, the T cell glycosylation state has been described to alter the ability of $CD8^+$ T cells to interact with major histocompatibility complex-I (MHC-I) molecules and the activation of subsequent signalling events [487]. Moreover, Perdicchio and co-authors reported that sialylated antigens on dendritic cells prevent the formation of effector $CD4^+$ and $CD8^+$ T cells and inhibit the function of the existing ones, demonstrating that α2,3-sialylation might affect T cell function [488]. In addition, it was also demonstrated that the reduction of tumour SA levels enhanced immunological tumour control by increasing effector T cell response and NK cells activation [489]. All these findings, in accordance with our results, support the idea that SA blockade potentiates killing of tumour cells by cytotoxic T-cells and evidence the need to decipher the molecular mechanisms by which SA-blockade on tumour cells enhance tumour killing by cytotoxic T cells and NK cells.

The data available so far provide preliminary evidence that the combination of SA inhibitors with existing cellular immunotherapies would be of special interest to improve their efficacy in PDA. Currently, there are diverse ongoing CAR T cell' clinical trials targeted to antigens that are overexpressed on tumour cells such as MSLN, CD33, EGFR, or Her2, as well as novel CAR strategies, although there are some barriers to overcome to make immunotherapy

efficient [141,490]. Considering that PDA TME accounts for up to 80% of the total tumour mass and it is highly desmoplastic, it is considered a physical barrier that prevents CAR T cells' action and limit their antitumour response by generating an immunosuppressive environment [72]. Thus, the use of a STs inhibitor, which could switch the immunosuppressive TME to a more permissive one, might improve CAR T cell immunotherapy outcome. In addition, despite the fact that PDA remains unresponsive to conventional immunotherapy with immune checkpoint-blocking antibodies like PD-1 and CTLA-4 [490,491], it would be interesting to assess whether the SA depletion on tumour cells might potentiate its effect. In this regard, our group is currently carrying out *in vitro* assays to explore if the tumour-cell killing by cytotoxic T cells could be enhanced by Ac_53F_{ax}-Neu5Ac treatment-induced SA blockade on BxPC-3, Capan-1 and Panc-1 PDA cells.

In conclusion, our preliminary *in vivo* assay evidenced the potency of the inhibitor Ac_53F_{ax}-Neu5Ac to reduce tumour growth via SA expression blockade on the tumour mass and an increase in the immune cell to tumour cell ratio. Repeated intratumoural injections of the ST inhibitor Ac_53F_{ax}-Neu5Ac generated an immune permissive TME, supporting the concept that SAs have a key role in tumour immune modulation and potentiate tumour immune evasion. For these reasons, the development of novel Ac_53F_{ax}-Neu5Ac analogues with improved efficacy and potency [492] represents a promising strategy to translate the use of these inhibitors into clinic, alone or in combination with existing immunotherapies.

CONCLUSIONS

From the first chapter of this thesis: **Impact of α2,3-sialyltransferases knockdown on EGFR signalling in BxPC-3 and Capan-1 PDA cells**

i. ST3GAL3 and ST3GAL4 KD PDA cells showed a trend to decrease the expression of sLe^x on EGFR, while the expression of α2,6-SA and α2,3-SA on EGFR was not significantly altered.

ii. ST3GAL3 KD BxPC-3 and ST3GAL4 KD Capan-1 cells presented a higher increase in EGFR phosphorylation levels upon EGF treatment compared to control cells, affecting specific residues of the receptor involved in the EGFR proliferative and internalization signalling networks. The increase in EGFR activation was translated into an increase in AKT phosphorylation for BxPC-3 ST KD cells, although no significant effect was observed for Capan-1 and MAPK protein phosphorylation in any of the cell lines.

iii. The higher activation of EGFR signalling pathway observed on STs KD BxPC-3 and Capan-1 cells led to an increase in EGFR homodimers formation upon EGF treatment on ST3GAL4 KD cells.

iv. ST3GAL3 KD and ST3GAL4 KD drove to an increase in the proliferation rate of BxPC-3 cells upon EGF-induction, in accordance with the increase in EGFR phosphorylation and higher activation of the AKT pathway, although no significant differences were observed for Capan-1 cells. Considering that Capan-1 cells express lower EGFR levels than BxPC-3, Capan-1 cell line might be less EGFR-dependent for their proliferation signalling.

v. The KD of ST3GAL3 and ST3GAL4 STs did not affect BxPC-3 and Capan-1 sensitivity to Erlotinib and Cetuximab, since the cell viability after the treatments was similar to that of BxPC-3 and Capan-1 control cells.

In relation to the second chapter of this thesis: **Reduction of sialic acid on PDA cells by a sialyltransferase inhibitor and study of its effect on E-selectin adhesion, migration and invasion capabilities of PDA cells *in vitro* and its potential to reduce tumour growth and alter tumour immune component in syngeneic mice**

vi. $Ac_5 3F_{ax}$-Neu5Ac treatment significantly reduced cell surface sialylation in BxPC-3 and Capan-1 cell lines, while AL-10 and SsaI inhibitors did not block cell sialyation in these PDA cells. $Ac_5 3F_{ax}$-Neu5Ac treatment has the potency to achieve the highest reduction of PDA cell sialoglycans, while the combined inhibition of STs with the ST3GAL4 KD and the $Ac_5 3F_{ax}$-Neu5Ac treatment did not show any additive effect.

vii. $Ac_5 3F_{ax}$-Neu5Ac treatment significantly impaired E-selectin binding in BxPC-3 and Capan-1 cells by reducing sLe antigen expression on these cell lines. In addition, the ST inhibitor reduced the migration and invasion of treated cells compared to their corresponding controls *in vitro*. Altogether, demonstrating that $Ac_5 3F_{ax}$-Neu5Ac treatment reverted the malignant phenotype of PDA cells by affecting key steps on tumour progression and metastasis.

viii. PDA MSB262 murine cells were sensitive to $Ac_5 3F_{ax}$-Neu5Ac *in vitro* as their treatment with the ST inhibitor caused a significant reduction on the cellular expression of α2,3-SA and α2,6-SA. Although the expression of sLe^x was not detectable on MSB262 murine cells, $Ac_5 3F_{ax}$-Neu5Ac treatment impaired the migration and invasion capacity of MSB262 cells.

ix. $Ac_5 3F_{ax}$-Neu5Ac treatment of PDA subcutaneous tumours generated in syngeneic mice with MSB262 cells reduced the tumour volume, their SA expression and modified the tumour immune component, by increasing the number of infiltrating $CD8^+$ T-cells and NK cells compared to non-treated control tumours, thus favouring anti-tumour immune surveillance.

x. The effect of $Ac_5 3F_{ax}$-Neu5Ac treatment in PDA cells *in vitro* and its impact on mice PDA tumours *in vivo* indicate that reducing SA expression in PDA by inhibiting cell STs has an important impact in PDA progress. Thus, $Ac_5 3F_{ax}$-Neu5Ac might be considered as a promising candidate to further evaluate the role of sialoglycans in tumour progression and for its translation into clinics.

REFERENCES

1. Sung H, Ferlay J, Siegel RL, et al. Global Cancer Statistics 2020: GLOBOCAN Estimates of Incidence and Mortality Worldwide for 36 Cancers in 185 Countries. *CA Cancer J Clin.* 2021;71(3):209-249. doi:10.3322/caac.21660

2. Siegel RL, Miller KD, Fuchs HE, Jemal A. Cancer statistics, 2022. *CA Cancer J Clin.* 2022;72(1):7-33. doi:10.3322/caac.21708

3. Fuster MM, Esko JD. The sweet and sour of cancer: Glycans as novel therapeutic targets. *Nat Rev Cancer.* 2005;5(7):526-542. doi:10.1038/nrc1649

4. Gupta GP, Massagué J. Cancer Metastasis: Building a Framework. *Cell.* 2006;127(4):679-695. doi:10.1016/j.cell.2006.11.001

5. Hanahan D, Weinberg RA. Hallmarks of cancer: The next generation. *Cell.* 2011;144(5):646-674. doi:10.1016/j.cell.2011.02.013

6. Hanahan D. Hallmarks of Cancer: New Dimensions. *Cancer Discov.* 2022;12(1):31-46. doi:10.1158/2159-8290.CD-21-1059

7. Brooks SA, Lomax-Browne HJ, Carter TM, Kinch CE, Hall DMS. Molecular interactions in cancer cell metastasis. *Acta Histochem.* 2010;112(1):3-25. doi:10.1016/j.acthis.2008.11.022

8. Langley RR, Fidler IJ. Tumor cell-organ microenvironment interactions in the pathogenesis of cancer metastasis. *Endocr Rev.* 2007;28(3):297-321. doi:10.1210/er.2006-0027

9. Felsher DW. Reversibility of oncogene-induced cancer. *Curr Opin Genet Dev.* 2004;14(1):37-42. doi:10.1016/j.gde.2003.12.008

10. Talmadge, Fidler. The Biology of Cancer Metastasis: Historical Perspective. *Cancer Res.* 2010;70(14):5649–5669. doi:10.1158/0008-5472.CAN-10-1040.AACR

11. Potente M, Gerhardt H, Carmeliet P. Basic and therapeutic aspects of angiogenesis. *Cell.* 2011;146(6):873-887. doi:10.1016/j.cell.2011.08.039

12. H.Plate K, Breier G, Risau W. Molecular mechanisms of developmental and tumor angiogenesis. *J Neurooncol.* 1994;50(1-2):63-70. doi:10.1023/A:1006414621286

13. Krock BL, Skuli N, Simon MC. Hypoxia-Induced Angiogenesis: Good and Evil. *Genes Cancer.* 2011;2(12):1117-1133. doi:10.1177/1947601911423654

14. Harris AL. Hypoxia - A key regulatory factor in tumour growth. *Nat Rev Cancer.* 2002;2(1):38-47. doi:10.1038/nrc704

15. McMahon G. VEGF Receptor Signaling in Tumor Angiogenesis. *Oncologist.* 2000;5(S1):3-10. doi:10.1634/theoncologist.5-suppl_1-3

16. Friedl P, Alexander S. Cancer invasion and the microenvironment: Plasticity and reciprocity. *Cell.* 2011;147(5):992-1009. doi:10.1016/j.cell.2011.11.016

17. Tsuruo T, Fujita N. Platelet aggregation in the formation of tumor metastasis. *Proc Jpn Acad Ser B Phys Biol Sci.* 2008;84(6):189-198. doi:10.2183/pjab.84.189

18. Biggerstaff JP, Seth N, Amirkhosravi A, et al. Soluble fibrin augments platelet/tumor cell adherence in vitro and in vivo, and enhances experimental metastasis. *Clin Exp Metastasis.* 1999;17(8):723-730. doi:10.1023/A:1006763827882

19. Gout S, Tremblay PL, Huot J. Selectins and selectin ligands in extravasation of cancer cells and organ selectivity of metastasis. *Clin Exp Metastasis.* 2008;25(4):335-344. doi:10.1007/s10585-007-9096-4

20. Kannagi R. Carbohydrate-mediated cell adhesion involved in hematogenous metastasis of cancer. *Glycoconj J.* 1997;14(5):577-584. doi:10.1023/A:1018532409041

21. Chambers AF, MacDonald IC, Schmidt EE, et al. Steps in tumor metastasis: new concepts from intravital videomicroscopy. *Cancer and Metastasis Reviews.* 1995;14(4):279-301. doi:10.1007/BF00690599

22. Akhtar M, Haider A, Rashid S, Al-Nabet ADMH. Paget's "seed and Soil" Theory of Cancer Metastasis: An Idea Whose Time has Come. *Adv Anat Pathol.* 2019;26(1):69-74. doi:10.1097/PAP.0000000000000219

23. Langley RR, Fidler IJ. The seed and soil hypothesis revisited-The role of tumor-stroma interactions in metastasis to different organs. *Int J Cancer.* 2011;128(11):2527-2535. doi:10.1002/ijc.26031

24. Benitez CM, Goodyer WR, Kim SK. Deconstructing pancreas developmental biology. *Cold Spring Harb Perspect Biol.* 2012;4(6):1-17. doi:10.1101/cshperspect.a012401

25. Kleeff J, Korc M, Apte M, et al. Pancreatic cancer. *Nat Rev Dis Primers.* 2016;2(April):1-23. doi:10.1038/nrdp.2016.22

26. Quante AS, Ming C, Rottmann M, et al. Projections of cancer incidence and cancer-related deaths in Germany by 2020 and 2030. *Cancer Med.* 2016;5(9):2649-2656. doi:10.1002/cam4.767

27. Rahib L, Smith BD, Aizenberg R, Rosenzweig AB, Fleshman JM, Matrisian LM. Projecting cancer incidence and deaths to 2030: The unexpected burden of thyroid, liver, and pancreas cancers in the united states. *Cancer Res.* 2014;74(11):2913-2921. doi:10.1158/0008-5472.CAN-14-0155

28. Orth M, Metzger P, Gerum S, et al. Pancreatic ductal adenocarcinoma : biological hallmarks , current status , and future perspectives of combined modality treatment approaches. *Radiat Oncol.* 2019;14(1):141. doi:10.1186/s13014-019-1345-6

29. Canto MI, Harinck F, Hruban RH, et al. International cancer of the pancreas screening (CAPS) consortium summit on the management of patients with increased risk for familial pancreatic cancer. *Gut.* 2013;62(3):339-347. doi:10.1136/gutjnl-2012-303108

30. Bardeesy N, DePinho RA. Pancreatic cancer biology and genetics. *Nat Rev Cancer.* 2002;2(12):897-909. doi:10.1038/nrc949

31. Kamisawa T, Wood LD, Itoi T, Takaori K. Pancreatic cancer. *The Lancet.* 2016;388(10039):73-85. doi:10.1016/S0140-6736(16)00141-0

32. Lynch HT, Lynch JF, Lanspa SJ. Familial pancreatic cancer. *Cancers (Basel).* 2010;2(4):1861-1883. doi:10.3390/cancers2041861

33. Gheorghe G, Diaconu CC, Ionescu V, et al. Risk Factors for Pancreatic Cancer: Emerging Role of Viral Hepatitis. *J Pers Med.* 2022;12(1):83. doi:10.3390/jpm12010083

34. Pereira SP, Oldfield L, Ney A, et al. Early detection of pancreatic cancer. *Lancet Gastroenterol Hepatol.* 2020;5(7):698-710. doi:10.1016/S2468-1253(19)30416-9

35. Landi S. Genetic predisposition and environmental risk factors to pancreatic cancer: A review of the literature. *Mutat Res Rev Mutat Res.* 2009;681(2-3):299-307. doi:10.1016/j.mrrev.2008.12.001

36. David SP, Murthy NV, Rabiner EA, et al. Identification of Sox9-dependent acinar-to-ductal reprogramming as the principal mechanism for initiation of pancreatic ductal adenocarcinoma. *Cancer Cell.* 2012;22(6):737-750. doi:10.1016/j.ccr.2012.10.025.Identification

37. Gidekel Friedlander SY, Chu GC, Snyder EL, et al. Context-Dependent Transformation of Adult Pancreatic Cells by Oncogenic K-Ras. *Cancer Cell.* 2009;16(5):379-389. doi:10.1016/j.ccr.2009.09.027

38. Yachida S, Jones S, Bozic I et al. Distant metastasis occurs late during the genetic evolution of pancreatic cancer. *Nature.* 2010;467(7319):1114-1117. doi:10.1038/nature09515

39. Ying H, Dey P, Yao W, et al. Genetics and biology of pancreatic ductal adenocarcinoma. *Genes Dev.* 2016;30(4):355-385. doi:10.1101/gad.275776.115

40. Hruban RH, Goggins M, Parsons J, Kern SE. Progression model for pancreatic cancer. *Clin Cancer Res.* 2000;6(8):2969-2972.

41. Kleeff J, Korc M, Apte M, et al. Pancreatic Cancer. *Nat Rev Dis Primers.* 2016;2(16022):1-1661. doi:10.1038/nrdp.2016.22

42. Vincent A, Herman J, Schulick R, Hruban RH, Goggins M. Pancreatic cancer. *Lancet.* 2011;11(2):168-180. doi:10.1002/ssu.2980110214

43. Maitra A, Hruban RH. Pancreatic cancer. *Annual Review of Pathology: Mechanisms of Disease.* 2008;3(2):157-188. doi:10.1146/annurev.pathmechdis.3.121806.154305

44. Real FX. A "catastrophic hypothesis" for pancreas cancer progression. *Gastroenterology.* 2003;124(7):1958-1964. doi:10.1016/S0016-5085(03)00389-5

45. Notta F, Chan-Seng-Yue M, Lemire M, et al. A renewed model of pancreas cancer evolution based on genomic rearrangement patterns. *Nature.* 2016;538(7625):378-382. doi:10.1038/nature19823

46. Real FX, Cibrián-Uhalte E, Martinelli P. Pancreatic Cancer Development and Progression: Remodeling the Model. *Gastroenterology.* 2008;135(3):724-728. doi:10.1053/j.gastro.2008.07.033

47. Hernández-Muñoz I, Skoudy A, Real FX, Navarro P. Pancreatic ductal adenocarcinoma: Cellular origin, signaling pathways and stroma contribution. *Pancreatology*. 2008;8(4-5):462-469. doi:10.1159/000151537

48. Maitra A, Fukushima N, Takaori K, Hruban RH. Precursors to invasive pancreatic cancer. *Adv Anat Pathol*. 2005;12(2):81-91. doi:10.1097/01.pap.0000155055.14238.25

49. Delpu Y, Hanoun N, Lulka H, et al. Genetic and Epigenetic Alterations in Pancreatic Carcinogenesis. *Curr Genomics*. 2011;12(1):15-24. doi:10.2174/138920211794520132

50. Koorstra JBM, Hustinx SR, Offerhaus GJA, Maitra A. Pancreatic carcinogenesis. *Pancreatology*. 2008;8(2):110-125. doi:10.1159/000123838

51. Jones S, Zhang X, Parsons DW, et al. Core signaling pathways in human pancreatic cancers revealed by global genomic analyses. *Science (1979)*. 2008;321(5897):1801-1806. doi:10.1126/science.1164368

52. Butz AM, Christopher S. von Bartheld JB and SHH. Integrated Genomic Characterization of Pancreatic Ductal Adenocarcinoma. *Physiol Behav*. 2017;176(12):139-148. doi:10.1016/j.ccell.2017.07.007.Integrated

53. Mueller S, Engleitner T, Maresch R, et al. Evolutionary routes and KRAS dosage define pancreatic cancer phenotypes. *Nature*. 2018;554(7690):62-68. doi:10.1038/nature25459

54. Makohon-Moore A, Iacobuzio-Donahue CA. Pancreatic cancer biology and genetics from an evolutionary perspective. *Physiol Behav*. 2017;176(5):139-148. doi:10.1038/nrc.2016.66.Pancreatic

55. Loc WS, Smith JP, Matters G, Kester M, Adair JH. Novel strategies for managing pancreatic cancer. *World J Gastroenterol*. 2014;20(40):14717-14725. doi:10.3748/wjg.v20.i40.14717

56. Buscail L, Bournet B, Cordelier P. Role of oncogenic KRAS in the diagnosis, prognosis and treatment of pancreatic cancer. *Nat Rev Gastroenterol Hepatol*. 2020;17(3):153-168. doi:10.1038/s41575-019-0245-4

57. Hustinx SR, Leoni LM, Yeo CJ, et al. Concordant loss of MTAP and p16/CDKN2A expression in pancreatic intraepithelial neoplasia: Evidence of homozygous deletion in a noninvasive precursor lesion. *Modern Pathology*. 2005;18(7):959-963. doi:10.1038/modpathol.3800377

58. Li D, Xie K, Wolff R, Abbruzzese JL. Pancreatic cancer. *Lancet*. 2004;4(1):4-5. doi:10.1159/000334593

59. Grant TJ, Hua K, Singh A. Molecular Pathogenesis of Pancreatic Cancer. *Prog Mol Biol Transl Sci*. 2016;144:241-275. doi:10.1016/bs.pmbts.2016.09.008

60. Gil YR, Sánchez PJ, Velasco RM, García AG, Lobo VJSA. Molecular alterations in pancreatic cancer: Transfer to the clinic. *Int J Mol Sci*. 2021;22(4):1-16. doi:10.3390/ijms22042077

61. Gits HC, Tang AH, Harmsen WS, et al. Intact SMAD-4 is a predictor of increased locoregional recurrence in upfront resected pancreas cancer receiving adjuvant therapy. *J Gastrointest Oncol*. 2021;12(5):2275-2286. doi:10.21037/jgo-21-55

62. Yakar DÖ, Bozkırlı BO, Ceyhan GO. Genetic landscape of pancreatic cancer: a narrative review. *Chin Clin Oncol*. 2022;11(1):5. doi:10.21037/cco-22-4

63. Yonezawa S, Higashi M, Yamada N, Goto M. Precursor Lesions of Pancreatic Cancer. *Gut Liver*. 2008;2(3):137-154. doi:10.5009/gnl.2008.2.3.137

64. Waddell N, Pajic M, Patch AM, et al. Whole genomes redefine the mutational landscape of pancreatic cancer. *Circ Res*. 2015;518(7540):495-501. doi:10.1038/nature14169

65. Li A, Omura N, Hong SM, et al. Pancreatic cancers epigenetically silence SIP1 and hypomethylate and overexpress miR-200a/200b in association with elevated circulating miR-200a and miR-200b levels. *Cancer Res*. 2010;70(13):5226-5237. doi:10.1158/0008-5472.CAN-09-4227

66. Szafranska AE, Davison TS, John J, et al. MicroRNA expression alterations are linked to tumorigenesis and non-neoplastic processes in pancreatic ductal adenocarcinoma. *Oncogene*. 2007;26(30):4442-4452. doi:10.1038/sj.onc.1210228

67. Wang J, Sen S. MicroRNA functional network in pancreatic cancer: From biology to biomarkers of disease. *J Biosci*. 2011;36(3):481-491. doi:10.1007/s12038-011-9083-4

68. Tjomsland V, Niklasson L, Sandström P, et al. The desmoplastic stroma plays an essential role in the accumulation and modulation of infiltrated immune cells in pancreatic adenocarcinoma. *Clin Dev Immunol*. 2011;2011:212810. doi:10.1155/2011/212810

69. Xie D, Xie K. Pancreatic cancer stromal biology and therapy. *Genes Dis.* 2015;2(2):133-143. doi:10.1016/j.gendis.2015.01.002

70. Opitz F v., Haeberle L, Daum A, Esposito I. Tumor microenvironment in pancreatic intraepithelial neoplasia. *Cancers (Basel).* 2021;13(24):6188. doi:10.3390/cancers13246188

71. Cortesi M, Zanoni M, Pirini F, et al. Pancreatic cancer and cellular senescence: tumor microenvironment under the spotlight. *Int J Mol Sci.* 2022;23(1):254. doi:10.3390/ijms23010254

72. Carvalho TMA, di Molfetta D, Greco MR, et al. Tumor microenvironment features and chemoresistance in pancreatic ductal adenocarcinoma: Insights into targeting physicochemical barriers and metabolism as therapeutic approaches. *Cancers (Basel).* 2021;13(23):6135. doi:10.3390/cancers13236135

73. Clark CE, Hingorani SR, Mick R, Combs C, Tuveson DA, Vonderheide RH. Dynamics of the immune reaction to pancreatic cancer from inception to invasion. *Cancer Res.* 2007;67(19):9518-9527. doi:10.1158/0008-5472.CAN-07-0175

74. Nielsen MFB, Mortensen MB, Detlefsen S. Key players in pancreatic cancer-stroma interaction: Cancer-associated fibroblasts, endothelial and inflammatory cells. *World J Gastroenterol.* 2016;22(9):2678-2700. doi:10.3748/wjg.v22.i9.2678

75. Sunami Y, Häußler J, Zourelidis A, Kleeff J. Cancer-Associated Fibroblasts and Tumor Cells in Pancreatic Cancer Microenvironment and Metastasis: Paracrine Regulators, Reciprocation and Exosomes. *Cancers (Basel).* 2022;14(3):744. doi:10.3390/cancers14030744

76. Ansari D, Carvajo M, Bauden M, Andersson R. Pancreatic cancer stroma: controversies and current insights. *Scand J Gastroenterol.* 2017;52(6-7):641-646. doi:10.1080/00365521.2017.1293726

77. Pothula SP, Xu Z, Goldstein D, Pirola RC, Wilson JS, Apte M v. Key role of pancreatic stellate cells in pancreatic cancer. *Cancer Lett.* 2016;381(1):194-200. doi:10.1016/j.canlet.2015.10.035

78. Xu Z, Pothula SP, Wilson JS, Apte M v. Pancreatic cancer and its stroma: A conspiracy theory. *World J Gastroenterol.* 2014;20(32):11216-11229. doi:10.3748/wjg.v20.i32.11216

79. Ikushima H, Miyazono K. TGFB 2 signalling: A complex web in cancer progression. *Nat Rev Cancer.* 2010;10(6):415-424. doi:10.1038/nrc2853

80. Schnittert J, Bansal R, Prakash J. Targeting Pancreatic Stellate Cells in Cancer. *Trends Cancer.* 2019;5(2):128-142. doi:10.1016/j.trecan.2019.01.001

81. Bhowmick NA, Neilson EG, Moses HL. Stromal fibroblasts in cancer initiation and progression. *Nature.* 2004;432(7015):332-337. doi:10.1038/nature03096

82. Erkan M, Kurtoglu M, Kleeff J. The role of hypoxia in pancreatic cancer: A potential therapeutic target? *Expert Rev Gastroenterol Hepatol.* 2016;10(3):301-316. doi:10.1586/17474124.2016.1117386

83. Li N, Li Y, Li Z, et al. Hypoxia inducible factor 1 (HIF-1) recruits macrophage to activate pancreatic stellate cells in ancreatic ductal adenocarcinoma. *Int J Mol Sci.* 2016;17(6):799. doi:10.3390/ijms17060799

84. Mahajan UM, Langhoff E, Goni E, et al. Immune Cell and Stromal Signature Associated With Progression-Free Survival of Patients With Resected Pancreatic Ductal Adenocarcinoma. *Gastroenterology.* 2018;155(5):1625-1639.e2. doi:10.1053/j.gastro.2018.08.009

85. Hu H, Hang JJ, Han T, Zhuo M, Jiao F, Wang LW. The M2 phenotype of tumor-associated macrophages in the stroma confers a poor prognosis in pancreatic cancer. *Tumor Biology.* 2016;37(7):8657-8664. doi:10.1007/s13277-015-4741-z

86. Daley D, Zambirinis CP, Seifert L, et al. γδ T Cells Support Pancreatic Oncogenesis by Restraining αβ T Cell Activation. *Cell.* 2016;166(6):1485-1499.e15. doi:10.1016/j.cell.2016.07.046

87. Pylayeva-Gupta Y, Das S, Handler JS, et al. IL-35 producing B cells promote the development of pancreatic neoplasia. *Cancer Discov.* 2016;6(3):247-255. doi:10.1158/2159-8290.CD-15-0843

88. Theocharis AD, Skandalis SS, Gialeli C, Karamanos NK. Extracellular matrix structure. *Adv Drug Deliv Rev.* 2016;97:4-27. doi:10.1016/j.addr.2015.11.001

89. Jiang H, Hegde S, Knolhoff BL, et al. Targeting focal adhesion kinase renders pancreatic cancers responsive to checkpoint immunotherapy. *Nat Med.* 2016;22(8):851-860. doi:10.1038/nm.4123

90. Li HY, Cui ZM, Chen J, Guo XZ, Li YY. Pancreatic cancer: diagnosis and treatments. *Tumor Biology.* 2015;36(3):1375-1384. doi:10.1007/s13277-015-3223-7

91. Adamska A, Domenichini A, Falasca M. Pancreatic Ductal Adenocarcinoma : Current and Evolving Therapies. *Int J Mol Sci.* 2017;18(7):1338. doi:10.3390/ijms18071338

92. Kanno A, Masamune A, Hanada K, et al. Multicenter study of early pancreatic cancer in Japan. *Pancreatology.* 2018;18(1):61-67. doi:10.1016/j.pan.2017.11.007

93. Wolfgang CL, Herman JM, Laheru DA, et al. Recent progress in pancreatic cancer. *Cancer J Clin.* 2013;63(5):318-348. doi:10.3322/caac.21190

94. Chang JC, Kundranda M. Novel diagnostic and predictive biomarkers in pancreatic adenocarcinoma. *Int J Mol Sci.* 2017;18(3):667. doi:10.3390/ijms18030667

95. Lee ES, Lee JM. Imaging diagnosis of pancreatic cancer: A state-of-the-art review. *World J Gastroenterol.* 2014;20(24):7864-7877. doi:10.3748/wjg.v20.i24.7864

96. Tummala P, Junaidi O, Agarwal B. Imaging of pancreatic cancer: An overview. *J Gastrointest Oncol.* 2011;2(3):168-174. doi:10.3978/j.issn.2078-6891.2011.036

97. Sperti C, Pasquali C, Bissoli S, Chierichetti F, Liessi G, Pedrazzoli S. Tumor relapse after pancreatic cancer resection is detected earlier by 18-FDG PET than by CT. *Journal of Gastrointestinal Surgery.* 2010;14(1):131-140. doi:10.1007/s11605-009-1010-8

98. Harinck F, Konings ICAW, Kluijt I, et al. A multicentre comparative prospective blinded analysis of EUS and MRI for screening of pancreatic cancer in high-risk individuals. *Gut.* 2016;65(9):1505-1513. doi:10.1136/gutjnl-2014-308008

99. Shin EJ, Topazian M, Goggins MG, et al. Linear-array EUS improves detection of pancreatic lesions in high-risk individuals: a randomized tandem study. *Gastrointest Endosc.* 2015;82(5):812-818. doi:10.1016/j.gie.2015.02.028

100. Cong L, Liu Q, Zhang R, et al. Tumor size classification of the 8th edition of TNM staging system is superior to that of the 7th edition in predicting the survival outcome of pancreatic cancer patients after radical resection and adjuvant chemotherapy. *Sci Rep.* 2018;8(1):10383. doi:10.1038/s41598-018-28193-4

101. Füzéry AK, Levin J, Chan MM, Chan DW. Translation of proteomic biomarkers into FDA approved cancer diagnostics: Issues and challenges. *Clin Proteomics.* 2013;10(1):13. doi:10.1186/1559-0275-10-13

102. E. Poruk K, Z. Gay D, Brown K, et al. The Clinical Utility of CA 19-9 in Pancreatic Adenocarcinoma: Diagnostic and Prognostic Updates. *Curr Mol Med.* 2013;13(3):340-351. doi:10.2174/156652413805076876

103. O'Brien DP, Sandanayake NS et al. Serum CA19-9 is significantly up-regulated up to 2 years prior to diagnosis with pancreatic cancer: implications for early disease detection. *Clin Cancer Res.* 2015;21(3):622-631. doi:10.1158/1078-0432.CCR-14-0365

104. Ferri MJ, Saez M, Figueras J, et al. Improved pancreatic adenocarcinoma diagnosis in jaundiced and non-jaundiced pancreatic adenocarcinoma patients through the combination of routine clinical markers associated to pancreatic adenocarcinoma Pathophysiology. *PLoS One.* 2016;11(1):e0147214. doi:10.1371/journal.pone.0147214

105. Harsha HC, Kandasamy K, Ranganathan P, et al. A compendium of potential biomarkers of pancreatic cancer. *PLoS Med.* 2009;6(4):e1000046. doi:10.1371/journal.pmed.1000046

106. Bettegowda C, Sausen M, Leary RJ, Kinde I, Wang Y. Detection of Circulating Tumor DNA in Early- and Late-Stage Human Malignancies. *Sci Transl Med.* 2014;6(224):2244ra24. doi:10.1126/scitranslmed.3007094

107. Kinugasa H, Nouso K, Miyahara K, et al. Detection of K-ras gene mutation by liquid biopsy in patients with pancreatic cancer. *Cancer.* 2015;121(13):2271-2280. doi:10.1002/cncr.29364

108. Pishvaian MJ, Bender RJ, Matrisian LM, et al. A pilot study evaluating concordance between blood-based and patient-matched tumor molecular testing within pancreatic cancer patients participating in the Know Your Tumor (KYT) initiative. *Oncotarget.* 2017;8(48):83446-83456. doi:10.18632/oncotarget.13225

109. Yi JM, Guzzetta AA, Bailey VJ, et al. Novel methylation biomarker panel for the early detection of pancreatic cancer. *Clinical Cancer Research.* 2015;19(23):6544-6555. doi:10.1158/1078-0432.CCR-12-3224

110. Kulemann B, Rösch S, Seifert S, et al. Pancreatic cancer: Circulating Tumor Cells and Primary Tumors show Heterogeneous KRAS Mutations. *Sci Rep.* 2017;7(1):4510. doi:10.1038/s41598-017-04601-z

111. Basturk O, Hong SM. A Revised Classification System and Recommendations From the Baltimore Consensus Meeting for Neoplastic Precursor Lesions in the Pancreas. *Am J Surg Pathol.* 2016;39(12):1730-1741. doi:10.1097/PAS.0000000000000533

112. Mayers JR, Wu C, Clish CB, et al. Elevated circulating branched chain amino acids are an early event in pancreatic adenocarcinoma development. 2014;20(10):1193-1198. doi:10.1038/nm.3686

113. Melo SA, Luecke LB, Kahlert C, Fernandez AF, Gammon ST. Glypican1 identifies cancer exosomes and facilitates early detection of cancer. *Nature.* 2015;523(7559):177-182. doi:10.1038/nature14581

114. Imamura T, Komatsu S, Ichikawa D, et al. Depleted tumor suppressor miR-107 in plasma relates to tumor progression and is a novel therapeutic target in pancreatic cancer. *Sci Rep.* 2017;7(1):5708. doi:10.1038/s41598-017-06137-8

115. Li Y, Sarkar FH. MicroRNA targeted therapeutic approach for pancreatic cancer. *Int J Biol Sci.* 2016;12(3):326-337. doi:10.7150/ijbs.15017

116. Silva MLS. Cancer serum biomarkers based on aberrant post-translational modifications of glycoproteins: Clinical value and discovery strategies. *Biochim Biophys Acta Rev Cancer.* 2015;1856(2):165-177. doi:10.1016/j.bbcan.2015.07.002

117. Balmaña M, Sarrats A, Llop E, et al. Identification of potential pancreatic cancer serum markers: Increased sialyl-Lewis X on ceruloplasmin. *Clinica Chimica Acta.* 2015;442:56-62. doi:10.1016/j.cca.2015.01.007

118. Balmaña M, Giménez E, Puerta A, et al. Increased α1-3 fucosylation of α-1-acid glycoprotein (AGP) in pancreatic cancer. *J Proteomics.* 2016;132:144-154. doi:10.1016/j.jprot.2015.11.006

119. Balmaña M, Duran A, Gomes C, et al. Analysis of sialyl-Lewis x on MUC5AC and MUC1 mucins in pancreatic cancer tissues. *Int J Biol Macromol.* 2018;112:33-45. doi:10.1016/j.ijbiomac.2018.01.148

120. Guerrero PE, Duran A, Ortiz MR, et al. Microfibril associated protein 4 (MFAP4) is a carrier of the tumor associated carbohydrate sialyl-Lewis x (sLex) in pancreatic adenocarcinoma. *J Proteomics.* 2021;231:104004. doi:10.1016/j.jprot.2020.104004

121. Martinez-Bosch N, Barranco LE, Orozco CA, et al. Increased plasma levels of galectin-1 in pancreatic cancer: Potential use as biomarker. *Oncotarget.* 2018;9(68):32984-32996. doi:10.18632/oncotarget.26034

122. Manji GA, Olive KP, Saenger YM, Oberstein P. Current and emerging therapies in metastatic pancreatic cancer. *Clinical Cancer Research.* 2017;23(7):1670-1678. doi:10.1158/1078-0432.CCR-16-2319

123. McGuigan A, Kelly P, Turkington RC, Jones C, Coleman HG, McCain RS. Pancreatic cancer: A review of clinical diagnosis, epidemiology, treatment and outcomes. *World J Gastroenterol.* 2018;24(43):4846-4861. doi:10.3748/wjg.v24.i43.4846

124. Howard B, Iii AB, Moore MJ, et al. Improvements in Survival and Clinical Benefit With Gemcitabine as First-Line Therapy for Patients With Advanced Pancreas Cancer: A Randomized Trial. *Journal of Clinical Oncology.* 1997;15(6):2403-2413. doi:10.1200/JCO.1997.15.6.2403

125. Kelley RK, Ko AH. Erlotinib in the treatment of advanced pancreatic cancer. *Biologics.* 2008;2(1):83-95. doi:10.2147/btt.s1832

126. Moore MJ, Goldstein D, Hamm J, et al. Erlotinib plus gemcitabine compared with gemcitabine alone in patients with advanced pancreatic cancer: A phase III trial of the National Cancer Institute of Canada Clinical Trials Group. *Journal of Clinical Oncology.* 2007;25(15):1960-1966. doi:10.1200/JCO.2006.07.9525

127. von Hoff DD, Ervin T, Arena FP, et al. Increased Survival in Pancreatic Cancer with nab-Paclitaxel plus Gemcitabine. *N Engl J Med.* 2013;369(18):1691-1703. doi:10.1056/NEJMoa1304369

128. Wang-Gillam A, Li CP, Bodoky G, et al. Nanoliposomal irinotecan with fluorouracil and folinic acid in metastatic pancreatic cancer after previous gemcitabine-based therapy (NAPOLI-1): A global, randomised, open-label, phase 3 trial. *The Lancet*. 2016;387(10018):545-557. doi:10.1016/S0140-6736(15)00986-1

129. Philip PA, Benedetti J, Corless CL, et al. Phase III study comparing gemcitabine plus cetuximab versus gemcitabine in patients with advanced pancreatic adenocarcinoma: Southwest oncology group-directed intergroup trial S0205. *Journal of Clinical Oncology*. 2010;28(22):3605-3610. doi:10.1200/JCO.2009.25.7550

130. Kim YJ, Jung K, Baek DS, Hong SS, Kim YS. Co-targeting of EGF receptor and neuropilin-1 overcomes cetuximab resistance in pancreatic ductal adenocarcinoma with integrin β1-driven Src-Akt bypass signaling. *Oncogene*. 2017;36(18):2543-2552. doi:10.1038/onc.2016.407

131. Haas M, Waldschmidt DT, Stahl M, et al. Afatinib plus gemcitabine versus gemcitabine alone as first-line treatment of metastatic pancreatic cancer: The randomised, open-label phase II ACCEPT study of the Arbeitsgemeinschaft Internistische Onkologie with an integrated analysis of the 'burden of . *Eur J Cancer*. 2021;146:95-106. doi:10.1016/j.ejca.2020.12.029

132. Wolpin BM, Hezel AF, Abrams T, et al. Oral mTOR inhibitor everolimus in patients with gemcitabine-refractory metastatic pancreatic cancer. *Journal of Clinical Oncology*. 2009;27(2):193-198. doi:10.1200/JCO.2008.18.9514

133. Javle MM, Shroff RT, Xiong H, et al. Inhibition of the mammalian target of rapamycin (mTOR) in advanced pancreatic cancer: Results of two phase II studies. *BMC Cancer*. 2010;10:368. doi:10.1186/1471-2407-10-368

134. Iriana S, Ahmed S, Gong J, Annamalai AA, Tuli R, Hendifar AE. Targeting mTOR in pancreatic ductal adenocarcinoma. *Front Oncol*. 2016;6:99. doi:10.3389/fonc.2016.00099

135. Kindler HL, Niedzwiecki D, Hollis D, et al. Gemcitabine plus bevacizumab compared with gemcitabine plus placebo in patients with advanced pancreatic cancer: Phase III trial of the Cancer and Leukemia Group B (CALGB 80303). *J Clin Oncol*. 2010;28(22):3617-3622. doi:10.1200/JCO.2010.28.1386

136. Mazur PK, Herner A, Mello SS, et al. Combined inhibition of BET family proteins and histone deacetylases as a potential epigenetics-based therapy for pancreatic ductal adenocarcinoma. *Nat Med*. 2015;21(10):1163-1171. doi:10.1038/nm.3952

137. Hodi FS, O'Day SJ, McDermott DF, et al. Improved Survival with Ipilimumab in Patients with Metastatic Melanoma. *N Engl J Med*. 2010;363(8):711-723. doi:10.1056/NEJMoa1003466

138. Borghaei H, Paz-Ares L, Horn L, et al. Nivolumab versus Docetaxel in Advanced Non-squamous Non- small Cell Lung Cancer. *N Engl J Med*. 2015;373(17):1627-1639. doi:10.1056/NEJMoa1507643

139. Le DT, Durham JN, Smith KN, et al. Mismatch-repair deficiency predicts response of solid tumors to PD-1 blockade. *Science (1979)*. 2017;357(6349):409-413. doi:10.1126/science.aan6733

140. Sahin IH, Askan G, I. Hu Z, O'Reilly EM. Immunotherapy in pancreatic ductal adenocarcinoma: An emerging entity? *Ann Oncol*. 2017;28(12):2950-2961. doi:10.1093/annonc/mdx503

141. Rangelova E, Kaipe H. Immunotherapy in pancreatic cancer-an emerging role: a narrative review. *Chin Clin Oncol*. 2022;11(1):4. doi:10.21037/cco-21-174

142. Hirooka Y, Itoh A, Kawashima H, et al. A combination therapy of gemcitabine with immunotherapy for patients with inoperable locally advanced pancreatic cancer. *Pancreas*. 2009;38(3):69-74. doi:10.1097/MPA.0b013e318197a9e3

143. Kimura Y, Tsukada J, Tomoda T, et al. Clinical and immunologic evaluation of dendritic cell-based immunotherapy in combination with gemcitabine and/or S-1 in patients with advanced pancreatic carcinoma. *Pancreas*. 2012;41(2):195-205. doi:10.1097/MPA.0b013e31822398c6

144. Posey Jr. AD, Schwab RD, Al E. Engineered CAR T Cells Targeting the Cancer-Associated Tn-Glycoform of the Membrane Mucin MUC1 Control Adenocarcinoma. *Immunity*. 2016;44(6):1444-1454. doi:10.1016/j.immuni.2016.05.014

145. Akce M, Zaidi MY, Waller EK, El-Rayes BF, Lesinski GB. The potential of CAR T cell therapy in pancreatic cancer. *Front Immunol*. 2018;9:2166. doi:10.3389/fimmu.2018.02166

146. Schlessinger J. Receptor tyrosine kinases: Legacy of the first two decades. *Cold Spring Harb Perspect Biol*. 2014;6(3):a008912. doi:10.1101/cshperspect.a008912

147. Guan H, Du Y, Ning Y, Cao X. A brief perspective of drug resistance toward EGFR inhibitors: The crystal structures of EGFRs and their variants. *Future Med Chem*. 2017;9(7):693-704. doi:10.4155/fmc-2016-0222

148. Shan Y, Eastwood MP, Zhang X, et al. Oncogenic mutations counteract intrinsic disorder in the EGFR kinase and promote receptor dimerization. *Cell*. 2012;149(4):860-870. doi:10.1016/j.cell.2012.02.063

149. Carpenter CD, Ingraham HA, Cochet C, et al. Structural analysis of the transmembrane domain of the epidermal growth factor receptor. *J Biol Chem*. 1991;266(9):5750-5755. doi:10.1016/s0021-9258(19)67659-3

150. Cymer F, Schneider D. Transmembrane helix-helix interactions involved in ErbB receptor signaling. *Cell Adh Migr*. 2010;4(2):299-312. doi:10.4161/cam.4.2.11191

151. Bell CA, Tynan JA, Hart KC, Meyer AN, Robertson SC, Donoghue DJ. Rotational coupling of the transmembrane and kinase domains of the Neu receptor tyrosine kinase. *Mol Biol Cell*. 2000;11(10):3589-3599. doi:10.1091/mbc.11.10.3589

152. Stamos J, Sliwkowski MX, Eigenbrot C. Structure of the epidermal growth factor receptor kinase domain alone and in complex with a 4-anilinoquinazoline inhibitor. *Journal of Biological Chemistry*. 2002;277(48):46265-46272. doi:10.1074/jbc.M207135200

153. Walton GM, Chen WS, Rosenfeld MG, Gill GN. Analysis of deletions of the carboxyl terminus of the epidermal growth factor receptor reveals self-phosphorylation at tyrosine 992 and enhanced in vivo tyrosine phosphorylation of cell substrates. *Journal of Biological Chemistry*. 1990;265(3):1750-1754. doi:10.1016/s0021-9258(19)40080-x

154. Huang Y, Ognjenović J, Karandur D, et al. A molecular mechanism for the generation of Ligand-dependent differential outputs by the epidermal growth factor receptor. *Elife*. 2021;10:e73218. doi:10.7554/eLife.73218

155. Adrain C, Freeman M. Regulation of receptor tyrosine kinase ligand processing. *Cold Spring Harb Perspect Biol*. 2014;6(1):a008995. doi:10.1101/cshperspect.a008995

156. Harris RC, Chung E, Coffey RJ. EGF receptor ligands. *Exp Cell Res*. 2003;284(1):2-13. doi:10.1016/S0014-4827(02)00105-2

157. Wilson KJ, Gilmore JL, Foley J, Lemmon MA, Riese DJ. Functional Selectivity of EGF Family Peptide Growth Factors: Implications for Cancer. *Pharmacol Ther*. 2009;122(1):1-8. doi:10.1016/j.pharmthera.2008.11.008

158. Sigismund S, Avanzato D, Lanzetti L. Emerging functions of the EGFR in cancer. *Mol Oncol*. 2018;12(1):3-20. doi:10.1002/1878-0261.12155

159. Barnard JA, Graves-Deal R, Pittelkow MR, et al. Auto- and cross-induction within the mammalian epidermal growth factor- related peptide family. *J Biol Chem*. 1994;269(36):22817-22822. doi:10.1016/s0021-9258(17)31718-0

160. Berasain C, Avila MA. Amphiregulin. *Semin Cell Dev Biol*. 2014;28:31-41. doi:10.1016/j.semcdb.2014.01.005

161. Zeng F, Harris RC. Epidermal growth factor, from gene organization to bedside. *Semin Cell Dev Biol*. 2014;28:2-11. doi:10.1016/j.semcdb.2014.01.011

162. Riese 2nd DJ, Cullum RL. Epiregulin: Roles in Normal Physiology and Cancer David. *Semin Cell Dev Biol*. 2014;28:49-56. doi:10.1016/j.semcdb.2014.03.005

163. Taylor SR, Markesbery MG, Harding PA. Heparin-binding epidermal growth factor-like growth factor (HB-EGF) and proteolytic processing by a disintegrin and metalloproteinases (ADAM): A regulator of several pathways. *Semin Cell Dev Biol*. 2014;28:22-30. doi:10.1016/j.semcdb.2014.03.004

164. Schneider MR, Yarden Y. Structure and function of epigen, the last EGFR ligand. *Semin Cell Dev Biol*. 2014;28:57-61. doi:10.1016/j.semcdb.2013.12.011.Structure

165. Singh B, Coffey RJ. From wavy hair to naked proteins: The role of transforming growth factor alpha in health and disease Bhuminder. *Semin Cell Dev Biol*. 2014;28:12-21. doi:10.1016/j.semcdb.2014.03.003

166. Dahlhoff M, Wolf E, Schneider MR. The ABC of BTC: Structural properties and biological roles of betacellulin. *Semin Cell Dev Biol*. 2014;28:42-48. doi:10.1016/j.semcdb.2014.01.002

167. Macdonald-Obermann JL, Pike LJ. Different epidermal growth factor (EGF) receptor ligands show distinct kinetics and biased or partial agonism for homodimer and heterodimer formation. *Journal of Biological Chemistry*. 2014;289(38):26178-26188. doi:10.1074/jbc.M114.586826

168. Ogiso H, Ishitani R, Nureki O, et al. Crystal structure of the complex of human epidermal growth factor and receptor extracellular domains. *Cell*. 2002;110(6):775-787. doi:10.1016/S0092-8674(02)00963-7

169. Savage Jr. RC, Hash JH, Cohen S. Epidermal growth factor: Location of disulfide bonds. *Journal of Biological Chemistry*. 1973;248(22):7669-7672. doi:10.1016/S0021-9258(19)43242-0

170. Conte A, Sigismund S. Chapter Six - The Ubiquitin Network in the Control of EGFR Endocytosis and Signaling. *Prog Mol Biol Transl Sci*. 2016;141:225-276. doi:10.1016/bs.pmbts.2016.03.002

171. Wee P, Wang Z. Epidermal growth factor receptor cell proliferation signaling pathways. *Cancers (Basel)*. 2017;9(5):52. doi:10.3390/cancers9050052

172. Sabbah DA, Hajjo R, Sweidan K. Review on Epidermal Growth Factor Receptor (EGFR) Structure, Signaling Pathways, Interactions, and Recent Updates of EGFR Inhibitors. *Curr Top Med Chem*. 2020;20(10):815-834. doi:10.2174/1568026620666200303123102

173. Lemmon MA, Schlessinger J. Cell signaling by receptor-tyrosine kinases. *Cell*. 2010;141(7):1117-1134. doi:10.1016/j.cell.2010.06.011

174. Tan X, Lambert PF, Rapraeger AC, Anders RA. Stress-induced EGFR trafficking: mechanisms, functions, and therapeutic implications. *Trends Cell Biol*. 2016;26(5):352-366. doi:10.1016/j.tcb.2015.12.006

175. Schneider MR, Wolf E. The epidermal growth factor receptor ligands at a glance. *J Cell Physiol*. 2009;218(3):460-466. doi:10.1002/jcp.21635

176. Repertinger SK, Campagnaro E, Fuhrman J, El-Abaseri T, Yuspa SH, Hansen LA. EGFR enhances early healing after cutaneous incisional wounding. *Journal of Investigative Dermatology*. 2004;123(5):982-989. doi:10.1111/j.0022-202X.2004.23478.x

177. Alroy I, Yarden Y. The ErbB signaling network in embryogenesis and oncogenesis: Signal diversification through combinatorial ligand-receptor interactions. *FEBS Lett*. 1997;410(1):83-86. doi:10.1016/S0014-5793(97)00412-2

178. Cho HS, Leahy DJ. Structure of the extracellular region of HER3 reveals an interdomain tether. *Science (1979)*. 2002;297(5585):1330-1333. doi:10.1126/science.1074611

179. Lemmon MA, Schlessinger J, Ferguson KM. The EGFR family: Not so prototypical receptor tyrosine kinases. *Cold Spring Harb Perspect Biol*. 2014;6(4):a020768. doi:10.1101/cshperspect.a020768

180. Jura N, Endres NF, Engel K, et al. Mechanism for Activation of the EGF Receptor Catalytic Domain by the Juxtamembrane Segment. *Cell*. 2009;137(7):1293-1307. doi:10.1016/j.cell.2009.04.025

181. Zhang X, Gureasko J, Shen K, Cole PA, Kuriyan J. An Allosteric Mechanism for Activation of the Kinase Domain of Epidermal Growth Factor Receptor. *Cell*. 2006;125(6):1137-1149. doi:10.1016/j.cell.2006.05.013

182. Pawson T. Specificity in Signal Transduction: From Phosphotyrosine-SH2 Domain Interactions to Complex Cellular Systems. *Cell*. 2004;116(2):191-203. doi:10.1016/S0092-8674(03)01077-8

183. Wang Z. *ErbB Receptor Signaling: Methods and Protocols*. Vol 1652.; 2017. doi:10.1007/978-1-4939-7219-7

184. Waterman H, Levkowitz G, Alroy I, Yarden Y. The RING finger of c-Cbl mediates desensitization of the epidermal growth factor receptor. *J Biol Chem*. 1999;274(32):22151-22154. doi:10.1074/jbc.274.32.22151

185. Countaway JL, Nairn AC, Davis RJ. Mechanism of desensitization of the epidermal growth factor receptor protein-tyrosine kinase. *Journal of Biological Chemistry*. 1992;267(2):1129-1140. doi:10.1016/s0021-9258(18)48406-2

186. Theroux SJ, Stanley K, Campbell DA, Davis RJ. Mutational removal of the major site of serine phosphorylation of the epidermal growth factor receptor causes potentiation of signal transduction: Role of receptor down-regulation. *Mol Endocrinol*. 1992;6(11):1849-1857. doi:10.1210/mend.6.11.1480174

187. Morrison DK. MAP Kinase Pathways. *Cold Spring Harb Perspect Biol.* 2012;4:a011254. doi:10.1101/cshperspect.a011254

188. Downward J. Mechanisms and consequences of activation of protein kinase B/Akt. *Curr Opin Cell Biol.* 1998;10(2):262-267. doi:10.1016/S0955-0674(98)80149-X

189. Castellano E, Downward J. Ras interaction with PI3K: More than just another effector pathway. *Genes Cancer.* 2011;2(3):261-274. doi:10.1177/1947601911408079

190. Sigismund S, Algisi V, Nappo G, et al. Threshold-controlled ubiquitination of the EGFR directs receptor fate. *EMBO Journal.* 2013;32(15):2140-2157. doi:10.1038/emboj.2013.149

191. Lo HW, Hung MC. Nuclear EGFR signalling network in cancers: Linking EGFR pathway to cell cycle progression, nitric oxide pathway and patient survival. *Br J Cancer.* 2006;94(2):184-188. doi:10.1038/sj.bjc.6602941

192. Wang YN, Yamaguchi H, Hsu JM, Hung MC. Nuclear trafficking of the epidermal growth factor receptor family membrane proteins. *Oncogene.* 2010;29(28):3997-4006. doi:10.1038/onc.2010.157

193. Lo HW, Hsu SC, Ali-Seyed M, et al. Nuclear interaction of EGFR and STAT3 in the activation of the iNOS/NO pathway. *Cancer Cell.* 2005;7(6):575-589. doi:10.1016/j.ccr.2005.05.007

194. Lee HJ, Lan L, Peng G, et al. Tyrosine 370 phosphorylation of ATM positively regulates DNA damage response. *Cell Res.* 2015;25(2):225-236. doi:10.1038/cr.2015.8

195. Santos SD, Verveer PJ, Bastiaens PI. Growth factor-induced MAPK network topology shapes Erk response determining PC-12 cell fate. *Nat Cell Biol.* 2007;9(3):324-330. doi:10.1038/ncb1543

196. Avraham R, Sas-Chen A, Manor O, et al. EGF decreases the abundance of MicroRNAs that restrain oncogenic transcription factors. *Sci Signal.* 2010;3(124):ra43. doi:10.1126/scisignal.2000876

197. Avraham R, Yarden Y. Feedback regulation of EGFR signalling: Decision making by early and delayed loops. *Nat Rev Mol Cell Biol.* 2011;12(2):104-117. doi:10.1038/nrm3048

198. Yarden Y, Sliwkowski MX. Untangling the ErbB signalling network. *Nat Rev Mol Cell Biol.* 2001;2(2):127-137. doi:10.1038/35052073

199. Herbst RS, Shin DM. Monoclonal antibodies to target epidermal growth factor receptor-positive tumors a new paradigm for cancer therapy. *Cancer.* 2002;94(5):1593-1611. doi:10.1002/cncr.10372

200. Roskoski R. The ErbB/HER family of protein-tyrosine kinases and cancer. *Pharmacol Res.* 2014;79:34-74. doi:10.1016/j.phrs.2013.11.002

201. Liu H, Zhang B, Sun Z. Spectrum of EGFR aberrations and potential clinical implications: insights from integrative pan-cancer analysis. *Cancer Commun.* 2020;40(1):43-59. doi:10.1002/cac2.12005

202. Levantini E, Maroni G, del Re M, Tenen DG. EGFR signaling pathway as therapeutic target in human cancers. *Semin Cancer Biol.* 2022;S1044-579X. doi:10.1016/j.semcancer.2022.04.002

203. Su Huang HJ, Nagane M, Klingbeil CK, et al. The enhanced tumorigenic activity of a mutant epidermal growth factor receptor common in human cancers is mediated by threshold levels of constitutive tyrosine phosphorylation and unattenuated signaling. *Journal of Biological Chemistry.* 1997;272(5):2927-2935. doi:10.1074/jbc.272.5.2927

204. Normanno N, Luca A de, Bianco C, et al. Epidermal growth factor receptor (EGFR) signaling in cancer. *Gene.* 2005;366(1):2-16. doi:10.1016/j.gene.2005.10.018

205. Tomas A, Futter CE, Eden ER. EGF receptor trafficking: Consequences for signaling and cancer. *Trends Cell Biol.* 2014;24(1):26-34. doi:10.1016/j.tcb.2013.11.002

206. Shan Y, Eastwood MP, Zhang X, et al. Oncogenic mutations counteract intrinsic disorder in the EGFR kinase and promote receptor dimerization. *Cell.* 2012;149(4):860-870. doi:10.1016/j.cell.2012.02.063

207. Linggi B, Carpenter G. ErbB receptors: new insights on mechanisms and biology. *Trends Cell Biol.* 2006;16(12):649-656. doi:10.1016/j.tcb.2006.10.008

208. Lo HW, Hung MC. Nuclear EGFR signalling network in cancers: Linking EGFR pathway to cell cycle progression, nitric oxide pathway and patient survival. *Br J Cancer.* 2006;94(2):184-188. doi:10.1038/sj.bjc.6602941

209. Wang SC, Hung MC. Nuclear translocation of the epidermal growth factor receptor family membrane tyrosine kinase receptors. *Clinical Cancer Research.* 2009;15(21):6484-6489. doi:10.1158/1078-0432.CCR-08-2813

210. Brand TM, Iida M, Luthar N, Starr MM, Huppert EJ, Wheeler DL. Nuclear EGFR as a molecular target in cancer. *Radiother and Oncol.* 2013;108(3):370-377. doi:10.1016/j.radonc.2013.06.010

211. Lin SY, Makino K, Xia W, et al. Nuclear localization of EGF receptor and its potential new role as a transcription factor. *Nat Cell Biol.* 2001;3(9):802-808. doi:10.1038/ncb0901-802

212. Zanetti-Domingues LC, Bonner SE, Martin-Fernandez ML, Huber V. Mechanisms of Action of EGFR Tyrosine Kinase Receptor Incorporated in Extracellular Vesicles. *Cells.* 2020;9(11):2505. doi:10.3390/cells9112505

213. Ettenberg SA, Rubinstein YR, Banerjee P, Nau MM, Keane MM, Lipkowitz S. cbl-b inhibits EGF-receptor-induced apoptosis by enhancing ubiquitination and degradation of activated receptors. *Mol Cell Biol Res Commun.* 1999;2(2):111-118. doi:10.1006/mcbr.1999.0157

214. Thomasson M, Hedman H, Guo D, Ljungberg B, Henriksson R. LRIG1 and epidermal growth factor receptor in renal cell carcinoma: A quantitative RT-PCR and immunohistochemical analysis. *Br J Cancer.* 2003;89(7):1285-1289. doi:10.1038/sj.bjc.6601208

215. Wang RY, Chen L, Chen HY, et al. MUC15 inhibits dimerization of EGFR and PI3K-AKT signaling and is associated with aggressive hepatocellular carcinomas in patients. *Gastroenterology.* 2013;145(6):1436-1448. doi:10.1053/j.gastro.2013.08.009

216. Zhang X, Pickin KA, Bose R, Jura N, Cole PA, Kuriyan J. Inhibition of the EGF Receptor by Binding to an Activating Kinase Domain Interface. *Nature.* 2007;450(7170):741-744. doi:10.1038/nature05998

217. Martinelli E, de Palma R, Orditura M, de Vita F, Ciardiello F. Anti-epidermal growth factor receptor monoclonal antibodies in cancer therapy. *Clin Exp Immunol.* 2009;158(1):1-9. doi:10.1111/j.1365-2249.2009.03992.x

218. Toolabi M, Moghimi S, Bakhshaiesh TO, et al. 6-Cinnamoyl-4-arylaminothienopyrimidines as highly potent cytotoxic agents: Design, synthesis and structure-activity relationship studies. *Eur J Med Chem.* 2020;185:111786. doi:10.1016/j.ejmech.2019.111786

219. Ayati A, Moghimi S, Salarinejad S, Safavi M, Pouramiri B, Foroumadi A. A review on progression of epidermal growth factor receptor (EGFR) inhibitors as an efficient approach in cancer targeted therapy. *Bioorg Chem.* 2020;99:103811. doi:10.1016/j.bioorg.2020.103811

220. Amelia T, Kartasasmita RE, Ohwada T, Tjahjono DH. Structural Insight and Development of EGFR Tyrosine Kinase Inhibitors. *Molecules.* 2022;27(3):819. doi:10.3390/molecules27030819

221. Yang JCH, Wu YL, Schuler M, et al. Afatinib versus cisplatin-based chemotherapy for EGFR mutation-positive lung adenocarcinoma (LUX-Lung 3 and LUX-Lung 6): Analysis of overall survival data from two randomised, phase 3 trials. *Lancet Oncol.* 2015;16(2):141-151. doi:10.1016/S1470-2045(14)71173-8

222. Soria JC, Wu YL, Nakagawa K, et al. Gefitinib plus chemotherapy versus placebo plus chemotherapy in EGFR-mutation-positive non-small-cell lung cancer after progression on first-line gefitinib (IMPRESS): A phase 3 randomised trial. *Lancet Oncol.* 2015;16(8):990-998. doi:10.1016/S1470-2045(15)00121-7

223. Song Z, Ge Y, Wang C, et al. Challenges and perspectives on the development of small-molecule EGFR inhibitors against T790M-mediated resistance in non-small-cell lung cancer. *J Med Chem.* 2016;59(14):6580-6594. doi:10.1021/acs.jmedchem.5b00840

224. Zhao HY, Xi XX, Xin M, Zhang SQ. Overcoming C797S mutation: The challenges and prospects of the fourth-generation EGFR-TKIs. *Bioorg Chem.* 2022;128(July):106057. doi:10.1016/j.bioorg.2022.106057

225. Leong S, Moss RA, Bowles DW, et al. A Phase I Dose-Escalation Study of the Safety and Pharmacokinetics of Pictilisib in Combination with Erlotinib in Patients with Advanced Solid Tumors. *Oncologist.* 2017;22(12):1491-1499. doi:10.1634/theoncologist.2017-0090

226. Mountzios G. Making progress in epidermal growth factor receptor (EGFR)-mutant non-small cell lung cancer by surpassing resistance: third-generation EGFR tyrosine kinase inhibitors (EGFR-TKIs). *Ann Transl Med.* 2018;6(8):140. doi:10.21037/atm.2017.10.04

227. Joanne L, Marx GM, MacDiarmid J, Brahmbhatt H, Ganju V. Interim data: Phase I/IIa study of EGFR-targeted EDV nanocells carrying cytotoxic drug PNU-159682 (E-EDV-D682) with immunomodulatory adjuvant EDVs carrying α-galactosyl ceramide (EDV-GC) in patients with

recurrent, metastatic pancreatic cancer. *Journal of Clinical Oncology*. 2020;38(15). doi:10.1200/JCO.2020.38.15_suppl.4632

228. Grapa CM, Mocan T, Gonciar D, et al. Epidermal growth factor receptor and its role in pancreatic cancer treatment mediated by nanoparticles. *Int J Nanomedicine*. 2019;14:9693-9706. doi:10.2147/IJN.S226628

229. Manzur A, Oluwasanmi A, Moss D, Curtis A, Hoskins C. Nanotechnologies in pancreatic cancer therapy. *Pharmaceutics*. 2017;9(4):39. doi:10.3390/pharmaceutics9040039

230. Varki A, Cummings RD, Esko JD, et al., eds. *Essentials of Glycobiology*. 4th ed. Cold Spring Harbor Laboratory Press; 2022. doi:10.1101/9781621824213

231. Varki A. Biological roles of glycans. *Glycobiology*. 2017;27(1):3-49. doi:10.1093/glycob/cww086

232. Pinho SS, Reis CA. Glycosylation in cancer: Mechanisms and clinical implications. *Nat Rev Cancer*. 2015;15(9):540-555. doi:10.1038/nrc3982

233. Josic D, Martinovic T, Pavelic K. Glycosylation and metastases. *Electrophoresis*. 2019;40(1):140-150. doi:10.1002/elps.201800238

234. Apweiler R, Hermjakob H, Sharon N. On the frequency of protein glycosylation, as deduced from analysis of the SWISS-PROT database. *Biochim Biophys Acta Gen Subj*. 1999;1473(1):4-8. doi:10.1016/s0304-4165(99)00165-8

235. Rakus JF, Mahal LK. New technologies for glycomic analysis: Toward a systematic understanding of the glycome. *Annual Review of Analytical Chemistry*. 2011;4:367-392. doi:10.1146/annurev-anchem-061010-113951

236. Stowell SR, Ju T, Cummings RD. Protein Glycosylation in Cancer. 2015;10:473-510. doi:10.1146/annurev-pathol-012414-040438

237. Reily C, Stewart TJ, Renfrow MB, Novak J. Glycosylation in health and disease. *Nat Rev Nephrol*. 2019;15(6):346-366. doi:10.1038/s41581-019-0129-4

238. Ohtsubo K, Marth JD. Glycosylation in Cellular Mechanisms of Health and Disease. *Cell*. 2006;126(5):855-867. doi:10.1016/j.cell.2006.08.019

239. Dell A, Galadari A, Sastre F, Hitchen P. Similarities and differences in the glycosylation mechanisms in prokaryotes and eukaryotes. *Int J Microbiol*. 2010;2010:148178. doi:10.1155/2010/148178

240. Zielinska DF, Gnad F, Wiśniewski JR, Mann M. Precision mapping of an in vivo N-glycoproteome reveals rigid topological and sequence constraints. *Cell*. 2010;141(5):897-907. doi:10.1016/j.cell.2010.04.012

241. Vliegenthart JFG. The impact of defining glycan structures. *Perspect Sci (Neth)*. 2017;11:3-10. doi:10.1016/j.pisc.2016.02.003

242. Bennett EP, Mandel U, Clausen H, Gerken TA, Fritz TA, Tabak LA. Control of mucin-type O-glycosylation: A classification of the polypeptide GalNAc-transferase gene family. *Glycobiology*. 2012;22(6):736-756. doi:10.1093/glycob/cwr182

243. Tran DT, ten Hagen KG. Mucin-type o-glycosylation during development. *J Biol Chem*. 2013;288(10):6921-6929. doi:10.1074/jbc.R112.418558

244. Bergstrom KS, Xia L. Mucin-type O-glycans and their roles in intestinal homeostasis. *Glycobiology*. 2013;23(9):1026-1037. doi:10.1093/glycob/cwt045

245. Kaur S, Kumar S, Momi N, Sasson AR, Batra SK. Mucins in pancreatic cancer and its microenvironment. *Nat Rev Gastroenterol Hepatol*. 2013;10(10):607-620. doi:10.1038/nrgastro.2013.120

246. Cohen M, Varki A. The sialome-far more than the sum of its parts. *OMICS*. 2010;14(4):455-464. doi:10.1089/omi.2009.0148

247. Angata T, Varki A. Chemical Diversity in the Sialic Acids and Related r -Keto Acids : An Evolutionary Perspective. *Chem Rev*. 2002;102(2):439-469. doi:10.1021/cr000407m

248. Pang X, Li H, Guan F, Li X. Multiple roles of glycans in hematological malignancies. *Front Oncol*. 2018;8:364. doi:10.3389/fonc.2018.00364

249. Harduin-lepers A, Vallejo-ruiz V, Krzewinki-Recchi MA, Samyn-petit B, Julien S, Delannoy P. The human sialyltransferase family. *Exp Cell Res*. 2001;410(1):112949. doi:10.1016/j.yexcr.2021.112949

250. Harduin-lepers A, Colomb F, Foulquier F, Groux- S, Delannoy P. Sialyltransferases functions in cancers. *Front Biosci (Elite Ed)*. 2012;4(1):499-515. doi:10.2741/e396

251. Ferreira IG, Pucci M, Venturi G, Malagolini N, Chiricolo M. Glycosylation as a Main Regulator of Growth and Death Factor Receptors Signaling. *Int J Mol Sci*. 2018;19(580). doi:10.3390/ijms19020580

252. Bate C, Nolan W, Williams A. Sialic Acid on the Glycosylphosphatidylinositol Anchor Regulates PrP-mediated Cell Signaling and Prion Formation. *Journal of Biological Chemistry*. 2016;291(1):160-170. doi:10.1074/jbc.M115.672394

253. Ilver D, Johansson P, Miller-Podraza H, Nyholm PG, Teneberg S, Karlsson KA. Bacterium–Host Protein–Carbohydrate Interactions. *Methods Enzymol*. 2003;363:134-157. doi:10.1016/S0076-6879(03)01049-8

254. Li Y, Chen X. Sialic acid metabolism and sialyltransferases: Natural functions and applications. *Appl Microbiol Biotechnol*. 2012;94(4):887-905. doi:10.1007/s00253-012-4040-1

255. Lehmann F, Tiralongo E, Tiralongo J. Sialic acid-specific lectins: occurrence, specificity and function. *Cellular and Molecular Life Sciences*. 2006;63(12):1331-1354. doi:10.1007/s00018-005-5589-y

256. Pendu J le, Marionneau S, Cailleau-Thomas A, Rocher J, le Moullac-Vaidye B, Clément M. ABH and Lewis histo-blood group antigens in cancer. *APMIS*. 2001;109(1):9-31. doi:10.1111/j.1600-0463.2001.tb00011.x

257. Dube DH, Bertozzi CR. Glycans in cancer and inflammation - Potential for therapeutics and diagnostics. *Nat Rev Drug Discov*. 2005;4(6):477-488. doi:10.1038/nrd1751

258. Hakomori S. Glycosylation defining cancer malignancy: New wine in an old bottle. *Proc Natl Acad Sci U S A*. 2002;99(16):10231-10233. doi:10.1073/pnas.172380699

259. Nakamori S, Kameyama M, Imaoka S, et al. Increased expression of sialyl Lewisx antigen correlates with poor survival in patients with colorectal carcinoma: clinicopathological and immunohistochemical study. *Cancer Res*. 1993;53(15):3632-3637.

260. Amado M, Carneiro F, Seixas M, Clausen H, Sobrinho-Simões M. Dimeric sialyl-Le(x) expression in gastric carcinoma correlates with venous invasion and poor outcome. *Gastroenterology*. 1998;114(3):462-470. doi:10.1016/s0016-5085(98)70529-3

261. Nakayama T, Watanabe M, Katsumata T, Teramoto T, Kitajima M. Expression of sialyl Lewis(a) as a new prognostic factor for patients with advanced colorectal carcinoma. *Cancer*. 1995;75(8):2051-2056. doi:10.1002/1097-0142(19950415)75:8<2051::aid-cncr2820750804>3.0.co;2-4

262. Ogawa J ichi, Sano A, Inoue H, Koide S. Expression of Lewis-related antigen and prognosis in stage I non-small cell lung cancer. *Ann Thorac Surg*. 1995;59(2):412-415. doi:10.1016/0003-4975(94)00866-6

263. Jørgensen T, Berner A, Kaalhus O, Tveter KJ, Danielsen HE, Bryne M. Up-regulation of the oligosaccharide sialyl LewisX: a new prognostic parameter in metastatic prostate cancer. *Cancer Res*. 1995;55(9):1817-1819.

264. Holgersson J, Löfling J. Glycosyltransferases involved in type 1 chain and Lewis antigen biosynthesis exhibit glycan and core chain specificity. *Glycobiology*. 2006;16(7):584-593. doi:10.1093/glycob/cwj090

265. Kukowska-Latallo JF, Larsen RD, Nair RP, Lowe J. A cloned human cDNA determines expression of a mouse stage-specific embryonic antigen and the Lewis blood group alpha(1,3/1,4)fucosyltransferase. *Genes Cancer*. 1990;4(8):1288-1303. doi:10.1101/gad.4.8.1288

266. Weston BW, Smith PL, Kelly RJ, Lowenii JB. Molecular Cloning of a Fourth Member of a Human alpha (1,3)Fucosyltransferase Gene Family. Multiple homologous sequences that determine expression of the Lewis x, sialyl Lewis x, and difucosyl sialyl Lewis x epitopes. *J Biol Chem*. 1992;267(34):24575-24584. doi:10.1016/S0021-9258(18)35803-4

267. Weston BW, Nairq RP, Larsenp RD, Loweq B. Isolation of a Novel Human alpha(1,3)Fucosyltransferase Gene and Molecular Comparison to the Human Lewis Blood Group alpha (1,3/1,4)fucosyltransferase gene. Syntenic, homologous, nonallelic genes encoding enzymes with distinct acceptor substrate specific. *J Biol Chem*. 1992;267(6):4152-4160. doi:10.1016/S0021-9258(19)50641-X

268. Natsukas S, Gerstens KM, Zenitas K, Kannagio R, Lowesnll JB. Molecular Cloning of a cDNA Encoding a Novel Human Leukocyte alpha-1,3-fucosyltransferase Capable o f Synthesizing the Sialyl Lewis x Determinant. *J Biol Chem.* 1994;269(24):16789-16794. doi:10.1016/S0021-9258(19)89461-9

269. Mondal N, Jr AB, Stolfa G, et al. ST3Gal-4 is the primary sialyltransferase regulating the synthesis of E-, P-, and L-selectin ligands on human myeloid leukocytes. *Blood.* 2015;125(4):687-697. doi:10.1182/blood-2014-07-588590

270. Pérez-Garay M, Arteta B, Pagés L, et al. A2,3-Sialyltransferase ST3Gal III Modulates Pancreatic Cancer Cell Motility and Adhesion in Vitro and Enhances Its Metastatic Potential in Vivo. *PLoS One.* 2010;5(9):e12524. doi:10.1371/journal.pone.0012524

271. Pérez-Garay M, Arteta B, Llop E, et al. α2,3-Sialyltransferase ST3Gal IV promotes migration and metastasis in pancreatic adenocarcinoma cells and tends to be highly expressed in pancreatic adenocarcinoma tissues. *Int J Biochem Cell Biol.* 2013;45(8):1748-1757. doi:10.1016/j.biocel.2013.05.015

272. Mondal N, Dykstra B, Lee J, et al. Distinct human alpha(1,3)-fucosyltransferases drive Lewis-X/sialyl Lewis-X assembly in human cells. *J Biol Chem.* 2018;293(19):7300-7314. doi:10.1074/jbc.RA117.000775

273. Trinchera M, Malagolini N, Chiricolo M, et al. The biosynthesis of the selectin-ligand sialyl Lewis x in colorectal cancer tissues is regulated by fucosyltransferase VI and can be inhibited by an RNA interference-based approach. *International Journal of Biochemistry and Cell Biology.* 2011;43(1):130-139. doi:10.1016/j.biocel.2010.10.004

274. Freeze HH, Aebi M. Altered glycan structures : the molecular basis of congenital disorders of glycosylation. *Curr Opin Struct Biol.* 2005;15(5):490-498. doi:10.1016/j.sbi.2005.08.010

275. Reis CA, Osorio H, Silva L, Gomes C, David L. Alterations in glycosylation as biomarkers for cancer detection. *J Clin Pathol.* 2010;63(4):322-329. doi:10.1136/jcp.2009.071035

276. Thomas D, Rathinavel AK, Radhakrishnan P. Altered glycosylation in cancer: A promising target for biomarkers and therapeutics. *Biochim Biophys Acta Rev Cancer.* 2021;1875(1):188464. doi:10.1016/j.bbcan.2020.188464

277. Oliveira-Ferrer L, Legler K, Milde-Langosch K. Role of protein glycosylation in cancer metastasis. *Semin Cancer Biol.* 2017;44:141-152. doi:10.1016/j.semcancer.2017.03.002

278. Carvalho S, Reis CA, Pinho SS. Cadherins Glycans in Cancer : Sweet Players in a Bitter Process. *Trends Cancer.* 2016;2(9):519-531. doi:10.1016/j.trecan.2016.08.003

279. Mereiter S, Balmaña M, Campos D, Gomes J, Reis CA. Glycosylation in the Era of Cancer-Targeted Therapy: Where Are We Heading? *Cancer Cell.* 2019;36(1):6-16. doi:10.1016/j.ccell.2019.06.006

280. Abbott KL, Nairn A v, Hall EM, et al. Focused glycomic analysis of the N -linked glycan biosynthetic pathway in ovarian cancer. *Proteomics.* 2008;8(16):3210-3220. doi:10.1002/pmic.200800157

281. Nguyen AT, Chia J, Ros M, Hui KM, Saltel F, Bard F. Organelle Specific O-Glycosylation Drives MMP14 Activation , Tumor Growth , and Metastasis. *Cancer Cell.* 2017;32(5):639-653.e6. doi:10.1016/j.ccell.2017.10.001

282. Wang Y, Ju T, Ding X, et al. Cosmc is an essential chaperone for correct protein. *Proc Natl Acad Sci USA.* 2010;107(20):9228-9233. doi:10.1073/pnas.0914004107

283. Itkonen HM, Minner S, Guldvik IJ, et al. O-GlcNAc Transferase Integrates Metabolic Pathways to Regulate the Stability of c-MYC in Human Prostate Cancer Cells. *Cancer Res.* 2013;73(16):5277-5287. doi:10.1158/0008-5472.CAN-13-0549

284. Lucena MC, Carvalho-cruz P, Donadio JL, et al. Epithelial Mesenchymal Transition Induces Aberrant Glycosylation through Hexosamine Biosynthetic Pathway. *J Biol Chem.* 2016;291(25):12917-12929. doi:10.1074/jbc.M116.729236

285. Munkley J, Elliott DJ. Hallmarks of glycosylation in cancer. *Oncotarget.* 2016;7(23):35478-35489. doi:10.18632/oncotarget.8155

286. Todeschini AR, Nilson J, Santos D, Handa K, Hakomori S itiroh. Ganglioside GM2-Tetraspanin CD82 Complex Inhibits Met and Its Cross-talk with Integrins , Providing a Basis for Control of

Cell Motility through Glycosynapse. *J Biol Chem*. 2007;282(11):8123-8133. doi:10.1074/jbc.M611407200

287. Park SY, Yoon SJ, Freire-de-lima L, Kim JH, Hakomori SI. Control of cell motility by interaction of gangliosides , tetraspanins , and epidermal growth factor receptor in A431 versus KB epidermoid tumor cells. *Carbohydr Res*. 2009;344(12):1479-1486. doi:10.1016/j.carres.2009.04.032

288. Julien S, Bobowski M, Steenackers A, Bourhis X le, Delannoy P. How Do Gangliosides Regulate RTKs Signaling? *Cells*. 2013;2(4):751-767. doi:10.3390/cells2040751

289. Guo HB, Johnson H, Randolph M, Lee I, Pierce M. Knockdown of GnT-Va expression inhibits ligand-induced downregulation of the epidermal growth factor receptor and intracellular signaling by inhibiting receptor endocytosis. *Glycobiology*. 2009;19(5):547-559. doi:10.1093/glycob/cwp023

290. Sato Y, Takahashi M, Shibukawa Y, et al. Overexpression of N-Acetylglucosaminyltransferase III Enhances the Epidermal Growth Factor-induced Phosphorylation of ERK in HeLaS3 Cells by Up-regulation of the Internalization Rate of the Receptors. *Journal of Biological Chemistry*. 2001;276(15):11956-11962. doi:10.1074/jbc.M008551200

291. Lau KS, Partridge EA, Grigorian A, et al. Complex N-Glycan Number and Degree of Branching Cooperate to Regulate Cell Proliferation and Differentiation. *Cell*. 2007;129(1):123-134. doi:10.1016/j.cell.2007.01.049

292. Mereiter S, Magalhães A, Adamczyk B, et al. Glycomic analysis of gastric carcinoma cells discloses glycans as modulators of RON receptor tyrosine kinase activation in cancer. *Biochim Biophys Acta Gen Subj*. 2016;1860(8):1795-1808. doi:10.1016/j.bbagen.2015.12.016

293. Gomes C, Osório H, Pinto MT, Campos D, Oliveira MJ, Reis CA. Expression of ST3GAL4 Leads to SLex Expression and Induces c-Met Activation and an Invasive Phenotype in Gastric Carcinoma Cells. *PLoS One*. 2013;8(6):e66737. doi:10.1371/journal.pone.0066737

294. Liwosz A, Lei T, Kukuruzinska MA. N -Glycosylation Affects the Molecular Organization and Stability of E-cadherin Junctions. *Journal of Biological Chemistry*. 2006;281(32):23138-23149. doi:10.1074/jbc.M512621200

295. Nita-Lazar M, Rebustini I, Walker J, Kukuruzinska MA. Hypoglycosylated E-cadherin promotes the assembly of tight junctions through the recruitment of PP2A to adherens junctions. *Exp Cell Res*. 2010;316(11):1871-1884. doi:10.1016/j.yexcr.2010.02.008

296. Nita-Lazar M, Noonan V, Rebustini I, Walker J, Menko AS, Kukuruzinska MA. Overexpression of DPAGT1 leads to aberrant N-glycosylation of E-cadherin and cellular discohesion in oral cancer. *Cancer Res*. 2010;69(14):5673-5680. doi:10.1158/0008-5472.CAN-08-4512

297. Harosh-davidovich S ben, Khalaila I. O -GlcNAcylation a ff ects β -catenin and E-cadherin expression , cell motility and tumorigenicity of colorectal cancer. *Exp Cell Res*. 2018;364(1):42-49. doi:10.1016/j.yexcr.2018.01.024

298. Osumi D, Takahashi M, Miyoshi E, et al. Core fucosylation of E-cadherin enhances cell – cell adhesion in human colon carcinoma WiDr cells. *Cancer Sci*. 2009;100(5):888-895. doi:10.1111/j.1349-7006.2009.01125.x

299. Bassagañas S, Carvalho S, Dias AM, et al. Pancreatic cancer cell glycosylation regulates cell adhesion and invasion through the modulation of α2β1 integrin and E-cadherin function. *PLoS One*. 2014;9(5):e98595. doi:10.1371/journal.pone.0098595

300. Zhou Y, Fukuda T, Hang Q, Hou S, Isaji T. Inhibition of fucosylation by 2-fluorofucose suppresses human liver cancer HepG2 cell proliferation and migration as well as tumor formation. *Sci Rep*. 2017;7(1):11563. doi:10.1038/s41598-017-11911-9

301. Lemieux GA, Bertozzi CR. Modulating cell surface immunoreactivity by metabolic induction of unnatural carbohydrate antigens. *Chem Biol*. 2001;8(3):265-275. doi:10.1016/S1074-5521(01)00008-4

302. Dall'Olio F, Malagolini N, Trinchera M, Chiricolo M. Mechanisms of cancer-associated glycosylation changes. *Frontiers in Bioscience*. 2012;17(2):670-699. doi:10.1109/epqu.2011.6128966

303. Varki NM, Varki A. Diversity in cell surface sialic acid presentations: Implications for biology and disease. *Lab Invest*. 2007;87(9):851-857. doi:10.1038/labinvest.3700656

304. Bogenrieder T, Herlyn M. Axis of evil: molecular mechanisms of cancer metastasis. *Oncogene*. 2003;22(42):6524-6536. doi:10.1038/sj.onc.1206757

305. Seales EC, Jurado GA, Brunson BA, Wakefield JK, Frost AR, Bellis SL. Hypersialylation of β 1 integrins, observed in colon adenocarcinoma, may contribute to cancer progression by up-regulating cell motility. *Cancer Res.* 2005;65(11):4645-4652. doi:10.1158/0008-5472.CAN-04-3117

306. Kariya Y, Kawamura C, Tabei T, Gu J. Bisecting GlcNAc residues on laminin-332 down-regulate galectin-3-dependent keratinocyte motility. *J Bi.* 2010;285(5):3330-3340. doi:10.1074/jbc.M109.038836

307. Ranjan A, Bane SM, Kalraiya RD. Glycosylation of the laminin receptor (α3β1) regulates its association with tetraspanin CD151 : Impact on cell spreading , motility , degradation and invasion of basement membrane by tumor cells. *Exp Cell Res.* 2014;322(2):249-264. doi:10.1016/j.yexcr.2014.02.004

308. Saoncella S, Echtermeyer F, Denhez F, et al. Syndecan-4 signals cooperatively with integrins in a Rho- dependent manner in the assembly of focal adhesions and actin stress fibers. *Proc Natl Acad Sci USA.* 1999;96(6):2805-2810. doi:10.1073/pnas.96.6.2805

309. Schultz MJ, Swindall AF, Bellis SL. Regulation of the metastatic cell phenotype by sialylated glycans. *Cancer and Metastasis Reviews.* 2012;31(3-4):501-518. doi:10.1007/s10555-012-9359-7

310. Dall'Olio F, Malagolini N, Trinchera M, Chiricolo M. Sialosignaling: Sialyltransferases as engines of self-fueling loops in cancer progression. *Biochim Biophys Acta Gen Subj.* 2014;1840(9):2752-2764. doi:10.1016/j.bbagen.2014.06.006

311. Yogeeswaran G, Salk P. Metastatic Potential Is Positively Correlated with Cell Surface Sialylation of Cultured Murine Tumor Cell Lines. *Science (1979).* 1981;212(4502):1514-1516. doi:10.1126/science.7233237

312. Dall'Olio F, Chiricolo M. Sialyltransferases in cancer. *Glycoconj J.* 2001;18(11-12):841-850. doi:10.1023/A:1022288022969

313. Kim YJ, Varki A. Perspectives on the significance of altered glycosylation of glycoproteins in cancer. *Glycoconj J.* 1997;14(5):569-576. doi:10.1023/A:1018580324971

314. Schultz MJ, Holdbrooks AT, Chakraborty A, et al. The tumor-associated glycosyltransferase ST6Gal-I regulates stem cell transcription factors and confers a cancer stem cell phenotype. *Cancer Res.* 2016;76(13):3978-3988. doi:10.1158/0008-5472.CAN-15-2834

315. Swindall AF, I. A, Londoño-Joshi, et al. ST6Gal-I protein expression is upregulated in human epithelial tumors and correlates with stem cell markers in normal tissues and colon cancer cell lines. *Cancer Res.* 2013;73(7):2368-2378. doi:10.1158/0008-5472.CAN-12-3424.ST6Gal-I

316. Gretschel S, Haensch W, Schlag PM, Kemmner W. Clinical Relevance of Sialyltransferases ST6GAL-I and ST3GAL-III in Gastric Cancer. *Oncology.* 2003;65(2):139-145. doi:10.1159/000072339

317. Swindall AF, Bellis SL. Sialylation of the Fas death receptor by St6Gal-I provides protection against Fas-mediated apoptosis in colon carcinoma cells. *Journal of Biological Chemistry.* 2011;286(26):22982-22990. doi:10.1074/jbc.M110.211375

318. Jones RB, Dorsett KA, Hjelmeland AB, Bellis SL. The ST6Gal-I sialyltransferase protects tumor cells against hypoxia by enhancing HIF-1alpha signaling. *J Biol Chem.* 2018;293(15):5659-5667. doi:10.1074/jbc.RA117.001194

319. Britain CM, Dorsett KA, Bellis SL. The glycosyltransferase ST6Gal-I protects tumor cells against serum growth factor withdrawal by enhancing survival signaling and proliferative potential. *Journal of Biological Chemistry.* 2017;292(11):4663-4673. doi:10.1074/jbc.M116.763862

320. Britain CM, Holdbrooks AT, Anderson JC, Willey CD, Bellis SL. Sialylation of EGFR by the ST6Gal-I sialyltransferase promotes EGFR activation and resistance to gefitinib-mediated cell death. *J Ovarian Res.* 2018;11(1):12. doi:10.1186/s13048-018-0385-0

321. Britain CM, Bhalerao N, Silva AD, et al. Glycosyltransferase ST6Gal-I promotes the epithelial to mesenchymal transition in pancreatic cancer cells. *J Biol Chem.* 2021;296:100034. doi:10.1074/jbc.RA120.014126

322. Rodrigues JG, Duarte HO, Gomes C, et al. Terminal α2,6-sialylation of epidermal growth factor receptor modulates antibody therapy response of colorectal cancer cells. *Cell Oncol (Dordr).* 2021;44(4):835-850. doi:10.1007/s13402-021-00606-z

323. Zhuo Y, Bellis SL. Emerging role of α2,6-sialic acid as a negative regulator of galectin binding and function. *J Biol Chem*. 2011;286(8):5935-5941. doi:10.1074/jbc.R110.191429

324. Peracaula R, Tabarés G, López-Ferrer A, Brossmer R, de Bolós C, Llorens R de. Role of sialyltransferases involved in the biosynthesis of Lewis antigens in human pancreatic tumour cells. 2005;22(3):135-144. doi:10.1007/s10719-005-0734-2

325. Bassagañas S, Pérez-Garay M, Peracaula R. Cell surface sialic acid modulates extracellular matrix adhesion and migration in pancreatic adenocarcinoma cells. *Pancreas*. 2014;43(1):109-117. doi:10.1097/MPA.0b013e31829d9090

326. Guerrero PE, Miró L, Wong BS, et al. Knockdown of α2,3-sialyltransferases impairs pancreatic cancer cell migration, invasion and E-selectin-dependent adhesion. *Int J Mol Sci*. 2020;21(17):6239. doi:10.3390/ijms21176239

327. Zhen Y, Caprioli RM, Staros J v. Characterization of glycosylation sites of the epidermal growth factor receptor. *Biochemistry*. 2003;42(18):5478-5492. doi:10.1021/bi027101p

328. Smith KD, Davies MJ, Bailey D, Renouf D v, Hounsell EF. Analysis of the glycosylation patterns of the extracellular domain of the epidermal growth factor receptor expressed in Chinese hamster ovary fibroblasts. *Growth Factors*. 1996;13(1-2):121-132. doi:10.3109/08977199609034572

329. Ullrich A, Coussens L, Hayflick JS, et al. Human epidermal growth factor receptor cDNA sequence and aberrant expression of the amplified gene in A431 epidermoid carcinoma cells. *Nature*. 1984;309(5967):418-425. doi:10.1038/309418a0

330. Soderquist AM, Carpenter G. Glycosylation of the epidermal growth factor receptor in A-431 cells. The contribution of carbohydrate to receptor function. *Journal of Biological Chemistry*. 1984;259(20):12586-12594. doi:10.1016/s0021-9258(18)90787-8

331. Liu YC, Yen HY, Chen CY, et al. Sialylation and fucosylation of epidermal growth factor receptor suppress its dimerization and activation in lung cancer cells. *Proc Natl Acad Sci USA*. 2011;108(28):11332-11337. doi:10.1073/pnas.1107385108

332. Takahashi M, Hasegawa Y, Maeda K, Kitano M, Taniguchi N. Role of glycosyltransferases in carcinogenesis; growth factor signaling and EMT/MET programs. *Glycoconj J*. 2022;39(2):167-176. doi:10.1007/s10719-022-10041-3

333. Takahashi M, Yokoe S, Asahi M, et al. N-glycan of ErbB family plays a crucial role in dimer formation and tumor promotion. *Biochim Biophys Acta*. 2008;1780(3):520-524. doi:10.1016/j.bbagen.2007.10.019

334. Gamou S, Shimizu N. Glycosylation of the epidermal growth factor receptor and its relationship to membrane transport and ligand binding. *J Biochem*. 1988;104(3):388-396. doi:10.1093/oxfordjournals.jbchem.a122478

335. Slieker LJ, Martensen TM, Lane MD. Synthesis of epidermal growth factor receptor in human A431 cells. Glycosylation-dependent acquisition of ligand binding activity occurs post-translationally in the endoplasmic reticulum. *J Biol Chem*. 1986;261(32):15233-15241. doi:10.1016/s0021-9258(18)66858-9

336. Slieker LJ, Lane MD. Post-translational processing of the epidermal growth factor receptor. Glycosylation-dependent acquisition of ligand-binding capacity. *Journal of Biological Chemistry*. 1985;260(2):687-690. doi:10.1016/s0021-9258(20)71149-x

337. Contessa JN, Bhojani MS, Freeze HH, Rehemtulla A, Lawrence TS. Inhibition of N-linked glycosylation disrupts receptor tyrosine kinase signaling in tumor cells. *Cancer Res*. 2008;68(10):3803-3809. doi:10.1158/0008-5472.CAN-07-6389

338. Kaszuba K, Grzybek M, Orlowski A, et al. N-Glycosylation as determinant of epidermal growth factor receptor conformation in membranes. *Proc Natl Acad Sci USA*. 2015;112(14):4334-4339. doi:10.1073/pnas.1503262112

339. Balmaña M, Diniz F, Feijão T, Barrias CC, Mereiter S, Reis CA. Analysis of the effect of increased α2,3-sialylation on RTK activation in MKN45 gastric cancer spheroids treated with crizotinib. *Int J Mol Sci*. 2020;21(3):722. doi:10.3390/ijms21030722

340. Duarte HO, Balmaña M, Mereiter S, Osório H, Gomes J, Reis CA. Gastric cancer cell glycosylation as a modulator of the ErbB2 oncogenic receptor. *Int J Mol Sci*. 2017;18(11):2262. doi:10.3390/ijms18112262

341. Taylor ES, Pol-fachin L, Lins RD, Lower SK. Conformational stability of the epidermal growth factor (EGF) receptor as influenced by glycosylation, dimerizatin and EGF hormone binding. *Proteins.* 2018;85(4):561-570. doi:10.1002/prot.25220

342. Freitas D, Campos D, Gomes J, et al. O-glycans truncation modulates gastric cancer cell signaling and transcription leading to a more aggressive phenotype. *EBioMedicine.* 2019;40:349-362. doi:10.1016/j.ebiom.2019.01.017

343. Chugh S, Meza J, Sheinin YM, Ponnusamy MP, Batra SK. Loss of N-acetylgalactosaminyltransferase 3 in poorly differentiated pancreatic cancer: Augmented aggressiveness and aberrant ErbB family glycosylation. *Br J Cancer.* 2016;114(12):1376-1386. doi:10.1038/bjc.2016.116

344. Sambrooks CL, Baro M, Quijano A, et al. Oligosaccharyltransferase Inhibition Overcomes Therapeutic Resistance to EGFR Tyrosine Kinase Inhibitors. *Physiol Behav.* 2018;176(3):139-148. doi:10.1158/0008-5472.CAN-18-0505

345. Lopez-Sambrooks C, Shrimal S, Khodier C, et al. Oligosaccharyltransferase Inhibition Induces Senescence in RTK-Driven Tumor Cells. *Physiol Behav.* 2016;176(5):139-148. doi:10.1038/nchembio.2194.Oligosaccharyltransferase

346. Tsuda T, Ikeda Y, Taniguchi N. The Asn-420-linked sugar chain in human epidermal growth factor receptor suppresses ligand-independent spontaneous oligomerization: Possible role of a specific sugar chain in controllable receptor activation. *J Biol Chem.* 2000;275(29):21988-21994. doi:10.1074/jbc.M003400200

347. Whitson KB, Whitson SR, Red-Brewer ML, et al. Functional effects of glycosylation at Asn-579 of the epidermal growth factor receptor. *Biochemistry.* 2005;44(45):14920-14931. doi:10.1021/bi050751j

348. Hasegawa Y, Takahashi M, Ariki S, et al. Surfactant protein D suppresses lung cancer progression by downregulation of epidermal growth factor signaling. *Oncogene.* 2015;34(7):838-845. doi:10.1038/onc.2014.20

349. Yao Y, Zhou L, Liao W, et al. HH1-1, a novel Galectin-3 inhibitor, exerts anti-pancreatic cancer activity by blocking Galectin-3/EGFR/AKT/FOXO3 signaling pathway. *Carbohydr Polym.* 2019;204:111-123. doi:10.1016/j.carbpol.2018.10.008

350. Wang X, Gu J, Ihara H, Miyoshi E, Honke K, Taniguchi N. Core fucosylation regulates epidermal growth factor receptor-mediated intracellular signaling. *J Biol Chem.* 2006;281(5):2572-2577. doi:10.1074/jbc.M510893200

351. Mathew MP, Tan E, Saeui CT, et al. Metabolic flux-driven sialylation alters internalization, recycling, and drug sensitivity of the epidermal growth factor receptor (EGFR) in SW1990 pancreatic cancer cells. *Oncotarget.* 2016;7(41):66491-66511. doi:10.18632/oncotarget.11582

352. Park JJ, Yi JY, Jin YB, et al. Sialylation of epidermal growth factor receptor regulates receptor activity and chemosensitivity to gefitinib in colon cancer cells. *Biochem Pharmacol.* 2012;83(7):849-857. doi:10.1016/j.bcp.2012.01.007

353. Yen HY, Liu YC, Chen NY, et al. Effect of sialylation on EGFR phosphorylation and resistance to tyrosine kinase inhibition. *Proc Natl Acad Sci USA.* 2015;112(22):6955-6960. doi:10.1073/pnas.1507329112

354. Liu N, Zhu M, Linhai Y, et al. Increasing HER2 a2,6 sialylation facilitates gastric cancer progression and resistance via the akt and ERK pathways. *Oncol Rep.* 2018;40(5):2997-3005. doi:10.3892/or.2018.6680

355. Cheng L, Cao L, Wu Y, et al. Bisecting N-Acetylglucosamine on EGFR Inhibits Malignant Phenotype of Breast Cancer via Down-Regulation of EGFR/Erk Signaling. *Front Oncol.* 2020;10:929. doi:10.3389/fonc.2020.00929

356. Kajihara Y, Kodama H, Wakabayashi T, Sato K ichi. Characterization of inhibitor activities and binding mode of synthetic 6 ' -modified methyl N-acetyl-beta-lactosaminide toward rat liver CMP-D-Neu5Ac: D-galactoside -(2-6)-alpha-D-sialyltransferase. *Carbohydr Res.* 1993;247:179-193. doi:10.1016/0008-6215(93)84251-z

357. Okazaki K, Nishigaki S, Ishizuka F, Ogawa S. Potent and specific sialyltransferase inhibitors : imino-linked 5a'-carbadisaccharides. *Org Biomol Chem.* 2003;1(13):2229-2230. doi:10.1039/b304695h

358. Wang L, Liu Y, Wu L, Sun XL. Sialyltransferase inhibition and recent advances. *Biochim Biophys Acta Proteins Proteom*. 2016;1864(1):143-153. doi:10.1016/j.bbapap.2015.07.007

359. Jeanneau C, Chazalet V, Augé C, et al. Structure-function analysis of the human sialyltransferase ST3Gal I: Role of N-glycosylation and a novel conserved sialylmotif. *J Biol Chem*. 2004;279(14):13461-13468. doi:10.1074/jbc.M311764200

360. Miyazaki T, Angata K, Seeberger PH, Hindsgaul O, Fukuda M. CMP substitutions preferentially inhibit polysialic acid synthesis. *Glycobiology*. 2009;18(2):187-194. doi:10.1093/glycob/cwm132

361. Al-saraireh YMJ, Sutherland M, Springett BR, et al. Pharmacological Inhibition of polysialyltransferase ST8SiaII Modulates Tumour Cell Migration. *PLoS One*. 2013;8(8):1-12. doi:10.1371/journal.pone.0073366

362. Li W, Niu Y, Xiong DC, Cao X, Ye XS. Highly Substituted Cyclopentane- CMP Conjugates as Potent Sialyltransferase Inhibitors. *J Med Chem*. 2015;58(20):7972-7990. doi:10.1021/acs.jmedchem.5b01181

363. Montgomery AP, Dobie C, Szabo R, et al. Design, synthesis and evaluation of carbamate-linked uridyl-based inhibitors of human ST6Gal I. *Bioorg Med Chem*. 2020;28(14):115561. doi:10.1016/j.bmc.2020.115561

364. Perez SJLP, Fu CW, Li WS. Sialyltransferase inhibitors for the treatment of cancer metastasis: Current challenges and future perspectives. *Molecules*. 2021;26(18):5673. doi:10.3390/molecules26185673

365. Burkart MD, Vincent SP, Düffels A, Murray BW, Ley S v, Wong CH. Chemo-Enzymatic Synthesis of Fluorinated Sugar Nucleotide: Useful Mechanistic Probes for Glycosyltransferases. *Bioorg Med Chem*. 2000;8(8):1937-1946. doi:10.1016/s0968-0896(00)00139-5

366. Rillahan CD, Antonopoulos A, Lefort CT, et al. Global Metabolic Inhibitors of Sialyl- and Fucosyltransferases. *Nat Chem Biol*. 2012;8(7):661-668. doi:10.1038/nchembio.999

367. Montgomery A, Szabo R, Skropeta D, Yu H. Computational characterisation of the interactions between human ST6Gal I and transition-state analogue inhibitors : insights for inhibitor design. *J Mol Recognit*. 2016;29(5):210-222. doi:10.1002/jmr.2520

368. Kuhn B, Greif M, Engel AM, Sobek H, Rudolph MG. The structure of human a -2 , 6-sialyltransferase reveals the binding mode of complex glycans research papers. *Acta Cryst*. 2013;69(Pt 9):1826-1838. doi:10.1107/S0907444913015412

369. Hinderlich S, Weidemann W, Yardeni T, Horstkorte R, Huizing M. UDP-GlcNAc 2-epimerase/ManNAc kinase (GNE), a master regulator of sialic acid synthesis Stephan. *Top Curr Chem*. 2015;366(464):97-137. doi:10.1007/128

370. Seppala R, Lehto VP, Gahl WA. Mutations in the human UDP-N-acetylglucosamine 2-epimerase gene define the disease sialuria and the allosteric site of the enzyme. *Am J Hum Genet*. 1999;64(6):1563-1569. doi:10.1086/302411

371. Büll C, Boltje TJ, Wassink M, et al. Targeting Aberrant Sialylation in Cancer Cells Using a Fluorinated Sialic Acid Analog Impairs Adhesion, Migration, and In Vivo Tumor Growth. *Mol Cancer Ther*. 2013;12(10):1935-1946. doi:10.1158/1535-7163.MCT-13-0279

372. Macauley MS, Arlian BM, Rillahan CD, et al. Systemic blockade of sialylation in mice with a global inhibitor of sialyltransferases. *J Biol Chem*. 2014;289(51):35149-35158. doi:10.1074/jbc.m114.606517

373. Büll C, Boltje TJ, van Dinther EA, et al. Targeted delivery of a sialic acid-blocking glycomimetic to cancer cells inhibits metastatic spread. *ACS Nano*. 2015;9(1):733-745. doi:10.1021/nn5061964

374. Natoni A, Farrell ML, Harris S, et al. Sialyltransferase inhibition leads to inhibition of tumor cell interactions with E-selectin, VCAM1, and MADCAM1, and improves sur vival in a human multiple myeloma mouse model. *Haematologica*. 2020;105(2):457-467. doi:10.3324/haematol.2018.212266

375. Heise T, Pijnenborg JFA, Büll C, et al. Potent Metabolic Sialylation Inhibitors Based on C-5-Modified Fluorinated Sialic Acids. *J Med Chem*. 2019;62(2):1014-1021. doi:10.1021/acs.jmedchem.8b01757

376. Hinou H, Sun X long, Ito Y. Systematic Syntheses and Inhibitory Activities of Bisubstrate-Type Inhibitors of Sialyltransferases. *J Org Chem*. 2003;68(14):5602-5613. doi:10.1021/jo030042g

377. Izumi M, Wada K, Yuasa H, Hashimoto H. Synthesis of Bisubstrate and Donor Analogues of Sialyltransferase and Their Inhibitory Activities. *J Org Chem.* 2005;70(22):8817-8824. doi:10.1021/jo0512608

378. Ortiz-Soto M elena, Reising S, Schlosser A, Seibel J. Structural and functional role of disulphide bonds and substrate binding residues of the human beta-galactoside alpha-2,3- sialyltransferase 1 (hST3Gal1). *Sci Rep.* 2019;9(1):17993. doi:10.1038/s41598-019-54384-8

379. Müller B, Schaub C, Schmidt RR. Efficient Sialyltransferase Inhibitors Based on Transition-State Analogues of the Sialyl Donor. *Angew Chem Int Ed Engl.* 1998;37(20):2893-2897. doi:10.1002/(SICI)1521-3773(19981102)37:20<2893::AID-ANIE2893>3.0.CO;2-W

380. Schaub C, Müller B, Schmidt RR. New sialyltransferase inhibitors based on CMP-quinic acid : development of a new sialyltransferase assay. *Glycoconj J.* 1998;15(4):345-354. doi:10.1023/a:1006917717161

381. Schwörer R, Schmidt RR. Efficient Sialyltransferase Inhibitors Based on Glycosides of N-Acetylglucosamine. *JACS.* 2002;124(8):163-1637. doi:10.1021/ja017370n

382. Rao F v, Rich JR, Rakic B, et al. Structural insight into mammalian sialyltransferases. *Nat Struct Mol Biol.* 2009;16(11):1186-1188. doi:10.1038/nsmb.1685

383. Montgomery AP, Skropeta D, Yu H. Transition state-based ST6Gal I inhibitors : Mimicking the phosphodiester linkage with a triazole or carbamate through an enthalpy-entropy compensation. *Sci Rep.* 2017;7(1):14428. doi:10.1038/s41598-017-14560-0

384. Guo J, Li W, Xue W, Ye XS. Transition State-Based Sialyltransferase Inhibitors: Mimicking Oxocarbenium Ion by Simple Amide. *J Med Chem.* 2017;60(5):2135-2141. doi:10.1021/acs.jmedchem.6b01644

385. Dobie C, Montgomery AP, Szabo R, Skropeta D, Yu H. Computer-aided design of human sialyltransferase inhibitors of hST8Sia III. *J Mol Recognit.* 2018;31(2):10.1002/jmr.2684. doi:10.1002/jmr.2684

386. Wu CY, Hsu CC, Chen ST, Tsai YC. Soyasaponin I, a potent and specific sialyltransferase inhibitor. *Biochem Biophys Res Commun.* 2001;284(2):466-469. doi:10.1006/bbrc.2001.5002

387. Hsu CC, Lin TW, Chang WW, et al. Soyasaponin-I-modified invasive behavior of cancer by changing cell surface sialic acids. *Gynecol Oncol.* 2005;96(2):415-422. doi:10.1016/j.ygyno.2004.10.010

388. Chang WW, Yu CY, Lin TW, Wang PH, Tsai YC. Soyasaponin I decreases the expression of α2,3-linked sialic acid on the cell surface and suppresses the metastatic potential of B16F10 melanoma cells. *Biochem Biophys Res Commun.* 2006;341(2):614-619. doi:10.1016/j.bbrc.2005.12.216

389. Chang KH, Lee L, Chen J, Li WS. Lithocholic acid analogues, new and potent α-2,3-sialyltransferase inhibitors. *Chemical Communications.* 2006;6(6):629-631. doi:10.1039/b514915k

390. Chen JY, Tang YA, Huang SM, et al. A Novel Sialyltransferase Inhibitor Suppresses FAK / Paxillin Signaling and Cancer Angiogenesis and Metastasis Pathways. *Cancer Res.* 2011;71(2):473-483. doi:10.1158/0008-5472.CAN-10-1303

391. Chiang CH, Wang CH, Chang HC, More S v., Li WS, Hung WC. A novel sialyltransferase inhibitor AL10 suppresses invasion and metastasis of lung cancer cells by inhibiting integrin-mediated signaling. *J Cell Physiol.* 2010;223(2):492-499. doi:10.1002/jcp.22068

392. Fu CW, Tsai HE, Chen WS, et al. Sialyltransferase Inhibitors Suppress Breast Cancer Metastasis. *J Med Chem.* 2021;64(1):527-542. doi:10.1021/acs.jmedchem.0c01477

393. Pietrobono S, Stecca B. Aberrant sialylation in cancer: Biomarker and potential target for therapeutic intervention? *Cancers (Basel).* 2021;13(9):2014. doi:10.3390/cancers13092014

394. Deer EL, Gonzalez-Hernandez J, Coursen JD, et al. Phenotype and Genotype of pancreatic cancer. *Pancreas.* 2010;39(4):425-435. doi:10.1097/MPA.0b013e3181c15963

395. Panosa C, Tebar F, Ferrer-Batallé M, et al. Development of an Epidermal Growth Factor Derivative with EGFR Blocking Activity. *PLoS One.* 2013;8(7):e69325. doi:10.1371/journal.pone.0069325

396. Uribe ML, Marrocco I, Yarden Y. EGFR in Cancer: Signaling Mechanisms, Drugs, and Acquired Resistance. *Cancers (Basel).* 2021;13(11):2748. doi:10.3390/cancers13112748

397. Li H, K AJ, Yong Tao ZX, Xiang Z. RPN2 promotes colorectal cancer cell proliferation through modulating the glycosylation status of EGFR. *Oncotarget*. 2017;8(42):72633-72651. doi:10.18632/oncotarget.20005

398. Qi F, Isaji T, Duan C, et al. ST3GAL3, ST3GAL4, and ST3GAL6 differ in their regulation of biological functions via the specificities for the α2,3-sialylation of target proteins. *FASEB J*. 2020;34(1):881-897. doi:10.1096/fj.201901793R

399. Rosell R, Moran T, Queralt C, et al. Screening for epidermal growth factor receptor mutations in lung cancer. *New England Journal of Medicine*. 2009;361(10):958-967. doi:10.1056/NEJMoa0904554

400. Attili I, Karachaliou N, Conte PF, Bonanno L, Rosell R. Therapeutic approaches for T790M mutation positive non-small-cell lung cancer. *Expert Rev Anticancer Ther*. 2018;18(10):1021-1030. doi:10.1080/14737140.2018.1508347

401. Engel J, Richters A, Getlik M, et al. Targeting Drug Resistance in EGFR with Covalent Inhibitors: A Structure-Based Design Approach. *J Med Chem*. 2015;58(17):6844-6863. doi:10.1021/acs.jmedchem.5b01082

402. Lu X, Yu L, Zhang Z, Ren X, Smaill JB, Ding K. Targeting EGFRL858R/T790M and EGFRL858R/T790M/C797S resistance mutations in NSCLC: Current developments in medicinal chemistry. *Med Res Rev*. 2018;38(5):1550-1581. doi:10.1002/med.21488

403. Naumov GN, Nilsson MB, Cascone T, et al. Combined Vascular Endothelial Growth Factor Receptor and Epidermal Growth Factor Receptor (EGFR) Blockade Inhibits Tumor Growth in Xenograft Models of EGFR Inhibitor Resistance. *Clin Cancer Res*. 2009;15(10):3484-3494. doi:10.1158/1078-0432.CCR-08-2904

404. Munkley J. The glycosylation landscape of pancreatic cancer (Review). *Oncol Lett*. 2019;17(3):2569-2575. doi:10.3892/ol.2019.9885

405. Vajaria BN, Patel PS. Glycosylation: a hallmark of cancer? *Glycoconj J*. 2017;34(2):147-156. doi:10.1007/s10719-016-9755-2

406. Drake PM, Cho W, Li B, et al. Sweetening the pot: adding glycosylation to the biomarker discovery equation. *Clin Chem*. 2010;56(2):223-236. doi:10.1373/clinchem.2009.136333

407. Llop E, Guerrero PE, Duran A, et al. Glycoprotein biomarkers for the detection of pancreatic ductal adenocarcinoma. *World J Gastroenterol*. 2018;24(24):2537-2554. doi:10.3748/wjg.v24.i24.2537

408. Magnani JL, Steplewski Z, Koprowsk H, Ginsburg V. Identification of The Gastrointestinal and Pancreatic Cancer-Associated Antigen Detected by Monoclonal Antibody 19–9 in the Sera of Patients as a Mucin. *Cancer Res*. 1983;43(11):5489-5492.

409. Yue T, Partyka K, Maupin K, et al. Identification of blood-protein carriers of the CA 19-9 antigen and characteriztion of prevalence in pancreatic diseases. *Proteomics*. 2012;11(18):3665-3674. doi:10.1002/pmic.201000827

410. Yue T, Maupin KA, Fallon B, et al. Enhanced discrimination of malignant from benign pancreatic disease by measuring the CA 19-9 antigen on specific protein carriers. *PLoS One*. 2011;6(12):e29180. doi:10.1371/journal.pone.0029180

411. Tang H, Partyka K, Hsueh P, et al. Glycans Related to the CA19-9 Antigen Are Increased in Distinct Subsets of Pancreatic Cancers and Improve Diagnostic Accuracy Over CA19-9. *Cmgh*. 2016;2(2):210-221.e15. doi:10.1016/j.jcmgh.2015.12.003

412. Singh S, Pal K, Yadav J, et al. Upregulation of Glycans Containing 3' Fucose in a Subset of Pancreatic Cancers Uncovered Using Fusion-Tagged Lectins. *J Proteome Res*. 2015;14(6):2594-2605. doi:10.1021/acs.jproteome.5b00142

413. Takahashi S, Oda T, Hasebe T, et al. Overexpression of sialyl Lewis x antigen is associated with formation of extratumoral venous invasion and predicts postoperative development of massive hepatic metastasis in cases with pancreatic ductal adenocarcinoma. *Pathobiology*. 2001;69(3):127-135. doi:10.1159/000048767

414. Rho J hyun, Mead JR, Wright WS, et al. Discovery of sialyl Lewis A and Lewis X modified protein cancer biomarkers using high density antibody arrays. *J Proteomics*. 2014;96:291-299. doi:10.1016/j.jprot.2013.10.030

415. Metzgar RS, Gaillard S, Levine SJ, Tuck FL, Bossen EH, Borowitz MJ. Antigens of human pancreatic adenocarcinoma cells defined by murine monoclonal antibodies. *Cancer Res.* 1982;42(2):601-608.

416. Pan S, Chen R, Tamura Y, et al. Quantitative glycoproteomics analysis reveals changes in N-glycosylation level associated with pancreatic ductal adenocarcinoma. *J Proteome Res.* 2014;13(3):1293-1306. doi:10.1021/pr4010184

417. Pan S, Tamura Y, Chen R, May D, McIntosh MW, Brentnall TA. Large-scale quantitative glycoproteomics analysis of site-specific glycosylation occupancy. *Mol Biosyst.* 2012;8(11):2850-2856. doi:10.1039/c2mb25268f

418. Park HM, Hwang MP, Kim YW, et al. Mass spectrometry-based N-linked glycomic profiling as a means for tracking pancreatic cancer metastasis. *Carbohydr Res.* 2015;413(1):5-11. doi:10.1016/j.carres.2015.04.019

419. Barrabés S, Pagès-Pons L, Radcliffe CM, et al. Glycosylation of serum ribonuclease 1 indicates a major endothelial origin and reveals an increase in core fucosylation in pancreatic cancer. *Glycobiology.* 2007;17(4):388-400. doi:10.1093/glycob/cwm002

420. Zhao J, Qiu W, Simeone DM, Lubman DM. N-linked glycosylation profiling of pancreatic cancer serum using capillary liquid phase separation coupled with mass spectrometric analysis. *J Proteome Res.* 2007;6(3):1126-1138. doi:10.1021/pr0604458

421. Cui HX, Wang H, Wang Y, et al. ST3Gal III modulates breast cancer cell adhesion and invasion by altering the expression of invasion-related molecules. *Oncol Rep.* 2016;36(6):3317-3324. doi:10.3892/or.2016.5180

422. Wang X, Zhang Y, Lin H, et al. Alpha2,3-sialyltransferase III knockdown sensitized ovarian cancer cells to cisplatin-induced apoptosis. *Biochem Biophys Res Commun.* 2017;482(4):758-763. doi:10.1016/j.bbrc.2016.11.107

423. Wen KC, Sung PL, Hsieh SL, et al. alpha2,3-sialyltransferase type I regulates migration and peritoneal dissemination of ovarian cancer cells. *Oncotarget.* 2017;8(17):29013-29027. doi:10.18632/oncotarget.15994

424. Larbouret C, Gaborit N, Chardès T, et al. In pancreatic carcinoma, dual EGFR/HER2 targeting with cetuximab/trastuzumab is more effective than treatment with trastuzumab/ erlotinib or lapatinib alone: Implication of receptors' down-regulation and dimers' disruption. *Neoplasia.* 2012;14(2):121-130. doi:10.1593/neo.111602

425. Wheeler DL, Dunn EF, Harari PM. Understanding resistance to EGFR inhibitors-impact on future treatment strategies. *Nat Rev Clin Oncol.* 2010;7(9):493-507. doi:10.1038/nrclinonc.2010.97

426. El-Hashim AZ, Khajah MA, Renno WM, et al. Src-dependent EGFR transactivation regulates lung inflammation via downstream signaling involving ERK1/2, PI3Kδ/Akt and NFϰB induction in a murine asthma model. *Sci Rep.* 2017;7(1):9919. doi:10.1038/s41598-017-09349-0

427. Qin H, Liu J, Yu M, et al. FUT7 promotes the malignant transformation of follicular thyroid carcinoma through α1,3-fucosylation of EGF receptor. *Exp Cell Res.* 2020;393(2):112095. doi:10.1016/j.yexcr.2020.112095

428. Soltoff SP, Carraway KL, Prigent SA, Gullick WG, Cantley LC. ErbB3 is involved in activation of phosphatidylinositol 3-kinase by epidermal growth factor. *Mol Cell Biol.* 1994;14(6):3550-3558. doi:10.1128/mcb.14.6.3550-3558.1994

429. Kim HH, Sierke SL, Koland JG. Epidermal growth factor-dependent association of phosphatidylinositol 3- kinase with the erbB3 gene product. *Journal of Biological Chemistry.* 1994;269(40):24747-24755. doi:10.1016/s0021-9258(17)31455-2

430. von Marschall Z, Cramer T, Höcker M, et al. De novo expression of vascular endothelial growth factor in human pancreatic cancer: Evidence for an autocrine mitogenic loop. *Gastroenterology.* 2000;119(5):1358-1372. doi:10.1053/gast.2000.19578

431. Song M, Bode AM, Dong Z, Lee MH. AKT as a therapeutic target for cancer. *Cancer Res.* 2019;79(6):1019-1031. doi:10.1158/0008-5472.CAN-18-2738

432. Colin M. Parsons, Muilenburg D, Tawnya L. Bowles, Virudachalam S, Bold RJ. The Role of Akt Activation in the Response to Chemotherapy in Pancreatic Cancer. *Anticancer Res.* 2010;30(9):3279-3289.

433. Takahashi M, Hasegawa Y, Gao C, Kuroki Y, Taniguchi N. N-glycans of growth factor receptors: Their role in receptor function and disease implications. *Clin Sci*. 2016;130(20):1781-1792. doi:10.1042/cs20160273

434. Sweeney C, Fambrough D, Huard C, et al. Growth Factor-specific Signaling Pathway Stimulation and Gene Expression Mediated by ErbB Receptors. *J Biol Chem*. 2001;276(25):22685-22698. doi:10.1074/jbc.M100602200

435. Yokoe S, Takahashi M, Asahi M, et al. The Asn 418 -linked N-glycan of ErbB3 plays a crucial role in preventing spontaneous heterodimerization and tumor promotion. *Cancer Res*. 2007;67(5):1935-1942. doi:10.1158/0008-5472.CAN-06-3023

436. Cao Q, Wang N, Ren L, Tian J, Yang S, Cheng H. MiR-125a-5p post-transcriptionally suppresses GALNT7 to inhibit proliferation and invasion in cervical cancer cells via the EGFR/PI3K/AKT pathway. *Cancer Cell Int*. 2020;20:117. doi:10.1186/s12935-020-01209-8

437. Wei A, Fan B, Zhao Y, et al. ST6Gal-I overexpression facilitates prostate cancer progression via the PI3K/Akt/GSK-3β/β-catenin signaling pathway. *Oncotarget*. 2016;7(40):65374-65388. doi:10.18632/oncotarget.11699

438. Sung PL, Wen KC, Horng HC, et al. The role of α2,3-linked sialylation on clear cell type epithelial ovarian cancer. *Taiwan J Obstet Gynecol*. 2018;57(2):255-263. doi:10.1016/j.tjog.2018.02.015

439. Gao Y, Luan X, Melamed J, Brockhausen I. Role of Glycans on Key Cell Surface Receptors That Regulate Cell Proliferation and Cell Death. *Cells*. 2021;10(5):1252. doi:10.3390/cells10051252

440. Chakraborty A, Dorsett KA, Trummell HQ, et al. ST6Gal-I sialyltransferase promotes chemoresistance in pancreatic ductal adenocarcinoma by abrogating gemcitabine-mediated DNA damage. *J Biol Chem*. 2018;293(3):984-994. doi:10.1074/jbc.M117.808584

441. Larbouret C, Robert B, Bascoul-Mollevi C, et al. Combined cetuximab and trastuzumab are superior to gemcitabine in the treatment of human pancreatic carcinoma xenografts. *Ann Oncol*. 2009;21(1):98-103. doi:10.1093/annonc/mdp496

442. Morgan MA, Parsels LA, Kollar LE, Normolle DP, Maybaum J, Lawrence TS. The combination of epidermal growth factor receptor inhibitors with gemcitabine and radiation in pancreatic cancer. *Clin C*. 2008;14(16):5142-5149. doi:10.1158/1078-0432.CCR-07-4072

443. Tonra JR, Deevi DS, Corcoran E, et al. Synergistic antitumor effects of combined epidermal growth factor receptor and vascular endothelial growth factor receptor-2 targeted therapy. *Clinical Cancer Research*. 2006;12(7 Pt I):2197-2207. doi:10.1158/1078-0432.CCR-05-1682

444. Poteet E, Liu D, Liang Z, van Buren G, Chen C, Yao Q. Mesothelin and TGF-α predict pancreatic cancer cell sensitivity to EGFR inhibitors and effective combination treatment with trametinib. *PLoS One*. 2019;14(3):e0213294. doi:10.1371/journal.pone.0213294

445. Azimzadeh Irani M, Kannan S, Verma C. Role of N-glycosylation in EGFR ectodomain ligand binding. *Proteins*. 2017;85(8):1529-1549. doi:10.1002/prot.25314

446. López J. *Anàlisi Dels Efectes de l'inhibidor de Les Sialiltransferases (Ac53FaxNeu5Ac) Sobre La Sialilació, El Fenotip Invasiu i La Citòlisi per Part Dels Limfòcits T En Línies Cel·lulars de Càncer de Pàncrees*. 2022.

447. Trinchera M, Aronica A, Dall'Olio F. Selectin Ligands Sialyl-Lewis a and Sialyl-Lewis x in Gastrointestinal Cancers. *Biology (Basel)*. 2017;6(4):16. doi:10.3390/biology6010016

448. Büll C, Boltje TJ, Balneger N, et al. Sialic acid blockade suppresses tumor growth by enhancing t-cell-mediated tumor immunity. *Cancer Res*. 2018;78(13):3574-3588. doi:10.1158/0008-5472.CAN-17-3376

449. Matsumura R, Hirakawa J, Sato K, et al. Novel antibodies reactive with sialyl Lewis X in both humans and mice define its critical role in leukocyte trafficking and contact hypersensitivity responses. *Journal of Biological Chemistry*. 2015;290(24):15313-15326. doi:10.1074/jbc.M115.650051

450. de Bolós C, Garrido M, Real FX. MUC6 apomucin shows a distinct normal tissue distribution that correlates with Lewis antigen expression in the human stomach. *Gastroenterology*. 1995;109(3):723-734. doi:10.1016/0016-5085(95)90379-8

451. Su ML, Chang TM, Chiang CH, et al. Inhibition of chemokine (C-C Motif) receptor 7 sialylation suppresses CCL19-stimulated proliferation, invasion and anti-anoikis. *PLoS One*. 2014;9(6):e98823. doi:10.1371/journal.pone.0098823

452. Chen JY, Tang YA, Huang SM, et al. A Novel Sialyltransferase Inhibitor Suppresses FAK/Paxillin Signaling and Cancer Angiogenesis and Metastasis Pathways. *Cancer Res.* 2011;71(2):473-483. doi:10.1158/0008-5472.CAN-10-1303

453. Takada A, Ohmori K, Yoneda T, et al. Contribution of Carbohydrate Antigens Sialyl Lewis A and Sialyl Lewis X to Adhesion of Human Cancer Cells to Vascular Endothelium. *Cancer Res.* 1993;53(2):354-361.

454. Phillips ML, Nudelman E, Gaeta FCA, et al. ELAM-1 Mediates Cell Adhesion by Recognition of a Carbohydrate Ligand , Sialyl-Le x. *Science (1979).* 1990;250(4984):1130-1132. doi:doi:10.1126/science.1701274

455. Yoshimoto K, Tajima H, Ohta T, et al. Increased E-selectin in hepatic ischemia-reperfusion injury mediates liver metastasis of pancreatic cancer. *Oncol Rep.* 2012;28(3):791-796. doi:10.3892/or.2012.1896

456. Takada A, Ohmori K, Takahashi N, et al. Adhesion of human cancer cells to vascular endothelium mediated by a carbohydrate antigen, sialyl Lewis A. *Biochem Biophys Res Commun.* 1991;179(2):713-719. doi:10.1016/0006-291X(91)91875-D

457. Iwai K, Ishikura H, Kaji M, et al. Importance of E-selectin (ELAM-1) and sialyl lewisa in the adhesion of pancreatic carcinoma cells to acttvated endothelium. *Int J Cancer.* 1993;54(6):972-977. doi:10.1002/ijc.2910540618

458. Aubert M, Panicot-Dubois L, Crotte C, et al. Peritoneal colonization by human pancreatic cancer cells is inhibited by antidense FUT3 sequence. *Int J Cancer.* 2000;88(4):558-565. doi:10.1002/1097-0215(20001115)88:4<558::AID-IJC7>3.0.CO;2-B

459. Zhan L, Chen L, Chen Z. Knockdown of FUT3 disrupts the proliferation, migration, tumorigenesis and TGF-β induced EMT in pancreatic cancer cells. *Oncol Lett.* 2018;16(1):924-930. doi:10.3892/ol.2018.8738

460. Aubert M, Panicot L, Crotte C, et al. Restoration of α(1,2) fucosyltransferase activity decreases adhesive and metastatic properties of human pancreatic cancer cells. *Cancer Res.* 2000;60(5):1449-1456.

461. Cavallaro U, Christofori G. Multitasking in tumor progression: Signaling functions of cell adhesion molecules. *Ann N Y Acad Sci.* 2004;1014:58-66. doi:10.1196/annals.1294.006

462. Li Q, Lan T, Xie J, Lu Y, Zheng D, Su B. Integrin-Mediated Tumorigenesis and Its Therapeutic Applications. *Front Oncol.* 2022;12:812480. doi:10.3389/fonc.2022.812480

463. Pinho S, Marcos NT, Ferreira B, et al. Biological significance of cancer-associated sialyl-Tn antigen: Modulation of malignant phenotype in gastric carcinoma cells. *Cancer Lett.* 2007;249(2):157-170. doi:10.1016/j.canlet.2006.08.010

464. Shen L, Luo Z, Wu J, et al. Enhanced expression of α2,3-linked sialic acids promotes gastric cancer cell metastasis and correlates with poor prognosis. *Int J Oncol.* 2017;50(4):1201-1210. doi:10.3892/ijo.2017.3882

465. Xu C, Wang S, Wu Y, Sun X, Yang D, Wang S. Recent advances in understanding the roles of sialyltransferases in tumor angiogenesis and metastasis. *Glycoconj J.* 2021;38(1):119-127. doi:10.1007/s10719-020-09967-3

466. Bhide GP, Colley KJ. Sialylation of N - glycans : mechanism , cellular compartmentalization and function. *Histochem Cell Biol.* 2017;147(2):149-174. doi:10.1007/s00418-016-1520-x

467. Christie DR, Shaikh FM, Lucas JA, Lucas JA, Bellis SL. ST6Gal-I expression in ovarian cancer cells promotes an invasive phenotype by altering integrin glycosylation and function. *J Ovarian Res.* 2008;1(1):3. doi:10.1186/1757-2215-1-3

468. Wu X, Tian Y, Yu M, Lin B, Han J, Han S. A fluorescently labelled sialic acid for high performance intraoperative tumor detection. *Biomater Sci.* 2014;2(8):1120-1127. doi:10.1039/c4bm00028e

469. Wu X, Yu M, Lin B, Xing H, Han J, Han S. A sialic acid-targeted near-infrared theranostic for signal activation based intraoperative tumor ablation. *Chem Sci.* 2015;6(1):798-803. doi:10.1039/c4sc02248c

470. Ino Y, Yamazaki-Itoh R, Shimada K, et al. Immune cell infiltration as an indicator of the immune microenvironment of pancreatic cancer. *Br J Cancer.* 2013;108(4):914-923. doi:10.1038/bjc.2013.32

471.   de Palma M, Lewis CE. Macrophage regulation of tumor responses to anticancer therapies. *Cancer Cell.* 2013;23(3):277-286. doi:10.1016/j.ccr.2013.02.013

472.   Khaled YS, Ammori BJ, Elkord E. Increased levels of granulocytic myeloid-derived suppressor cells in peripheral blood and tumour tissue of pancreatic cancer patients. *J Immunol Res.* 2014;2014:879897. doi:10.1155/2014/879897

473.   Goulart MR, Stasinos K, Fincham REA, Delvecchio FR, Kocher HM. T cells in pancreatic cancer stroma. *World J Gastroenterol.* 2021;27(46):7956-7968. doi:10.3748/wjg.v27.i46.7956

474.   Büll C, den Brok MH, Adema GJ. Sweet escape: Sialic acids in tumor immune evasion. *Biochim Biophys Acta Rev Cancer.* 2014;1846(1):238-246. doi:10.1016/j.bbcan.2014.07.005

475.   Torphy RJ, Schulick RD, Zhu Y. Understanding the immune landscape and tumor microenvironment of pancreatic cancer to improve immunotherapy. *Mol Carcinog.* 2020;59(7):775-782. doi:10.1002/mc.23179

476.   van de Wall S, Santegoets KCM, van Houtum EJH, Büll C, Adema GJ. Sialoglycans and Siglecs Can Shape the Tumor Immune Microenvironment. *Trends Immunol.* 2020;41(4):274-285. doi:10.1016/j.it.2020.02.001

477.   Adams OJ, Stanczak MA, von Gunten S, Läubli H. Targeting sialic acid-Siglec interactions to reverse immune suppression in cancer. *Glycobiology.* 2018;28(9):640-647. doi:10.1093/glycob/cwx108

478.   Rodriguez E, Boelaars K, Brown K, et al. Sialic acids in pancreatic cancer cells drive tumour-associated macrophage differentiation via the Siglec receptors Siglec-7 and Siglec-9. *Nat Commun.* 2021;12(1):1270. doi:10.1038/s41467-021-21550-4

479.   Seidenfaden R, Krauter A, Schertzinger F, Gerardy-Schahn R, Hildebrandt H. Polysialic Acid Directs Tumor Cell Growth by Controlling Heterophilic Neural Cell Adhesion Molecule Interactions. *Mol Cell Biol.* 2003;23(16):5908-5918. doi:10.1128/mcb.23.16.5908-5918.2003

480.   Yamaji T, Mitsuki M, Teranishi T, Hashimoto Y. Characterization of inhibitory signaling motifs of the natural killer cell receptor Siglec-7: Attenuated recruitment of phosphatases by the receptor is attributed to two amino acids in the motifs. *Glycobiology.* 2005;15(7):667-676. doi:10.1093/glycob/cwi048

481.   Nicoll G, Avril T, Lock K, Furukawa K, Bovin N, Crocker PR. Ganglioside GD3 expression on target cells can modulate NK cell cytotoxicity via siglec-7-dependent and -independent mechanisms. *Eur J Immunol.* 2003;33(6):1642-1648. doi:10.1002/eji.200323693

482.   Hudak JE, Canham SM, Bertozzi CR. Glycocalyx engineering reveals a Siglec-based mechanism for NK cell immunoevasion. *Nat Chem Biol.* 2014;10(1):69-75. doi:10.1038/nchembio.1388

483.   Daly J, Carlsten M, O'Dwyer M. Sugar free: Novel immunotherapeutic approaches targeting siglecs and sialic acids to enhance natural killer cell cytotoxicity against cancer. *Front Immunol.* 2019;10:1047. doi:10.3389/fimmu.2019.01047

484.   Meril S, Harush O, Reboh Y, Matikhina T, Barliya T, Cohen CJ. Targeting glycosylated antigens on cancer cells using siglec-7/9-based CAR T-cells. *Mol Carcinog.* 2020;59(7):713-723. doi:10.1002/mc.23213

485.   Martinez-Bosch N, Vinaixa J, Navarro P. Immune evasion in pancreatic cancer: From mechanisms to therapy. *Cancers (Basel).* 2018;10(1):6. doi:10.3390/cancers10010006

486.   Lee HC, Wondimu A, Liu Y, Ma JSY, Radoja S, Ladisch S. Ganglioside Inhibition of CD8 + T Cell Cytotoxicity: Interference with Lytic Granule Trafficking and Exocytosis. *J Immunol.* 2012;189(7):3521-3527. doi:10.4049/jimmunol.1201256

487.   Daniels MA, Devine L, Miller JD, et al. CD8 binding to MHC class I molecules is influenced by T cell maturation and glycosylation. *Immunity.* 2001;15(6):1051-1061. doi:10.1016/S1074-7613(01)00252-7

488.   Perdicchio M, Ilarregui JM, Verstege MI, et al. Sialic acid-modified antigens impose tolerance via inhibition of T-cell proliferation and de novo induction of regulatory T cells. *Proc Natl Acad Sci U S A.* 2016;113(12):3329-3334. doi:10.1073/pnas.1507706113

489.   Perdicchio M, Cornelissen LAM, Streng-Ouwehand I, et al. Tumor sialylation impedes T cell mediated anti-tumor responses while promoting tumor associated-regulatory T cells. *Oncotarget.* 2016;7(8):8771-8782. doi:10.18632/oncotarget.6822

490.   Yeo D, Giardina C, Saxena P, Rasko JEJ. The next wave of cellular immunotherapies in pancreatic cancer. *Mol Ther Oncolytics.* 2022;24:561-576. doi:10.1016/j.omto.2022.01.010

491. Feig C, Jones JO, Kraman M, et al. Targeting CXCL12 from FAP-expressing carcinoma-associated fibroblasts synergizes with anti-PD-L1 immunotherapy in pancreatic cancer. *Proc Natl Acad Sci U S A*. 2013;110(50):20212-20217. doi:10.1073/pnas.1320318110

492. Moons SJ, Rossing E, Janssen MACH, et al. Structure − Activity Relationship of Metabolic Sialic Acid Inhibitors and Labeling Reagents. *ACS Chem Biol*. 2022;17(3):590-597. doi:10.1021/acschembio.1c00868